KIT SCIENTIFIC REPORTS 7654

Proceedings of the 17th IEA International Workshop on Ceramic Breeder Blanket Interactions (CBBI-17)

September 12-14, 2013, Barcelona, Spain

Regina Knitter, Lorenzo V. Boccaccini, Angel Ibarra (eds)

KIT Scientific Publishing

Regina Knitter, Lorenzo V. Boccaccini, Angel Ibarra (eds)

Proceedings of the 17th IEA International Workshop on Ceramic Breeder Blanket Interactions (CBBI-17)

September 12-14, 2013, Barcelona, Spain

Karlsruhe Institute of Technology
KIT SCIENTIFIC REPORTS 7654

Proceedings of the 17th IEA International Workshop on Ceramic Breeder Blanket Interactions (CBBI-17)

September 12-14, 2013, Barcelona, Spain

by
Regina Knitter, Lorenzo V. Boccaccini, Angel Ibarra (eds)

Scientific
Publishing

Report-Nr. KIT-SR 7654

Impressum

KIT Scientific Publishing

Karlsruher Institut für Technologie (KIT)
KIT Scientific Publishing
Straße am Forum 2
D-76131 Karlsruhe

KIT Scientific Publishing is a registered trademark of Karlsruhe Institute of Technology. Reprint using the book cover is not allowed.

www.ksp.kit.edu

Print on Demand 2014

ISSN 1869-9669
ISBN 978-3-7315-0101-5

PREFACE

The Seventeenth International Workshop on Ceramic Breeder Blanket Interaction was held in Barcelona, Spain, on September, 12-14, 2013 under the auspices of the IEA Implementing Agreement and the Japan-US Fusion Collaboration Framework on the Nuclear Technology of Fusions Reactors.

The CBBI-17 provided a forum of specialists involved in the design, research, development and testing of materials and components for lithium ceramic based breeding blankets. The workshop was organized by CIEMAT supported by KIT as a satellite meeting of the 11th International Symposium on Fusion Nuclear Technology (ISFNT-11) and was hosted by IREC, Barcelona, Spain.

The workshop was attended by 30 participants from China, the European Union, Japan, Korea, the Russian Federation and the United States. 24 presentations were given on the four topics: (1) Ceramic Breeder Fabrication and Properties, (2) Pebble Bed Properties, (3) Tritium Release, Extraction and Permeation, (4) Status of Breeder Blankets. In addition, three Topical Discussions were focussed on the subjects “New Material Productions”, “Tritium Permeation in the Breeding Zone” and “Life Limiting Factors and Achievable Peak Power Density for Solid Breeder Blankets”.

EDITORS

R. Knitter, L.V. Boccaccini (KIT) and A. Ibarra (CIEMAT)

PROGRAM ADVISORY COMMITTEE

M. Abdou (UCLA), L.V. Boccaccini (KIT), P. Chaudhuri (IPR), X. Chen (CAEP), S. Cho (NFRI),
R. K. Ellappan (IPR), M. Enoeda (JAEA), K. Feng (SWIP), V. Konvalenko (NIKIET),
A. Ibarra (CIEMAT), Edward Stevens (US-DOE), A. Leshukov (NIKIET), T. Terai (Univ. Tokyo),
R. Knitter (KIT), Scientific Secretary

LOCAL ORGANIZING COMMITTEE

M. Garcia (CIEMAT), O. Nomen (IREC), M. Sanmarti (IREC)

CONTENT

page

Final Programme

17th IEA International Workshop:

Ceramic Breeder Blanket Interactions (CBBI-17)

12-14 September 2013

IREC, Jardins de les Dones de Negre, 1, 2ª pl.
08930 Sant Adrià de Besòs, Barcelona, Spain

	Thursday, 12 September 2013
09:00	**Welcome / Introduction to CBBI-17** (A. Ibarra)
	Topic 1: **Ceramic Breeder Fabrication and Properties** (A. Ibarra)
•	Fabrication method of ceramic pebble using PVA-boric acid reaction Y.-H. Park, NFRI
•	Recent progress on lithium ceramic breeder materials in CAEP X. Chen, CEAP
•	Development of lithium meta-titanate ceramic powder with solid state reaction for Indian LLCB TBM A. Shrivastava, IPR
	Coffee Break
	Topic 1: **Ceramic Breeder Fabrication and Properties**, cont. (K. Feng)
•	Recent developments of the melt-based production of lithium orthosilicate pebbles O. Leys, KIT
•	Vaporization property of lithium metatitanate and orthosilicate pebbles by high temperature mass spectrometry K. Mukai, Univ. Tokyo
•	Behavior of advanced ceramic breeder pebbles in long-term heat treatment M. Kolb, KIT
	Lunch Break
	Topic 1: **Ceramic Breeder Fabrication and Properties**, cont. (M. Kolb)
•	Chemical compatibility of lithium meta-titanates with low-activation ferritic steel F82H T. Terai, Univ. Tokyo
•	Correlation between electrical behaviour and tritium release in γ-irradiated Li_4SiO_4 breeder pellets and pebbles E. Carella, CIEMAT
	Topical Discussion (R. Knitter, X. Chen): New Material Productions
	End of Day 1

	Friday, 13 September 2013
09:00	Topic 2: **Pebble Bed Properties** (M.-Y. Ahn)
•	A study on fluid flow of helium purge gas with tritium transfer released from lithium titanate in a solid breeder test blanket module M. Enoeda, JAEA
•	Design & fabrication of experimental set up for packed bed effective thermal conductivity measurement A. Shrivastava, IPR
•	Experimental investigation of thermal properties of the Li_4SiO_4 pebble beds Y. Feng, SWIP
•	Progress on pebble bed thermomechanics modeling for solid breeder designs: DEM and FEM approaches J. Van Lew, UCLA
	Coffee Break
	Topic 3: **Tritium Release, Extraction and Permeation** (V. Kapyshev)
•	Tritium recovery experiment on water cooled ceramic breeder blanket under DT neutron irradiation K. Ochiai, JAEA
•	Examination of tritium release properties of advanced tritium breeders by DT neutron K. Ochiai, JAEA
•	Basic studies on new neutron multiplier and breeder materials K. Munakata, Akita Univ.
	Lunch Break
	Topic 3: **Tritium Release, Extraction and Permeation**, cont. (T. Terai)
•	Advanced tritium extraction process for HCPB breeding blanket D. Demange, KIT
•	Influence of the microstructure on the light species behaviour in ceramic breeder blanket materials E. Carella, CIEMAT
•	He thermal-induced diffusion in lithium titanate M. Gonzales, CIEMAT
•	Recent progress on the development of erbium oxide coatings for tritium permeation barrier T. Chikada, Univ. Tokyo
	Topical Discussion (T. Terai, D. Demange): Tritium Permeation in the Breeding Zone
	End of Day 2

	Saturday, 14 September 2013
09:00	Topic 4: **Status of Breeder Blankets** (A. Ying)
•	Development and qualification of ceramic breeder materials for the EU Test Blanket Module: Strategy and R&D achievements M. Zmitko, F4E
•	Initial design and test of the tritium breeder monitoring system for the test breeder module of the ITER V. Kapyshev, NIKIET
•	Current status of design and accident analysis for Korean HCCR TBS M.-Y. Ahn, NFRI
	Coffee Break
	Topic 4: **Status of Breeder Blankets**, cont. (M. Zmitko)
•	Status of development of water cooled ceramic breeder test blanket M. Enoeda, JAEA
•	Recent developments of the design of the EU solid breeder blanket for DEMO L.V. Boccaccini, KIT
	Topical Discussion (A. Ying, M. Enoeda): Life Limiting Factors and Achievable Peak Power Density for Solid Breeder Blankets
	Closing remarks of CBBI-17 (L.V. Boccaccini)
13:00	End of CBBI-17 workshop

PARTICIPANTS OF CBBI-17

	Name	Affiliation	Email address
(1)	**Ahn**, Mu-Young	NFRI	myahn74@nfri.re.kr
(2)	**Boccaccini**, Lorenzo V.	KIT	lorenzo.boccaccini@kit.edu
(3)	**Carella**, Elisabetta	CIEMAT	elisabetta.carella@ciemat.es
(4)	**Chen**, Xiaojun	CAEP	xiaojunchen@caep.ac.cn
(5)	**Chikada**, Takumi	Univ. Tokyo	chikada@nuclear.jp
(6)	**Cho**, Seungyon	NFRI	Sycho@nfri.re.kr
(7)	**Demange**, David	KIT	david.demange@kit.edu
(8)	**Enoeda**, Mikio	JAEA	enoeda.mikio@jaea.go.jp
(9)	**Feng**, Kaiming	SWIP	fengkm@swip.ac.cn
(10)	**Feng**, Yongjin	SWIP	fengyj@swip.ac.cn
(11)	**González**, Maria	CIEMAT	maria.gonzalez@ciemat.es
(12)	**Hirose**, Takanori	JAEA	hirose.takanori@jaea.go.jp
(13)	**Ibarra**, Angel	CIEMAT	angel.ibarra@ciemat.es
(14)	**Kapyshev**, Victor	NIKIET	kapyshev@nikiet.ru
(15)	**Knitter**, Regina	KIT	regina.knitter@kit.edu
(16)	**Kolb**, Matthias	KIT	matthias.kolb@kit.edu
(17)	**Leys**, Oliver	KIT	oliver.leys@kit.edu
(18)	**Mukai**, Keisuke	Univ. Tokyo	kmukai@nuclear.jp
(19)	**Munakata**, Kenzo	Univ. Akita	kenzo@gipc.akita-u.ac.jp
(20)	**Nomen,** Oriol	IREC	onomen@irec.cat
(21)	**Ochiai**, Kentaro	JAEA	ochiai.kentaro@jaea.go.jp
(22)	**Park**, Yi-Hyun	NFRI	yhpark@nfri.re.kr
(23)	**Sanmarti**, Manel	IREC	msanmarti@irec.cat
(24)	**Shrivastava**, Aroh	IPR	aroh@ipr.res.in
(25)	**Stevens**, Edward	US-DOE	Edward.Stevens@science.doe.gov
(26)	**Terai**, Takayuki	Univ. Tokyo	tera@n.t.u-tokyo.ac.jp
(27)	**Van Lew**, Jon	UCLA	jtvanlew@fusion.ucla.edu
(28)	**Ying**, Alice	UCLA	ying@fusion.ucla.edu
(29)	**Zarins**, Arturs	Univ. Riga	arturs.zarins@lu.lv
(30)	**Zmitko**, Milan	F4E	milan.zmitko@f4e.europa.eu

Participants on September, 12, 2013

Participants on September, 14, 2013

TOPIC 1: CERAMIC BREEDER FABRICATION AND PROPERTIES

Fabrication method of ceramic pebble using PVA-boric acid reaction
Yi-Hyun Park, Seungyon Cho, Mu-Young Ahn, Chang-Shuk Kim, Duck Young Ku and Soon Chang Park

Recent progress on lithium ceramic breeder materials in CAEP
Xiaojun Chen, Chengjian Xiao, Xiaoling Gao, Chunmei Kang, Shuming Peng and Xiaolin Wang

Development of lithium meta-titanate ceramic powder with solid state reaction for Indian LLCB TBM
Aroh Shrivastava, Mayank Makwana, P. Chaudhuri, and E. Rajendrakumar

Recent developments of the melt-based production of lithium orthosilicate pebbles
Oliver Leys, Matthias Kolb, Aniceto Goraieb and Regina Knitter

Vaporization property of lithium metatitanate and orthosilicate pebbles by high temperature mass spectrometry
K. Mukai, M. Yasumoto, T. Terai, T. Hoshino, R. Knitter and A. Suzuki

Behavior of advanced ceramic breeder pebbles in long-term heat treatment
M.H.H. Kolb, O.H.J.B. Leys, C. Odemer, C. Frey and R. Knitter

Chemical compatibility of lithium meta-titanates with low-activation ferritic steel F82H
T. Terai, R. Ishioka, K. Uozumi, K. Mukai, A. Suzuki and M. Koyama

Correlation between electrical behaviour and tritium release in γ-irradiated Li_4SiO_4 breeder pellets and pebbles
E. Carella, M.T. Hernandez, A. Ibarra, E. Chinarro and B. Moreno

Topical Discussion: New Material Productions

Fabrication Method of Ceramic Pebble using PVA-Boric Acid Reaction

Yi-Hyun Park[1], Seungyon Cho[1], Mu-Young Ahn[1], Chang-Shuk Kim[1], Duck Young Ku[1] and Soon Chang Park[1]

[1] *National Fusion Research Institute, Yuseong-gu, Daejeon, Republic of Korea*

The Helium Cooled Ceramic Reflector (HCCR) TBM concept has been developed by Korea in order to acquire experimental results through the TBM Program for the breeding blanket of demonstration power reactor (DEMO). In the solid breeding blanket for fusion reactor, lithium-containing ceramics have been selected as tritium breeding material. The breeding material is used in pebble-bed form to reduce the uncertainty of the interface thermal conductance. The one of the candidate for the breeding material of the HCCR TBM is lithium metatitanate (Li_2TiO_3) pebble because of their high mechanical strength, low activation property and chemical stability. The aim of this study is to develop fabrication method considering mass production of the Li_2TiO_3 pebble.

Polyvinyl alcohol (PVA) solutions which was used as binder material prepared by dissolving PVA powder in distilled water. Li_2TiO_3 slurry was prepared by mixing Li_2TiO_3 powder and PVA solution. The slurry was dropped into glycerin including boric acid by a syringe needle. The slurry droplet was cured by cross-linking reaction with PVA and boric acid in glycerin. Finally, the dried green pebble was sintered at 1200 °C in air atmosphere. The morphology and microstructure of the sintered Li_2TiO_3 pebble was observed by optical microscopy and scanning electron microscopy (SEM). The crush load was evaluated by micro-force material test machine. The elemental concentration was analyzed by inductively coupled plasma-optical emission spectroscopy (ICP-OES). The shape of Li_2TiO_3 green pebbles was affected by slurry viscosity, PVA content and boric acid content. The grain size and average crush load of sintered Li_2TiO_3 pebble were controlled by the sintering time. Additionally, the boron in the sintered pebble was not detected. It was expected that the fabrication process using PVA-boric acid method was easily-controllable, low cost and high yield process for mass production of solid breeder pebbles.

Ministry of Science, ICT and Future Planning

NFRI

Fabrication Method of Ceramic Pebble using PVA - Boric Acid Reaction

17th IEA International Workshop :
Ceramic Breeder Blanket Interactions (CBBI-17)
Barcelona, Spain, 12 - 14 Sep. 2013

Yi-Hyun Park

TBM Technology Team

National Fusion Research Institute

iter KOREA DOMESTIC AGENCY

Contents

I Background – Korean HCCR TBM

II R&D Status of Solid Breeder for HCCR TBM

- Development of Li_4SiO_4 Pebble (CBBI-16)
- Development of Li_2TiO_3 Pebble
- Characteristics of Li_2TiO_3 Pebble

III Summary and Future Works

Korean HCCR TBM

➢ **Helium Cooled Ceramic Reflector (HCCR) TBM**
(DEMO-relevant Breeding Breeder Concept)

Parameter	Values
FW heat flux	Average 0.3 MW/m^2 Peak 0.5 MW/m^2
Neutron wall load	0.78 MW/m^2
Thermal Power	1.01 MW
Tritium Breeding Ratio	1.1
Structural material	RAFM (< 550 °C)
Breeder	Li_2TiO_3 pebble bed or Li_4SiO_4 pebble bed < 920 °C
Multiplier	Be pebble bed < 650 °C
Reflector	Graphite pebble bed
Coolant	8 MPa He 0.973 kg/s FW (300 °C / 390 °C) Breeding Zone(390 °C/500 °C)
Purge	He with 0.1 % H_2

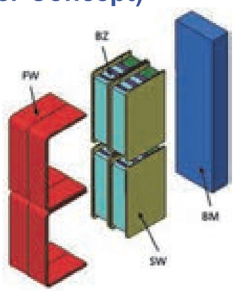

(Cross-section of TBM)

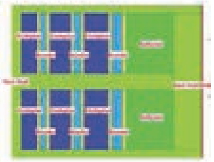

- Structural Material
  - ✓ RAFM
- 7 Layer Breeding Zone
  - ✓ 3 Multipliers (Be)
  - ✓ 3 Breeders (Li-ceramics)
  - ✓ 1 Reflector (Graphite)

- 4 sub-module concept
  - ✓ Manufacturability
  - ✓ PIE & Transportation of irradiated TBM
- Graphite pebble as reflector
  - ✓ Reduce the amount of Be multiplier
  - ✓ Comparable nuclear performance for tritium breeding and shielding in the last layer

Contents

Fabrication Process of Li_4SiO_4 Pebble

➢ Slurry Droplet Wetting Method by using Hydrogen Peroxide Solution

Li_4SiO_4 Powder + PVA solution → Mixing → **Dropping into H_2O_2 solution** → Drying → Sintering

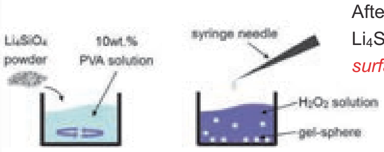

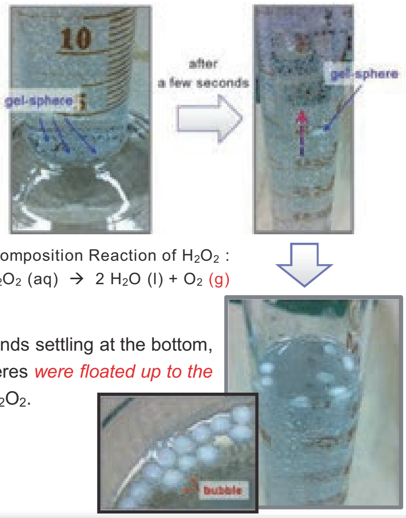

Decomposition Reaction of H_2O_2 :
$2\ H_2O_2\ (aq) \rightarrow 2\ H_2O\ (l) + O_2\ (g)$

After a few seconds settling at the bottom, Li_4SiO_4 gel-spheres *were floated up to the surface* of the H_2O_2.

Appearance and Microstructure of Li_4SiO_4 Pebble

PVA content		10 wt.%	15 wt.%	5 wt.%
Dried gel-spheres				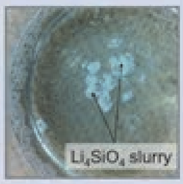
Sintered pebbles	OM and SEM (sintering temp. : 950 °C)	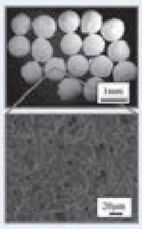		
	Diameter	0.86 mm	0.90 mm	
	Sphericity	< 1.03	< 1.03	
	Porosity	24.5 %	32.3 %	

- The sintered pebbles kept the shape of sphere during sintering process in spite of shrinkage.
- The dropped slurry with PVA content of 5 wt.% was spread in the solution and failed to form the sphere.

Crush Load of Sintered Pebble

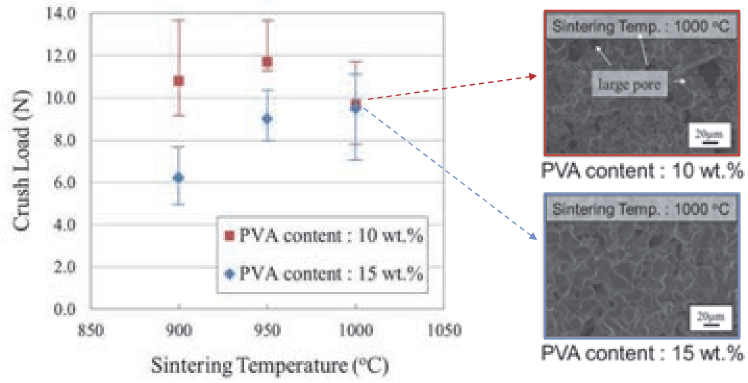

- Several large pores and abnormal grain growth were observed at high sintering temperature.
- Appropriate sintering temperature for stable microstructure of Li_4SiO_4 pebble is less than 1000 °C.

Contents

Fabrication Process for Li_2TiO_3 Pebble

- Slurry Droplet Wetting Method based on the Reaction between PVA and Boric-acid

Fabrication Process

Li_2TiO_3 Powder → Mixing ← PVA Solution

Mixing → Dropping into Glycerin including Boric Acid → Drying → Sintering

Mixing

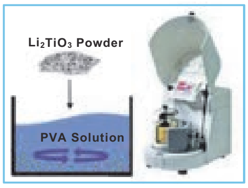

Shaping

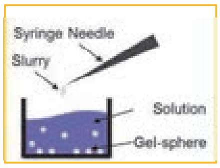

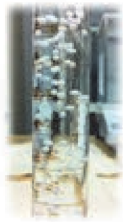

Sintering

Reaction between PVA and Boric Acid

- Cross-linking Reaction between PVA and Boric Acid

  - Boric acid accepts a hydroxide OH^- from water and glycerin.

$$H_3BO_3 \quad + \quad OH^- \quad \longrightarrow \quad B(OH)^-_4$$

  - Ionized molecule act in a condensation reaction with PVA.

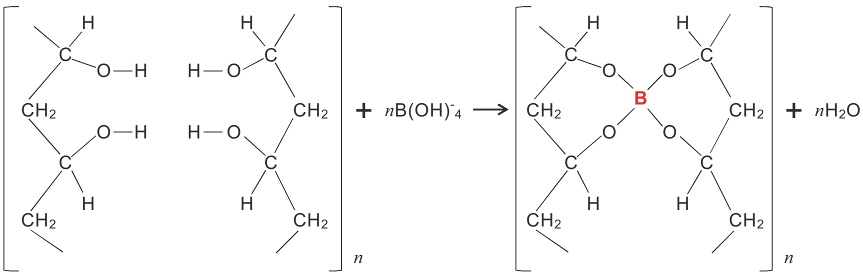

Parameter Study (1)

➢ Effect of Milling Time on Particle Size of Li_2TiO_3 Powder

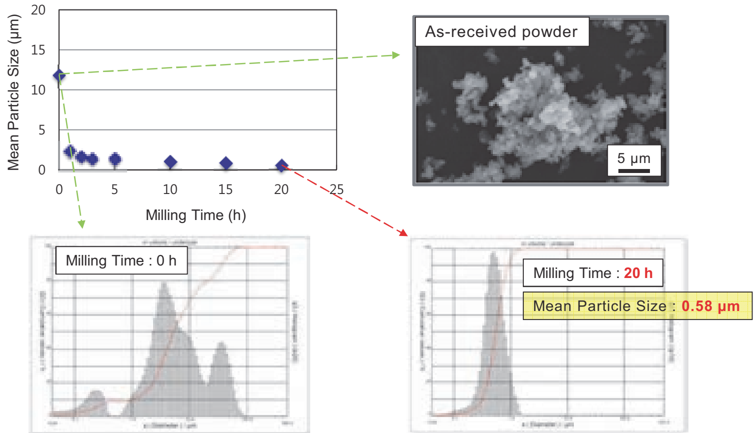

- Commercial Li_2TiO_3 powder was aggregated with small particles.
- Aggregated particles were separated by the ball-milling process.

Parameter Study (2)

➢ Effect of Slurry Viscosity

- Measuring Conditions
  - Instrument : Brookfield Viscometer (rotational viscometer)
  - Rotating Speed : 1 rpm
  - Measuring Temperature : 24 °C

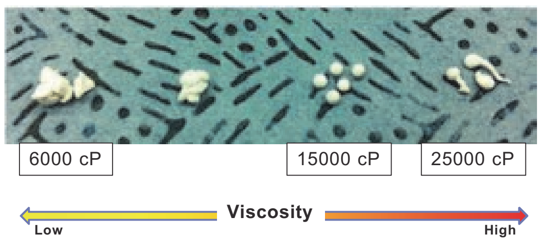

- Slurry droplet of low viscosity was not able to keep the shape.
- High viscosity slurry formed the tail of a droplet.

Parameter Study (3)

- Effect of PVA Content on Shaping

PVA Content : 5 wt.% | PVA Content : 10 wt.% | PVA Content : 15 wt.% | PVA Content : 20 wt.%

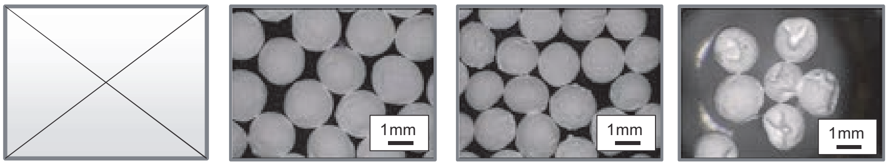

- The dropped slurry with PVA content of 5 wt.% was spread in the glycerin.

- Effect of Boric Acid Content on Shaping

BA Content : 3 wt.% | BA Content : 5 wt.% | BA Content : 10 wt.% | BA Content : 15 wt.%

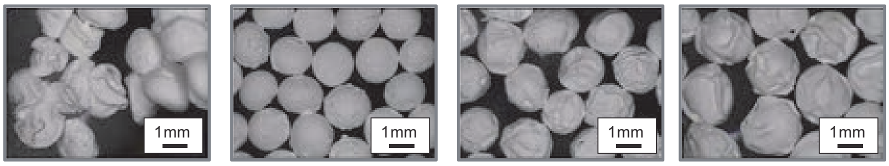

- The content of boric acid had an effect on the reaction speed with PVA.
- Excessive addition of boric acid caused formation of crease on the surface of green body.

Parameter Study (4)

- Effect of Sintering Time (1200°C, air atmosphere)

Sintering Time : 1 h | Sintering Time : 2 h | Sintering Time : 3 h | Sintering Time : 4 h

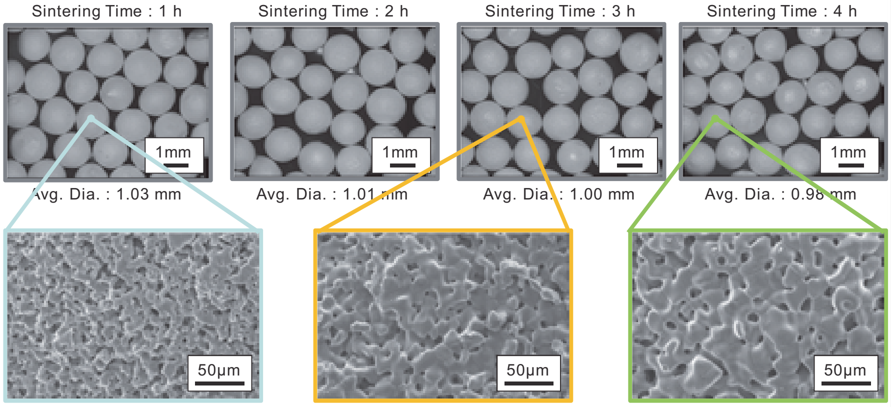

Grain Size : 8 μm | Grain Size : 10 μm | Grain Size : 20 μm

- Grain size was increased with increasing sintering time.
- The whole pore of the sintered pebble was open type.
- The open porosity was about 10 %. (Sintering Time : 3 h)

Contents

Crush Load and Fracture

➢ Crush Load of Sintered Pebble

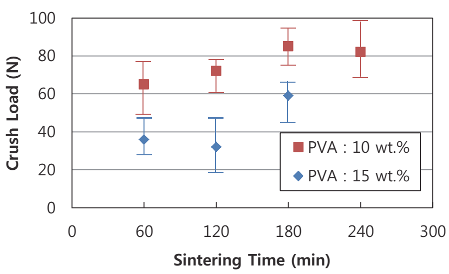

Experimental Conditions

- Equipment : INSTRON 5969
- Crosshead Speed : 0.1 mm/min
- Experimental Mode : Single Compression
- Number of Specimens : 15 EA

➢ Fracture Surface (PVA : 10 wt.%)

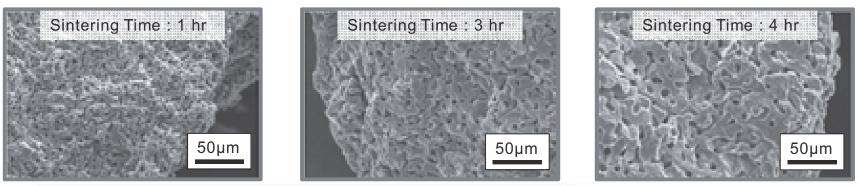

Impurities of Li_2TiO_3 Powder and Pebble

➢ Analysis Results by ICP-OES

(unit : ppm)

Element	Powder	Green Body (Before Sintering)	Pebble (After Sintering)
Al	5.49	10.71	4077.56
B	N.D.	2555.05	N.D.
Ca	70.07	58.85	290.71
Co	629.11	515.98	662.61
Cr	34.57	28.87	38.09
Fe	6.54	6.57	12.63
K	N.D.	N.D.	N.D.
Mg	20.92	17.07	52.77
Na	144.40	102.03	41.46

- The binder and hardening agent, especially boron, were perfectly removed during sintering process.
- The development of high purity starting powder is necessary and important.

Summary

☺ Li_2TiO_3 pebbles were fabricated by **slurry droplet wetting method** based on the **cross-linking reaction** between PVA and boric acid.

☺ Fabrication parameters were investigated to establish suitable process conditions for high-quality ceramic breeder pebbles.

☺ The average diameter and grain size of the Li_2TiO_3 pebble were about **1 mm and 10 µm**, respectively. The whole pore of the pebble was open type and the **open porosity was about 10 %**. The pebble has extremely high strength, about **80 N**, due to the **stable and uniform microstructure**.

☺ Binder and hardening agent were **perfectly removed** during the final sintering process.

☺ In Korea, an automatic dispensing system of the high viscosity ceramic slurry is being developed for **mass production** of the ceramic breeder pebbles. Also, development of the **powder synthesis** process for the high purity and fine grain is ongoing.

Recent Progress on Lithium Ceramic Breeder Materials in CAEP

Xiaojun Chen, Chengjian Xiao, Xiaoling Gao, Chunmei Kang, Shuming Peng, Xiaolin Wang
Institute of Nuclear Physics and Chemistry, China Academy of Engineering Physics, Mian Yang, 621900, China

Abstract: Lithium ceramic breeder materials serve as tritium breeding materials in solid concept TBM in fusion reactor. The overall performance of the ceramic breeder will affect the function of TBM in fusion reactor severely, for instance, tritium breeding and energy converting. In recently, optimizing the fabrication process and properties research work is on going in CAEP. To get higher phase contents of Li_4SiO_4, lithium hydroxide and silicone dioxide are served as the raw materials to produce Li_4SiO_4 powder. The Li_4SiO_4 ceramic pebbles were fabricated using freeze-sintering wet process. A special liquid sintering method was used in the sintering process. The Li_4SiO_4 pebbles show good properties, including high crush load, higher phase structure and small grain size of 10 μm (a.v.). The $LiAlO_2$ pebble with good properties was also fabricated with the freeze-sintering process.

Out-of-pile tritium release experiment was performed using the Li_4SiO_4 pebbles and $LiAlO_2$ pebble. In order to elucidate the fundamental mechanism of tritium release, tritium release kinetics of Li_4SiO_4 pebble irradiated with low thermal-neutron fluence was studied by isochronal and isothermal annealing experiments. It was found that the trace tritium produced in Li_4SiO_4 pebble was released mainly in the chemical form of tritiated water. The apparent desorption activation energy of HTO(g) for isochronal experiments was identical to the diffusion activation energy for isothermal experiments. The Arrhenius relation expression of the overall diffusion coefficient at the temperatures from 450 to 600 K was $D = 1\times10^{-7.0}\exp(-40.3\times10^{3}/RT)$ cm^2s^{-1}. Water content measurement is performed on samples treated under different experimental procedures. It was found that water was adsorbed on the sample during its transferring and storage process. A strong dependence of tritium release behavior on water uptake was determined. By adding H_2 in the sweep gas, formation of water was observed in addition to the isotope exchange reaction with H_2 gas.

Out-of-pile tritium release experiments were also performed to investigate the tritium release properties of $LiAlO_2$ pebble fabricated by freeze-sintering process. The experimental results indicate that the migration of tritium in $LiAlO_2$ is more difficult compared with other ceramic breeder, such as Li_4SiO_4 and Li_2TiO_3. The bred tritium in $LiAlO_2$ pebble requires a higher temperature region to be released. Tritiated water (HTO) was the dominant chemical form of the released tritium with pure helium as the sweep gas. Hydrogen addition to the sweep gas or catalytic metal loaded on the pebble, could significantly change the released form of the tritium. The tritium desorption activation energy of the $LiAlO_2$ pebble is evaluated to 128.7 ± 28.6 kJ/mol.

中国工程物理研究院
CHINA ACADEMY OF ENGINEERING PHYSICS

CBBI-17

Recent Progress on Lithium Ceramic Breeder Materials in CAEP

Presented by: CHEN Xiaojun

Fusion energy materials research group

E-mail Address: xiaojunchen@caep.ac.cn & cxj839@hotmail.com

Institute of Nuclear Physics and Chemistry, CAEP, China

Barcelona, Spain, 12-14 September, 2013

中国工程物理研究院
CHINA ACADEMY OF ENGINEERING PHYSICS

CBBI-17

Outline

- Introduction
- Development of freeze-sintering process
- Tritium release properties(Li_4SiO_4/ γ-$LiAlO_2$)
- Outlook & Summary

2

中国工程物理研究院
CHINA ACADEMY OF ENGINEERING PHYSICS

CBBI-17

Introduction

TBM: tritium breeding
energy extraction

Properties of the tritium breeders will directly affect the TBM

TBR	Radioactivity	Thermal-mechanical
Irradiation	Li Recovery	… …

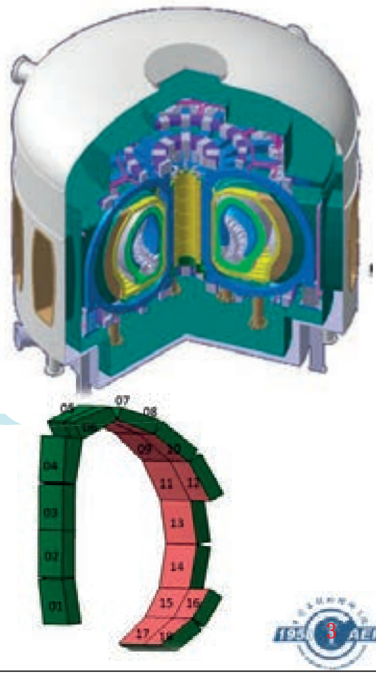

中国工程物理研究院
CHINA ACADEMY OF ENGINEERING PHYSICS

CBBI-17

Introduction

Present status for ceramic breeder

- ✓ Optimize of present fabrication process
- ✓ Fundamental characterization of ceramic pebble
- ✓ Tritium release properties of ceramic pebble
- ✓ Supplement of tritium breeder database

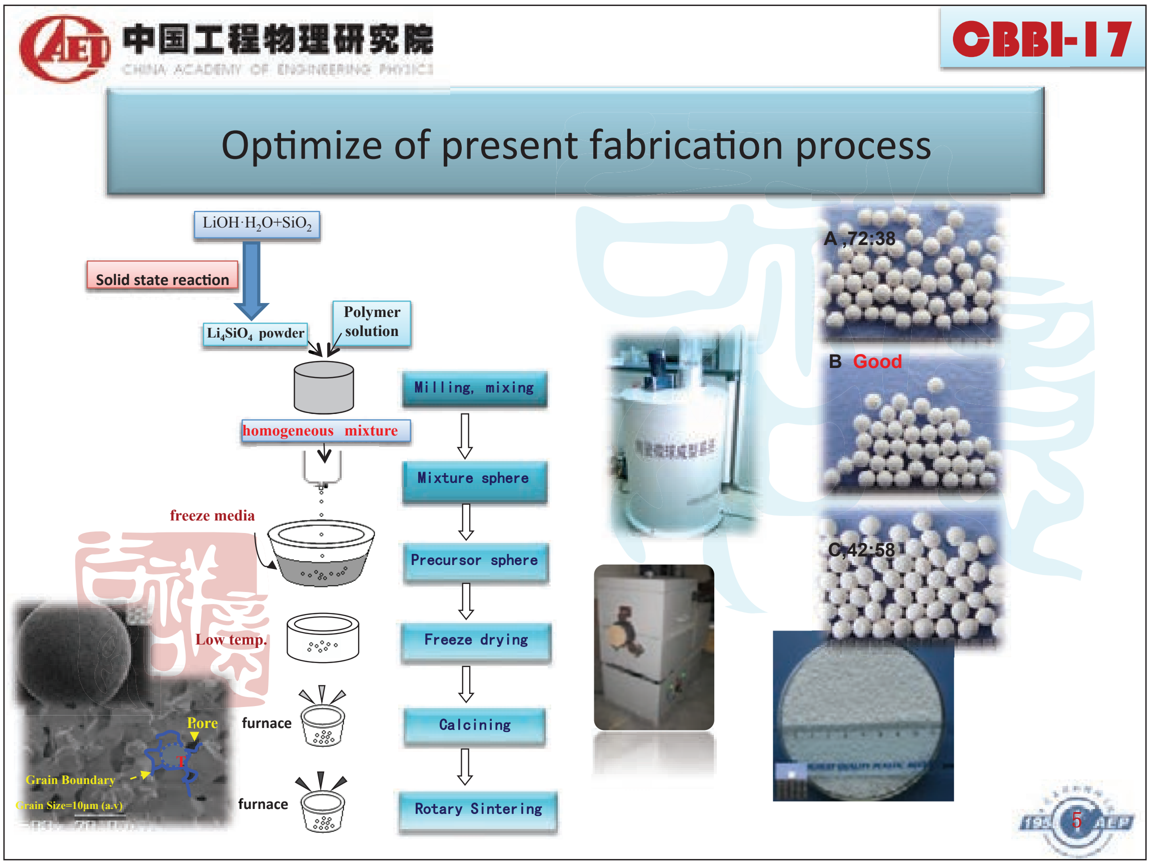
中国工程物理研究院
CHINA ACADEMY OF ENGINEERING PHYSICS
CBBI-17
Optimize of present fabrication process
LiOH·H2O+SiO2
Solid state reaction
Li4SiO4 powder
Polymer solution
homogeneous mixture
freeze media
Low temp.
furnace
furnace
Pore
Grain Boundary
Grain Size=10μm (a.v)
Milling, mixing
Mixture sphere
Precursor sphere
Freeze drying
Calcining
Rotary Sintering
A 72:38
B Good
C 42:58
5

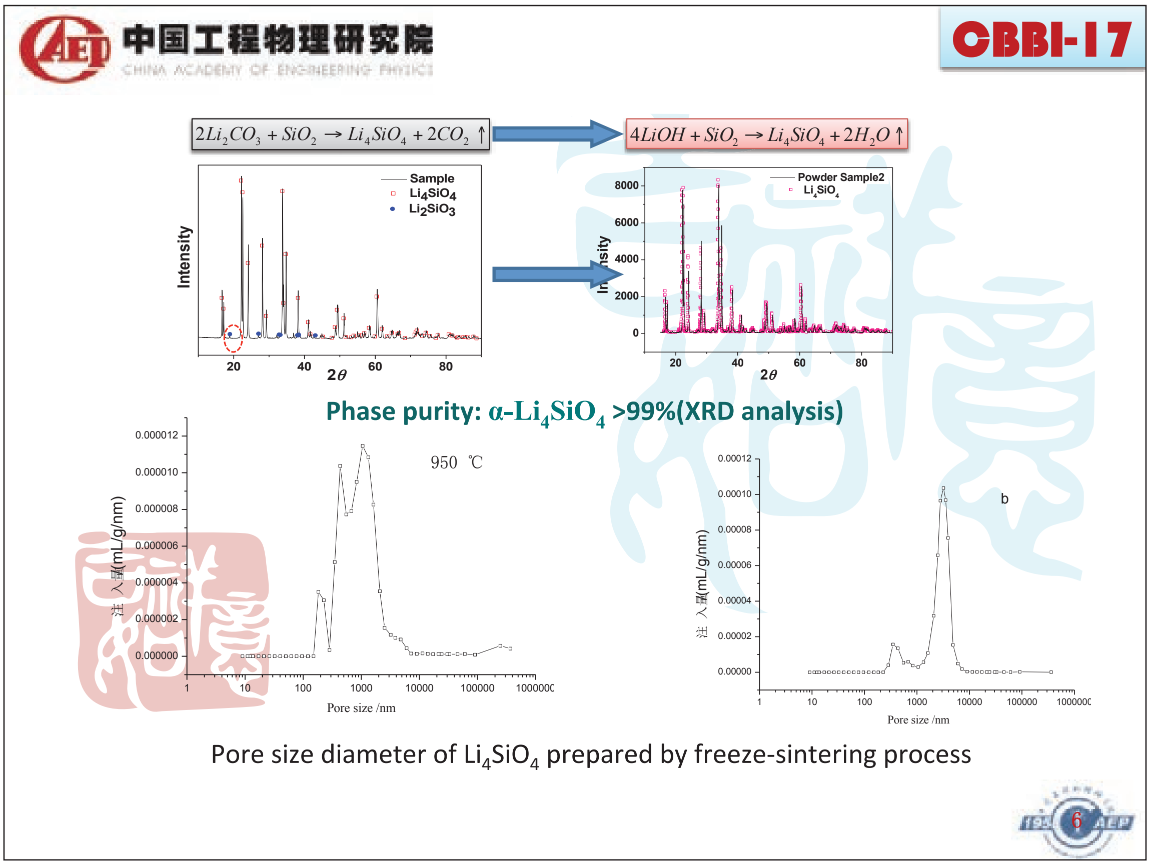
中国工程物理研究院
CHINA ACADEMY OF ENGINEERING PHYSICS
CBBI-17
$2Li_2CO_3 + SiO_2 \rightarrow Li_4SiO_4 + 2CO_2\uparrow$
$4LiOH + SiO_2 \rightarrow Li_4SiO_4 + 2H_2O\uparrow$
Sample
Li4SiO4
Li2SiO3
Intensity
20
40
60
80
2θ
Powder Sample2
Li4SiO4
8000
6000
4000
2000
0
Phase purity: α-Li4SiO4 >99%(XRD analysis)
950 ℃
Pore size /nm
b
Pore size /nm
Pore size diameter of Li4SiO4 prepared by freeze-sintering process
6

Sintering condition（1020℃）

Pebble

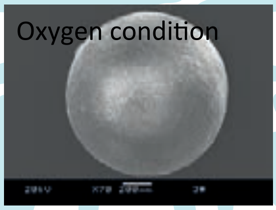

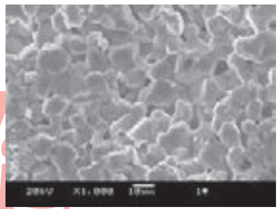

Fracture

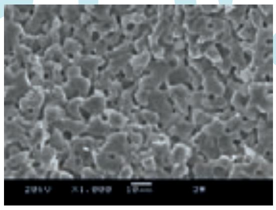

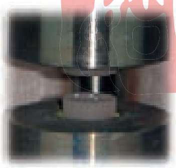

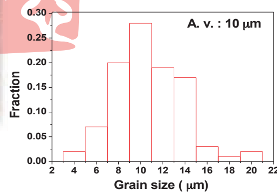

Grain size distribution

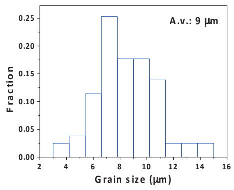

中国工程物理研究院
CHINA ACADEMY OF ENGINEERING PHYSICS
CBBI-17

Element analysis of Li_4SiO_4 pebble(ICP-MS)

element	Be	Sc	V	Cr	Co	Ni	Cu	Zn	Ga	Rb	Sr
(μg/g)	0.431	20.9	0.487	1.43	1.13	1.74	2.31	9.04	0.068	0.267	0.67
element	Y	Nb	Mo	Cd	In	Sb	Cs	Ba	La	Ce	Pr
(μg/g)	0.038	0.278	0.535	0.031	0.005	0.118	0.029	6.87	0.044	0.156	0.01
element	Nd	Sm	Eu	Gd	Tb	Dy	Ho	Er	Tm	Yb	Lu
(μg/g)	0.026	0.01	0.009	0.003	0.003	0.013	0.002	0.006	0.001	0.007	0.001
element	Ta	W	Re	Tl	Pb	Bi	Th	U	Zr	Hf	Sum up
(μg/g)	1.29	0.608	未检出	0.009	0.528	0.05	0.056	0.085	0.982	0.109	50.385

中国工程物理研究院
CHINA ACADEMY OF ENGINEERING PHYSICS

CBBI-17

Characterization of Li_4SiO_4 Pebble

Item	
Pebble diameter	~1.0 mm
Grain size	10 μm (a.v.)
Impurity	～ 0.005%
Sphericity	<1.04
Chemical phase	α- Li_4SiO_4， >99% (XRD)
Crush load	24 N (a.v.)
Porosity	14.8%
Specific area	26.22 (m^2/g)
Coefficient of heat conductivity	0.34 (W/m·K)
Coefficient of Thermal Expansion	23.76E-06 （300℃）
Density	81.2% T.D.
Packing density	apparent density: 1.23 (g/cm^3) tap density: 1.31 (g/cm^3)

9

中国工程物理研究院
CHINA ACADEMY OF ENGINEERING PHYSICS

CBBI-17

Neutron-irradiated Li_4SiO_4 pebbles

Sample
Li_4SiO_4 pebble:~81% T.D,
pebbles size: 1.0 mm(a.v),
grain diameter: 10um(a.v) .
Pretreatment: 773 K for 3h in vacuum.

Neutron Irradiation
$5.5*10^{12}$ $n.cm^{-2}.s^{-1}$, 1 min and 100min

Annealing
TDS:1-20K/min,R.T-800°C ;
Isothermal:450-600 K;
Purge gas:He,15 ml/min.

Measurement
P.C(HTO+HT),LSC(HTO)

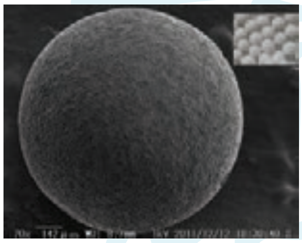

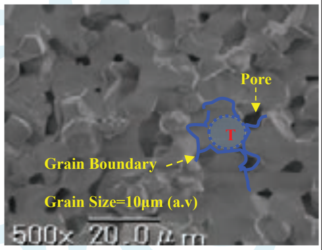

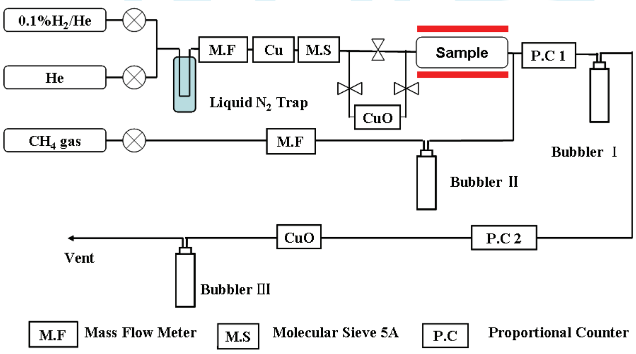

Flow chart of tritium release experiments

10

中国工程物理研究院
CHINA ACADEMY OF ENGINEERING PHYSICS

CBBI-17

Neutron-irradiated Li_4SiO_4 pebbles

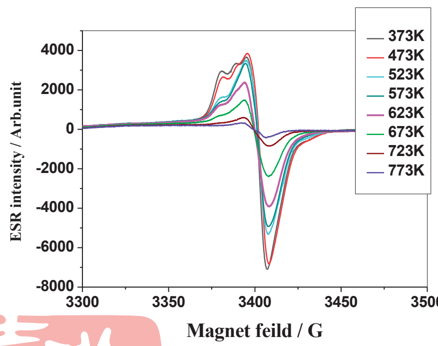

Defect of Li_4SiO_4 pebble

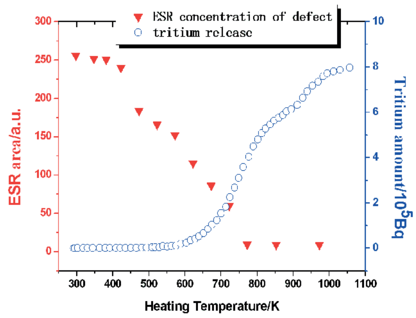

Relationship of tritium release and irradiation defect (Li_4SiO_4 pebble)

- A large number of defects annihilated at temp. around 400-600K.
- The diffusion of trium in Li_4SiO_4 pebbles was affected by the neutron fluence at temp. around 450-600 K possibly due to the irradiation defects.

11

中国工程物理研究院
CHINA ACADEMY OF ENGINEERING PHYSICS

CBBI-17

Neutron-irradiated Li_4SiO_4 pebbles

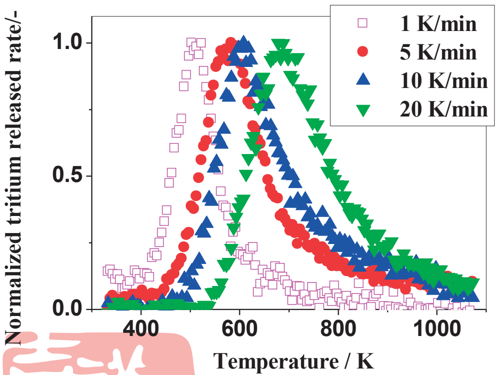

Tritium TDS spectra of Li_4SiO_4 pebble irradiated at $5.5*10^{12}$ $s^{-1}cm^{-2}$ for 1min.

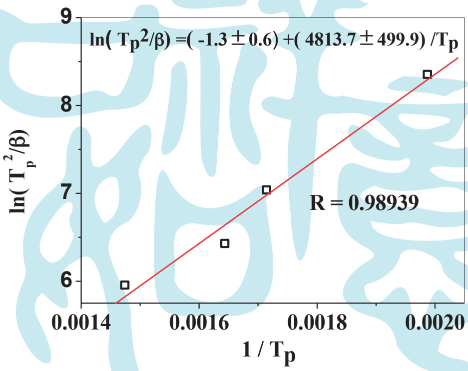

$$\ln\frac{T_P^2}{\beta}=\frac{E_d}{RT_P}+\ln\frac{E_d}{R\nu_n n}-(n-1)\ln(\sigma)$$

Tritium released at low temp. from Li_4SiO_4 pebbles.

Desorption Activation Energy
E_d= (40.0±4.2) kJ/mol

12

中国工程物理研究院
CHINA ACADEMY OF ENGINEERING PHYSICS

CBBI-17

Neutron-irradiated Li_4SiO_4 pebbles

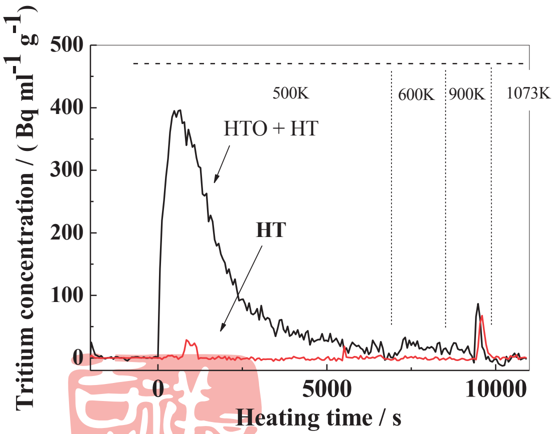

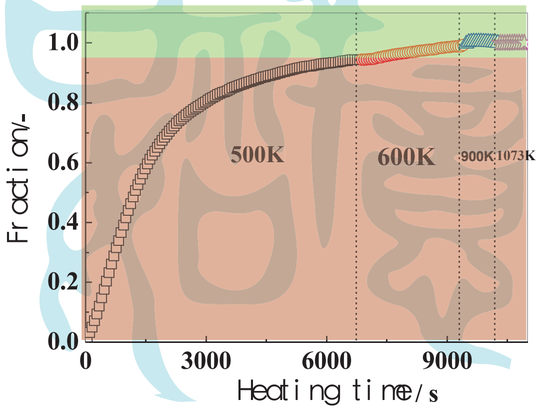

Isothermal tritium release from Li_4SiO_4 pebble irradiated at $5.5*10^{12}$ $s^{-1}cm^{-2}$ for 1min

The tritium release was mainly controlled by one process

中国工程物理研究院
CHINA ACADEMY OF ENGINEERING PHYSICS

CBBI-17

Neutron-irradiated Li_4SiO_4 pebbles

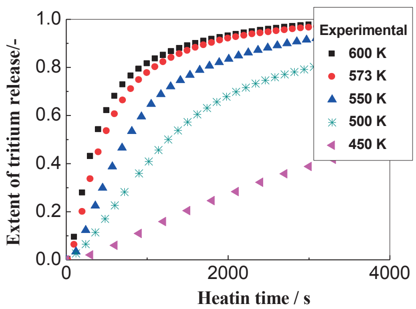

Isothermal exp. of 1 min-irra. Li_4SiO_4 (1min, 3.3×10^{14} n cm^{-2})

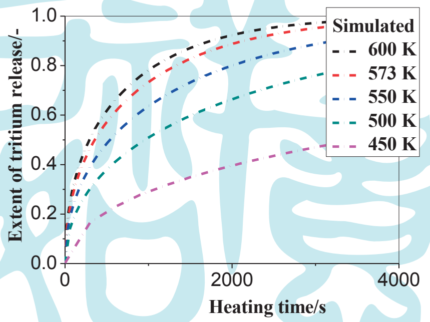

Simulated curves by diffusion equation

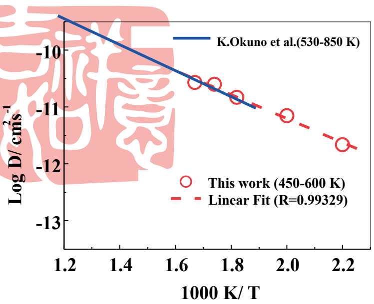

Arrhenius plots of diffusion coefficients for tritium

$$\alpha = 1 - \frac{6}{\pi}\sum_{n=1}^{\infty}\frac{1}{n^2}\exp\left(\frac{-Dn^2\pi^2 t}{a^2}\right)$$

$$D = D_0 \exp(E_a/RT)$$

Log D_0 = -7.0 ±0.3 cm^2s^{-1}
E_a = (40.3±2.7) kJ/mol

中国工程物理研究院
CHINA ACADEMY OF ENGINEERING PHYSICS

CBBI-17

Neutron-irradiated Li_4SiO_4 pebbles

Influence of neutron fluence

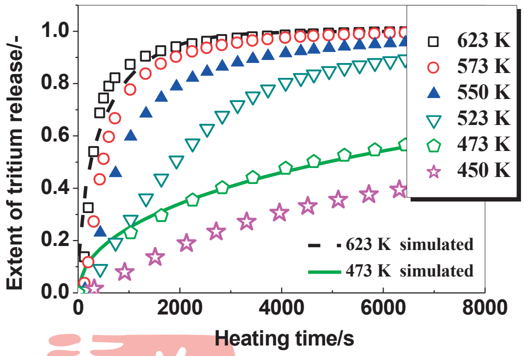

Isothermal exp. of 100 min-irra. Li_4SiO_4 (3.3×10^{16} n cm^{-2})

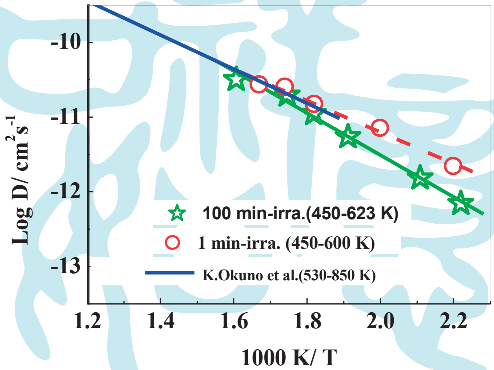

Neutron fluence	Log D_0	E/kJ mol^{-1}	Author
3.3×10^{14}	-7.0 ±0.3	40.3±2.7	This work
3.3×10^{16}	-5.9 ±0.3	53.7±3.4	This work
2.5×10^{16}	-6.7±0.1	43.8±0.9	K.Okuno[1]

[1] K.Okuno, H. Kudo. Fusion Engineering and Design 8(1989)355-358

- The HTO release of 100 min-irra. sample obeys the diffusion-controlled kinetics.
- The diffusion coefficient of 100 min-irra. sample was slightly smaller than that of 1 min-irra. sample at temp. around 450-600 K.
- Activation energy was increased with increasing irra. time(irradiation defects).

15

中国工程物理研究院
CHINA ACADEMY OF ENGINEERING PHYSICS

CBBI-17

Neutron-irradiated Li_4SiO_4 pebbles

Effect of sweep gas composition

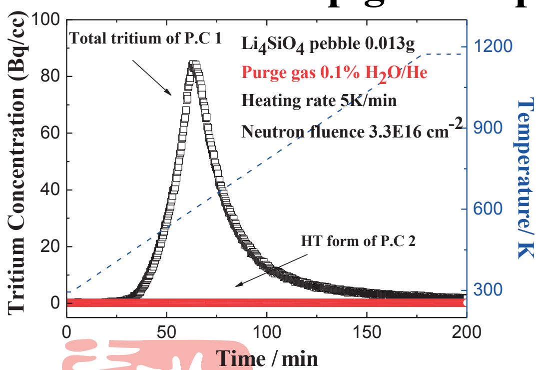

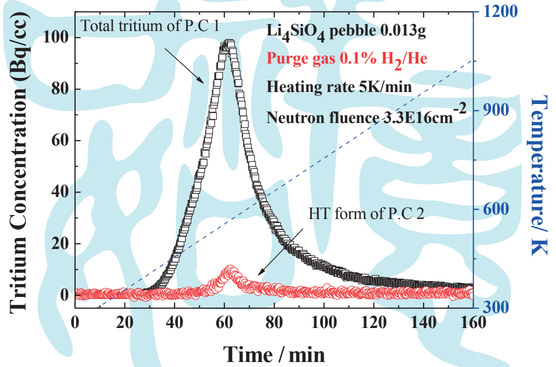

Purge gas	Peak	HTO fraction
0.1%H_2O+He	600 K	100%
He	-	>95%
0.1%H_2+He	594 K	93.7%

- Regardless of sweep gas composition, HTO is the main chemical form of the released tritium.
- The addition of hydrogen to He sweep gas slightly affects the tritium release behavior.

Low temp.: -OT (ads.) + H_2O(g)= -OH (ads.) + HTO (g)
High temp.: -OT (ads.) + H_2 (g)= -OH (ads.) + HT (g)

The isotope exchange reaction of the tritium on the grain surface and H_2 in the sweep gas is slower at the temperatures lower than 600K.[3]

Isotope exchange reaction activation energy: 110~120 kJ/mol

16

☐Neutron-irradiated $LiAlO_2$

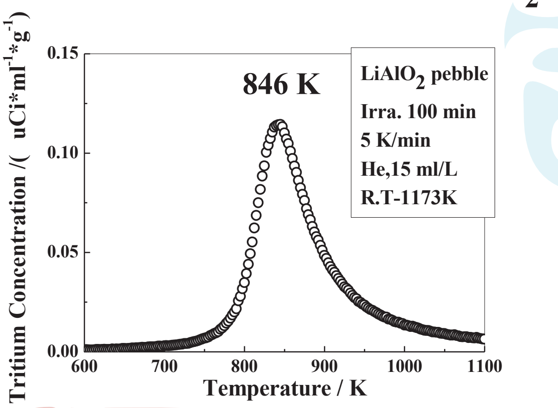

$LiAlO_2$ pebbles (0.9mm, Grain size = 15.6 um(a.v))

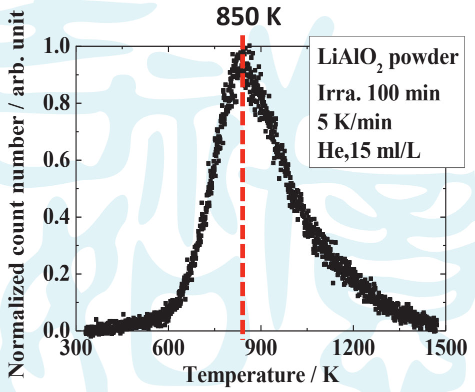

$LiAlO_2$ powder (grain size < 5 um)

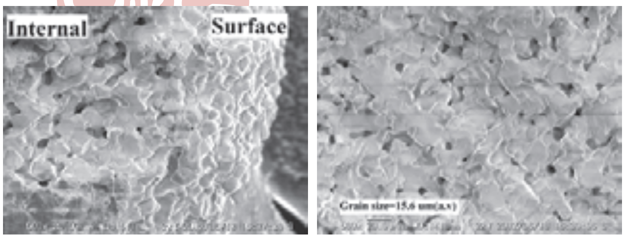

- Tritium release region: 800~1000K·
- HTO of total tritium: ~99%
- The tritium release behavior of $LiAlO_2$ pebbles is similar to that of powder.

Pebble size play a limited role in tritium release behavior

中国工程物理研究院
CHINA ACADEMY OF ENGINEERING PHYSICS
CBBI-17

☐Neutron-irradiated $LiAlO_2$ pebbles

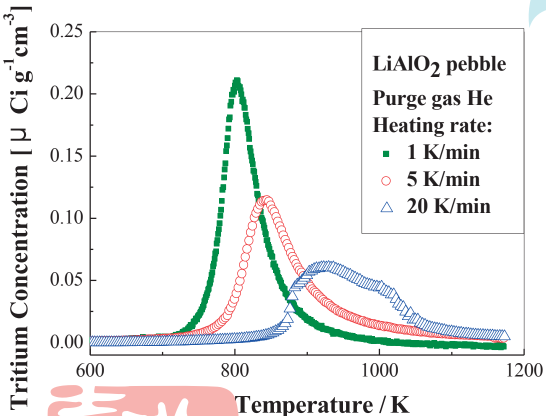

Heating rate	Peak top / K	Fraction of HTO
1	804	>99 %
5	846	>99 %
20	930	>99 %

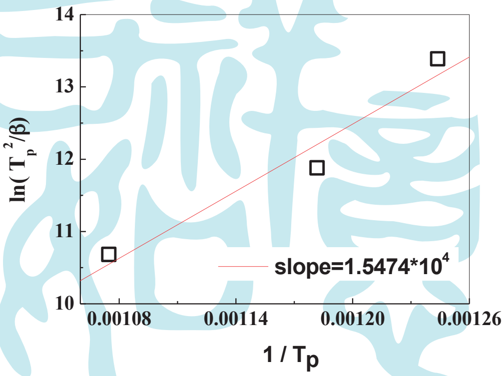

$$\ln\frac{T_P^2}{\beta}=\frac{E}{RT_P}+\ln\frac{E}{R\nu_n n}-(n-1)\ln(\sigma)$$

E_d = (128.7±28.6) kJ/mol

中国工程物理研究院
CHINA ACADEMY OF ENGINEERING PHYSICS

CBBI-17

□Neutron-irradiated $LiAlO_2$ pebbles

➢Isothermal tritium release

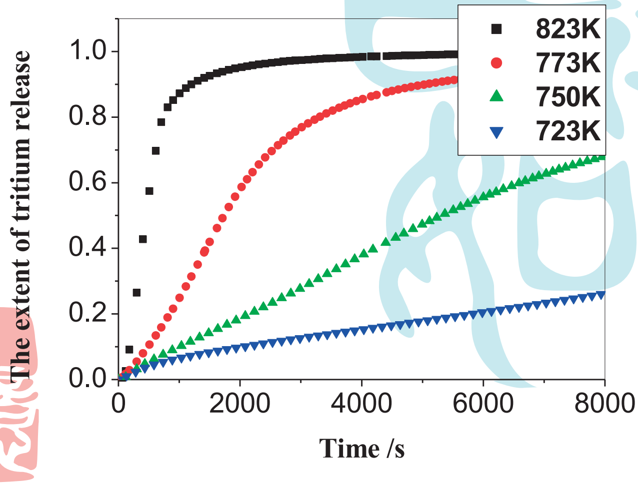

- The trtium release curves can't be fitted well by the equation of diffusion-controled kinetics.

中国工程物理研究院
CHINA ACADEMY OF ENGINEERING PHYSICS

CBBI-17

□Neutron-irradiated $LiAlO_2$ pebbles

➢Effect of sweep gas composition

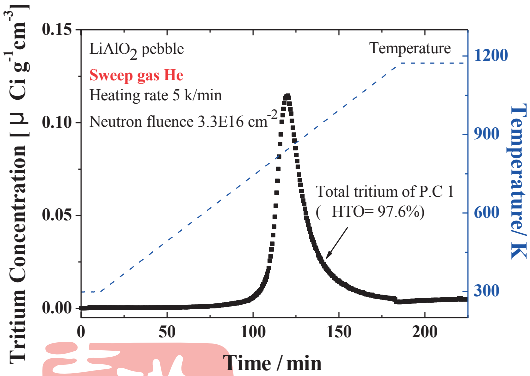

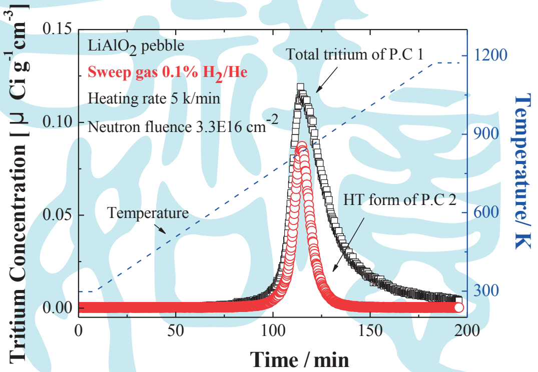

Purge gas	Peak	HTO fraction
0.1%H_2O+He (15ml/min)	855 K	92.9%
He (15ml/min)	846	**97.6%**
0.1%H_2+He (15ml/min)	~830 K	**66.8%**
1%H_2+He (100ml/min)	~840 K	**30.2%**

➢The addition of hydrogen to He sweep gas significantly affected the tritium release behavior:increasing the HT fraction .

•Desorption activation energy ($LiAlO_2$)): ~120 kJ/mol (this work)

•Isotope exchange reaction activation energy[ref]: 110~120 kJ/mol

中国工程物理研究院
CHINA ACADEMY OF ENGINEERING PHYSICS

CBBI-17

Outlook & Summary

- Optimize the fabrication process to meet CFETR demand

  Lab scale industry scale … …

- Development of advanced ceramic breeder

  Higher performance (lithium density, melting temperature…)

- In-pile test to be performed with high neutron flux

  in situ tritium release higher irradiation fluence

  pebble bed… …

21

中国工程物理研究院
CHINA ACADEMY OF ENGINEERING PHYSICS

CBBI-17

实验内容

轮次	辐照时间 /h	辐照位置	增殖剂温度 /℃	载带气体 成份	载带气体 流量/mL·min^{-1}	实验目的
1	13	D1	29→633(分 8 个台阶)	He+0.1%H_2	100	温度影响
2	28	A2	557→665	He+0.1%H_2	100	温度影响
3	28	A2	608→540→610→664→544	He+0.1%H_2	100	温度影响
4	28	A2	609	纯 He→He+0.1%H_2	100	加微氢影响
5	45	D1	511	He+0.1%H_2	100→50→100	载气流量影响

Irradiation system

Control system

22

Design of Control system

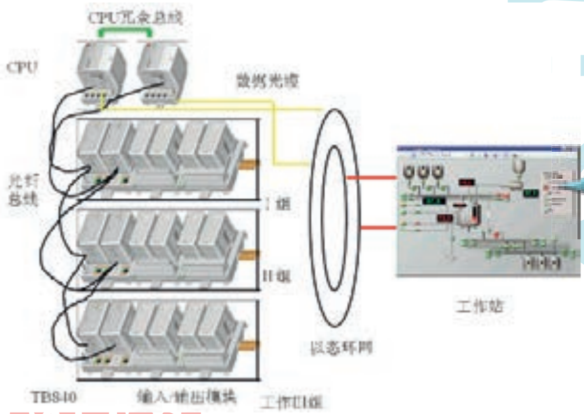

In order to remotely measure and control the in-pile tritium release process

Measuring and controlling System

中国工程物理研究院
CHINA ACADEMY OF ENGINEERING PHYSICS
CBBI-17

Optimize design of the capsule

Thickness of pebble bed : 12mm

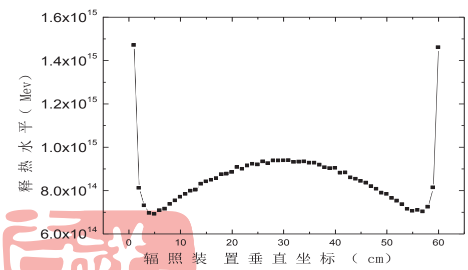

Heat production distribution

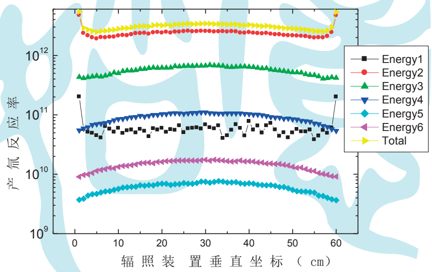

Reaction rate distribution

中国工程物理研究院
CHINA ACADEMY OF ENGINEERING PHYSICS

CBBI-17

Calculation of thermo-hydraulic neutron

In order to understand the fundamental physical and thermodynamic properties of the capsule .
Used software: MCNP and Fluent

Item	Results
Li_4SiO_4	792g
Netron flux	$4.2\times10^{13}n\cdot cm^{-2}s^{-1}$
Reaction cross section	109b
Shield factor	0.435
Tritium production(/d)	0.76Ci
Total heat productivity	8.2kW

25

中国工程物理研究院
CHINA ACADEMY OF ENGINEERING PHYSICS

CBBI-17

Outlook & Summary

- **Data base for the present candidate materials**

  Present candidate advanced breeder… …

- **Cooperation in the worldwide to be strengthen**

  Conference, workshop, cooperation experiment, sample exchange… …

26

Development of Lithium meta-titanate Ceramic powder with solid state reaction for Indian LLCB TBM

Aroh Shrivastava, Mayank Makwana, P. Chaudhuri, E. Rajendrakumar

Institute for Plasma Research, Gandhinagar, Gujarat, India-382428
Email: aroh@ipr.res.in

Abstract

The Indian Lead-Lithium Ceramic Breeder (LLCB) Test Blanket Module (TBM) is the Indian DEMO relevant blanket module which will be tested in ITER machine through the TBM program. Lithium meta titanate (Li_2TiO_3) will be used in Indian Lead Lithium Ceramic Breeder (LLCB) concept to be tested in ITER. Li_2TiO_3 is being considered as one of the promising tritium breeding materials for future DEMO reactors because of its reasonable lithium atom density, prominent tritium release rate at low temperatures, its low activation characteristics, low thermal expansion coefficient & high thermal conductivity etc.

Among the various methods of preparation of Li_2TiO_3 powders, Indian TBM team is involved in developing this tritium breeder material by solid state reaction and solution combustion method. Lithium carbonate (Li_2CO_3) and titanium di-oxide (TiO_2) are used as a raw material for solid state methods. The reactant powder is mixed & grinded in planetary ball mill. The reaction parameters were optimized with thermo gravimetric analyzer. The final powder has been characterized for its phase purity, grain size and its true density with XRD, SEM & with Helium-Pycnometer. Finally Li_2TiO_3 pebbles were prepared by the extrusion followed by the spheronization with diameter range from 0.8 mm to 1.5 mm. Prepared pebbles were tested for mechanical strength using crush strength measurement, pebble size distribution and pore size distribution and their analysis by Mercury porosimeter and Archimedes principle. The details of the powder synthesization, pebble formation and their various characterizations will be discussed in this paper.

Key words – Li_2TiO_3, solid state reaction, thermo gravimetric, extrusion & spheronization

Development of Lithium meta-titanate Ceramic powder with solid state reaction for Indian LLCB TBM

Aroh Shrivastava
Institute For Plasma Research, India
E- mail: aroh@ipr.res.in

Outline

- ❑ Introduction
- ❑ IN-LLCB TBM materials
- ❑ Li_2TiO_3 Preparations at IPR
- ❑ Solid State reaction
- ❑ Extrusion & Spheronization (Pebble preparation)
- ❑ Characterizations of Li_2TiO_3
- ❑ Conclusion
- ❑ Critical issues

Introduction

India has proposed Lead Lithium ceramic breeder concept (LLCB) in which helium would be used at high pressure of 8 MPa for cooling of first wall channels. Lead lithium will be used as a neutron multiplier, tritium generation as well as coolant of the ceramic breeder channels

Among the various lithium ceramic materials like Li_2O, $LiAlO_2$, Li_4SiO_4, Li_2TiO_3 & Li_2ZrO_3. Lithium titanate (Li_2TiO_3) is considered as a possible tritium breeding material for Indian Lead lithium ceramic breeder concept due to its eminent properties like reprocessing & tritium release at low temperature.

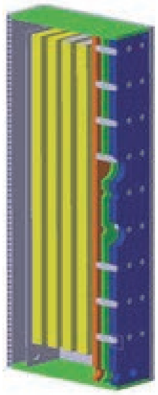

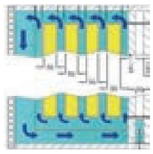

IN-LLCB TBM Materials

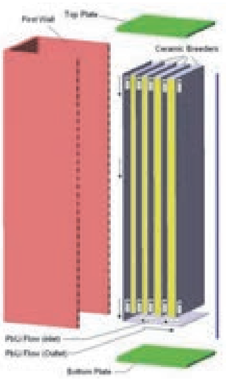

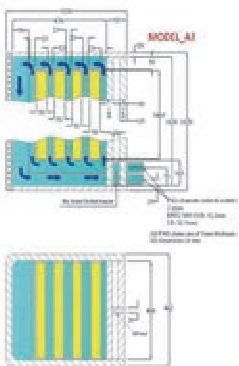

Breeding material	$Li_2TiO_{3,}$ PbLi
Structure	Reduced Activation Ferritic Martinsitic Steel (RAFMS)
Coolant	Helium
Purge	Helium + $\%H_2$

Li_2TiO_3 Preparation at IPR

- Solid state reaction
- Solution combustion method*

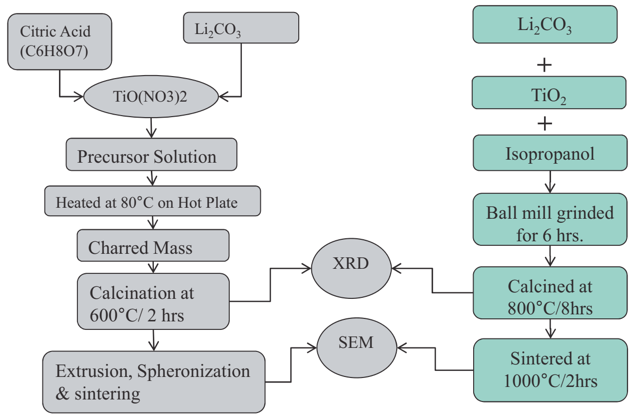

*A. Shrivastava et. al. "Preparation & Characterization of the Lithium meta-titanate Ceramics by Solution Combustion Method for Indian LLCB TBM" Accepted in FST

Solid State reaction

$$\boxed{Li_2CO_3(s) + TiO_2(s) = Li_2TiO_3(s) + CO_2(g)}$$

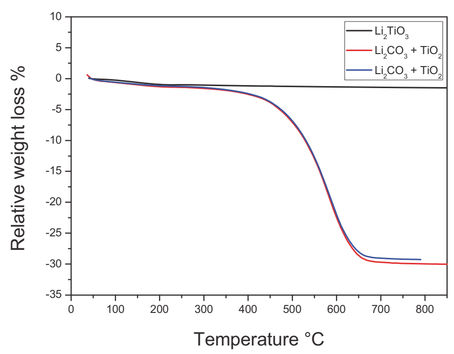

TG Analysis of Raw Powder & calcined powder

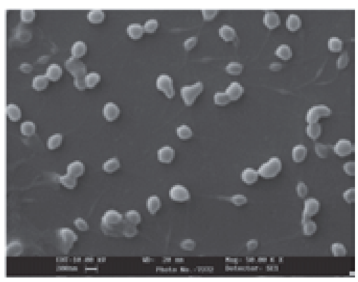

SEM Analysis of grinded raw powder

Extrusion & spherodization (Pebble fabrication)

Extrude of Li_2TiO_3 powder 1 .00 mm diameter

Spheronization of Li_2TiO_3 extrudes 1 .00 mm diameter

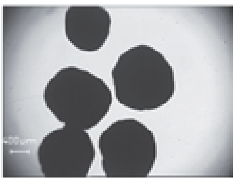

Microscopic image of Pebbles

Obtained pebbles after sintering

Physical Properties for Li_2TiO_3

Crystal Structure

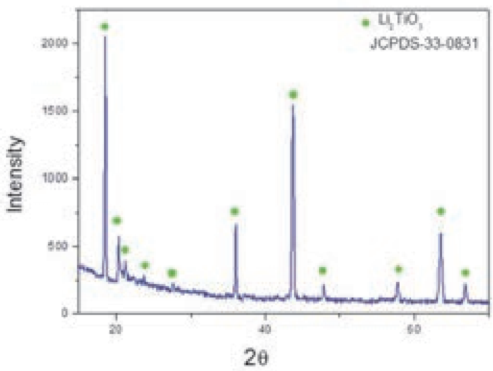

XRD pattern of Solid State reaction powder

- The Crystal structure is observed monoclinic, The average crystallite size is 52 nm.

Microstructure Analysis

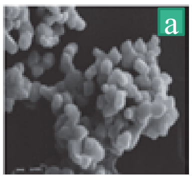

Calcined powder at 800°C

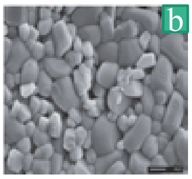

Sintered pellet at 900°C, 2 hrs

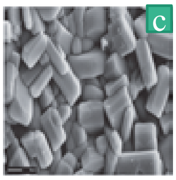

Sintered pellet at 900°C, 10 hrs

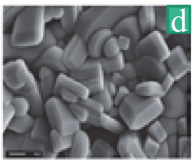

Sintered pellet at 900°C, 15 hrs

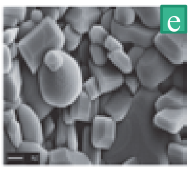

Sintered pellet at 900°C, 20 hrs

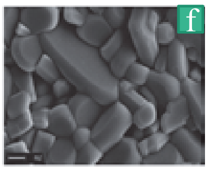

Sintered pellet at 900°C, 25 hrs

Pellets Sintered at 1000°C

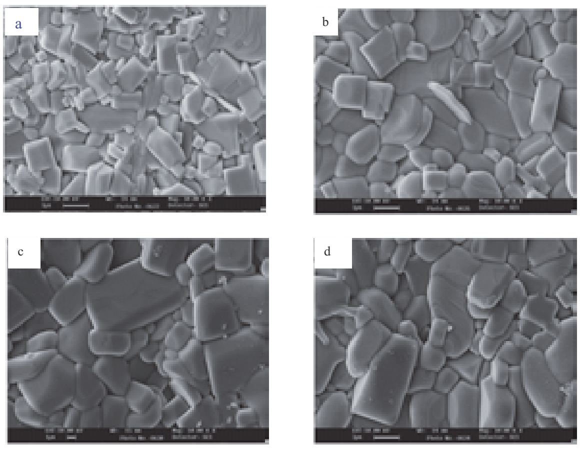

(a) Sintered Li_2TiO_3 pellet at 1000°C for 2 hours (b) Sintered Li_2TiO_3 pellet at 1000°C for 10 hours (c) Sintered Li_2TiO_3 pellet at 1000°C, 15 hours (d) Sintered Li_2TiO_3 pellet at 1000°C for 20 hrs

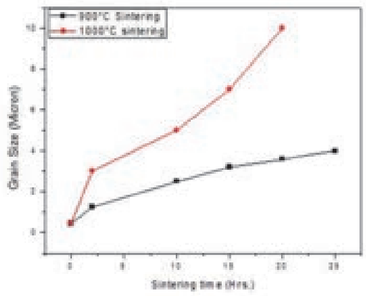

Effect of sintering temp and time on grain size

Thermal Diffusivity measurement

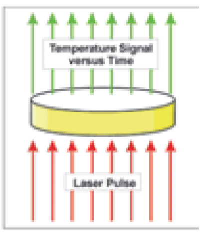

$$a = 0.1338 \cdot \frac{d^2}{t_{1/2}}$$

$$\alpha = \frac{k}{\rho c_p}$$

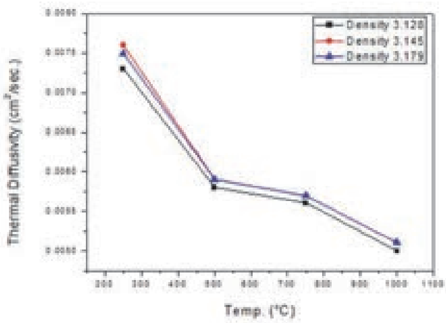

Temperature V/s. Diffusivity

Pellet Diameter – 12.7 mm, Thickness – 2 mm

Thermal Expansion & shrinkage measurement

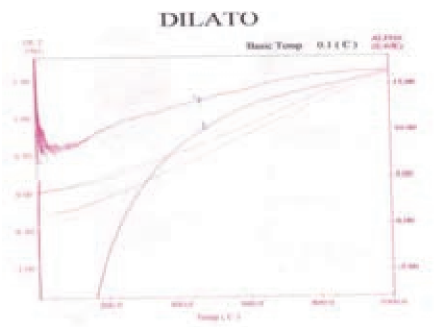

Thermal expansion of Li_2TiO_3 sintered pellet

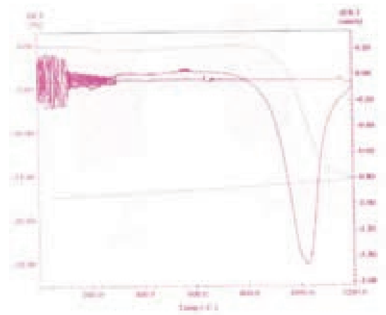

Thermal shrinkage of Li_2TiO_3 green pellet

Porosity measurement (Mercury porosimeter)

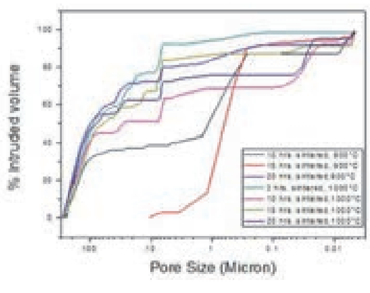

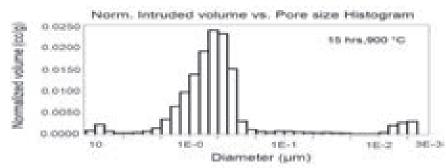

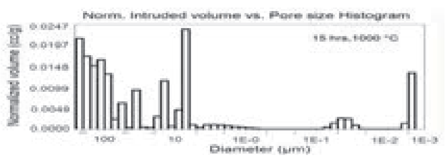

Effect of sintering on pore size

Crush Strength test

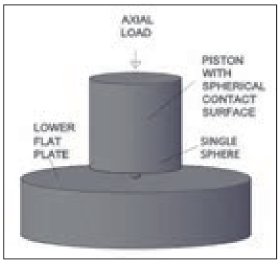

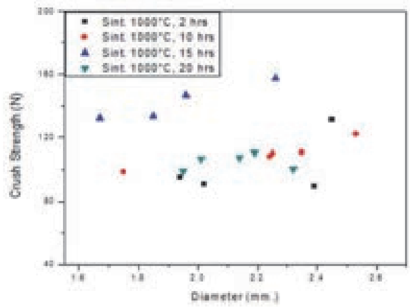

<u>Li_2TiO_3 pebbles sintered at 1000°C, 5 % PVA, 500-100</u>

Achieved parameter

S.No.	Property	
1.	Bulk Density (g/cc)	2.75
2.	Crystallite size	52 nm
3.	Crystal Structure	Monoclinic
4.	Porosity	20-22 %
5.	Thermal Diffusivity Cm^2/Sec. -500°C	0.0059
6.	Pebble Size (mm)	1 – 1.5 mm
7.	Cush Strength (N) (for diameter > 1.5 mm)	>100
8.	Co-efficient of Thermal expansion @ 500°C (E-6/°K)	13
9.	Grain size (Micron)	2-7

Conclusion

- ❑ Phase pure Li_2TiO_3 is prepared with solid state reaction. Monoclinic crystal structure was observed.
- ❑ The process parameters of powder preparation and sintering parameters of the pebbles have been optimized. large quantities can be prepared.
- ❑ Pebbles have been prepared with extrusion and spheronization however the sphericity is needs to be improved further.
- ❑ The sintering parameters were taken as 1000°C for isothermal 15 hrs for further experiments.
- ❑ Thermal diffusivity of Li_2TiO_3 is decreasing with temperature. The density dependence on thermal conductivity is needs to analyzed.
- ❑ Further characterization of pebbles (Physical, mechanical, chemical, thermal) are also planned for the future work.

Critical issues

- ❑ Purity of raw materials
- ❑ Development of fabrication route
- ❑ Characterization of pebbles (Physical, mechanical, chemical, thermal)
- ❑ Out of Pile Experiments (Thermo-Mech. Studies & Tritium inventory studies)
- ❑ Tritium and heat generation rate : Irradiation Experiments (~3 dpa)
    - Fast-reactors
    - High Flux Fission Reactors
- ❑ Li-6 enrichment in pebbles
- ❑ Final qualification of pebbles for ITER (Data base generation for licencing)
- ❑ Large scale production
- ❑ Recycling technology

Recent Developments of the Melt-based Production of Lithium-Orthosilicate Pebbles

Oliver Leys[1], Matthias Kolb[1], Aniceto Goraieb[2], Regina Knitter[1]

[1]*Karlsruhe Institute of Technology, Institute for Applied Materials (IAM-WPT), 76021 Karlsruhe, Germany*
[2]*Goraieb Versuchstechnik (GVT), 76227 Karlsruhe, Germany*

Introduction

Lithium orthosilicate is the material of choice in the European Union for the breeding of tritium inside future fusion reactors, allowing them to be self-sustainable. The ceramic compound is to be featured inside the blanket of the reactor wall in the form of pebble beds with pebbles being approximately 1 mm in size. Recent material developments have seen the addition of lithium metatitanate as a secondary phase to improve various physical properties. Experiments to determine the optimum operating pressure and cooling methods have also been conducted to maximise the yield of the process. Periodic sampling and high-speed camera analysis at the nozzle have also been conducted to understand the dynamics of pebble formation.

Experimental

a. Addition of a secondary phase to the melt

In order to add a secondary phase of lithium metatitanate phase to the end product, TiO2 was added to the melt. Different batches were produced with lithium metatitanate contents of up to 40 mol%.

b. Liquid nitrogen spray cooling

To minimise the thermal shock effect of quenching the pebbles directly in liquid nitrogen, a liquid nitrogen spray was developed, which reduces the temperature inside the cooling tower as well as dispersing micro-droplets.

c. Analysis of pressure effects on distribution

Periodic time sampling was used to generate 3-dimensional plots of time vs droplet size vs quantity. Pebbles were extracted from the process at regular intervals by intercepting the molten jet. This was repeated for multiple batched with different operating pressures.

d. High-speed camera analysis

In order to analyse the droplet formation, a high-speed camera was set up to film directly at the nozzle. Using a specially written program, various process characteristics were then determined from the acquired images.

Results

a. Addition of a secondary phase to the melt

It was shown that a secondary phase of lithium metatitanate resulted in an increase in both the crush-load and the closed porosity.

b. Liquid Nitrogen spray cooling

Batches made using the liquid nitrogen spray cooling method have displayed an increase in the crush-load as well as a slight increase in the Weibull modulus. The yield has also drastically increased.

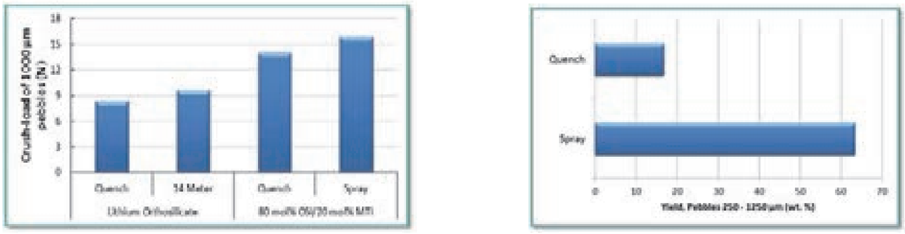

Figure 1: l) Process effects on the crush-load r) Average yield for quench and spray cooling

c. Analysis of pressure effects on distribution

In order to form a stable jet, a low pressure is preferred. This reduces the amount of under-sized pebbles being formed due to the ‘spraying’ of the jet as well as reduces the amount of over-sized pebbles from agglomerations that occur due to irregular break-up of the jet.

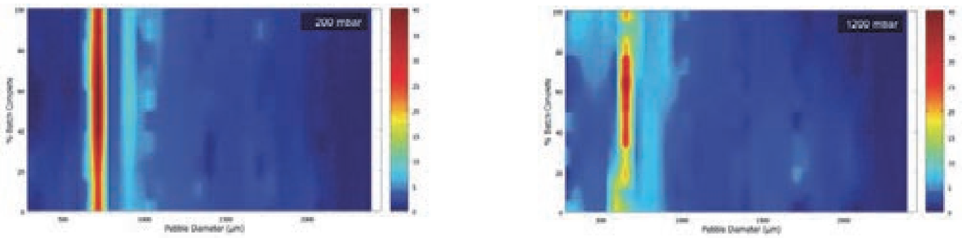

Figure 2: Effect of operating pressure on pebble size distribution. l) 200 mbar r) 1200 mbar

d. High-speed camera analysis

Some process characteristics that were determined include pebble size after jet-break-up and pebble generation frequency.

Summary

One of the main targets of research has been to increase the mechanical strength of the pebbles. This has been achieved by the addition of lithium metatitanate as a secondary phase as well as the targeted cooling of the liquid nitrogen spray. The yield has also been increased as an additional effect of the liquid nitrogen spray, presumably by minimising the agglomerations of liquid drops after break-up from the jet.

Droplet formation dynamics and the effect of the operating pressure have also been studied, which will allow further optimisation of process parameters to allow stable jets to be formed, hence also increasing the yield.

Recent Developments of the Melt-based Production of Lithium Orthosilicate Pebbles

Oliver Leys[1], Matthias Kolb[1], Aniceto Goraieb[2], Regina Knitter[1]

[1]Karlsruhe Institute of Technology, Institute for Applied Materials – Material Process Technology (IAM-WPT), 76021 Karlsruhe, Germany
[2]Goraieb Versuchstechnik (GVT), 76227 Karlsruhe, Germany

Overview

- Introduction
- Recent Developments
- Future Plans
- Summary

Introduction

- Lithium Orthosilicate (Li_4SiO_4) ceramic pebbles have been produced at KIT since 2008 after the collaboration with Schott AG discontinued
- Since then, a melt-based process has been developed which allows room for various process parameters as well as optimistation
- This presentation will give an overview of the developments undertaken on the process since the last CBBI meeting

Addition of a Secondary Strengthening Phase

- Lithium Metatitanate was introduced to the pebbles as a secondary phase.
- It was observed that an increase in the metatitanate content causes a significant increase in the crush-load of the pebbles
- The closed porosity also shows an increase with metatitanate content

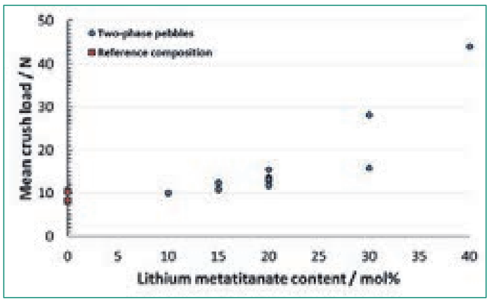

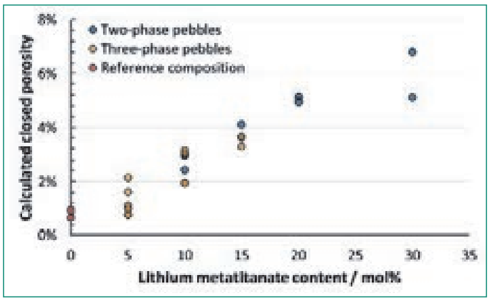

Addition of a Secondary Strengthening Phase

- Li-orthosilicate and Li-metatitanate solidify dendritically
  - Between 20 and 30 mol% metatitanate a distinct change in crystallisation behaviour can be observed.
  - At 30 mol%, the metatitanate dominates the crystallisation; a strong sign that it solidified first.

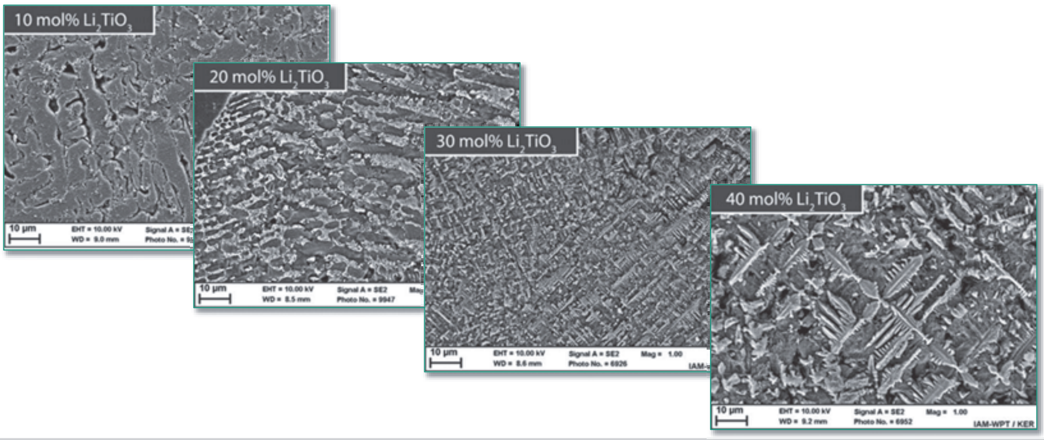

High Speed Camera Analysis

- A high-speed camera is used to analyse the dynamics of droplet formation.
- Using a quartz-window, it is possible to zoom in on the nozzle which is at approximately 1300 °C.
- A platinum mirror is used to create sufficient contrast between the pebbles and the background
- An offline program has been developed to evaluate various process characteristics

High Speed Camera Analysis

- Example of an observable process characteristic:

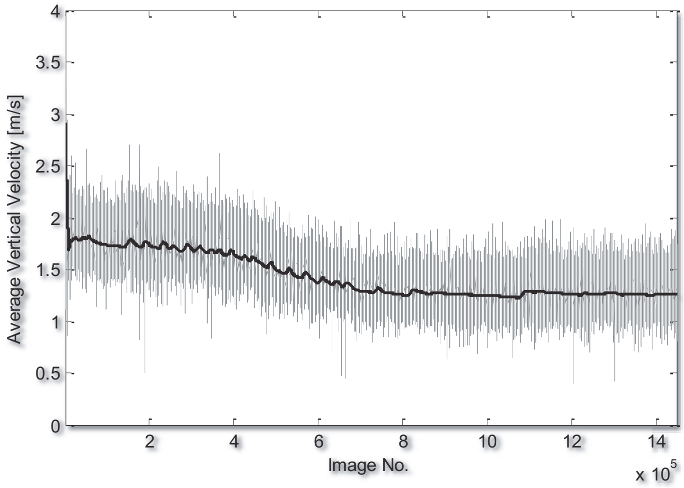

Pebble velocity after break off from the jet

Liquid Nitrogen Spray Cooling

- A liquid nitrogen spray has recently been developed to solidify the droplets after jet break-up at the nozzle
- Avoidance of the thermal shock that occurred previously when a bath of liquid nitrogen was used to solidify the droplet
- Control of the spray intensity to match various other process parameters (e.g. nozzle size)

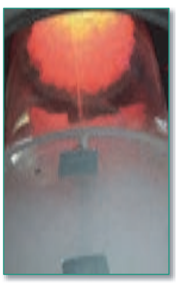

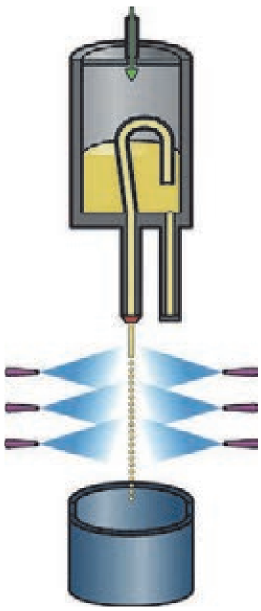

Liquid Nitrogen Spray Cooling

- Preliminary results, from the liquid nitrogen spray, indicate an increase in the pebble crush-load and a slight increase in the Weibull modulus
- The spray has also increased the overall yield of process, presumably by solidifying many pebbles before they have the chance to agglomerate during free-fall
- Further optimisation of the spray is expected to lead to even better results

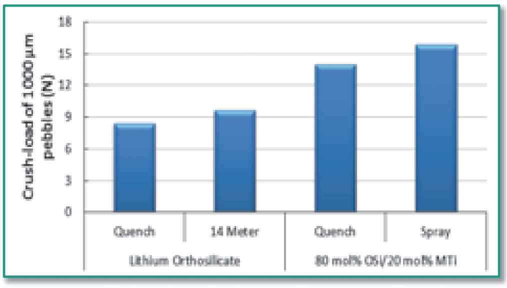

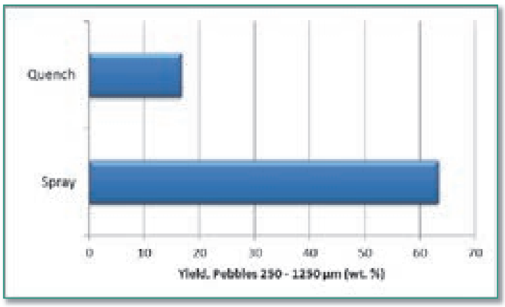

O. Leys, M.H.H. Kolb, A. Goraieb, R. Knitter

Pebble Size Distribution

- Manual sampling was used to monitor the change in pebble size distribution over time for different pressures

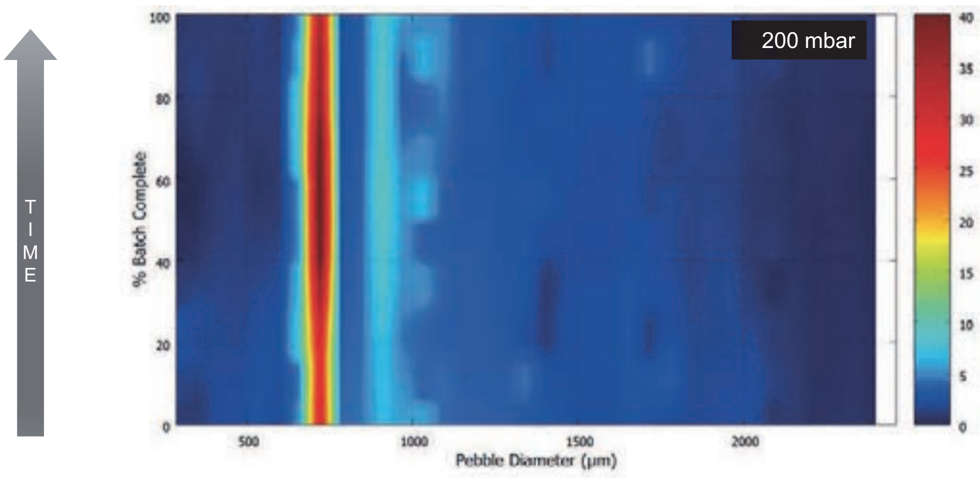

O. Leys, M.H.H. Kolb, A. Goraieb, R. Knitter
CBBI-17 Workshop , 12th September 2013, Barcelona
Institute for Applied Materials (IAM-WPT)

Nozzle Design

- The design of the nozzle is crucial for the formation of a stable liquid jet.
- An increase in the angle between the jet and the nozzle allows lower operating pressures to be achieved due to a reduction in the effectiveness of wetting factors

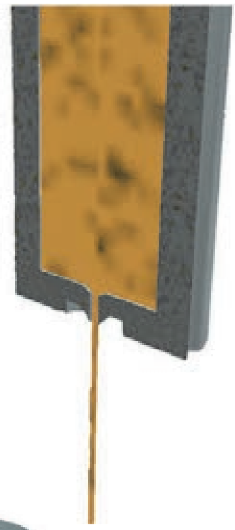

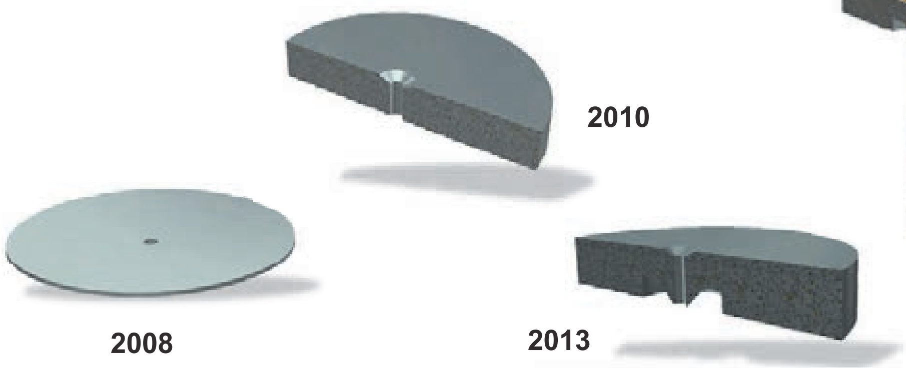

Modifications to the Reaction Crucible

- The current crucible design allows for the production of up to 1 kg with one batch
- Increased wall thickness and selected welding look to lengthen the crucible life expectancy and minimise crucible maintenance costs
- A large inner-tube allows for the start of production to be controlled by the operator
- The crucible has also been designed so that in the future, multiple jets can be ejected from the nozzle without interacting with each other

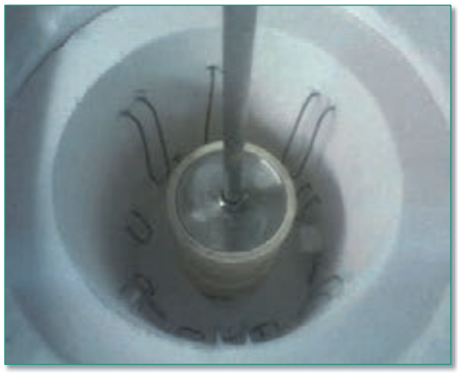

Process Upgrade 2013

- The process is currently undergoing a significant upgrade, which is due to be completed by autumn
- One considerable change is the installation of 3 separate cooling zones, which will allow different cooling procedures depending on the process
- Focus will also be on increasing the stability of the process, for example by minimizing external influences
- The new process set-up will also feature a control center for monitoring, controlling and recording process data
- High-end pressure and flow controllers will be used to control the jet dynamics

Future Work

- Installation of new process components
- Set-up of centralised control system
- Optimise pebble properties
- Increase the yield
- Increase the production capacity

Summary

- **Major developments of the process include:**

- Addition of a lithium metatitanate phase to the pebbles
  - Increase in crush-loads and porosity
- High-speed-camera to analyse droplet formation dynamics at the nozzle
- Controlled cooling with the use of a liquid nitrogen spray
  - Increase in crush-load and yield
- New nozzle design; enhancing the stability of the jet
- Process upgrade to take place this year

Vaporization property of lithium metatitanate and orthosilicate pebbles by high temperature mass spectrometry

K. Mukai[1], M. Yasumoto[1], T. Terai[1], T. Hoshino[2], R. Knitter[3], A. Suzuki[1]

1 The University of Tokyo Tokyo, Japan
2 Japan Atomic Energy Agency, Aomori, Japan
3 Karlsruhe Institute of Technology, Karlsruhe, Germany
Corresponding author: kmukai@nuclear.jp

1. Introduction

Vaporization behavior of a breeder material at high temperature is one of a key chracteristic for predicting tritium chemical form as well as lithium loss in a fusion blanket during operation. High temperature mass spectrometry (HTMS) has been developed to obtain thermodynamic quantities such as equilibrium constant and enthalpy of vapor reaction. Up to now, the measurement on lithium metatianate (MTi) and orthosilicate (OSi) have already reported in the temperature range of 1373-1673 K [1] and 1188-1422 K [2] respectively. However, the effects of the phase transformation on the equilibrium constants of the vapor reactions at 1473 K [3] and 1297 K [4], where lithium metatitanate and orthosilicate changes from β-phase into γ-phase and from metasilicate (s) into metasilicate (l) respectively, have been ignored. For the accurate understandings of the vaporization properties from the breeder materials, the measurements in proper temperature ranges are required. The objective of this work is to investigate the vaporization behavior of OSi and MTi pebbles in a proper temperature range under D_2 atmosphere by atmosphere controllable high temperature mass spectrometry.

2. Methods

2.1 High temperature mass spectrometer

In this study, the vasporization properties of lithium metatitanate and orthosilicate were studied by the atomosphere controllable high temperature mass spectrometry. The measured ion intensity I_i of the vapor species i was converted into the corresponding partial pressure P_i at temperature T by the equation

$$\mathrm{P}_i = \frac{K_m I_i T_{KC}}{\sigma_i \gamma_i} \qquad (1)$$

where K_m is the pressure calibration constant, σ_i is the relative ionization cross-section, γ_i is the gain of the electron multiplier.

2.2 Equations for analysis

Third low Enthalpy ΔH^o_{298} of a vapor reaction was calculated by

$$\Delta H^\circ_{298} = -T(R \ln K + \Delta fef) \qquad (2)$$

where T is temperature, R is gas constant, K is equilibrium constant, Δfef is free energy function. Total pressure of lithium containing species P_{Li}^{total} of the breeder material in various conditions, defined as $P_{Li}^{total} = P_{Li} + P_{LiOD}$, was calculated from equilibrium constants of vapor reactions.

2.3 Breeder pebbles

OSi pebble (2.5 % SiO_2 excess) and stoichiometric MTi pebble (Li/Ti = 2.00±0.02 analyzed by ICP-AES), which were fabricated by spray method at KIT and sol-gel process at JAEA respectively, were used for high temperature mass spectrometry. Before the measurements, these pebbles were heated at 600°C for 12 hours in Knudsen cell in order to avoid impurity effect such as absorbed water and Li_2CO_3.

3. Results and Discussion

The fittings by Rietveld analysis on the powder XRD patterns from the MTi specimen was done in β- Li_2TiO_3 [5] (R_{wp} = 14.5, R_e =7.35). Then, the diffraction pattern in 2θ = 10-100^o except 2θ = 20–30^o was used for the refinement because of the broad peak in that region. The fitting on the pattern from the OSi specimen, which was more satisfactory (R_{wp} = 7.78, R_e =3.35) than that of MTi, indicated multi-phase of Li_4SiO_4 [6] with 7.14 wt % of Li_2SiO_3 [7].

By the measurement of high temperature mass spectrometry, the detected gas phases in the Knudsen cell with MTi and OSi pebbles were Li(g), LiOD(g), D_2 (g) and D_2O (g). Then, the following vapor reactions were considered.

$$Li_2TiO_3(s) \rightleftarrows 2Li\ (g) + 0.5O_2\ (g) + TiO_2\ (s) \quad (3)$$
$$Li_2TiO_3(s) + D_2O\ (g) \rightleftarrows 2LiOD\ (g) + TiO_2\ (s) \quad (4)$$
$$Li_4SiO_4(s) \rightleftarrows 2Li\ (g) + 0.5O_2\ (g) + Li_2SiO_3\ (s) \quad (5)$$
$$Li_4SiO_4(s) + D_2O\ (g) \rightleftarrows 2LiOD\ (g) + Li_2SiO_3\ (s) \quad (6)$$
$$D_2 + 0.5O_2\ (g) \rightleftarrows D_2O(g)_2 \quad (7)$$

The equilibrium constants K_3, K_4, K_5 and K_6 were calculated from the equilibrium pressure P_i of these gas phases. Here, K_7 was calculated by using MALT-2 software because the pressure of O_2 (g) from the pebbles were less than the detectable level. K_7 was calculated as $K_7 = 1.23 \times 10^{-3}\exp(3.03 \times 10^4/T)$. Since the change of the temperature dependence on equilibrium pressures at the phase transformation temperature of MTi at 1473 K (β-γ transformation) was clearly observed, the measured pressure of the low temperature phase (β- Li_2TiO_3) was employed for the following calculation and estimation.

The equilibrium constants obtained by high temperature mass spectrometry were $K_3 = 9.93 \times 10^{16}\exp(-1.20 \mathrm{X}\ 10^5/T)$, $K_4 = 1.65 \times 10^1\exp(-6.15 \times 10^4/T)$, $K_5 = 1.57 \times 10^5 \exp(-8.66 \times 10^4/T)$ and $K_6 = 9.78 \times 10^5 \exp(-2.60 \times 10^4/T)$. From equation (2) and these equilibrium constants provided 3rd low enthalpies of equation (3)-(6). The vapor reaction where solid state of Li_2TiO_3 or Li_4SiO_4 decomposes into Li (g) and O_2 (g) showed $\Delta H^o_{298}(3)$ = 992.82 ± 49.6 kJ/mol and $\Delta H^o_{298}(5)$ = 1003.5 ± 50.2 kJ/mol. Compared with the previous study [8] and the calculated value, the difference was within the measurement error. The 3rd low enthalpy of the vapor reaction where the solid state decomposes into LiOD (g) were calculated as $\Delta H^o_{298}(4)$ = 426.38 ± 21.3 kJ/mol, and $\Delta H^o_{298}(6)$ =437.8 ± 21.9 kJ/mol. The obtained $\Delta H^o_{298}(6)$ value in this work was slightly smaller than the reported value ($\Delta H^o_{298}(6)$ = 471.2 ± 4.3) by R. D. Penzhorn et al.[9].

Finally, by calculating the total pressure of lithium containing species $P_{Li}^{total} = P_{Li} + P_{LiOD}$ under D_2 sweep gas condition (P_{D2} = 0.1%) from the equibrium constants of equation (3)-(7), P_{Li}^{total} in various temperature and moisture pressure were estimated in the region of P_{D2O} = 0.01-100 Pa. The estimation sugested that P_{Li}^{total} from MTi and OSi pebble can be minimized by controlling P_{D2O} as 0.25 Pa and 0.10 Pa. Taking the suggested P_{Li}^{total} value (P_{Li}^{total} < 0.01 Pa) [10] into account, D_2O in a blanket with MTi and OSi pebble should be controlled less than 36 Pa and 4.0 Pa respectively.

4. Summary

The vaporization properties of Li_4SiO_4 (multi-phase with 7.14 wt% of Li_2SiO_3) and the single phase of β-Li_2TiO_3 were studied by atmosphere controllable high temperature mass spectrometry (HTMS). Although the obtained 3rd low enthalpy of the vapor reactions were comparable to the previous report and the calculated value by MALT2, the slight difference was confirmed in the reaction where Li_4SiO_4 (s) decomposes into LiOD (g) and Li_2SiO_3 (s). The estimation of P_{Li}^{total} suggested that moisture pressure in a blanket with metatitanate and orthosilicate pebbles should be controlled less than 36 Pa and 4.0 Pa. In a future study, the vaporization properties of advanced breeder materials (Li excessive metatitanate and $Li_4SiO_4$with Li_2TiO_3, are going to be studied by high temperature mass spectrometry.

5. References

[1] M. Yamawaki, A. Suzuki, et al., Journal of Nuclear Materials 247 (1997) 11-16

[2] R.-D. Penzhorn, H.R. Ihle, S et al., J. Nuclear Materials 191 - I94 (1992) 173- I77

[3] H. Kleykamp, Fusion Engineering and Design 61/62 (2002) 361/366
[4] H. Migge, J. Nuclear Materials 151 (1988) 101-107
[5] JICST powder diffraction pattern, 8604
[6] Crystallography Open Database (COD), 2101200
[7] JICST powder diffraction pattern, 1935
[8] M. Yamawaki, A. Suzuki, et al., Journal of Nuclear Materials 247 (1997) 11-16
[9] R. D. Penzhorn, H.R. Ihle, S. Huber, P. Schuster and H,J. Ache J. Nuclear Materials 191 - I94 (1992) 173- I77
[10] H.R. Ihle, R.-D. Penzhom, P. Schuster, SOFT Conf, Rome, Italy, Sept. 1992.

Vaporization property of lithium metatitanate and orthosilicate pebbles by high temperature mass spectrometry

CBBI 12–14 September 2013, Barcelona Spain

Keisuke Mukai[1], Masaru Yasumoto[1], Takayuki Terai[1],
Tsuyoshi Hoshino[2], Mathias Kolb[3], Regina Knitter[3], Akihiro Suzuki[1]

1 THE UNIVERSITY OF TOKYO 2 JAEA 3 KIT Karlsruhe Institute of Technology

kmukai@nuclear.jp

THE UNIVERSITY OF TOKYO

Outline

1 Introduction
- Background
- Purpose

2 Method
- Experimental
- Equations for analysis

3 Results & Discussion
- X-ray analysis
- High temperature mass spectroscopy

4 Conclusion

2

Outline

1 Introduction
- Background
- Purpose

2 Method
- Experimental
- Equations for analysis

3 Results & Discussion
- X-ray analysis
- High temperature mass spectroscopy

4 Conclusion

THE UNIVERSITY OF TOKYO

Introduction

Vaporization behavior under sweep gas condition is important from the view point of Li-loss and T behavior in a blanket

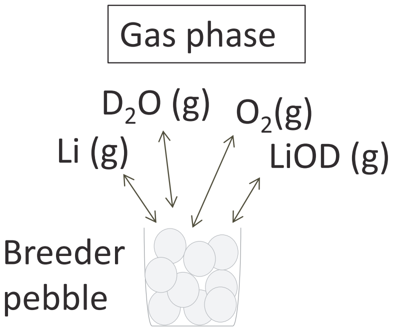

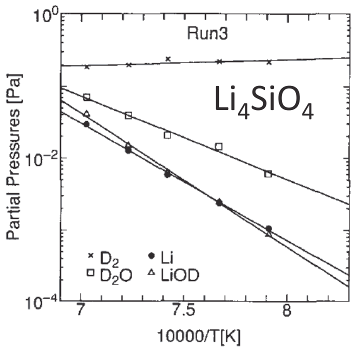

High temperature mass spectrometry (HTMS) measures fundamental thermodynamic quantities of vapor reactions from ceramic breeder
- Equilibrium constant K
- Enthalpy change ΔH^{o}_{298}

Past study by HTMS

Breeder material	Past study Measurement Temperature	in the temperatu range[3, 4]	Phase in blanket temperature range
Li_2TiO_3 (MTi)[1]	1373-1673 K	γ-MTi (s) (T > 1473 K) β-MTi (s) (T <1473 K)	β-MTi
Li_4SiO_4 (OSi) + Li_2SiO_3 (MSi)[2]	1188-1422 K	OSi(s) + MSi (Liq) (T>1297 K) OSi (s) + MSi (s) (T<1297 K)	OSi (s) + MSi (s)

different

For accurate understanding on vaporization behavior of ceramic breeder material, HTMS measurement in the blanket temperature range is required

1 M. Yamawaki, A. Suzuki, et al., Journal of Nuclear Materials 247 (1997) 11-16
2 R.-D. Penzhorn, H.R. Ihle, S et al., J. Nuclear Materials 191 - I94 (1992) 173- I77
3 H. Kleykamp, Fusion Engineering and Design 61/62 (2002) 361/366
4 H. MIgge, J. Nuclear Materials 151 (1988) 101-107

THE UNIVERSITY OF TOKYO

Purpose & research flow

Purpose

To understand the vaporization behavior of OSi and MTi pebbles in a proper temperature range under D_2 atmosphere by atmosphere controllable high temperature mass spectrometry

- evaluate enthalpy change due to vapor reaction
- reveal the preferable condition which minimizes Li loss by vaporization

Research flow

1. Measurement of vapor Pressure from breeder pebbles
2. Calculation of 3rd low enthalpy ΔH^o_{298}
3. Estimation of Li loss (P_{Li}^{total}) in various conditions

Outline

THE UNIVERSITY OF TOKYO

Breeder pebbles

- OSi (orthosilicate) pebble
  Li_4SiO_4 (2.5 weight % SiO_2 excess)
  Spray process
  Fabricated by KIT

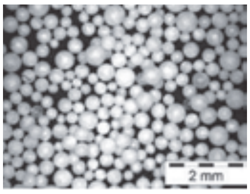

- MTi (metatitanate) pebble
  Li_2TiO_3 stoichiometric
  (Li/Ti = 2.00±0.02)
  Sol-gel process
  Fabricated by JAEA

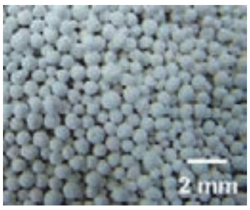

Before HTMS measurement, the phases of the pebbles were confirmed by Powder Xray diffraction and Rietveld analysis (PDXL)

THE UNIVERSITY OF TOKYO

High temperature mass spectrometer (HTMS)

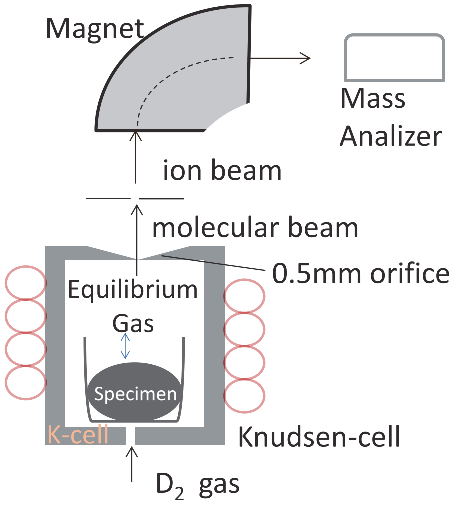

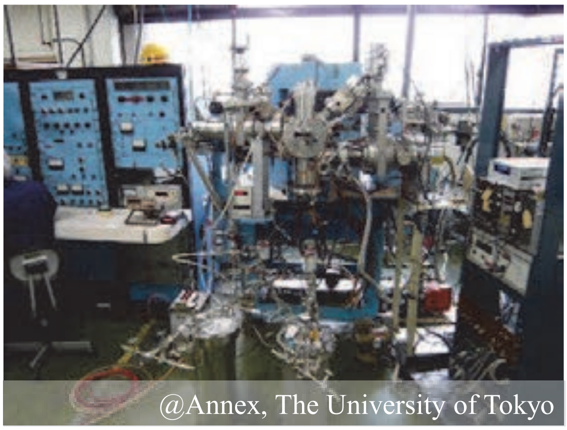

- HTMS can measure equilibrium pressure P_i of vapor gas in Knudsen -cell
- Atmosphere in the Knudsen cell is controllable
- Heated at 873 K for 12 h before measurement to avoid impurity effect

THE UNIVERSITY OF TOKYO

Equation for analysis

1. Measurement of Vaporization pressure P[Pa]

$$P_i = \frac{K_m I_i T_{KC}}{\sigma_i \gamma_i}$$

K_m : Equipment constant
I_i : Ion current=(1.609*10^{-19}*count rate)
T_{KC} : Temperature of K-cell[K]

σ_i :ionization cross section [m^{-2}]
γ_i : isotope ratio[%]

2. Calculation of Third law Enthalpy change ΔH^o_{298} due to vaporization

Ex. $$D_2(g) + \frac{1}{2}O_2(g) \rightarrow D_2O(g) + \Delta H$$

then K: Equilibrium constant is $K = \dfrac{a_{D_2O}}{a_{D_2} a_{O_2}^{0.5}}$

a: activity
Pure solid: a = 1
Gas: a=P/P_0 (P is its partial pressure, P_0 = 101325 Pa)

$$\Delta H^{\circ}_{298} = -T(R \ln K + \Delta fef)$$

R:gas constant（Jmol）
fef: free energy function

3. Estimation of total loss of Li-containing species P^{total}_{Li} [Pa]

$$P_{Li}^{total} = P_{Li} + P_{LiOD} = (P_0^2 P_{D_2} K_7 K_9 / P_{D_2O})^{0.5} + (K_8 P_0 P_{D_2O})$$

P_{D2}=101.3Pa =sweep gas condition (0.1%)

Calculation of thermodynamic parameter

Thermodynamic database, JANAF-table and MALT2 were used for the calculation of fef (free function energy), Equilibrim constant K_0 and enthalpy ΔH^o_{298}.

Equilibrium constant: K_0

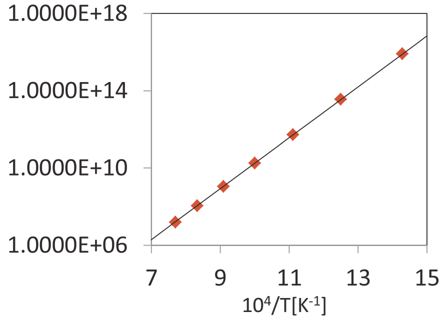

$D_2(g) + 0.5O_2(g) \leftrightarrow D_2O(g)$ ･･･(0)

$K_0 = a_{D2O}/a_{D2}a_{O2}^{0.5}$
$= 1.23 \times 10^{-3} \exp(3.03 \times 10^4/T)$

Outline

3 Results & Discussion

THE UNIVERSITY OF TOKYO

Crystal structure

Powder x-ray diffraction and Rietveld analysis (by PDXL)

MTi pebble

(analyzed except pattern in 2θ=20-30°)

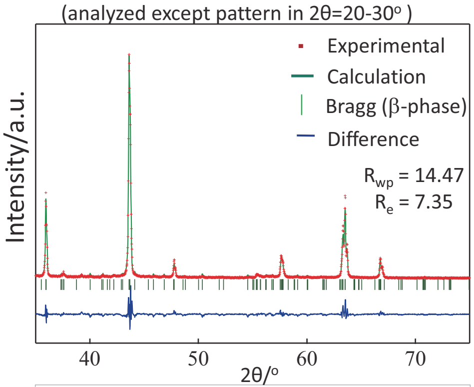

Single phase
β-Li_2TiO_3

Input parameter
Li2TiO3: JICST, 8604

OSi pebble

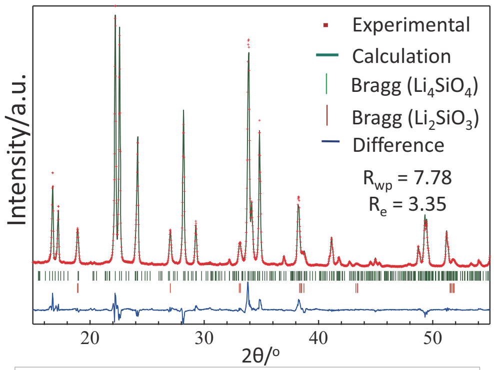

Multi-phase
Li_4SiO_4 with 7.14 wt % of Li_2SiO_3

Input parameter
Li4SiO4: Crystallography Open Database, 2101200
Li2SiO3: JICST, 1935

13

3 Results & Discussion

THE UNIVERSITY OF TOKYO

HTMS Results: MTi pebble (1573-1173K)

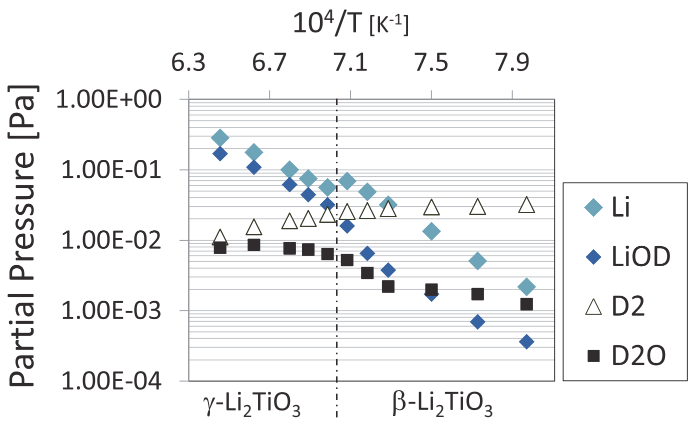

Equilibrium constant: K

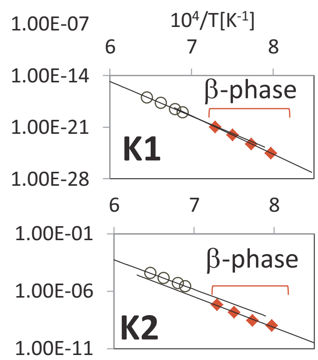

Eq.	Vapor raeaction	Equilibrium constant (β-phase)
1	$Li_2TiO_3(s) \rightarrow 2Li(g) + \frac{1}{2}O_2(g) + TiO_2(s)$	$K_1=P_{Li}{}^2P_{O2}{}^{0.5}$= 9.93 X 10^{16} exp(-1.20 X 10^5/T)
2	$Li_2TiO_3(s) + D_2O(g) \rightarrow 2LiOH(g) + TiO_2(s)$	$K_2=P_{LiOD}{}^2/P_{D2O}$= 1.65 X 10^{12} exp(-6.15 X 10^4/T)

14

3 Results & Discussion

THE UNIVERSITY OF TOKYO

HTMS Results: OSi pebble (1193-1153K)

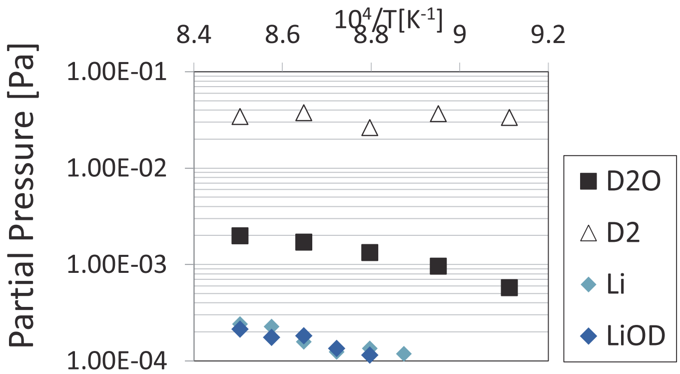

Equilibrium constant: K

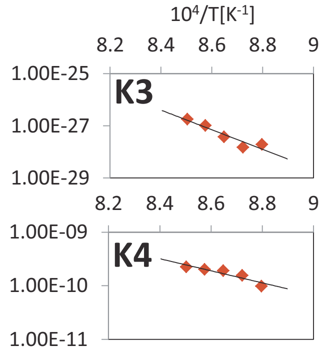

Eq.	Vapor raeaction	Equilibrium constant
3	$Li_4SiO_4(s) \leftrightarrow 2Li(g) + \frac{1}{2}O_2(g) + Li_2SiO_3(s)$	$K_3=P_{Li}^2P_{O2}^{0.5}$= 1.57 X 10^5 exp(-8.66 X 10^4/T)
4	$Li_4SiO_4(s) + D_2O(g) \leftrightarrow 2LiOH(g) + Li_2SiO_3(s)$	$K_4=P_{LiOD}^2/P_{D2O}$= 9.78 X 10^5 exp(-2.60 X 10^4/T)

3 Results & Discussion

THE UNIVERSITY OF TOKYO

3rd low enthalpy ΔH^o_{298}

Calc.: MALT calculation

Li_2TiO_3

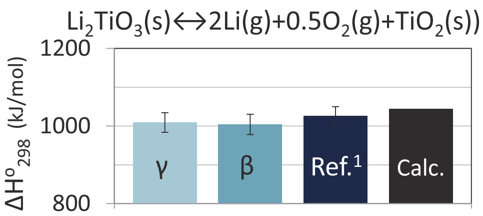

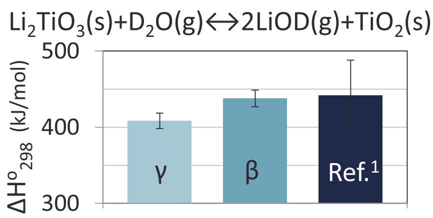

Li_4SiO_4

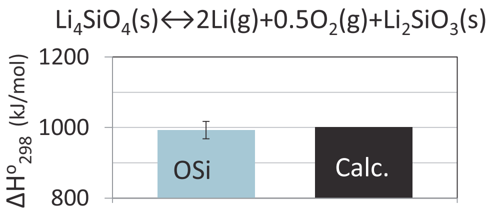

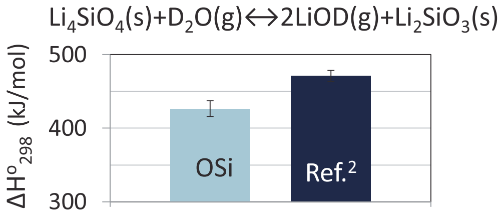

Ref.1 M. Yamawaki, A. Suzuki, et al., Journal of Nuclear Materials 247 (1997) 11-16
Ref.2 R.-D. Penzhorn, H.R. Ihle, S. Huber, P. Schuster and H,J. Ache J. Nuclear Materials 191 - I94 (1992) 173- I77

3 Results & Discussion

THE UNIVERSITY OF TOKYO

Estimation of P_{Li}^{total} from β-Li_2TiO_3

$P_{Li}^{total} = P_{Li} + P_{LiOD}$

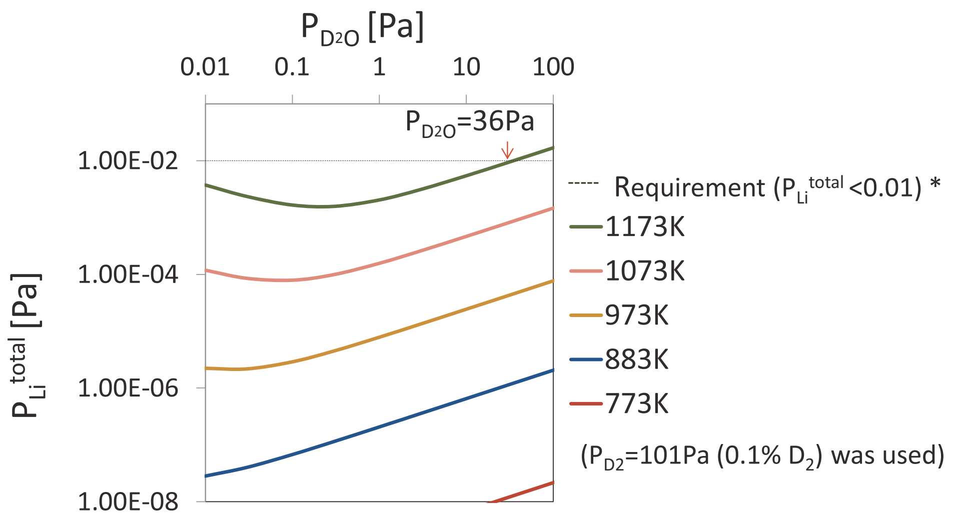

Moisture Pressure in Li_2TiO_3 pebble blanket should be controlled P_{D2O} < 36 Pa

*H.R. Ihle, R.-D. Penzhom, P. Schuster, SOFT Conf, Rome, Italy, Sept. 1992.

17

3 Results & Discussion

THE UNIVERSITY OF TOKYO

Estimation of P_{Li}^{total} from Li_4SiO_4

$P_{Li}^{total} = P_{Li} + P_{LiOD}$

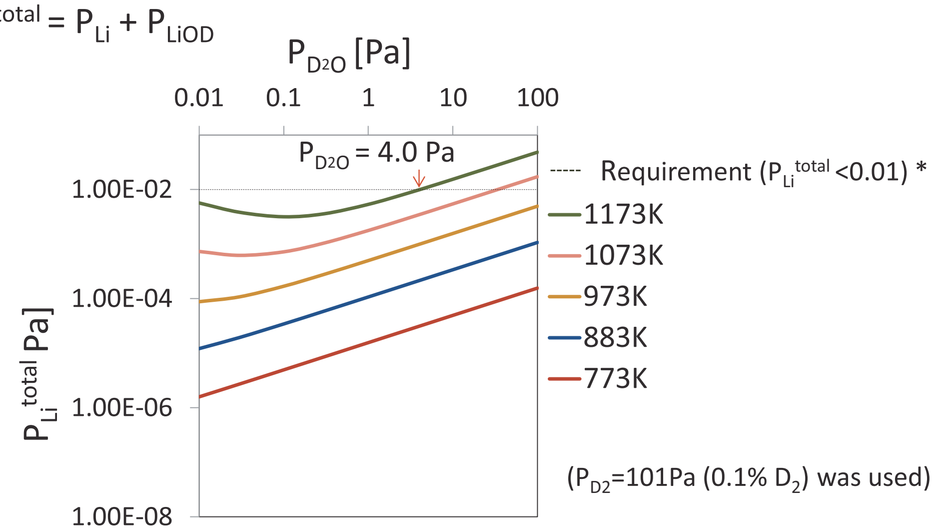

- More sensitive to P_{D2O} than Li_2TiO_3
- Moisture Pressure in Li_4SiO_4 pebble blanket should be controlled P_{D2O} < 4.0 Pa

*H.R. Ihle, R.-D. Penzhom, P. Schuster, SOFT Conf, Rome, Italy, Sept. 1992.

18

THE UNIVERSITY OF TOKYO

Outline

4

THE UNIVERSITY OF TOKYO

Conclusion

Vaporization properties of Li_4SiO_4 (Multi-phase with Li_2SiO_3) and the single phase of β-Li_2TiO_3 have been studied by atmosphere controllable high temperature mass spectrometer (HTMS).

- 3rd low Enthalpy ΔH^o_{298}
  - ΔH^o_{298} (Li_4SiO_4(s)→2Li(g)+0.5O_2(g)+Li_2SiO_3(s)) = 992.82±49.6 kJ/mol
  - ΔH^o_{298} (Li4SiiO4(s)+D2O(g)→2LiOH(g)+Li2SiO3(s)) = 426.38±21.3 kJ/mol
  - ΔH^o_{298} (Li_2TiO_3(s)→2Li(g)+0.5O_2(g)+TiO_2(s)) = 1003.5±50.2kJ/mol
  - ΔH^o_{298} (Li_2TiO_3(s)+D_2O(g)→2LiOH(g)+TiO_2(s)) = 437.8±21.9 kJ/mol
- Proposed moisture pressure in a blanket
  - P_{H2O} < 4.0 [Pa] for OSi pebble
  - P_{H2O} < 36 [Pa] for MTi pebble
- Future study

  Advanced breeder (Li excessive metatitanate (Li/Ti>2.0), Li_4SiO_4+Li_2TiO_3) are going to be studied by the HTMS

BEHAVIOR OF ADVANCED CERAMIC BREEDER PEBBLES IN LONG-TERM HEAT TREATMENT

M.H.H. KOLB, O.H.J.B. LEYS, C. ODEMER, C. FREY, R. KNITTER

Karlsruhe Institute of Technology, Institute for Applied Materials (IAM-WPT), 76021 Karlsruhe, Germany

INTRODUCTION

Usually, ceramic breeder pebbles are characterized right after fabrication and thus their quality is estimated. While this is effective for developing different breeder ceramics and fabrication techniques, the determined properties may not be indicative of the pebble properties after a significant time of use within a breeder blanket module. As the design of the blanket modules relies, amongst other data, on the pebble properties, it is necessary to provide for relevant data.

So-called long-term annealing experiments were relatively frequently carried out at KIT/FZK in the years 1997 to 2002. The goal of these experiments was to determine the changes of the pebble properties, after exposing them to high, blanket relevant temperatures and a constantly purging, blanket relevant gas atmosphere (Helium with 0.1% H2), as a function of time. The experiments were carried out with reference breeder pebbles available at the time. However, since 2011 ceramic breeder pebbles produced by the melt-based KALOS process consisting of Lithium Orthosilicate as the main constituent and Lithium Metatitanate as strengthening phase are available. To characterize these pebbles in the same way, another long-term annealing experiment was carried out.

EXPERIMENTAL

The annealing was performed in a modified rotary kiln with three separate alumina tubes. These tubes are connected to influent and effluent gas tubing by water-cooled flanges. The temperature of each alumina tube is monitored by an individual thermocouple.

On the influent and effluent gas tubing of each alumina tube a digital mass flow controller and a digital absolute pressure controller is installed, respectively. Between these controllers a defined pressurized atmosphere is established, independent of the environmental atmospheric pressure. Within this section of the tubing, four optical Oxygen sensors are installed, as the Oxygen measurements are sensitive towards pressure changes. One of the sensors is placed on an influent line and three are placed on the effluent side of each alumina tube. To also monitor the humidity of the purge gas, four moisture probes are installed. Only the probes that monitor the effluent gas streams are placed in the pressurized section. The moisture sensors as well as the Oxygen sensors monitor the temperature of the purge gas. All sensors and controllers are connected to a PC-based data acquisition and control system.

Three different compositions of pebbles, i.e. 20 mol% Lithium Metatitanate, 25 mol% Lithium Metatitanate and 30 mol% Lithium Metatitanate, were annealed at 900 °C. The samples were dried in a vacuum furnace at 300 °C for 1 hour before placing them in the alumina tubes. During the annealing a constant gas flow of 1200 ml/h and a constant absolute pressure of 1200 mbar, which is slightly above the environmental atmospheric pressure, was established. The pebble samples were placed in special platinum boats (20 mol% Lithium Metatitanate & 30 mol% Lithium Metatitanate) and alumina boats (25 mol% Lithium Metatitanate). All samples held in platinum boats were placed in one alumina tube, while the alumina boats were placed in a second alumina tube. After 4 days, 32 days and 64 days of annealing, one boat of each sample type was extracted from the kiln. During the sampling the temperature was reduced to 300 °C.

The extracted samples were split into several sub-samples according to the different characterization techniques. 40 pebbles of 500 µm diameter and 40 pebbles of 1000 µm diameter of each sample were singly, uniaxially compressed until fracture to determine their crush load. The density of the samples was determined by Helium pycnometry, thus the closed porosity was calculated. With Mercury porosimetry the open porosity of the pebbles was measured and by multi-point BET N2 adsorption the specific surface area of the pebbles was determined.

RESULTS & DISCUSSION

During the first 4 days of annealing, the pebbles, although carefully dried before the experiment, still emit a significant amount of water, as the dew point of the effluent gas of both alumina tubes (maximum at about 10 °C) lies well above that of the influent gas (about -45 °C). During the subsequent annealing a relatively constant and low release of water from the samples establishes. During the sampling, atmospheric water and also Oxygen is introduced into the system, yet both gases are purged quickly. The samples held by alumina boats apparently release more water than the samples held in platinum boats, other than that, the shapes of the release curves look very similar. A significant effect of the sample types on the release behavior cannot be determined.

The emitted Oxygen from the pebbles during annealing is in general relatively. Similar to the observations for the water release, the Oxygen release curves of the two alumina tubes resemble each other a lot. During the first third of the annealing experiment, the release of Oxygen rises slowly until it starts to diminish for the rest of the annealing. For the platinum boats, this decrease leads to a net consumption of Oxygen in the last third of annealing. However, in the effluent gas from the tube filled with the alumina boats the detected Oxygen content is constantly higher than that of the influent gas, i.e. a net release of Oxygen. Apparently there is a constant offset of released Oxygen towards higher oxygen release in comparison to the curve of the platinum boats.

Yet, the composition of the effluent gas does not seem to be significantly influenced by the sample composition, neither in terms of Oxygen nor water release. Obviously, the alumina boats emit a significant amount of Oxygen, which is not surprising as alumina readily forms Oxygen vacancies in reducing atmospheres. The so-emitted Oxygen may partly react to water, which can explain the differences in the release curves.

The effect of the annealing on the microstructure is relatively little. The cross sections of the pebbles show the characteristic dendritic/eutectic microstructure of pebbles fabricated by a melt-based process, depending of the Lithium Metatitanate content. Significant grain growth after 4 days of annealing is only observed for the pebbles containing 30 mol% Lithium Metatitanate. Annealing these pebbles for longer times does not increase the grain size perceivably. The 25 mol% Lithium Metatitanate pebbles, showing fine lamellae of Lithium Metatitanate, do not exhibit significant changes of the microstructure until 64 days of annealing, when the lamella structure starts to coalesce to sphere or cylinder shaped structures. Yet there are still large areas where the coalescence has not taken place. After 64 days of annealing, the Lithium Metatitanate phase is still finely dispersed within the Lithium Orthosilicate matrix in all sample types. The negligible solubility and the therefore little diffusion rate of Silicon or Titanium ions in the respective phase is presumably the cause for the high thermal stability of the microstructure.

The crush load of all pebble samples changes significantly after 4 days of annealing. While pebbles with a lower Lithium Metatitanate content loose some of their strength, the crush load of the 30 mol% Lithium Metatitanate samples increases by about 50%. These effects are observable for pebbles of 500 µm diameter and 1000 µm diameter alike. Annealing the pebbles for longer times, i.e. 32 days and 64 days, consolidates the crush load values at a certain level near the values of the 4 days samples. However, the 1000 µm pebbles with 30 mol% Lithium Metatitanate cannot keep their high strength and approach a value, still higher than that of the as-received samples. Several effects are eligible for the observed behavior. However, a partly healing of defects may explain the rise in the crush loads for the 30 mol% Lithium Metatitanate pebbles.

As for the crush load, the specific surface area of the pebble samples, with the exception of the 20 mol% Lithium Metatitanate samples, shows a substantial change within the first 4 days of annealing to a then constant value for longer annealing times. The specific surface area of these samples decreases, which is synonymic for a smoothing of the pebble surface, to about 0.06 m^2/g, while the 20 mol% Lithium Metatitanate samples reach this value after 64 days of constant surface smoothing. The most significant reduction in the surface area is measured for the 30 mol% Lithium Metatitanate samples. To some degree, a smoothing of the surface can reduce the severity of cracks and therefore the crush load can be improved.

The open porosity of the samples does not change a lot as a function of the annealing duration. However, the closed porosity is significantly increased after 4 days of annealing. Analogous to the development of the crush loads, the closed porosity approaches a constant value after long annealing durations. This constant value lies between the high 4 day values and the low initial level. The reason for an increase of the closed porosity is usually the formation of a gaseous species within the sample. As the release of water vapor from the pebbles is substantial during the first 4 days of annealing, this might be an explanation.

CONCLUSION

The properties of the pebble samples change significantly as a function of annealing duration. Most changes happen during the first 4 days of annealing with a subsequent stabilization at a certain level. The processes that govern the changes are not understood completely and therefore have to be investigated in the future. Also a thorough XRD analysis and an elemental analysis are planned to be performed in addition to the presented characterization. In general, the properties of all pebble samples are still acceptable after 64 days of annealing for an application in a breeder blanket.

Behavior of advanced ceramic breeder pebbles in long-term heat treatment

M.H.H. Kolb, O.H.J.B. Leys, C. Odemer, C. Frey, R. Knitter

INSTITUTE FOR APPLIED MATERIALS - MATERIAL PROCESS TECHNOLOGY

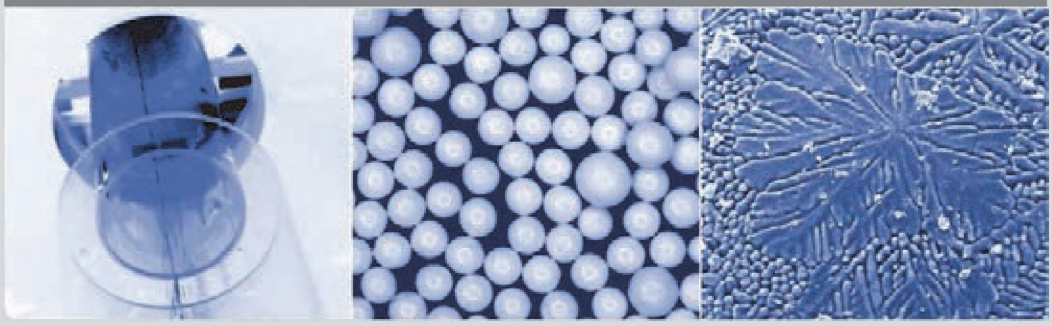

Introduction

- Goal
  - Time-resolved analysis of the evolution of breeder materials in a relevant environment
- Previous work
  - Four long-term annealing experiments (1997-2002)
    - Reference grade lithium orthosilicate (Li_2CO_3 or LiOH as starting materials)
    - Other candidate breeders (Li_2TiO_3, Li_2ZrO_3)
    - 970 °C annealing temperature
    - Maximum of 96 days of annealing
- This work
  - Focus on advanced tritium breeder materials
    - JAEA
    - EU
  - Part of EU BroaderApproach DEMO activities

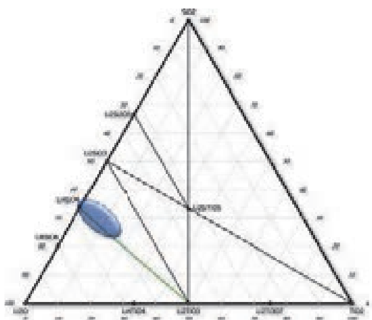

Contents

- Experimental set-up
- Release of gaseous species
- Microstructure of the pebbles
- Evolution of the mechanical rigidity
- Porosity and specific surface area

Experimental parameters

Annealing temperature	900° C
Heating rates	5 K/min
Sampling after	4, 32, 64, 128 days
Temperature during sampling	300° C
Atmosphere/purge gas	He/H_2 0.1%, 1200 mbar(a) and 1200 ml/h
Samples	KALOS (20, 25, 30 mol% Li_2TiO_3) JAEA (Sol-Gel, Emulsion method)
Sample preparation	1 h of drying at 300° C in a vacuum oven

Experimental set-up

Alumina boats for 25 mol% MTi-pebbles

Platinum boats for 20 mol% & 30 mol% MTi-pebbles

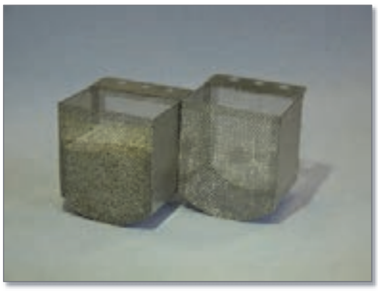

Experimental set-up

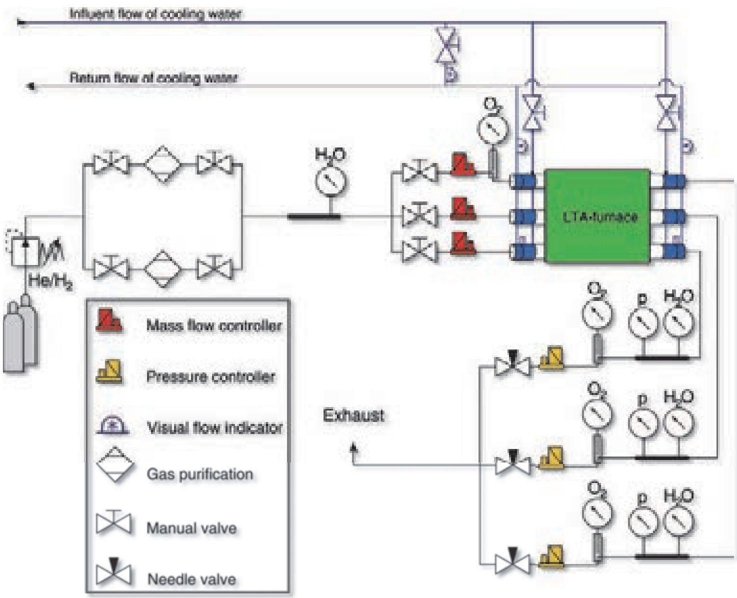

Sensors

- Attachment of 3 thermocouples on the alumina tubes for precise temperature monitoring
  - An additional thermocouple monitors the temperature of the flanges on the alumina tubes
- Installation of 4 optical oxygen sensors (detection limit: ~100 ppm)
- Recalibration of the moisture detection system and its 4 sensors
- Installation of 3 digital mass flow controllers and 3 digital absolute pressure controllers
  - Providing a constant environment for the oxygen sensors independent of the environmental atmospheric pressure
  - Precise calculation of the number densities of molecules
- Measurement, data logging and control system on PC basis

Recorded values

- Temperature
  - Each alumina tube
  - Alumina tube flange
  - He/H_2 gas, influent and effluent from each alumina tube
- Moisture
  - He/H_2 gas, influent and effluent from each alumina tube
- Pressure
  - Each alumina tube
- Gas mass flow
  - Each alumina tube
- Oxygen concentration
  - Influent and effluent from each alumina tube

Release of water and oxygen

- Release of water vapor
  - Significant release of water during the first four
  - Constant release of water vapor during the following heat treatment
  - Little effect of the sample type
- Release of oxygen
  - Slow increase of the released oxygen during the first ~40 days
  - “Consumption” of oxygen during the later days of heat treatment
  - Little effect of the sample type
  - Very low concentration of oxygen

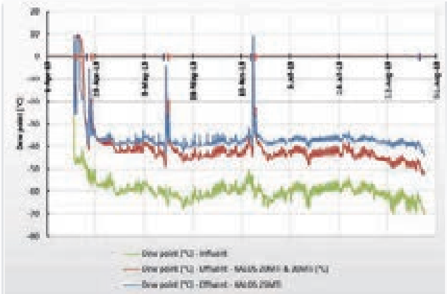

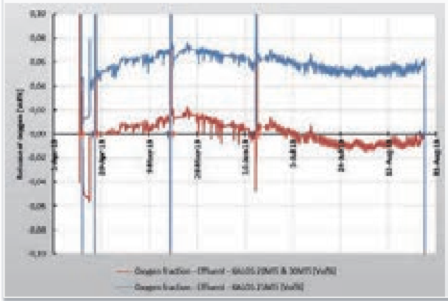

9 12.09.2013 M. Kolb Behavior of advanced ceramic breeder pebbles in long-term heat treatment Institute for Applied Materials (IAM-WPT)

Microstructural evolution

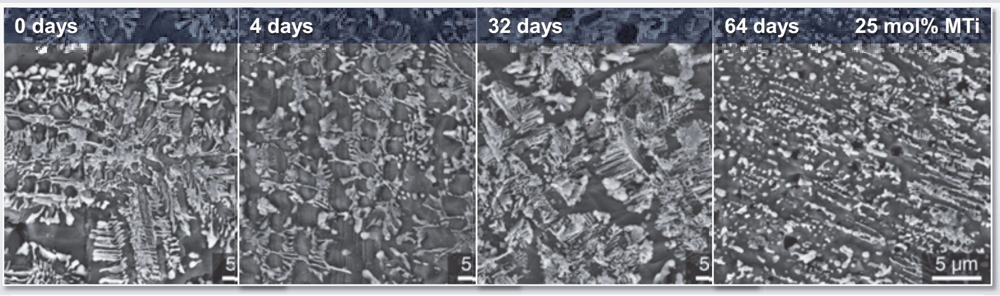

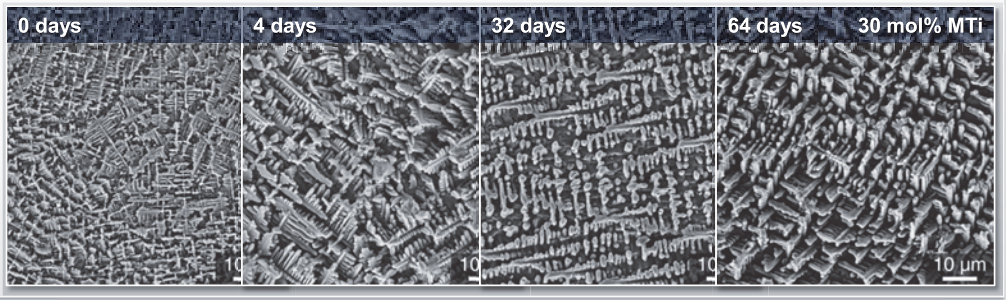

10 12.09.2013 M. Kolb Behavior of advanced ceramic breeder pebbles in long-term heat treatment Institute for Applied Materials (IAM-WPT)

Mechanical characterization

- Reduction of the mechanical strength of 20 mol% & 25 mol% MTi pebbles
  - Decrease of maximum crush load
    - Plateau strength for 20 mol% & 25 mol% pebbles
  - Form of corrosion?
- Increase of crush load of 30 mol% pebbles
  - Substantial increase of minimum crush loads
  - Healing of defects?

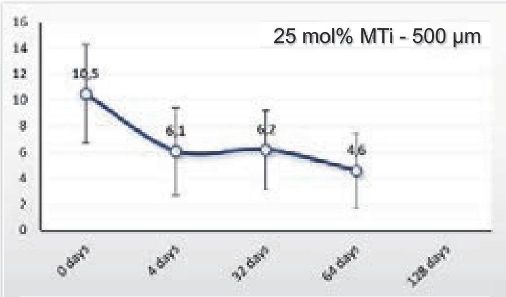

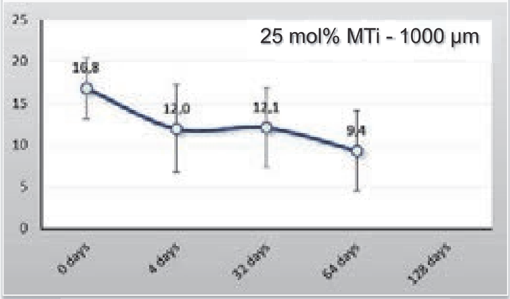

Mechanical characterization

- Reduction of the mechanical strength of 20 mol% & 25 mol% MTi pebbles
  - Decrease of maximum crush load
    - Plateau strength for 20 mol% & 25 mol% pebbles
  - Form of corrosion?
- Increase of crush load of 30 mol% pebbles
  - Substantial increase of minimum crush loads
  - Healing of defects?

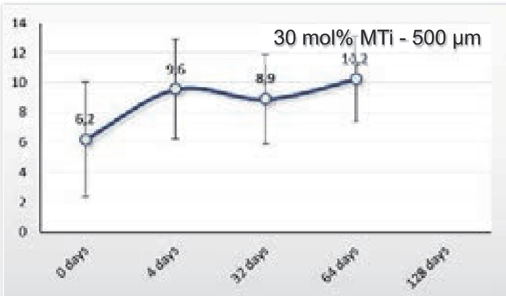

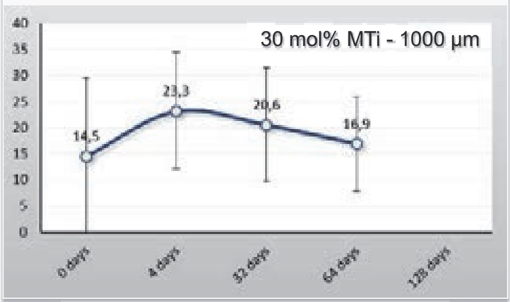

Effect on porosity & surface area

- Fast smoothing of the pebble surface for pebbles with high MTi-content
  - Possible defect healing effect
- Lower limit at ~0.06 m²/g

- Evolution of porosity depends significantly on the pebble composition
  - Closed porosity significantly increases within 4 days
    - Coincides with the release of water vapor
  - Followed by a decrease of closed porosity to constant value
  - Little change in open porosity

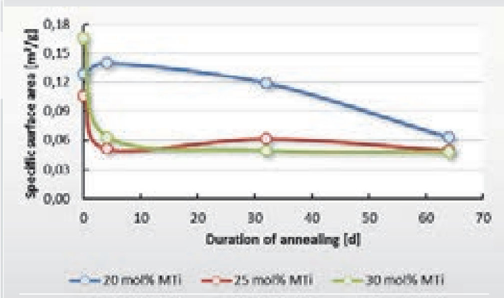

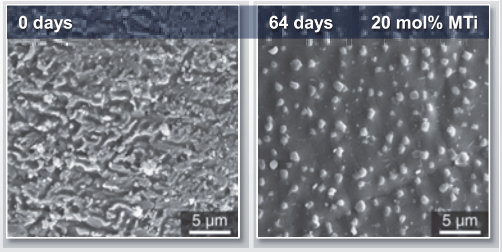

13 12.09.2013 M. Kolb Behavior of advanced ceramic breeder pebbles in long-term heat treatment Institute for Applied Materials (IAM-WPT)

Effect on porosity & surface area

- Fast smoothing of the pebble surface for pebbles with high MTi-content
  - Possible defect healing effect
- Lower limit at ~0.06 m²/g

- Evolution of porosity depends significantly on the pebble composition
  - Closed porosity significantly increases within 4 days
    - Coincides with the release of water vapor
  - Followed by a decrease of closed porosity to constant value
  - Little change in open porosity

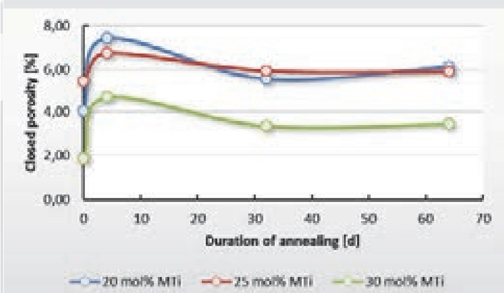

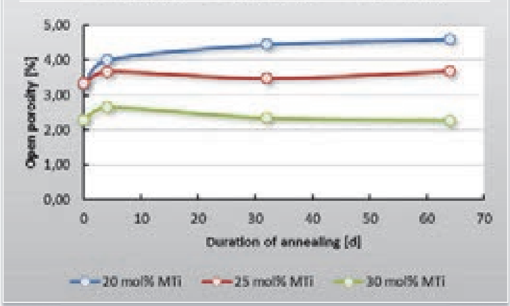

14 12.09.2013 M. Kolb Behavior of advanced ceramic breeder pebbles in long-term heat treatment Institute for Applied Materials (IAM-WPT)

Summary

- 128 day heat treatment of advanced tritium breeder pebbles in blanket relevant atmosphere

- Microstructure, mechanical properties & morphology
  - Continuing and slow grain growth
    - Lithium metatitanate phase is (still) finely dispersed
  - Evolution of mechanical rigidity is strongly dependent of the pebble composition
    - Possible defect healing for 30 mol% MTi pebbles
  - Peculiar increase of the closed porosity during the first four days
  - Fast smoothing of the pebble surface for high MTi content pebbles

- Analysis yet to be performed
  - Chemical analysis
  - 128 days samples
  - In-depth XRD analysis

Chemical compatibility of lithium meta-titanates with low-activation ferritic steel F82H

T. Terai[1], R. Ishioka[1], K. Uozumi[2], K. Mukai[1], A. Suzuki[1], M. Koyama[2]

[1]*School of Engineering, The University of Tokyo, Tokyo, 113-8656 Japan*
[2]*Central Research Institute of Electric Power Industry, Komae, Tokyo, 201-8511 Japan*
Corresponding author: tera@n.t.u-tokyo.ac.jp

Lithium meta-titanate with excess lithium is proposed as a candidate tritium breeding material because of its high concentration of lithium, which is consumed in fusion reactor blanket due to vaporization and nuclear transmutation. The chemical reactivity of the material is a great concern because the lithium activity in the material is anticipated to be larger than that in the stoichiometeric lithium meta-titanate. In this study, the chemical compatibility of the material with low-activation ferritic steel F82H was investigated in comparison with that of the stoichiometric compound at 600 °C or 800 °C for 100 – 600 h.

Lithium meta-titanate pebbles with excess lithium and stoichiometric composition were supplied by JAEA. Both were confirmed to be 2.27 and 2.01 in Li/Ti ratio, respectively, by chemical analysis and to have only the monoclinic-Li_2TiO_3 phase by XRD. Pebbles of each compound were heat-treated in contact with a F82H specimen supplied by JAEA under the contacting pressure of 3700 Pa in the atomosphere of He+0.1%H_2 at 600 °C or 800 °C for 100 h, 200 h, 400 h or 800 °C. The surface and the cross-section of each specimen after the experiment were analyzed by XRD, EPMA and SIMS.

On the surfaces of lithium meta-titanates with stoichiometric composition and with excess lithium, only small Li_2FeO_2 peaks were detected besides the peaks derived from monoclinic-Li_2TiO_3 phase and no significant diffusion of the elements from F82H into the lithium meta-titanates was observed. On the surface of F82H specimen, on the other hand, $LiCrO_2$ peaks were detected as well as F82H-derived peaks and the cross-sectional observation of the F82H specimens by EPMA and SIMS gave some important information about the corrosion and the diffusion of Li , O and Cr in the near-surface region. In case of stoichiometric lithium meta-titanate, Cr diffused to the surface from the F82H bulk to form $LiCrO_2$ on the surface. In case of excess Li compound, in contrast, Cr_2O_3 phase was formed in the deep region as well as the formation of $LiCrO_2$ in the adjoining near-surface region. These results mean the diffusion of Li and O is enhanced presumably by the larger activities of the elements in the excess compound. Apparent O diffusivity observed in the experiment suggests that the corrosion depth by the excess compound is at most 117 micro-meters at 320 °C for 2 years, which will not a significant problem in the actual blanket operation condition.

Chemical Compatibility of Reduced-activation Ferritic Steel F82H with Lithium Meta-titanates

Takayuki TERAI, Rika ISHIOKA, Keisuke MUKAI, Akihiro SUZUKI

U. Tokyo

Koichi UOZUMI, Tadafumi KOYAMA

CRIEPI

CBBI-17

@Barcelona, 12-14 September, 2013

Outline

1. Introduction
   - Research purpose
2. Experimental
   - Apparatus and condition
3. Results
   - Phase characterization on the surface by XRD
   - Cross-sectional characterization by EPMA and SIMS
4. Discussion
   - Reaction mechanism in thermodynamics and kinetics
5. Conclusion

2

Stoichiometric and hyper-stoichiometric lithium meta-titanates

lithium meta-titanates : Li_2TiO_3

○high chemical stability ○good T release characteristic

×Low Li density than other solid breeders (Li_2O, Li_4SiO_4…etc.)

Hyper-stoichiometric lithium meta-titanate (Li/Ti > 2.0) is investigated in Japan for the improvement of Li loss due to burn-up and vaporization

Phase diagram of Li_2O-TiO_2

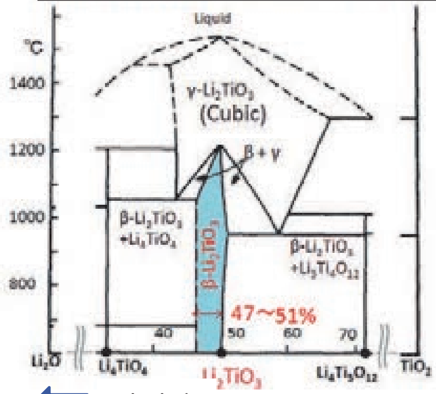

Li rich

β-Li_2TiO_3 phase in the range of 1.88 ≦ Li/Ti ≦ 2.25 (starting material)

Hyper-stoichiometric lithium meta-titanates

$Li_{2+x}TiO_{3+y}$

(Li/Ti ratio > 2.0)

○ high Li density

○ high chemical stability in reduced atmosphere (He+H_2)

after Hoshino

3

RAFS F82H

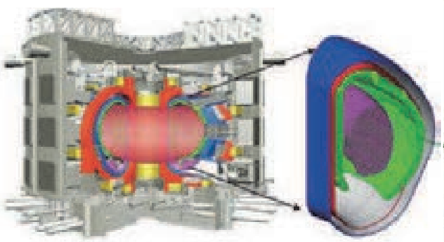

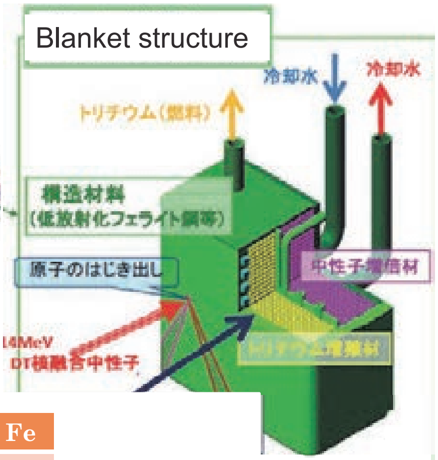

Chemical composition of F82H (wt.%)

	C	Cr	W	V	Ta	Mn	Si	Fe
F82H	0.1	8.0	2.0	0.2	0.04	0.5	0.1	bal.

Design parameters of water cooled solid blanket	
Structural	F82H
T breeder	Li_2TiO_3
Atmosphere	He+0.1%vol H_2

T_{max} at boundary is 320 C

4

Purpose of this study

In the previous study on the compatibility between stainless steel (HT-9, SUS316) and Li bearing oxides (Li_2O, $LiAlO_2$, Li_2SiO_3, etc.), some new Li bearing oxide compounds were formed due to the diffusion of Li and O, which may influences the mechanical properties of the structural materials.

No study has been done on the compatibility between RAFS and lithium meta-titanate.
In particular, no data is available on hyper-stoichiometric phase $Li_{2+x}TiO_{3+y}$.

Purpose
To clarify the compatibility between F82H and lithium meta-titanates (stoichimetric Li_2TiO_3 and hyper-stoichiometric $Li_{2+x}TiO_{3+y}$).

5

Outline

1. Introduction
   - Research purpose
2. Experimental
   - Apparatus and condition
3. Results
   - Phase characterization on the surface by XRD
   - Cross-sectional characterization by EPMA and SIMS
4. Discussion
   - Reaction mechanism in thermodynamics and kinetics
5. Conclusion

6

Experimental

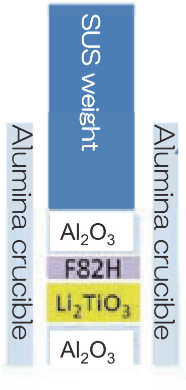

Contacting F82H with Li_2TiO_3 at high temperature

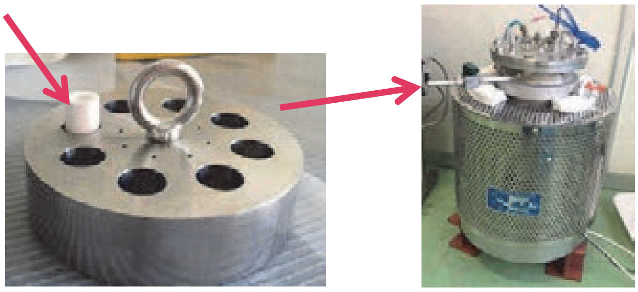

Contact pressure: about 3600Pa

Atmosphere : He + 0.1vol%H_2 flow
Temperature : 600 C,800 C
Period : 100h, 200h, 400h, 600h
Structural : F82H
Solid breeder : stoichiometric Li_2TiO_3 pellet(Li/Ti=2.03)
hyper-stoichiometric Li_2TiO_3 pellet(Li/Ti=2.27)
Both kinds of pellets were monoclinic phase of Li_2TiO_3 and >88% TD.

7

Outline

1. Introduction
   - Research purpose
2. Experimental
   - Apparatus and condition
3. Results
   - Phase characterization on the surface by XRD
   - Cross-sectional characterization by EPMA and SIMS
4. Discussion
   - Reaction mechanism in thermodynamics and kinetics
5. Conclusion

8

Characterization of Reaction Products on the surfaces by XRD

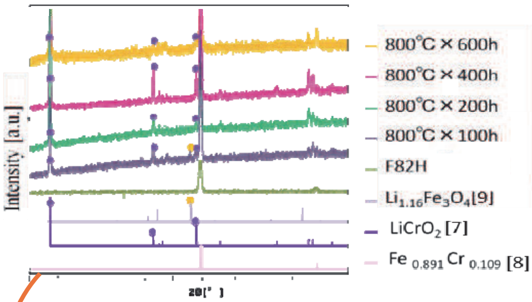

XRD pattern of F82H surface contacting Li_2TiO_3

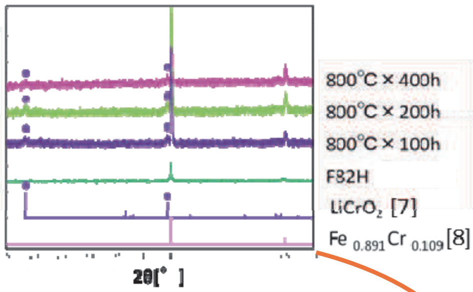

XRD pattern of F82H surface contacting $Li_{2+x}TiO_{3+y}$

Peaks of Cr_2O_3 due to oxidation by atmosphere on the opposite side of F82H

F82H

Mainly peaks of $LiCrO_2$, TiO_2 as well as F82H in both cases

F82H

Stoichiometric Li_2TiO_3

Mainly peaks of Li_2TiO_3 only
No significant change in EPMA cross-sectional image
→ Focusing on F82H side

Hyper-stoichiometric Li_2TiO_3

9

Cross-sectional Element Distribution of F82H Contacting Stoichiometric Li_2TiO_3 by SEM/EPMA

800 C×400 h

boundary

F82H resin

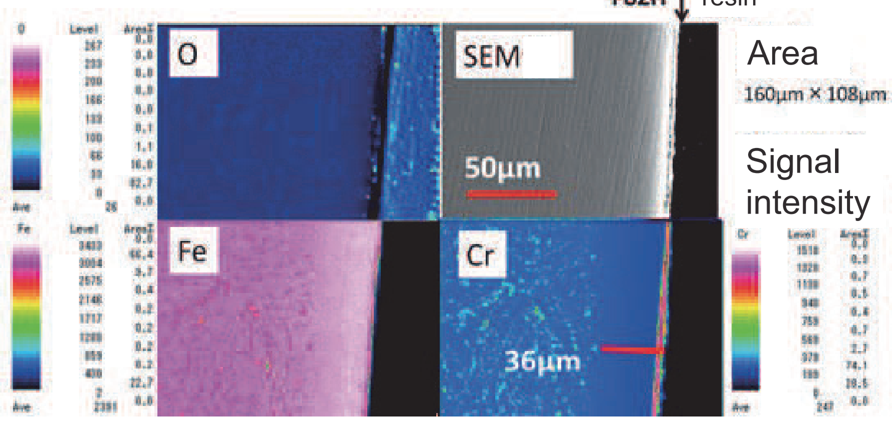

Cr migration to the surface from the depth of 36μm.
The same phenomena at 600 C

In case of F82H contacting stoichiometric Li_2TiO_3, Cr migrated from the depth to the surface of F82H.

10

Cross-sectional Element Distribution of F82H Contacting Hyper-stoichiometric

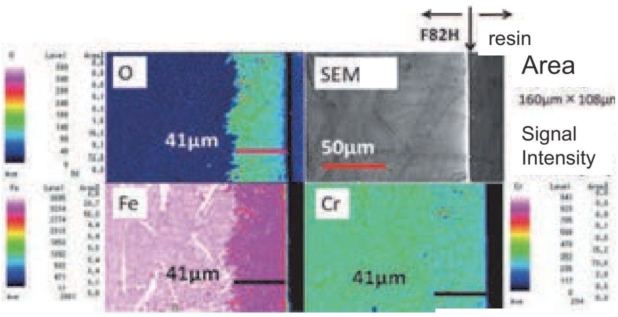

F82H contacting $Li_{2+x}TiO_{3+y}$ at 600 C for 600 h

O invasion to the depth of 41µm with Fe concentration decreasing.
High concentration region of Cr and O in the depth.

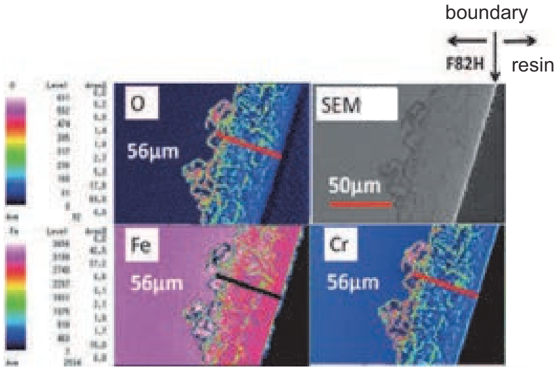

F82H contacting $Li_{2+x}TiO_{3+y}$ at 800 C for 400 h

O invasion to the depth of 56µm with Fe concentration decreasing. Clear high concentration region of Cr and O in the depth.

Diffusion of O and Cr from the surface to the depth of F82H contacting $Li_{2+x}TiO_{3+y}$

11

Cross-sectional elemental distribution and by SIMS

Li can be observed by SIMS.

F82H contacting stoichiometric Li_2TiO_3 at 800 C for 600h

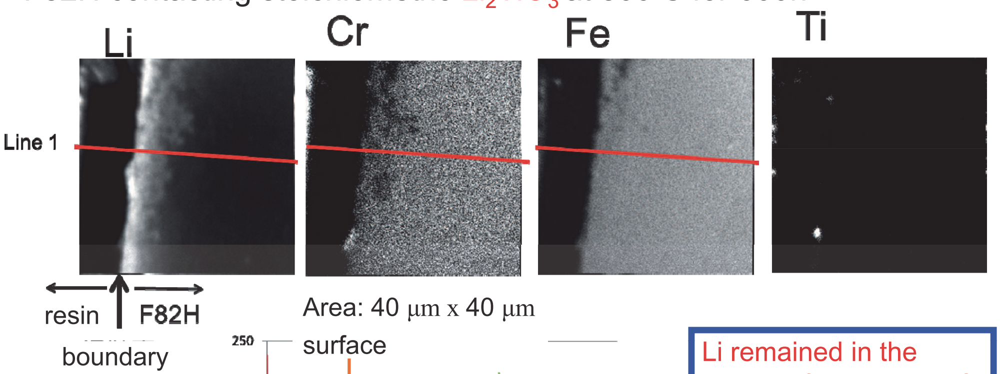

Area: 40 µm x 40 µm

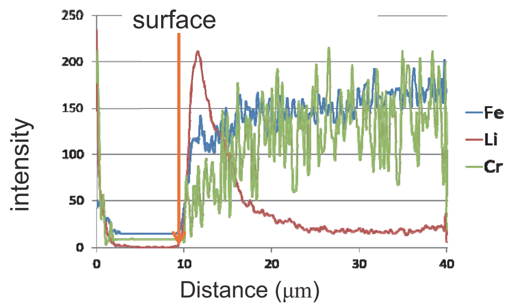

Li remained in the near-surface region of F82H contacting stoichiometric Li_2TiO_3

12

Cross-sectional elemental distribution by SIMS

F82H contacting hyper-stoichiometric $Li_{2+x}TiO_{3+y}$ at 600 C for 600h

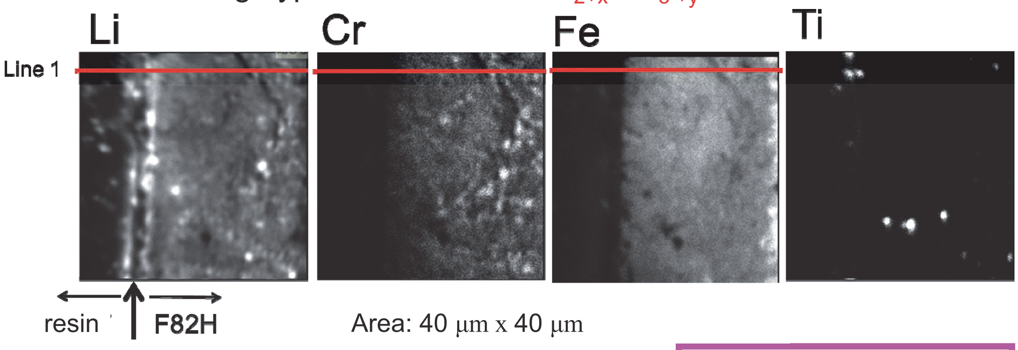

Area: 40 μm x 40 μm

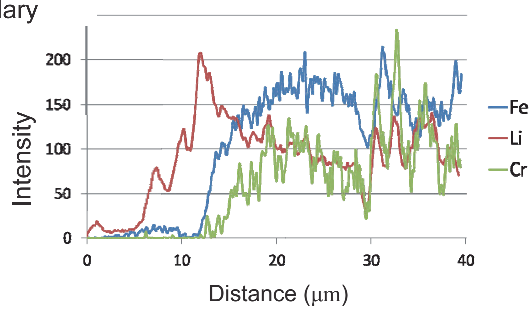

Li diffused to the depth as well as in the surface region of F82H contacting hyper-stoichiometric $Li_{2+x}TiO_{3+y}$

13

Outline

1. Introduction
   - Research purpose
2. Experimental
   - Apparatus and condition
3. Results
   - Phase characterization on the surface by XRD
   - Cross-sectional characterization by EPMA and SIMS
4. Discussion
   - Reaction mechanism in thermodynamics and kinetics
5. Conclusion

14

Calculation of Apparent Li Diffusivity

Fick's Law

$$C = C_0 \mathrm{erfc}\left(\frac{x}{2\sqrt{Dt}}\right)$$

C : concentration at x C_0 : surface concentration

x : distance t : time D : diffusivity

Apparent D value [cm^2/sec] of Li in F82H contacting Li_2TiO_3	Apparent D value [cm^2/sec] of Li in F82H contacting $Li_{2+x}TiO_{3+y}$
600 C	600 C
1×10^{-14}	(1) 2×10^{-13}, (2) 5×10^{-13}, (3) 1×10^{-12} $2\sim10\times10^{-13}$

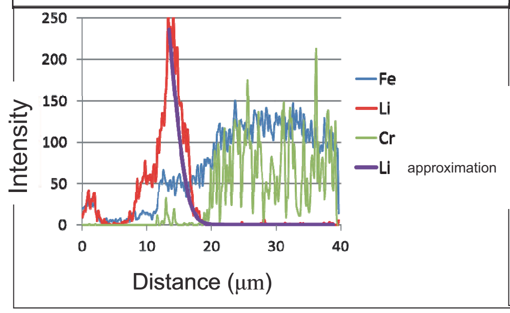

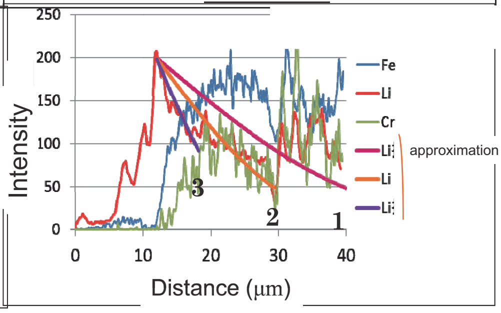

Apparent Li Diffusivity is larger in F82H contacting $Li_{2+x}TiO_{3+y}$ than that in Li_2TiO_3.

15

Calculation of Apparent O Diffusivity ($Li_{2+x}TiO_{3+y}$ case)

O Diffusion distance was defined as the distance of O reaching from the surface in this study.

Diffusivity D[cm^2/sec]

$$D = \frac{x^2}{t}$$

x : distance[cm]
t : time [sec]

Apparent diffusivity D of O [cm^2/sec]	
600℃	$(7.7\pm0.2)\times10^{-12}$
800℃	(1) 100h : 6.4×10^{-11}
	(2) 200h : 3.6×10^{-11}
	(3) 400h : 2.2×10^{-11}

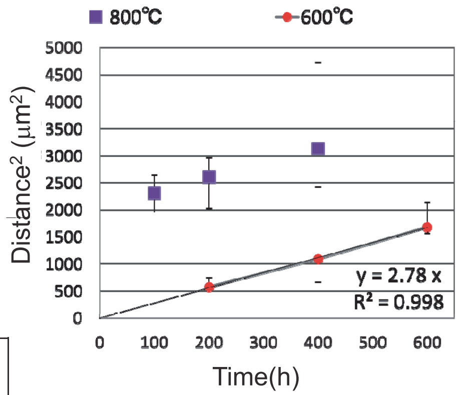

Apparent O diffusivity is larger than that of Li at 600 C ($2\sim10\times10^{-13}$)

Apparent diffusivity decreased with duration time

16

Thermodynamic Analysis by MALT for Windows

Stable products formed from the thermodynamic point of view were obtained by the equilibrium calculation program “gem” in MALT for windows
⇒In chemical equilibrium,
$LiCrO_2$, Ti_2O_3, etc. (F82H with Li_2TiO_3)
Cr_2O_3 (F82H in the experimental atmosphere)

Consistent with XRD results
$LiCrO_2$ and Cr_2O_3 were stably formed.

The following reactions occurred on the boundary and in the bulk.

Surface : $Li_2TiO_3 + Cr_2O_3 = 2\ LiCrO_2 + TiO_2$

Inside : diffusion of Li^+ and O^{2-} and $Li^+ + 2O^{2-} + Cr = LiCrO_2$

Inside : diffusion of Li^+ and O^{2-} and $3O^{2-} + 2Cr = Cr_2O_3$

17

Summary on the Reaction Mechanism

Apparent Li diffusivity in F82H

Contacting Li_2TiO_3 < Contacting $Li_{2+x}TiO_{3+y}$

In F82H contacting $Li_{2+x}TiO_{3+y}$

Apparent diffusivity of Li < Apparent diffusivity of O

The apparent O diffusivity decreased with time at 800 C may be influenced by the formation of the stable compound Cr_2O_3 in the depth.

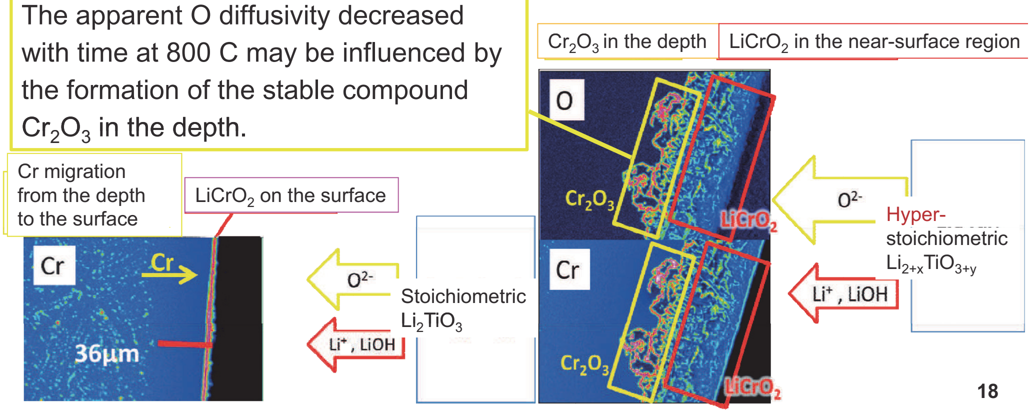

18

Evaluation of O Diffusion in the actual blanket condition

Arrhenius Equation

$$D = D_0 \exp\left(\frac{-E_A}{kT}\right)$$

D : diffusion distance[cm²/sec]
T : temperature[K]
E_A : activation energy [eV]
k : Boltzmann constant [eV/K]

Maximum temperature at boundary between structural material and breeder: 320 C
Operation period: 2 years
→Evaluation of O diffusion distance using O diffusivity at 320 C calculated by Arrhenius Equation

Maximum O diffusion distance in F82H contacting hyper-stoichiometric $Li_{2+x}TiO_{3+y}$	
Activation energy [eV]	0.20
Diffusivity D at 320 C [cm²/sec]	2.2×10^{-12}
Diffusion distance for 2 years [μm]	117

This result indicates that the corrosion of F82H wall (1.5 mm in thickness in the blanket design) by hyper-stoichiometric $Li_{2+x}TiO_{3+y}$ may be no significant problem in the actual blanket condition.

19

Conclusion

Compatibility of F82H and lithium meta-titanates (Li_2TiO_3 and $Li_{2+x}TiO_{3+y}$)

- On the side of lithium meta-titanates, no significant chemical change observed
- On the side of F82H contacting Li_2TiO_3, Cr migration to the surface to form $LiCrO_2$ formation
- On the side of F82H contacting $Li_{2+x}TiO_{3+y}$, $LiCrO_2$ formation in the near-surface region and Cr_2O_3 formation in the depth

Reaction mechanisms are different between two cases, $Li_{2+x}TiO_{3+y}$ shows larger reactivity than Li_2TiO_3 .
The chemical potentials of Li and O in $Li_{2+x}TiO_{3+y}$ are larger than those of Li_2TiO_3, and then Li and O migrate into deeper region.

Diffusion distance of O at 320 C was calculated to be 117μm in 2 years. This result indicates no significant problem in the blanket condition, because the thickness of the structural material is designed to be 1.5 mm.

20

Correlation between electrical behaviour and tritium release in γ-irradiated Li_4SiO_4 breeder pellets and pebbles.

E.Carella[1], M.T. Hernandez[1], A.Ibarra[1], E.Chinarro[2], B.Moreno[2]

[1]LNF-CIEMAT, Materials for Fusion Group, Av. Complutense 40, Madrid, Spain.
[2]ICV-CSIC, Dpto. de Vidrios, c/Kelsen 5, Madrid, Spain.

Lithium orthosilicate (Li_4SiO_4) is considered one of the best candidates for the solid Breeder Blanket system (BBs). In the blanket zone electric and magnetic field may cause important changes in the properties of these materials. Furthermore during reactor operation, the pebbles will be bombarded by neutrons and gamma radiation which may alter their composition and properties, leading to important changes in the effectiveness of processes like tritium diffusion and release.

The need to understand the Tritium behaviour during reactor operation brings to the necessity of study the main properties and the microstructure of these ceramics. The detailed diffusion pathways of Li in the bulk and the occupancy of the ion in the lattice as well as the influence of the defects are critically important for understanding the ceramic behaviour. If the blanket zone changes its insulating behaviour, electrical and magnetic fields may cause a closed electrical circuit, thus affecting to the shielding role of the TBM.

The electrical measurements represent therefore, a useful implement for the analysis of physico-chemical processes and the degradation occurring during irradiation [[i],[ii]]. The Electrochemical Impedance Spectroscopy (EIS) is chosen as a non-destructive tool to elucidate transfer mechanisms and dynamics of the principal charge carrier, presumed to be the Li^+ [[iii],[iv]], although the other ions (like O) may be mobile to a certain extent. It represents a simple and roughly technique with the great advantage of being performed *in-situ* during irradiation.

Starting from Li_4SiO_4 fabricated in our laboratories by two synthesis methods, the ceramics were irradiated by a ^{60}Co source at different doses, from 0,5 MGy to 13MGy. The γ-ray bombardment was performed at room temperature (30 ºC +/- 2 ºC) in a sample holder immersed in dry nitrogen or only in one case, at 250 ºC by a thermocouple controlled oven. After irradiation all the samples became darker along the entire volume.

The EIS measurements were carried out using a frequency analyser model Solartron 1255B with platinum as blocking electrodes, all inserted in a tubular oven varying the temperature between 20 ºC and 800 ºC, over a frequency range from 0.1 Hz to 10^9 Hz. The conductivity measurements were taken after 15 minutes stabilization heating ramps.

The bulk conductivity at 26 ºC in as-prepared conditions is of 3,16 x 10^{-8} S/cm and it slightly increases with irradiation damage (i.e.: 1,68 x 10^{-7} S/cm for 15 MGy of irradiation-doses).

The conductivity rises with temperature, as expected when phonon lattice movements together with point defects are considered [v].

In the case of 0,5 MGy irradiated ceramics, the electrical tests were performed on compressed pebbles fabricated by Spray Dryer method and compared to sintered pellets fabricated by rotary-evaporator route.

The thermal annealing processes brought to a recombination of defects through the movement of charge carriers, implying a slight difference between the electrical conductivity in as prepared and damaged samples.

The electrical behaviour of SiO_2 was also studied. Observing the bulk conductivity it is evident that even presenting at room temperature an insulating behaviour, with a value of 6,8 x 10^{-8} S/cm likewise the orthosilicate one, the energy provided by thermal activation does not imply a great increase in ionic movement, confirming the charge carrier role of Li^+ (and possibly Li^{2+}) ions under thermal excitation [vi].

At relatively low temperatures grain boundaries (GB) diffusion is mediated by the motion of individual point defects. The point defect dominating the diffusion depends on several factors such as the GB structure, the temperature and even the diffusion direction [vii]. In the low temperature regime, few diffusive events dominate the overall conductivity with the result that the GB diffusion coefficient follows the Arrhenius law and determines the entire process.

The change in charge state given by the gamma irradiation alters the electrical properties, actually one of the phenomenon largely studied in insulators is the Radiation Induced Conductivity (RIC). Structural imperfections in the crystal, such as impurities, create trapping sites for the diffusing electrons and holes which further modify the electrical conductivity behavior.

The increases in the RIC (Radiation Induced Conductivity) observed with increasing temperature are attributed to the thermal release of electrons from shallow and deep electron traps [viii]. Decrease in the conductivity with high gamma doses are then attributed to a release of trapped holes and a subsequent quenching of the conductivity trough the recombination of these holes with irradiated electrons.

Following Mott predictions [ix] it is possible to propose a model in which charge is transported by the thermally assisted hopping of electrons between states localized near randomly distributed traps, created as by the introduction of impurities during fabrication process as by electrical damage.

The information about structural changes under irradiation and the comparison with silica samples, confirms the hypothesis of Li^+ as charge carriers. Since the diffusion of tritium is not interstitial but is related to the creation of Li vacancies, the rate of occurrence of such vacancies determines the diffusion of already formed tritium. Its movement at high doses can be expected to lag Li diffusion by a complex hopping process which results in a lower diffusion coefficient.

The correlation between the annihilation process of irradiation defects and the tritium release in irradiated solid breeder materials is been reported by several authors [x] and here confirmed, making of EIS measurements a powerful tool for the *in-situ* characterization of breeding blanket materials in Fusion technology.

---

i E. H. Farnum et al.; *RADIATION-INDUCED ELECTRICAL DEGRADATION EXPERIMENTS IN THE JAPAN MATERIALS TESTING REACTOR*; J. of Nucl. Mat., 228 (1996),117-128.

ii O.D. Slagle et al.; *The FUBR-1B irradiation experiment — Tritium release and physical stability of solid breeder materials;* J. of Nucl. Mat.,843 (1991), 179-183.

iii F. Alessandrini et al.; *In-situ tritium release (CORELLI-2 experiment) and ex-reactor ionic conductivity of substoichiometric LiAlO2 breeder ceramics;* J. of Nucl. Mat., 224 Is. 3 (1995), 236–244.

iv Th. Fehr, E. Schmidbauer; *Electrical conductivity of Li2TiO3 ceramics*; Solis State Ionics, 178 (2007), 35-41.

v J.W. Fergus; *Ceramic and polymeric solid electrolytes for lithium-ion batteries*; J. of Power Sources, 195, No. 15. (2010), 4554-4569.

vi E. Feldbach et al.; *Low-temperature irradiation effects in lithium orthosilicates*; NIMB 250, 1-2. (2006), 159-163.

vii A Suzuki, Y Mishin; *Atomic mechanisms of grain boundary diffusion:Low versus high temperatures*; J. Mater Sci., 40 (2005), 3155-3161.

viii R.W.Klaffky, B.H. Rose, A.N. Goland, G.J. Dienes; *Radiation-induced conductivity of Al2O3: Experiment and theory;* Phys. Rev. B, 21 (1980), 3610-3634.

ix N.F. Mott; *Conduction in glasses containing transition metal ions;* J. of Non-Cryst. Sol.,1, (1968), 1-17.

x Y. Nishikawa et al.; *Correlation between tritium release and thermal annealing of irradiation damage in neutron-irradiated Li2SiO3*; J. of Nucl. Mat., 367-370 (2007), 1371-1376.

Ceramic Breeder Blanket Interactions 12-14 September 2013, Barcelona, Spain

Correlation between electrical behaviour and tritium release in γ-irradiated Li_4SiO_4 breeder pellets and pebbles.

E.Carella[1], M.T. Hernandez[1], A.Ibarra [1], E.Chinarro[2], B.Moreno[2]

[1]LNF-CIEMAT, Materials for Fusion Group Madrid, Spain

[2]ICV-CSIC, Glass Department, Madrid, Spain

Outline

- An indirect monitoring of Tritium Breeding Ratio (TBR).
- Overview of Li_4SiO_4 electrical behaviour under different conditions:
  - synthesis method,
  - calcination status,
  - damage conditions.
- Study and understand lithium kinetics.

Why Electrical properties?

Besides the main task to produce Tritium, the BBs must exhibit a long-term stability.

Electrical properties are of great importance concerning the degradation BBs can suffer in fusion reactors during plasma operations but also regarding the tritium behavior.

elisabettacarella@gmail.com

Tritium Breeder Ratio

A key parameter for talking about reactor Tritium self-sufficiency is the Tritium Breeder Ratio (TBR)

$$\text{TBR} = \frac{\text{Tritium generated in Breeder Blanket}}{\text{Tritium consumed in plasma}}$$

The TBM Tritium production & predictability will be validated experimentally under ITER environmental conditions.

..meanwhile

SOME INDIRECT MEASUREMENTS

	HCPB
^6Li enrichment in breeder	40% ^6Li for Li_4SiO_4 70% ^6Li for Li_2TiO_3 (Pack. Fraction ~63%)
Breeder radial depth	460 mm
Tritium Breeding Ratio	TBR = 1.14

elisabettacarella@gmail.com

Electrical properties as an indirect measurement

The migration of the T is assumed to occur by hopping from O to O ion in lattice, having to overcome the barrier of electrostatic repulsion due to Li ions.
Since the Li is supposed to migrate through vacancy mechanism and considering its transmutation, then the repulsive force decreases and the T can easily migrate.
So the lithium ion conductivity → the tritium diffusion.

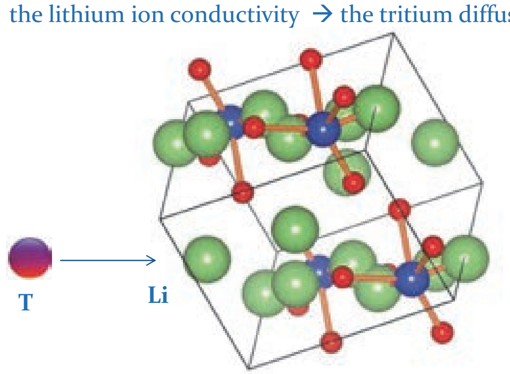

Monoclinic structure, with isolated SiO_4 tetrahedra and Li atoms floating around them

Ceramic Breeder Blanket Interactions 12-14 September 2013, Barcelona, Spain

So, what is EIS?

Probing an electrochemical system with a small ac-perturbation, $V_o \cdot e^{j\omega t}$, over a range of frequencies.
The **impedance** (resistance) is given by:

$$Z(\omega) = \frac{V(\omega)}{I(\omega)} = \frac{V_0 \; e^{j\omega t}}{I_0 \; e^{j(\omega t + \varphi)}} = \frac{V_0}{I_0}[\cos\varphi - j\sin\varphi]$$

$\omega = 2\pi f$
$j = \sqrt{-1}$

The magnitude and phase shift depend on frequency.

Also: **admittance** (conductance), inverse of impedance:

$$Y(\omega) = \frac{1}{Z(\omega)} = \frac{I_0 \, e^{j(\omega t + \varphi)}}{V_0 \, e^{j\omega t}} = \frac{I_0}{V_0}[\cos\varphi + j\sin\varphi]$$

"real +j·imaginary"

A parallel R-C combination

The parallel combination of a resistance and a capacitance, start in the admittance representation:

$$Y(\omega) = \frac{1}{R} + j\omega C$$

Transform to impedance representation:

$$Z(\omega) = \frac{1}{Y(\omega)} = \frac{1}{1/R + j\omega C} \cdot \frac{1/R - j\omega C}{1/R - j\omega C} =$$

$$\frac{R - j\omega R^2 C}{1+\omega^2 R^2 C^2} = R\frac{1-j\omega\tau}{1+\omega^2\tau^2}$$

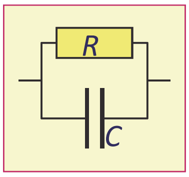

A semicircle in the impedance plane!

Cole–Cole (Nyquist) Diagram

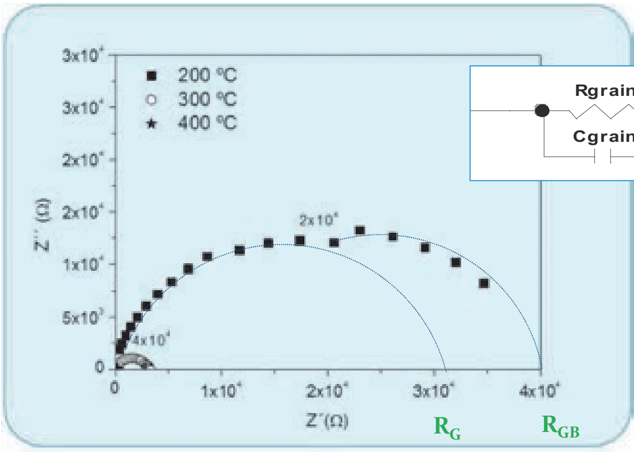

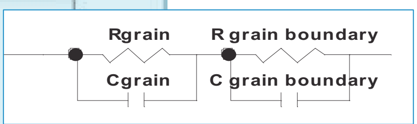

Arrhenius plot of the bulk conductivity

Starting from the sample dimension (S and A), it is possible to find an Arrhenius relation between the conductivity and the temperature:

$$\sigma \approx \sigma_o \exp(-E_A/KT)$$

↓

$$\ln \sigma = -\frac{E_A}{KT} + ln\sigma_0$$

From which we obtain the activation energy of the electrical conduction process.

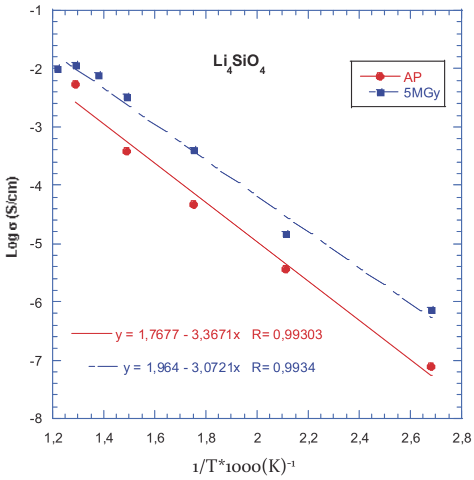

Ceramic Breeder Blanket Interactions 12-14 September 2013, Barcelona, Spain

Electrical Impedance Spectroscopy

The silver electrodes by a high conductivity paste.
A sample holder temperature range: from RT to 800 ºC.
Frequency analyser (Solartron 1255B) between 0,1 Hz and 10^9 Hz.
The conductivity measurements were taken after each 15 min/stabilized heating ramp.

The EIS spectra were fitted using the “EQUIVCRT” (Equivalent Circuit Programme)
The software required the knowledge of the geometry of the sample: its thickness and surface area.

Electrical Impedance Spectroscopy system

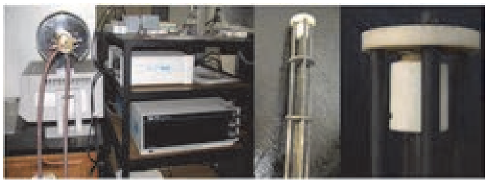

LNF-CIEMAT laboratories: 2 fabrication routes

Gel $SiO_2 + Li_3C_6H_5O_7$

$xC_8H_{12}O_8Si + xC_2H_3O_2Li$

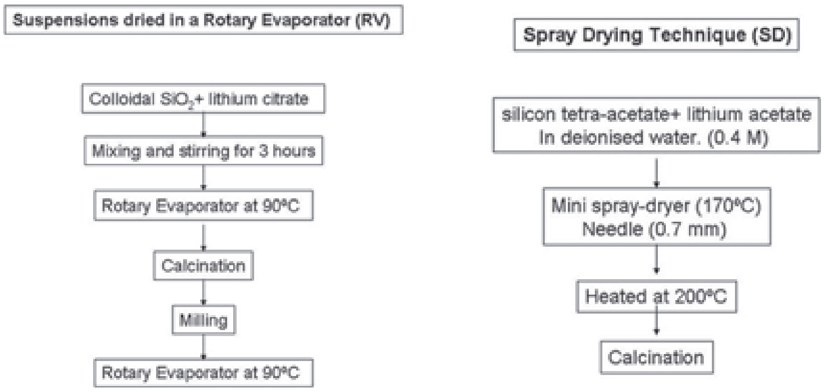

Flow chart for the preparation of **Li4SiO4** powders

Comparison between fabrication methods

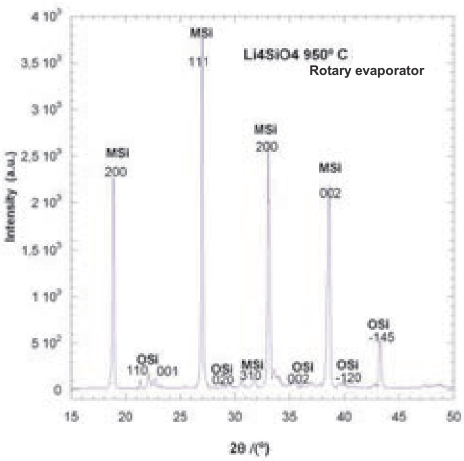

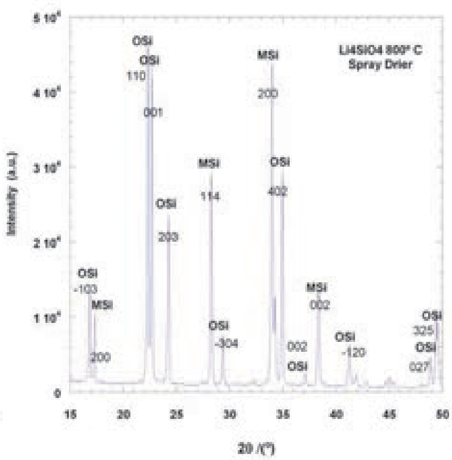

Comparison between fabrication methods

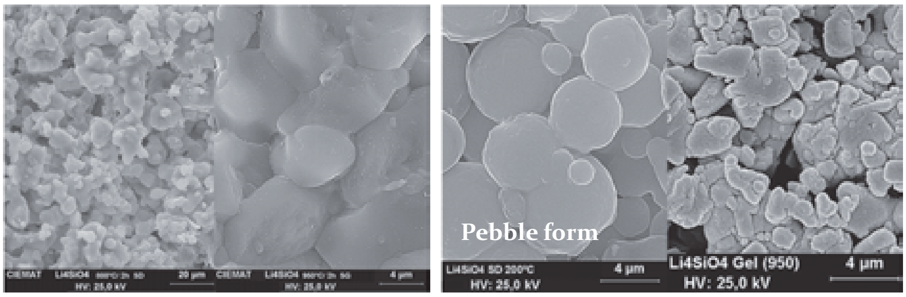

Suspension in RV **Spray drying**

Gamma-irradiation

Nayade irradiation pool
[60] Co source with a rate of 6Gy/s (30 ºC +/- 2 ºC) in a sample holder immersed in dry nitrogen or, only in one case, at 250 ºC by a thermocouple controlled oven

ATR-IR spectra:
Slow change in vibrational band →
No phase neither metamorphic transformation

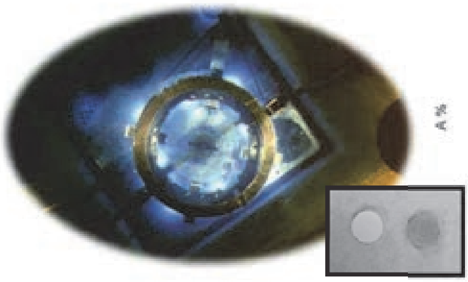

Before – After

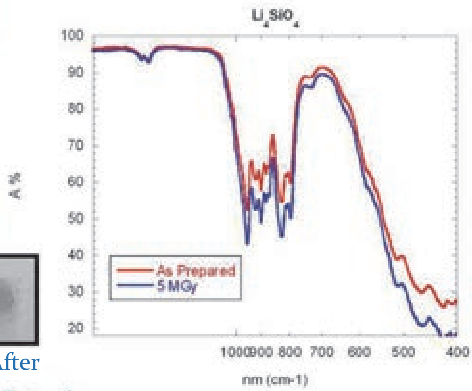

Comparison between fabrication methods

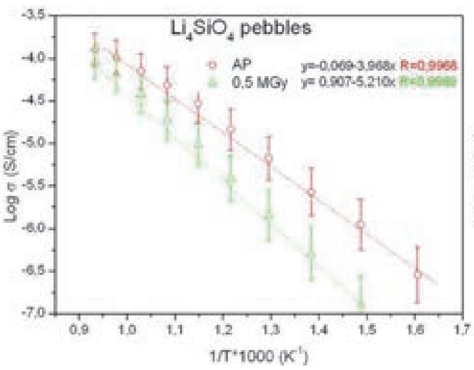

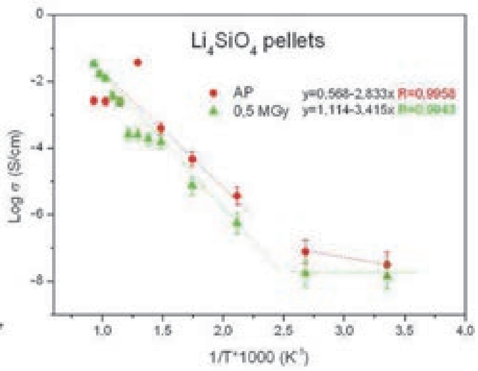

Li_4SiO_4	Pebbles	Pellets	Pebbles + 0.5 MGy	Pellets + 0.5MGy
E_A (eV)	0.78	0.57	1.03	0.71
σ(S/cm) (400 ºC)	$1.12*10^{-6}$	$1.30*10^{-3}$	$1.25*10^{-7}$	$3.11*10^{-4}$

Gamma damage at different doses

Li_4SiO_4	5MGy	10MGy	13MGy	AP
E_A (eV)	0,62	0,64	0,65	0,66

Constant activation energy

Same conduction mechanism!

Top at 5 MGy!

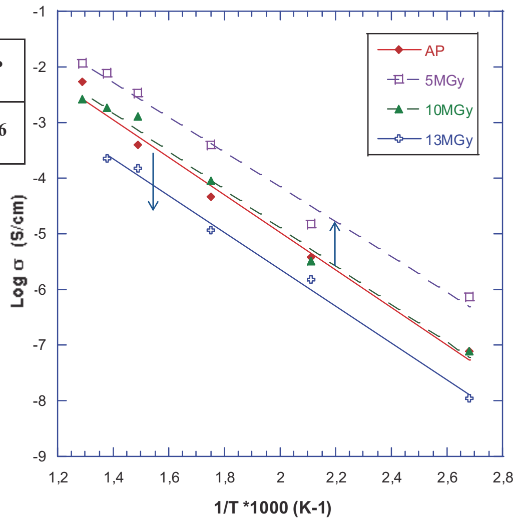

Reproducibility

The electrical damage is permanent

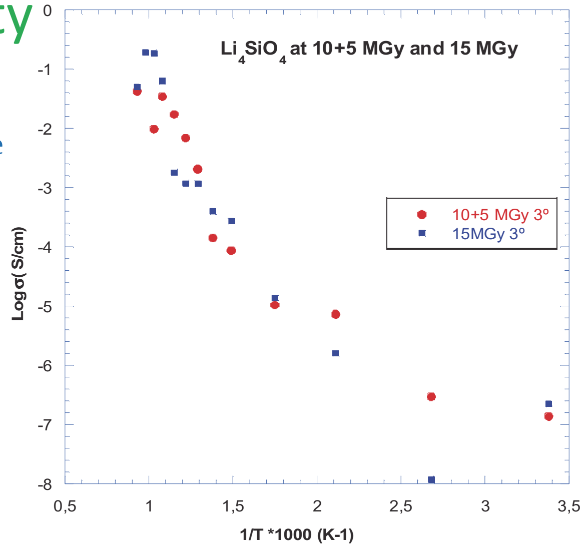

elisabettacarella@gmail.com

Ceramic Breeder Blanket Interactions 12-14 September 2013, Barcelona, Spain

Temperature effect

The value of σ decrease with thermal treatment (250ºC) → it is facilitate the defect recombination!

The electrical conductivity mechanism does not change → Same E_A

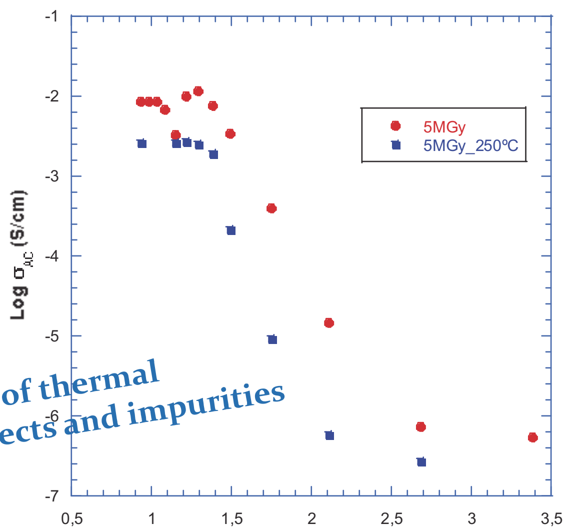

Relocation effect of thermal annealing on defects and impurities

elisabettacarella@gmail.com

SiO_2 vs Li_4SiO_4 behaviour

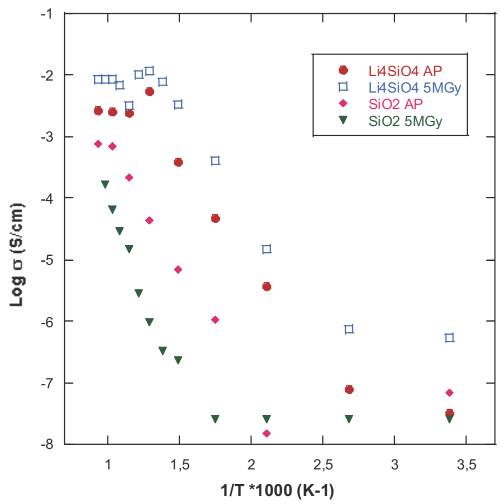

OSi follows silica conduction model

y = 0,30199 - 2,598x R= 0,93837

y = 0,32529 - 2,1626x R= 0,8897

y = 0,90204 - 4,0613x R= 0,99537

y = 0,86232 - 5,0433x R= 0,97589

E_A values:
Li4SiO4≈ 0,48 eV
SiO2 ≈0,89 eV

Li atoms are able to move easily

Ceramic Breeder Blanket Interactions 12-14 September 2013, Barcelona, Spain

Over stoichiometric ceramics

Ceramics with different Li:Si proportion

Light ions are responsibles of electrical conductivity variation

Thermal assisted HOPPING of charge between states localized near randomly distributed traps [*]

Correlation with tritium behavior

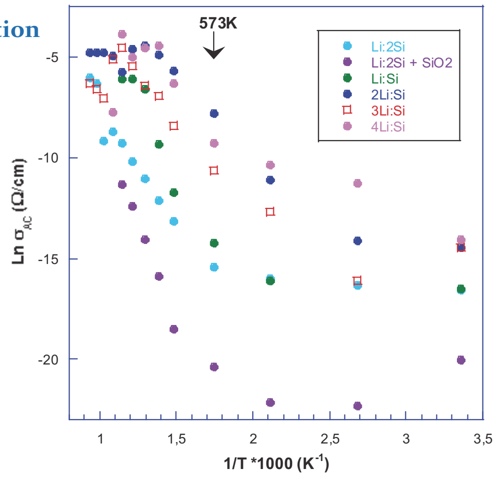

* N.F. Mott, *J.Non-cryst. Sol.1* (1968)

Conclusions

- Electrical conductivity is caused by lithium- ions diffusivity.
- A good electrical recombination is found under gamma irradiation, confirming a nice Li_4SiO_4 physico-chemical stability.
- The change in charge state given by γ-irradiation (Radiation-induced electrical degradation) is attributed to the thermal release of charge from shallow and deep electron traps.
- As previously observed (Ohno et al. 1985) a relation between the tritium diffusion and the Lithium behaviour could be find.
- EIS technique is a cheap, easy and useful tool for Ceramic Breeder Blanket electrical characterization.

TOPICAL DISCUSSION: NEW MATERIAL PRODUCTIONS (summarized by R. Knitter)

The following issues were discussed under this topic:

(1) What do we want to test in the first TBM phase?

The electromagnetic phase is only interesting for the liquid breeder concept. There are no criteria, i.e. no explicit specification for the breeder material. Yet, safety issues have to be considered, such as clogging of the purge gas by possibly generated ceramic powder (dust).

ITER is the first step to DEMO and will generate important data to evaluate the TBM concepts. ITER is a unique opportunity for the testing and evaluation of the TBMs.

(2) Selection of the breeder material

Lithium orthosilicate and lithium metatitanate are the materials considered as solid breeders for ITER. All ITER partners selected a so called reference material for their TBM, however, most of them also consider the other material as a back-up alternative. Lithium orthosilicate is the reference material for Europe, China and Korea, and the TBM designs are based on the properties of this material. However, lithium metatitanate may be considered because of its inherent, higher mechanical strength.

(3) Neutron irradiation experiments

All newly developed ceramic breeder materials have to be investigated under neutron irradiation to check their in-pile performance and particularly the tritium release/retention behavior. However, there is only very limited access to suitable reactors and neutron sources. Russia is planning to irradiate pebble bed assemblies (PBA) with the focus on safety issues and tritium inventory.

(4) Lithium enrichment

Presently most of the partners are not well prepared to provide enriched lithium. The US possess a relatively large storage of enriched lithium, and they may be willing to provide Li-6 for the fabrication of enriched ceramic breeder pebbles.

(5) Joint meeting day with beryllium workshop

Several aspects of the development of functional materials are of interest for both, the multiplier and the breeder community. It was therefore proposed to organize the workshops at the same location and the same time to enable a joint meeting day of CBBI and Be workshops in the future.

TOPIC 2: PEBBLE BED PROPERTIES

A study on fluid flow of helium purge gas with tritium transfer released from lithium titanate in a solid breeder test blanket module.

Y. Seki[1], M. Enoeda[1], S. Fukada[2]

1: *Japan Atomic Energy Agency, Naka-shi, Ibaraki-ken, 311-0193 Japan, seki.yohji @jaea.go.jp*
2: *Kyushu University, Fukuoka-shi, Fukuoka-ken, 812-8581, Japan*

Development of Water Cooled Solid Breeder (WCSB) TBM is being performed as the primary candidate of ITER Test Blanket Module (TBM) of Japan. Prior to the installation of each TBM, it is necessary to develop the capability of the analyses of all essential functions of the blanket, because the validation of the analyses tools by the TBM performance data under the real fusion environment of ITER enables extrapolation of the design and performance analyses to DEMO blanket. Especially the prediction tool of tritium concentration in the blanket system is one of the most important issues to control tritium recovery. From this view point, this paper discusses the flow phenomena of the helium purge gas in the pebble bed. A purpose of our research is to establish and verify a method for a prediction of the flow of the helium purge gas in the pebble bed. Moreover, the database contributes to the total tritium behavior simulation taking into account all essential tritium transfer process.

The pressure drop (ΔP) of the purge gas in the breeder pebble bed experimentally has been studied, using pebble bed of comparably-size of the TBM as shown in Fig. 1. Two cross-section shapes for containers of pebbles are applied. One is simple rectangle and the other is rectangle-shaped with pipe-laying. A Cross-section area and a flow length of two containers are same values, 3864 mm^2 and 500 mm, respectively. Breeder pebbles (Li_2TiO_3, diameter of 1 mm) which will be used in TBM were packed in the containers. The packing factors in containers were obtained as 65.4% for the simple rectangle and as 64.4% for the rectangle-shaped with pipe laying one. The range of the flow rate of helium purge gas in room temperature is set to be up to 100 L/min. Figure 2 shows the experimental result. It indicates that the laminar flow is dominant. Reliability of the prediction ability of the ΔP derived from Ergun's equation was validated by this experiment within the flow rate which is less than 40 L/min and also less than 2.9 of the Reynolds number normalized by the pebble-diameter. On the other hand, slight difference between the experimental result and the Ergun's equation appears within the range of flow rate from 40 L/min to 100 L/min. However, the results demonstrated that prediction accuracy of ΔP calculated by Ergun's equation and general formulae such as the laminar flow is enough for contribution to the engineering design of the blanket up to flow rate of 100 L/min as to be applied to the TBM from 40 to 50 L/min.

It is necessary to further investigate the effect of near-wall packing fraction to efficiently recover tritium and to predict permeation. A preliminary experiment with using a particle imaging velocimetry (PIV) has been started to demonstrate a flow distribution near the wall and at the center of pebble bed as shown in Fig. 3.

A numerical simulation for the flow of water through the pebble bed also has been performed to predict a velocity in the pebble bed and to be compared to the PIV data. Figure 4 shows the calculated velocity field in the pebble bed. It indicates that the magnitude of the velocity near the wall is larger than that in the center of the pebble bed. From the point of view of the empirical equations, the preferential flow-path is also indicated by the prediction of the larger porosity near the wall than that in the center of pebble bed.

For building the integrated simulation approach of heat and mass transfer in whole domain of the blanket, this study achieved to recognize the flow phenomena with tritium in the pebble bed. Consequently, the results of the experiment and the numerical simulation contribute to establishment of the prediction method of the total tritium behavior simulation taking consideration into all essential tritium transfer process for an engineering design of a blanket.

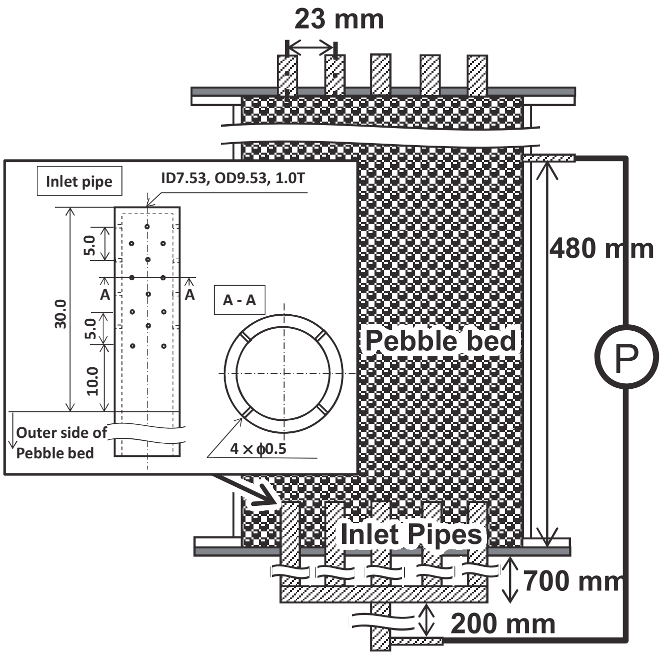

Fig. 1 Experimental apparatus to measure the pressure drop of helium purge gas passing the pebble bed.

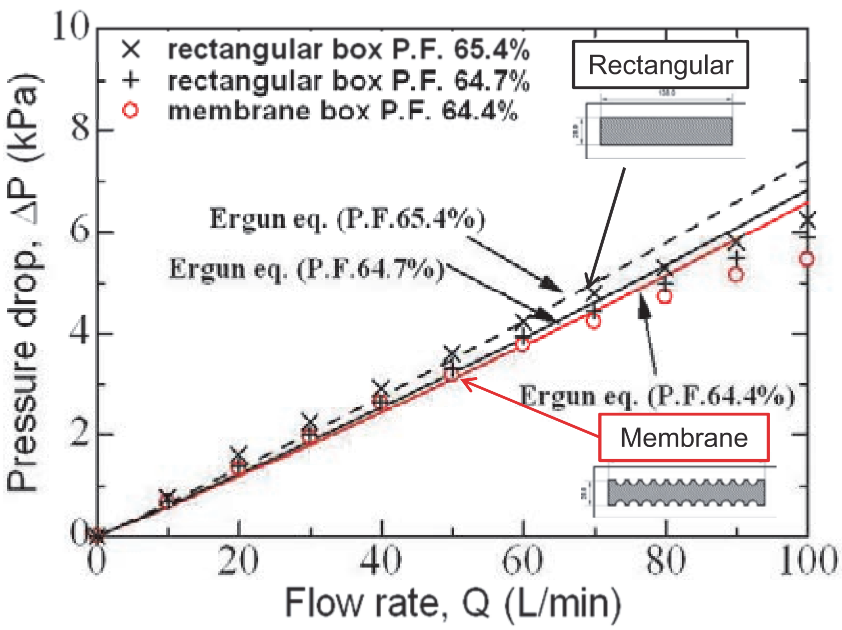

Fig. 2 Dependence of pressure drop on cross-section shape of container.

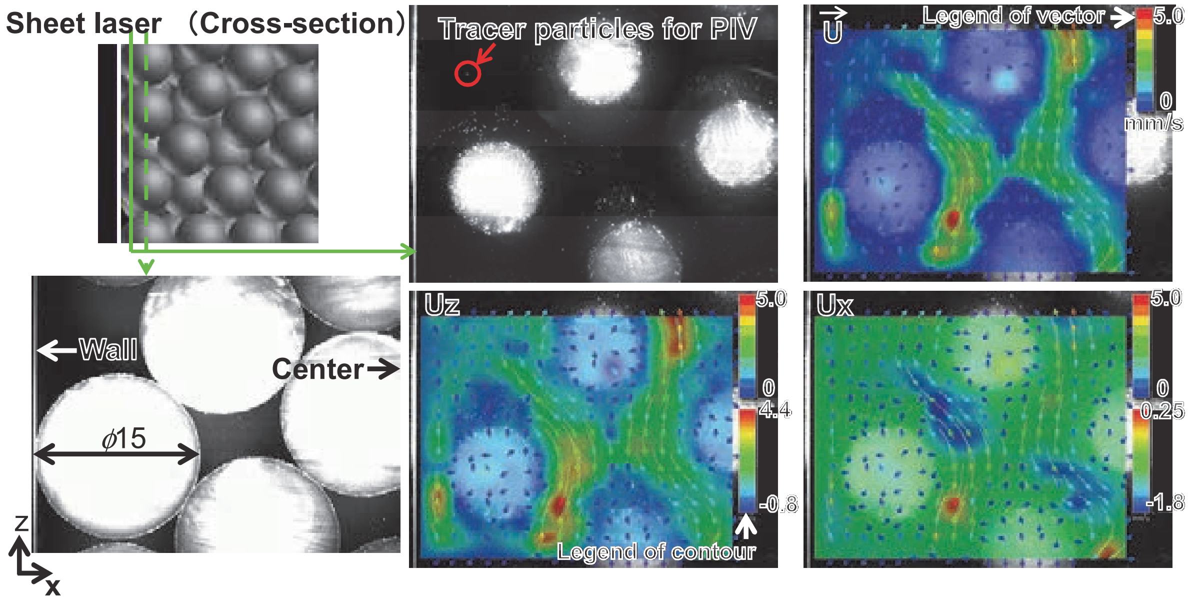

Fig. 3 Visualization of flow phenomena in pebble bed

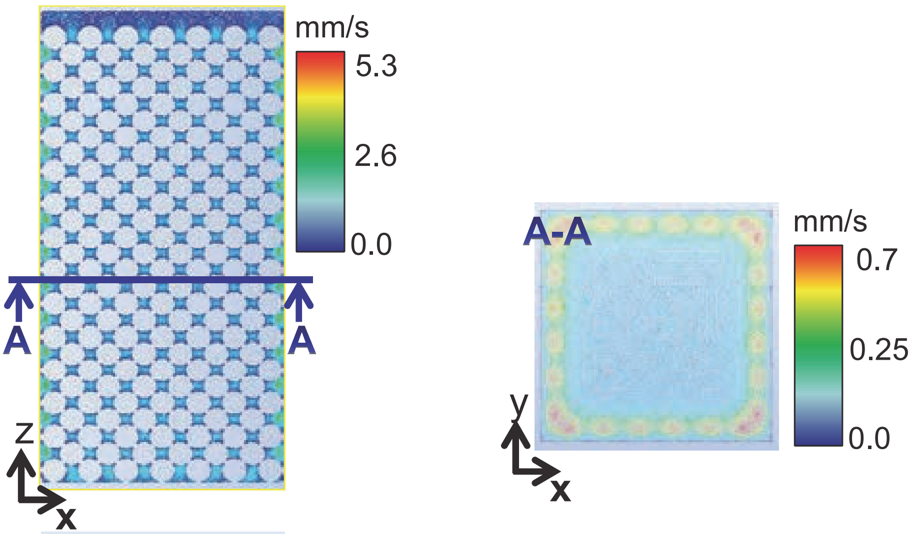

Fig. 4 3-D numerical simulation for the water flow in pebble bed

A study on fluid flow of helium purge gas with tritium transfer released from lithium titanate in a solid breeder test blanket module

17th International Workshop on Ceramic Breeder Blanket Interactions (CBBI-17),
Barcelona, Spain
13 September 2013

Y. Seki (Japan Atomic Energy Agency)
M. Enoeda (Japan Atomic Energy Agency)
S. Fukada (Kyushu Univ.)

(Contact: seki.yohji@jaea.go.jp)

Outlines

- Background and objective
  - Scope of this work
- Experimental study of a pressure drop in the breeder pebble bed
  - Check the pressure drop estimated by Ergun's equation
  - Dependence of the pressure drop on cross-section shape of container
- 2-D Analysis of behavior of He purge gas in breeder pebble beds
  - Numerical simulation for Darcy flow in porous media
- Verification test of flow distribution in the pebble bed
  - Experimental equipment for PIV in Mexflon's pebble bed
  - Visualization of flow phenomena in pebble bed
  - Verification test with a use of 3-D numerical simulation
- 3-D numerical simulation in pebble bed to predict flow and tritium transfer.
- Conclusions

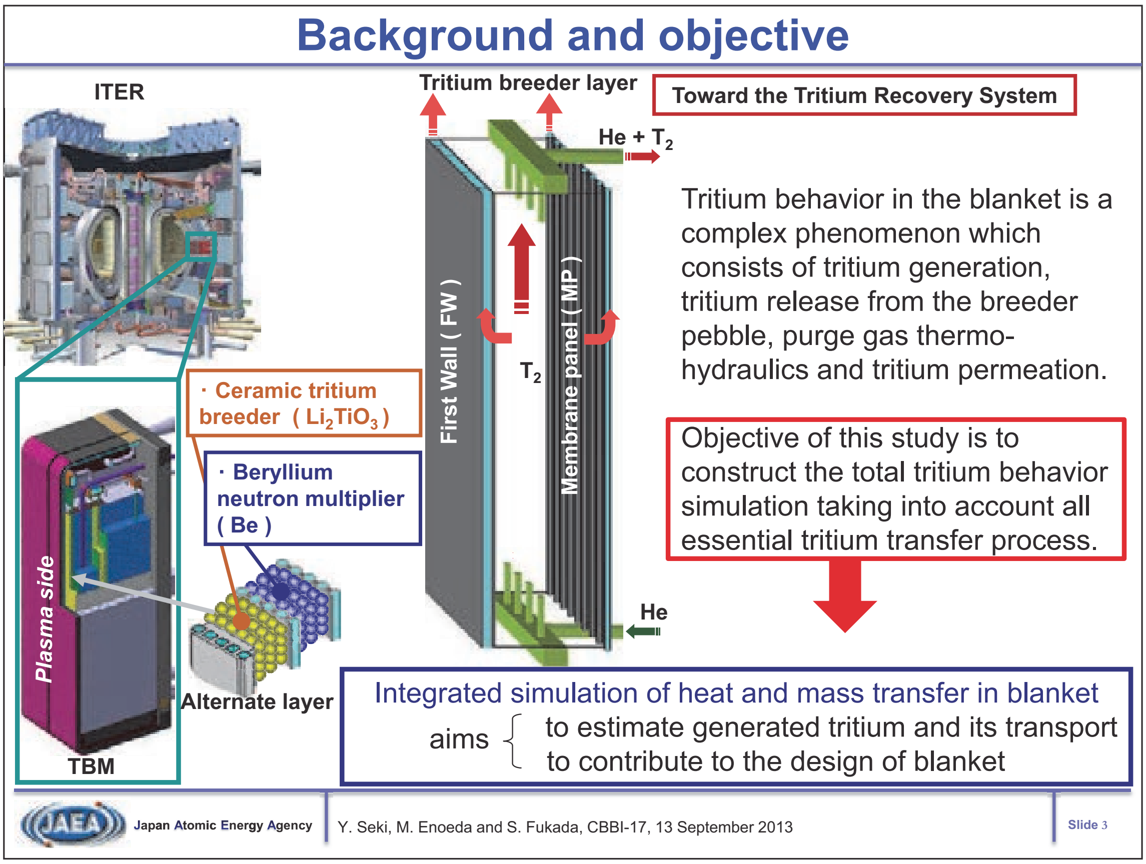
Background and objective
ITER
Tritium breeder layer
Toward the Tritium Recovery System
He + T_2
Tritium behavior in the blanket is a complex phenomenon which consists of tritium generation, tritium release from the breeder pebble, purge gas thermo-hydraulics and tritium permeation.
First Wall (FW)
Membrane panel (MP)
T_2
· Ceramic tritium breeder (Li_2TiO_3)
· Beryllium neutron multiplier (Be)
Objective of this study is to construct the total tritium behavior simulation taking into account all essential tritium transfer process.
Plasma side
He
Alternate layer
TBM
Integrated simulation of heat and mass transfer in blanket
aims
to estimate generated tritium and its transport
to contribute to the design of blanket
Japan Atomic Energy Agency
Y. Seki, M. Enoeda and S. Fukada, CBBI-17, 13 September 2013
Slide 3

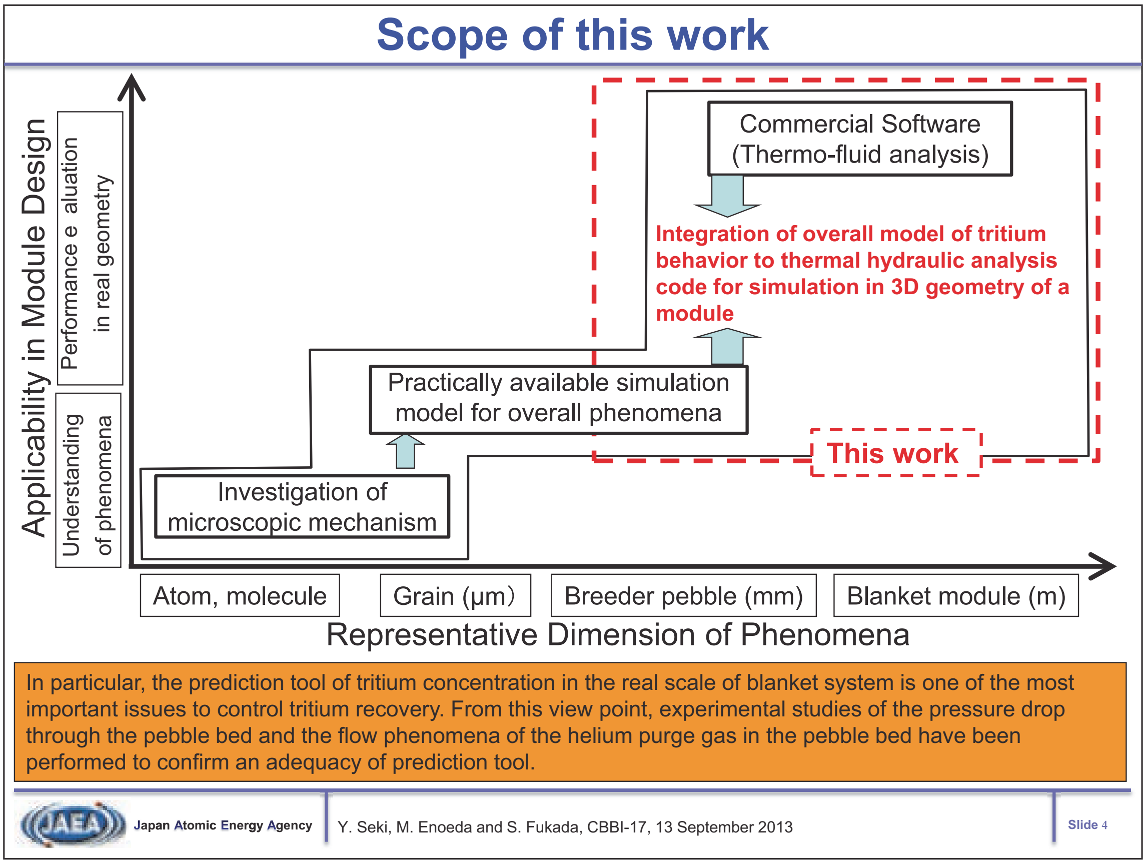
Scope of this work
Applicability in Module Design
Performance e aluation in real geometry
Understanding of phenomena
Commercial Software (Thermo-fluid analysis)
Integration of overall model of tritium behavior to thermal hydraulic analysis code for simulation in 3D geometry of a module
Practically available simulation model for overall phenomena
This work
Investigation of microscopic mechanism
Atom, molecule
Grain (μm)
Breeder pebble (mm)
Blanket module (m)
Representative Dimension of Phenomena
In particular, the prediction tool of tritium concentration in the real scale of blanket system is one of the most important issues to control tritium recovery. From this view point, experimental studies of the pressure drop through the pebble bed and the flow phenomena of the helium purge gas in the pebble bed have been performed to confirm an adequacy of prediction tool.
Japan Atomic Energy Agency
Y. Seki, M. Enoeda and S. Fukada, CBBI-17, 13 September 2013
Slide 4

Outlines

- Background and objective
  - Scope of this work
- Experimental study of a pressure drop in the breeder pebble bed
  - Check the pressure drop estimated by Ergun's equation
  - Dependence of the pressure drop on cross-section shape of container
- 2-D Analysis of behavior of He purge gas in breeder pebble beds
  - Numerical simulation for Darcy flow in porous media
- Verification test of flow distribution in the pebble bed
  - Experimental equipment for PIV in Mexflon's pebble bed
  - Visualization of flow phenomena in pebble bed
  - Verification test with a use of 3-D numerical simulation
- 3-D numerical simulation in pebble bed to predict flow and tritium transfer.
- Conclusions

Experimental study of pressure drop in pebble bed

Issues

- To prevent obstruction in a purge gas pipe and the pebble bed.
- Suppression of tritium permeation

Selection of pump head by an estimation of pressure drop in pebble bed.

Objective of this experiment to measure the pressure drop in pebble bed

- Verification of accuracy of Ergun's equation.
- Dependence of pressure drop on cross-section shape of container.

The experiment provides

- that the pressure drop from Ergun's equation and general formulae is enough for contribution to the engineering design of the blanket.
- to build database of a pressure drop for contribution to the tritium recovery system

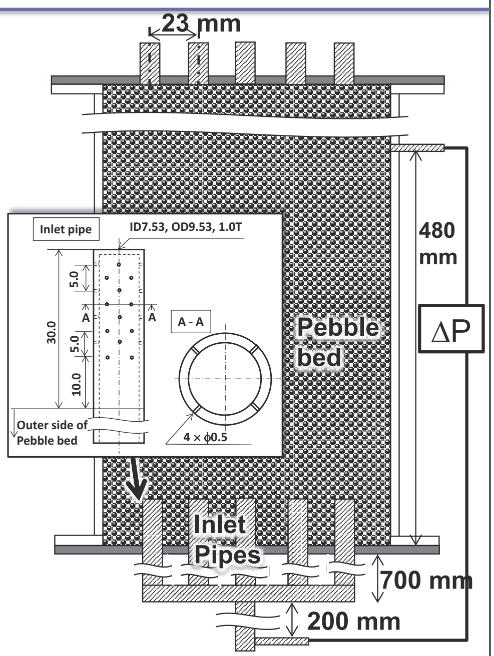

Experimental apparatus to measure the pressure drop of helium purge gas passing the pebble bed.

Experimental study of pressure drop in the breeder pebble bed

Estimation of pressure drop of purge gas through a porous media

Motion equation of fluid in porous media

$$\rho\frac{\partial v_{si}}{\partial t}-\rho(v_{si}\cdot\nabla)\left(\frac{v_{si}}{\varepsilon}\right)=\boxed{-\nabla(\varepsilon p)}-[\nabla\cdot\varepsilon\tau_i]+\rho\varepsilon g_i+\boxed{\varepsilon F_i}$$

Press. grad. External Force of Solid

Assuming steady state and uniform velocity

$$\frac{dp}{dx_i}=F_i$$

Ergun equation

$$F_i=\boxed{-\frac{150\mu}{{d_p}^2}\frac{(1-\varepsilon)^2}{\varepsilon^3}v_{si}}\boxed{-\frac{1.75\rho}{d_p}\frac{1-\varepsilon}{\varepsilon^3}|v_{si}|v_{si}}$$

Laminar term (Blake-Kozeny) Turbulence term (Burke-Plummer)

d_p : Diameter	g_i : Gravity force
ε : Porosity	τ_i : Shear stress
v_{si} : Darcy velocity, εv_i	ρ : Density
p : Pressure	v_i : actual velocity

The pressure drop of the purge gas in the breeder pebble bed experimentally has been studied, using pebble bed of comparably-size of the blanket module.

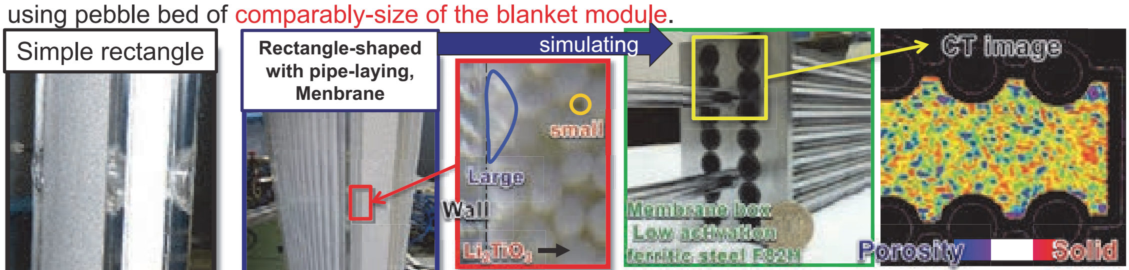

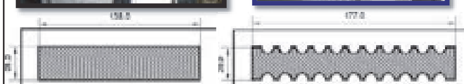

Porosity near the wall ε_w > Porosity at center ε_∞. Approximately, Porosity within $y/d_p<1/2$ is expressed as following:

$$\varepsilon_w=1-0.513\frac{D/d_p-7/8}{D/d_p-1/2}$$

P.F.64.7%, ε = 0.353,
ε_w = 0.492, ε_c = 0.346

H. Martin, Chem. Eng. Sci. 38, pp. 913, 1978 .

Estimation of pressure drop by a use of Ergun equation

ΔP inside the pebble bed of 64.7% P.F. without inlet pipes of the rectangular box

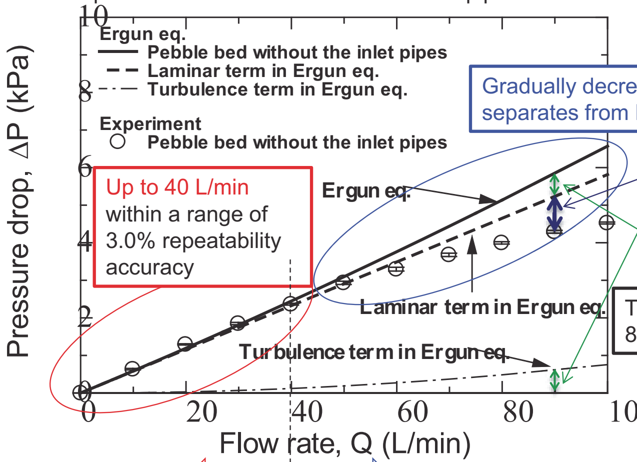

Cross section of Rectangular box

Laminar term is larger than experimental data.

Contribution of turbulence term

The ΔP of the laminar term constitutes 80% of total ΔP up to 80 L/min.

Good prediction ⇦ ⇨ Gradually decreases

$$\Delta P=\boxed{\frac{150\mu}{{d_p}^2}\frac{(1-\varepsilon)^2}{\varepsilon^3}v_{si}L}+\boxed{\frac{1.75\rho}{d_p}\frac{1-\varepsilon}{\varepsilon^3}|v_{si}|v_{si}L}$$

Laminar(Blake-Kozeny) Turbulence(Burke-Plummer)

The difference of ΔP between the experimental value and Ergun's prediction is caused by not only a lack of a contribution from the turbulent flow but also a basic flow phenomenon in pebble bed such as spatial distribution of flow rate in the cross section.

The ΔP predicted by Ergun eq. is able to apply to pebble beds within whole lines of the helium purge gas including tritium recovery system because the predicted ΔP is not underestimated.

Dependence of pressure drop on cross-section shape of container

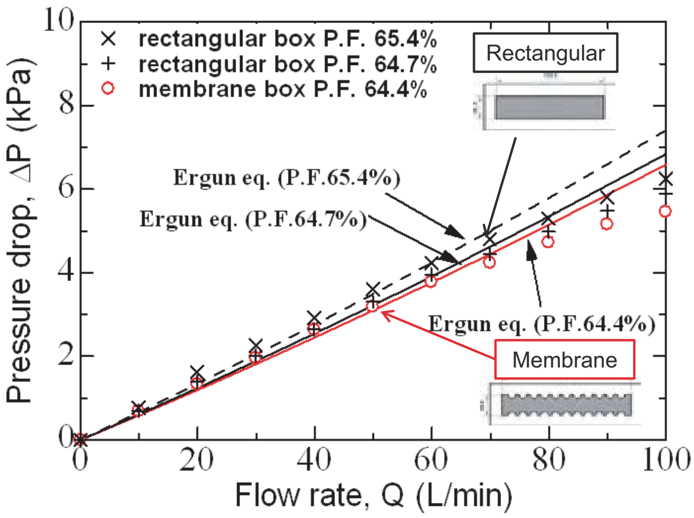

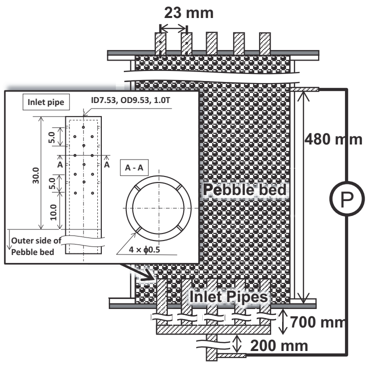

Experimental apparatus to measure the pressure drop of helium purge gas passing the pebble bed.

The ⊿P of the rectangular box is close agreement with that of membrane box. The reason of slightly difference of ⊿P is the result of the different P.F. It indicates that the geometric difference of the cross-sections does not significantly affect ⊿P.

This experiment demonstrated that prediction accuracy of ⊿P calculated by Ergun's eq. is enough for contribution to the engineering design of the blanket up to flow rate of 100 L/min without underestimation as to be applied to the TBM from 40 to 50 L/min.

Outlines

- Background and objective
  - Scope of this work
- Experimental study of a pressure drop in the breeder pebble bed
  - Check the pressure drop estimated by Ergun's equation
  - Dependence of the pressure drop on cross-section shape of container
- 2-D Analysis of behavior of He purge gas in breeder pebble beds
  - Numerical simulation for Darcy flow in porous media
- Verification test of flow distribution in the pebble bed
  - Experimental equipment for PIV in Mexflon's pebble bed
  - Visualization of flow phenomena in pebble bed
  - Verification test with a use of 3-D numerical simulation
- 3-D numerical simulation in pebble bed to predict flow and tritium transfer.
- Conclusions

2D-Computational Configuration

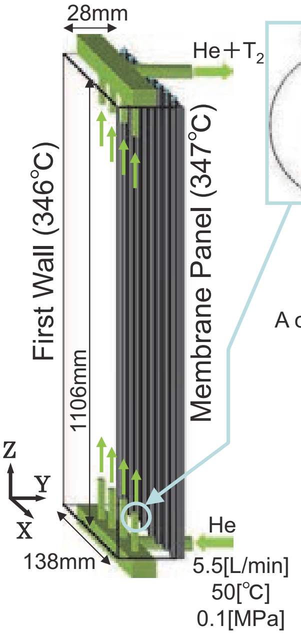

2 types for inlet and outlet

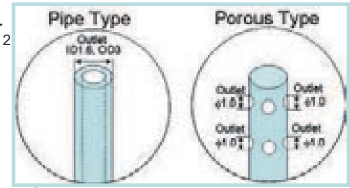

【Porous type】
number of inlet is 4.
A outlet is perforated cover plate.

- **porosity: 0.35**
- **Reynolds number:**

$$Re_p = \frac{u_m D_p}{\nu} = 0.3$$

u_m : Bulk mean velocity
D_p : Sphere Diameter (2mm)
ν : kinematic viscosity

Mesh

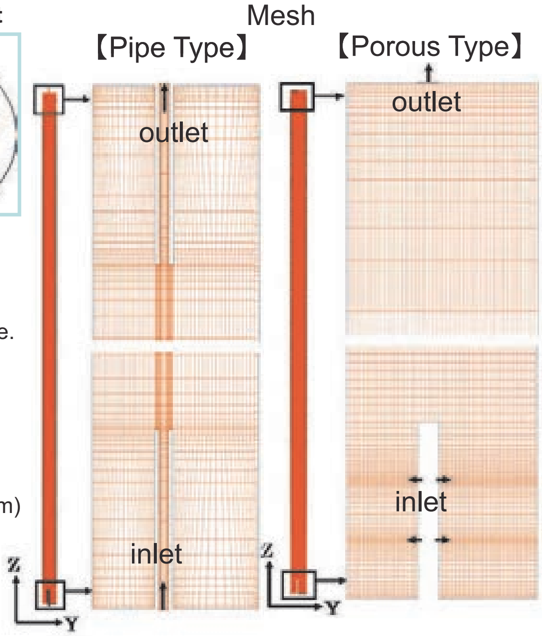

Different inlet and outlet types are applied.

Analysis results of velocity and tritium (T_2) concentration

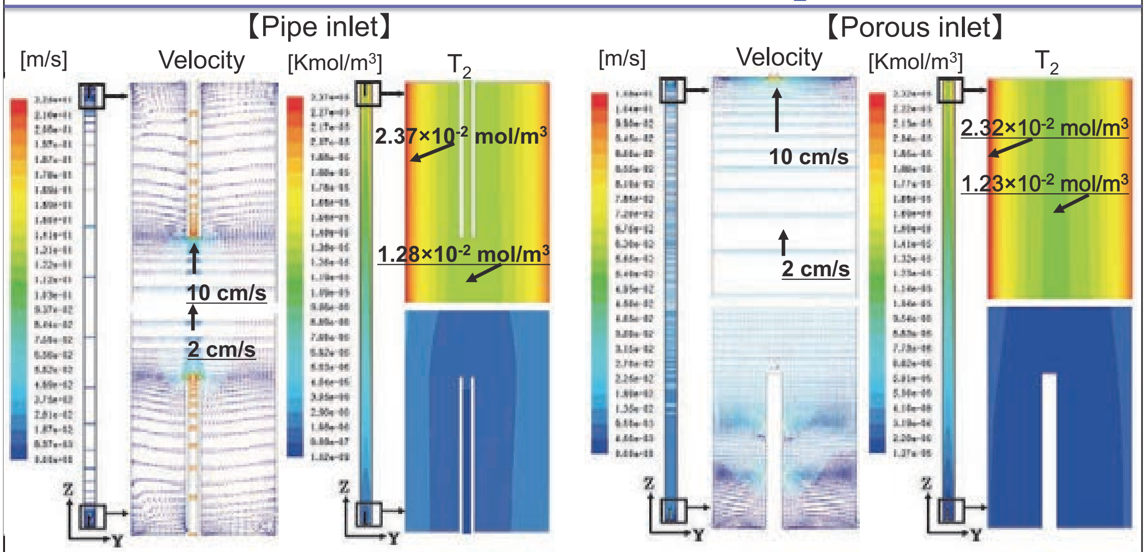

Convective diffusion → small
Molecular diffusion of T_2 → small

Especially, the high concentration of T_2 stays near the first wall and the membrane panel.

It is necessary to further investigate the effect of near-wall packing fraction. An experiment has been started to demonstrate a flow distribution near the wall and at the center of pebble bed.

Verification test of flow distribution in pebble bed

The flow in the porous media is simulated with the uniform porosity.
What is difference of flow field between in uniform porosity and in pebble bed?→ Different porosity
A detail flow distribution in a pebble bed is clarified by **Particle Imaging Velocimetry (PIV).**

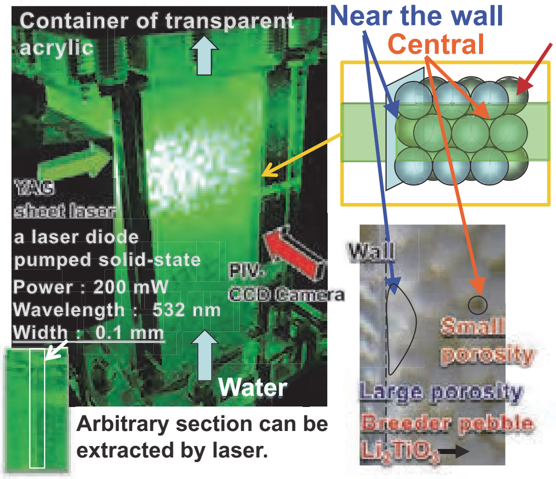

Refractive index of Mexflon (fluororesin) is identical to that of water to prevent loss of tracer particle caused by reflection of light. It adapts to PIV.

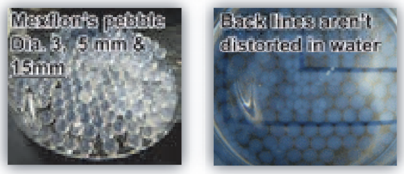

Visualization of flow in the pebble bed

⇩

Comparison between near wall flow rate and bulk pebble bed flow rate

⇩

Comparison with calculation

It is qualitatively well known that the velocity near the wall is larger than that at a center of pebble bed because of the different porosity. **It aims to compare velocity distribution near the wall and at a center of pebble bed with quantitative experimental data. Preliminary test for visualization of flow in the Mexflon's pebble bed has been performed by PIV.**

Visualization of flow phenomena in pebble bed

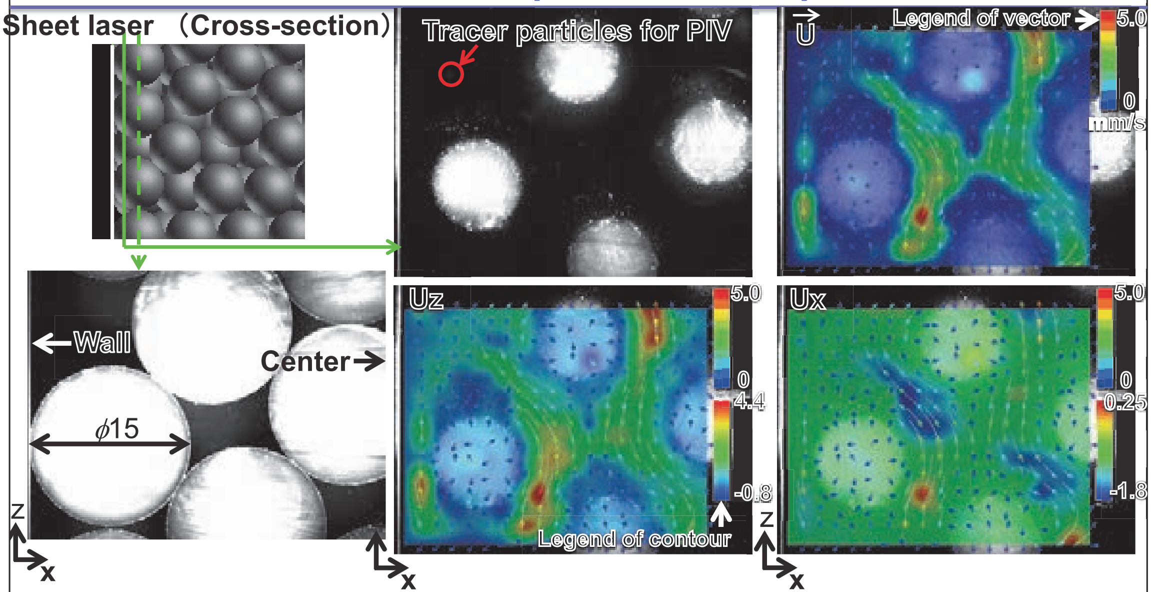

The velocity distributions are quantitatively obtained at near wall and the center region in the pebble bed by preliminary test of PIV.

The velocity near the wall increases more than about three times velocity in central region.

3-D numerical simulation for the water flow in pebble bed

After pebbles are packed in a container with a vibration by a use of a discrete element method (LIGGGHTS), computational grids are created in void of pebble bed.

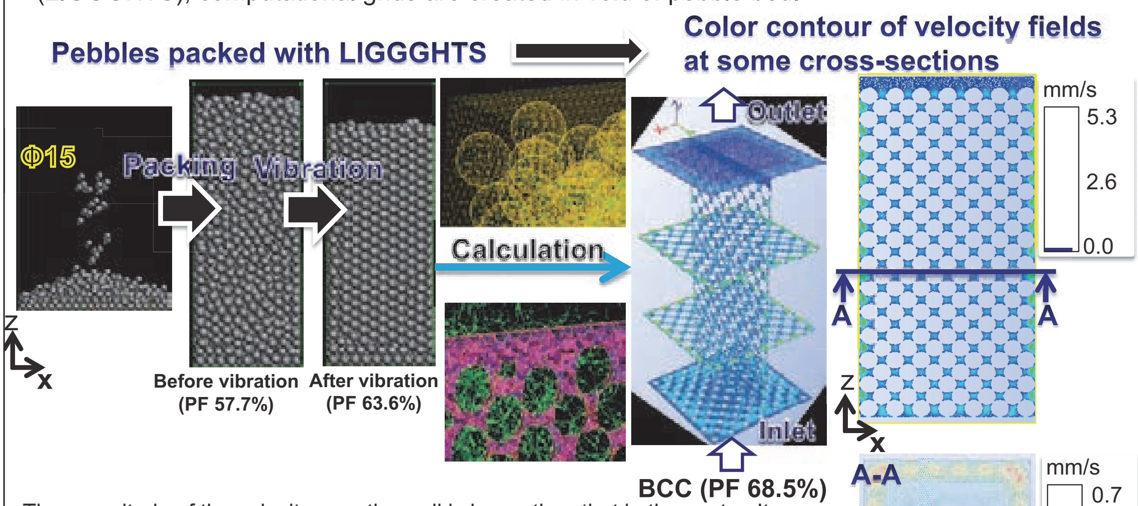

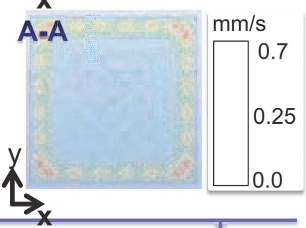

The magnitude of the velocity near the wall is larger than that in the center. It indicates that the preferential flow-paths are formed within a half of the pebble dia. The distribution and magnitude of the velocity in numerical simulation corresponds to the experimental data.

Flow field in pebble bed can be predicted by the numerical simulation with a high accuracy in comparison to the experiment.

Numerical simulation for the flow of the helium purge gas in pebble bed

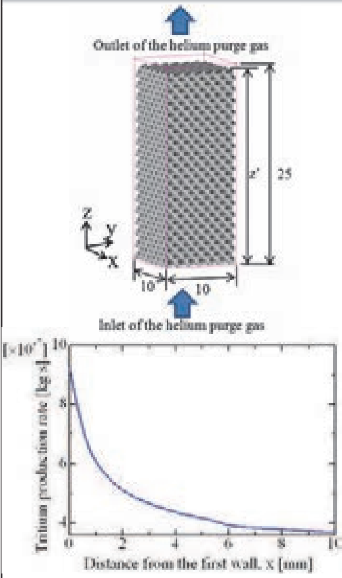

The box		
x-way length of the box	9.49	mm
y-way length of the box	9.49	mm
z-way length of the box	25.0	mm
The pebble bed		
Height of the pebble bed, z'	24.3	mm
Smallest grid size near the wall	0.08	mm
Pebble diameter, *d*	1.02	mm
Packing factor, P.F.	70.8	%
Porosity, ε	0.292	-

Helium		
Temperature of the helium	20.0	°C
Density, ρ	1.66×10^{-1}	kg/m^3
Kinematic viscosity, ν	1.18×10^{-4}	m^2/s
Reynolds number, Re_p	3.68	-
Flow rate, F.R.	6.37×10^{-6}	kg/s
Volumetric flow rate	2.30	L/min
Bulk velocity of the inlet, *u*	0.426	m/s
Binary diffusion coef. of He and T	1.32×10^{-4}	m^2/s
ΔP derived from Ergun's eq.	623	Pa

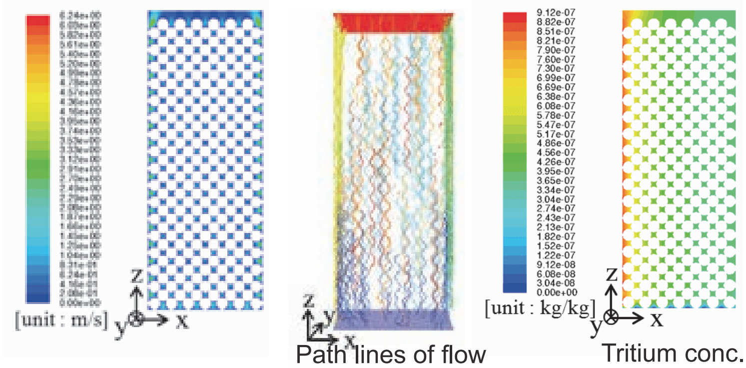

The path-lines in the meander channel do not almost pass transversely across the pebble bed. The convective diffusion does not take place. The diffusion of tritium is caused by the effect of a molecular diffusion. ➔To examine an effect of this tritium concentration on permeability to the wall, further detailed research with carefully considering a permeability rate is required.

Conclusions

- Dependence of pressure drop on cross-section shape of container
  - The pressure drop of the purge gas in the breeder pebble bed experimentally has been studied, using pebble bed of comparably-size of the TBM.
  - The experimental results demonstrated that prediction of DP calculated by Ergun's equation may contain about 10% but not underestimate. Thus, Ergun's equation is enough applicable to the engineering design of the blanket up to flow rate of 100 L/min as to be applied to the TBM from 40 to 50 L/min.
  - Difference of geometry of packed bed cross-section on pressure drop was not observed.
- Flow experiments and numerical simulation of tritium behavior in purge gas flow in the breeder pebble bed
  - Visualization of flow phenomena in pebble bed by using PIV and pebbles made by Mexflon was successful.
  - By the verification of the numerical simulation with experimental results, important information was obtained for the establishment of the prediction method of the total tritium behavior simulation which takes into account all essential tritium transfer process for an engineering design of a breeding blanket.

Design & Fabrication of Experimental set up for Packed Bed Effective Thermal conductivity Measurement

Aroh Shrivastava, Maulik Panchal, P. Chaudhuri, E. Rajendrakumar

Institute for Plasma Research, Gandhinagar, Gujarat, India-382428
Email: aroh@ipr.res.in

Abstract
International thermonuclear experimental reactor is one step more towards the demo reactor. ITER will demonstrate the scientific & technical feasibility of the fusion. The two isotopes of hydrogen i.e. deuterium D & tritium T will produce high energy neutron. These neutrons will react with Lithium compounds to produce tritium which would be put inside the test blanket module. India had proposed lead lithium ceramic breeder concept for test blanket module. These blankets will contain Lithium titanate Li2TiO3 in form of 1 mm pebbles. The development of Li2TiO3 is under progress. The measurement of the thermal profile inside of the TBM is very important factor for proper & economic design. Li2TiO3 pebble bed is having lower thermal conductivity compared to other materials inside the TBM therefore measurement for the effective thermal conductivity is important. A preliminary setup for measurement of Keff is developed in IPR. Setup is based on the axial heat flow comparative method. Various analyses had been carried out with the reference materials and the analysis is also carried out on alumina packed bed. Alumina pebbles were taken approx. 3.5 mm in diameter. Thermal conductivity of various standard materials like SS 304, aluminium, copper & brass were measured in this setup which were calibrated with the values obtained from the laser flash system. Experiments were carried out at various bed temperatures at air atmosphere. The details of the experimental setup & the current measured values will be discussed in this paper.

Keywords – effective thermal conductivity, packing fraction

Design & Fabrication of Experimental setup for packed bed Effective Thermal Conductivity Measurement

Aroh Shrivastava, M. Panchal
Institute For Plasma Research, India
E- mail: aroh@ipr.res.in

Introduction

- The effective thermal conductivity of the packed bed is the conductivity of hypothetical solid mass which is to be completely equivalent to a portion of packed bed.
- In LLCB TBM concept there are four ceramic breeder zones. Each housed in FMs structure and cooled by the liquid lead lithium metal which is flowing through the ceramic breeder zone.
- The temperature profile in the four ceramic breeder zone is strongly dependent on lead lithium flow velocity and the effective thermal conductivity of packed bed.

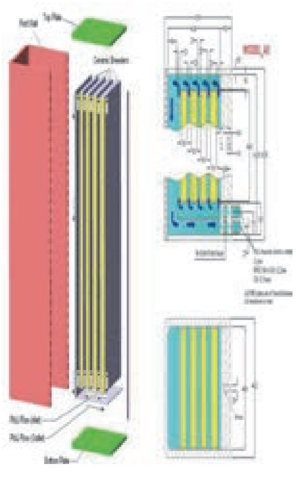

if the pebbles are considerably smaller than the dimensions of the pebble bed than the bed can be treated as homogeneous medium and the heat transfer parameters can be reduced two coefficients the effective thermal conductivity of pebble bed and the heat transfer co efficient at the wall .

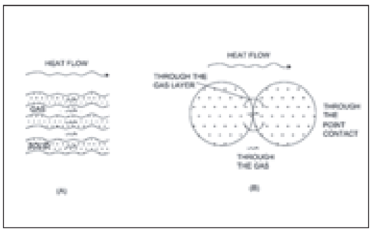

$$keff = \varepsilon kg + (1-\varepsilon)ks$$

$$keff = \varepsilon kg + (1-\varepsilon)ks\left[\frac{1}{\left\{\varphi b\left(\frac{ks}{kg}\right)+\left(\frac{2}{3}\right)\right\}}\right]$$

Kunni & smith model

Parameters affecting ETC

- Conductivity of pebbles
- Conductivity of gas
- Ratio of solid to gas conductivity
- Gas pressure
- Bed packing fraction
- Pebble size
- Pebble surface roughness
- Contact area and bed deformation

Methods for measuring thermal conductivity

- Axial Flow method
- Guarded hot plate method
- Hot wire method

$$Q_{Conduction} = -k * A * \frac{dT}{dx}$$

- ❑ This experimental setup is designed to study the Li_2TiO_3 pebble bed (PB) thermal conductivity based on the principles of the steady state and axial heat flow methods.
- ❑ The temperature gradient across the PB is generated which creates 1-D heat transfer in the PB region. Temperatures of the PB at different locations are measured by thermocouples.
- ❑ effective thermal conductivity of PB is calculated by measuring the heat flux and temperatures across the pebble bed using Fourier's law of heat conduction after steady state conditions are reached.

Schematic of Experimental set up

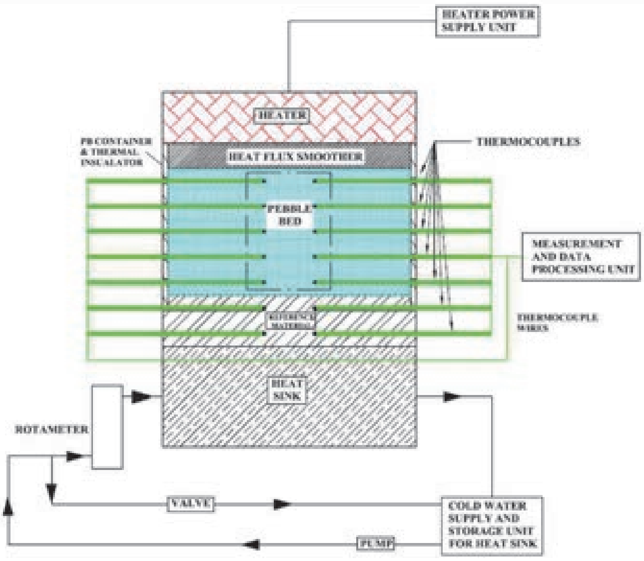

Details of Experimental set up

- ❑ Ceramic Band heater - 2200 W
- ❑ Heating element – Kanthal A1 grade
- ❑ Thermo couple 1 mm. Diameter – K type accuracy : 1.1°C or +/- 0.4 % T which ever is greater
- ❑ Insulation – Microtherm Super A (k = 0.03 w/m°K at 500°C)
- ❑ Area Meter for water flow (5 lt./hour)
- ❑ Material of Construction – SS 304 (Reference block, Test section), coolant channel – Copper , Heat flux smoother – graphite
- ❑ Power supply unit – Libratherm PID copntroller,
- ❑ DAQ unit – Masibus 48 channels

Simulation Study

- A 2D Axis symmetry model is consider for predicting the temperature profile inside the test section.
- 2 models were simulated, 1 with insulation and 1 without insulation
- Model was considered with heater section (with insulation) and test section (without insulation)
- The outer boundaries are considered as convection cooled.
- The test material was taken SS 304 block
- Reference material was also taken as SS 304.

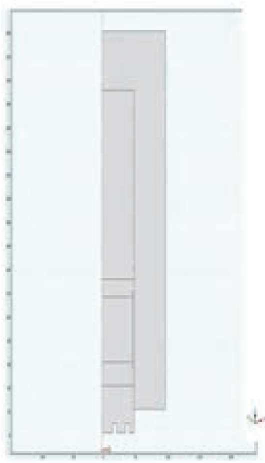

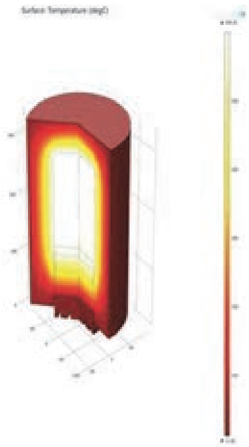

Simulation Study

Objective - To Determine 1 D heat transfer region

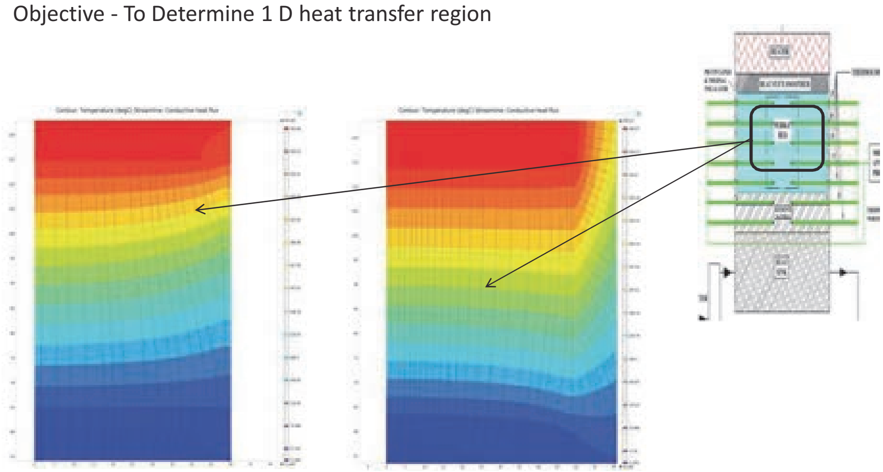

No insulation on test section

Microtherm insulation on test section

Bed Temp. Profile with time

Ramp rate – 5°C / Min.

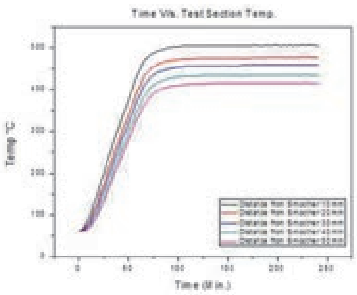

SS 304 block in test section

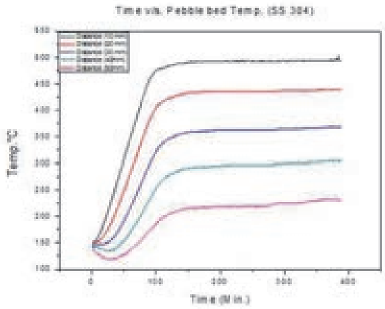

SS 304 Spheres in test section

Bed Temp. Profile with Interface distance

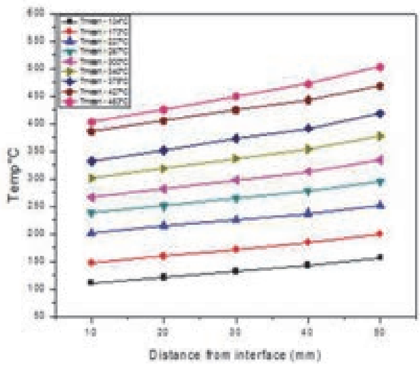

SS 304 block in test section

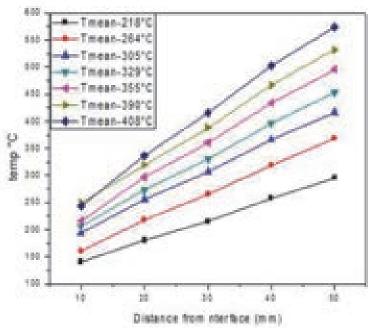

SS 304 Spheres in test section

Comparison with Laser flash results

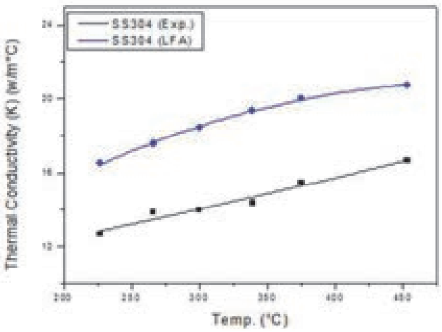

SS 304 block Thermal Conductivity Exp. results

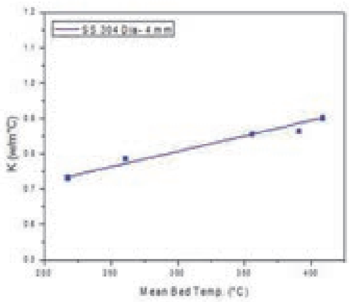

SS 304 Spheres effective Thermal Conductivity
Experimental results

Limitations with current Exp. set up

- Radiation losses
- Heat Flux measurement
- Maximum experimental temperature
- 1 D heat profile
- Constant boundary conditions
- Thermocouple positioning
- Interface temperature measurement for HTC

Modified Experimental Set up

The experiments are planned for the packed bed under helium gas. Therefore new experimental setup is planned with following arrangements.

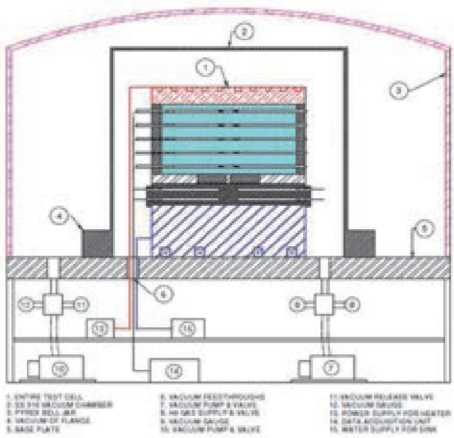

Schematic of Test set up

Modified Experimental Set up

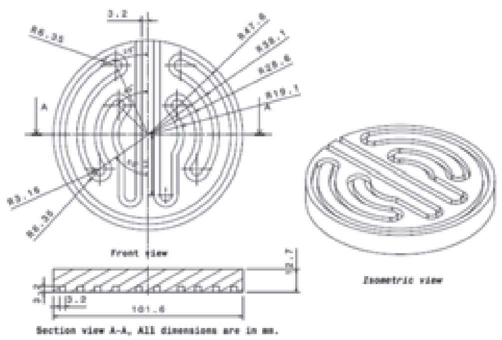

Heater body with tungsten heating element layout*

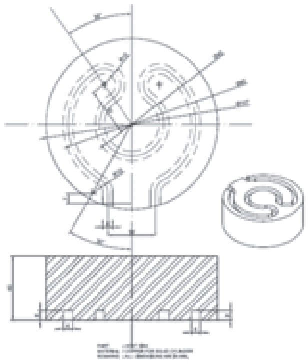

Schematic of Cooling Block**

*William M. Healy , ANSYS Users' Group Conference Proceedings. October 2, 2001
**A. Abou Sena, Alice ying, M.Abdou "Experimental measurement of the effective thermal conductivity & interface thermal conductance of lithium ceramic pebble bed

Fabrication Challenges

- A lot of instrumentations in small chamber.
- Vacuum sealing for 10E-5 torr
- Positioning & thickness of heat flux sensors
- High temperature extension cables
- Prevention of Heat loss to surroundings
- Vacuum feed through & their positioning
- Working temperature range up to 900°C
- Protection of seal gaskets

Conclusion

- The preliminary experiments are performed on the SS 304 blocks and sphere bed in air atmosphere with various mean bed temperature.
- The obtained thermal conductivity results of SS 304 block is compared with laser flash results. 20 % deviation is observed through out the temperature.
- The current experimental set up is needs to be modified in order to minimize surrounding heat loss through.
- The pebble bed temperature is also needs to increase up to 900°C.
- The number of experiments are needed with various variables like packing factor, purge gas pressure, single or binary size pebbles etc.

Experimental Investigation of Thermal Properties of the Li_4SiO_4 Pebble Beds

Yongjin Feng[a], Kaiming Feng[a], Yinfen Cheng[a], Yang Liu[a], Jin Hu[b]

[a]*Southwestern Institute of Physics, P.O. Box 432, Chengdu, Sichuan, China*
[b]*Kunming University of Science and Technology, Kunming, Yunnan, China.*

1. Introduction

Lithium ceramics breeding blanket is considered one the most promising fusion blankets and worldwide efforts have been devoted to its R&D. The helium-cooled ceramic breeder (HCCB) with the pebble bed concept was selected as Chinese test blanket module (TBM) design. In the HCCB TBM, Lithium orthosilicate (Li_4SiO_4) is considered as the first candidate tritium breeder and beryllium is used for neutron multiplication. The material-form options for the tritium breeders and neutron multiplier are pebble bed. Using pebble beds in breeder blanket has several advantages. First, bed characteristics can be tailored to obtain the required thermal characteristics. Second, the effective thermal conductivity can be controlled by adjusting bed characteristic. Third, tritium produced in the pebble beds can be easily removed by the purge gas. In the thermal mechanical design of the HCCB TBM with pebble beds, the thermal properties of the pebble beds is one of the most important design parameters which decides the optimum breeder and multiplier arrangement to keep the appropriate temperature ranges of the breeder and multiplier materials. The pebbles are surrounded by flowing helium which carries away the tritium produced in pebbles. However the helium velocity is so small that the effective thermal conductivity of the bed is not affected by the helium flow and the bed behaves like a stagnant bed. The heat produced in the pebbles is carried away by means of cooling tubes containing high pressure helium(≈8MPa) .

In the present paper, a new technique (Transient Plane Source method) applied to measure the thermal parameters of tritium breeder pebble bed. Then, temperature dependence and thermal properties, with respect to thermal diffusivity, thermal conductivity and specific heat, were investigated.

2 Experimental

2.1 Method

The Transient Plane Source (TPS) method for measuring the thermal conductivity and thermal diffusivity has been used in a variety of situation and for a number of different materials. The experimental principle of the TPS method is based on the transient temperature response of an infinite medium to step heating of a disk-shaped plane source. In the measurement of the TPS method, the sensor serves both as a heater and a temperature detector. The temperature rise in the sensor surface is accurately determined through resistance measurement. The temperature rise in the sensor surface is also highly dependent on the thermal transport properties of the test specimen surrounding the sensor.

In this study, the apparatus used was thermal constant analyzer test system (TPS 2500S, Hot Disk, Sweden). The Mica sensor (a type of sensor for high temperature measurement) was horizontally embedded in the center of the pebble bed. The radius of the sensor is 9.719 mm and the thickness is 0.1

mm. The temperature range of the electric furnace is from ambient to 600℃. Stagnant helium at atmosphere pressure was used as a filling gas. After reaching the steady state for each experimental run, the sensor is then heated by a constant electrical current for a short period of time. The generated heat dissipates from the sensor into the surrounding sample material, causing a rise in temperature of the sensor and surrounding sample material.

2.2 Material

The Li_4SiO_4 pebbles with the diameter 1.0 mm, used in this study as shown in Fig. 1, were fabricated using the melt-spraying technique. These pebbles were conditioned by annealing at 1000℃ for 2h to obtain the thermodynamically stable phase, lithium orthosilicate and metasilicate and a homogeneous microstructure in all pebbles. Using the Hg-porosimetry a density of approximately 94% T.D. (T.D. = 2.40 g/cm^3) and an open porosity of 5.2% were measured; while a closed porosity of 3.2% was measured by He-pycnometry. SEM (Scanning Electron Microscopy) was used to study the microstructure of the pebble surface, see Fig. 2. Li_4SiO_4 pebbles exhibits the known dendritic solidification microstructure due to rapid cooling. The pebbles were packed into a container made of stainless steel and tapped into place by hand. Diameter of the packed bed was 45mm and height 50mm, see Fig. 3. The packing ratio, which is the ratio of the total volume of pebbles to the volume of a pebble container, is about 60.5%.

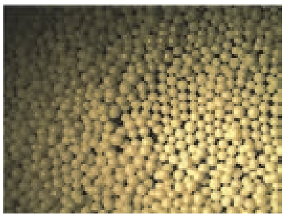

Fig. 1 Photograph of Li_4SiO_4 pebbles

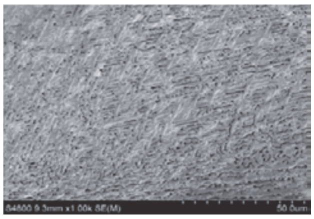

Fig. 2 Morphology of pebble's surface

Fig. 3 Pebble container and test sensor

3. Results and Discussion

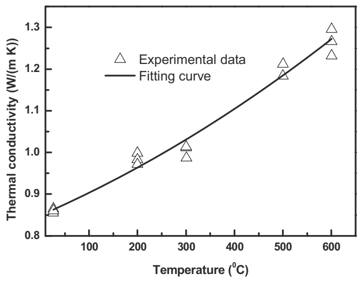

Fig. 4. Temperature dependence of thermal conductivity for Li_4SiO_4 pebble beds.

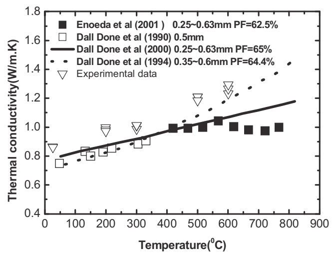

Fig. 5. Comparison with previous experimental data

Figure 4 shows the measured effective thermal conductivity, λ, of the bed of Li_4SiO_4 pebbles versus the bed average temperature. From this figure, the effective thermal conductivity of pebble bed increases with the increase of the pebble bed temperature. In other words, the effective thermal conductivity increase from values of about 0.86 W/m K at ambient temperature to values of about 1.29 W/m K at 600℃. The data was correlated in the temperature range of R.T.-600℃ by the following equation: $\lambda = 0.97198+5.04496\times10^{-4}T+3.30432\times10^{-7}T^2$.

In the heat transfer process, the pebble beds is considered as two-phase (pebbles/gas medium). Thermal conduction through the solid pebbles and thermal conduction through the contact areas are expected to dominate when the filling gas is stagnant and its thermal conductivity is small compared to that of the pebbles. During initial packing process, all the pebbles are randomly packed into a container and the pebbles are almost point-point contact. With the temperature increase, the pebble beds will generate the thermal deformation. The point-point contact can evolve to area-area contact. The effective thermal conductivity of pebble beds are influenced by many parameters with different degree. Some of these parameters have significant impact on thermal conductivity of the pebble beds, such as thermal conductivity of solid pebbles and filling gas, bed deformation and bed packing fraction. Other parameters have less impact such as pebble size and surface roughness. Thermal conductivities of pebbles and filling gas have direct impact on effective conductivity of the pebble beds. When this ratio is high, the heat flux prefers to follow the path of higher conductivity regions (pebbles and contact areas). Because the helium conductivity is much lower than that of pebbles, the contact area between pebbles directly affects the amount of heat flux across it. It was concluded that the effect of deformation on thermal conductivity cannot be neglected for lithium ceramic pebble beds.

Figure 5 shows the measured effective conductivity of the Li_4SiO_4 pebble beds compared with the previous data. These results indicate the effective thermal conductivity have the same trend of increasing thermal conductivity with the temperature increase. But the measured data are higher than the other previous experimental data especially at temperature 500℃ and 600℃. The reason comes from the different measure methods. The contact areas between pebbles with sensor using TPS are larger than hot wire method.

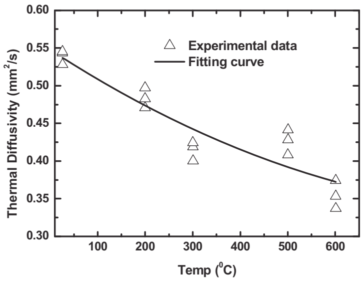

Fig. 6. Temperature dependence of thermal diffusivity for Li_4SiO_4 pebble beds.

Figure 6 shows the measured thermal diffusivity, α, of the Li_4SiO_4 pebble bed versus the bed average temperature. The thermal diffusivity of the Li_4SiO_4 pebble bed has the tendency to decrease with the temperature increase. From the results, the thermal diffusivity of pebble beds was about 0.53 mm^2/s at room temperature, falling to about 0.33-0.37 mm^2/s. The experimental points are fitted by the follow correlation, $\alpha = 0.54761 - 4.08679\times10^{-4}T + 1.95265\times10^{-7}T^2$.

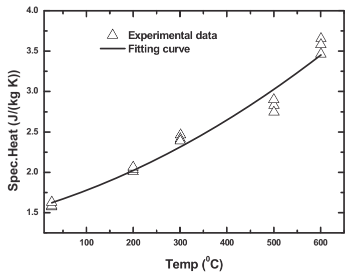

Fig. 7. Temperature dependence of specific heat for Li_4SiO_4 pebble beds.

Figure 7 shows the measured specific heat of the Li_4SiO_4 pebble bed versus the bed average temperature. From the results, the specific heat of Li_4SiO_4 pebble bed increased with increasing temperature. The empirical equation obtained here is given as follows: $c_p = 1.57753 + 0.00179T + 2.22244\times10^{-6}T^2$.

4. Conclusion

The transient plane source method has been applied to measure the thermal properties of single size Li4SiO4 pebble beds. The correlations have been developed which describe thermal properties as a function of temperature. It was found that the effective thermal conductivity and effective specific heat increase with the increase of the temperature of the bed. The thermal diffusivity decreased with the increase of the temperature of the bed.

More experimental studies, with acceptable level of confidence and accuracy, are still required especially for compressed Li_4SiO_4 pebble beds. These experiments will help to create a database of the thermal properties of Li_4SiO_4 pebble beds which can be used for the design and analysis of tritium breeder blankets.

References

[1] K.M. Feng, C.H. Pan, G.S. Zhang et al,. Progress on design and R&D for helium-cooled ceramic breeder TBM in China. Fusion Engineering and Design 87 (2012) 1138-1145.

[2] M. Dalle Donne, A. Goraieb and G. Sordon, Measurements of the effective thermal conductivity of a bed of Li_4SiO_4 pebbles of 0.35-0.6mm diameter and of a mixed bed of Li_4SiO_4 and aluminum pebbles, Journal of Nuclear Materials 191-194 (1992) 149-152.

[3] Hu Gang et al, "Updated Design and development route for CH HCCB TBM and its mockup", Proceedings of the 2013 21st International Conference on Nuclear Engineering ICONE21, July 29- August 2, 2013, Chengdu, China.

[4] J. Reimann and S. Hermsmeyer, Thermal conductivity of compressed ceramic breeder pebble beds, Fusion Engineering and Design 61-62 (2002) 345-351.

[5] M. Enoeda, et al, Effective thermal conductivity measurements of the binary pebble beds by hot wire method for the breeding blanket, Fusion Technology 34 (1998) 877-881

[6] M. Enoeda, Y. Ohara, N. Roux, A. Ying, G. Piazza, S. Malang, Effective Thermal Conductivity Measurement of the Candidate Ceramic Breeder Pebble Beds by the Hot Wire Method, Fusion Technology 39 (2001) 612-616

[7] H. Tanigawa, T. Hatano, M. Enoeda, M. Akiba, Effective thermal conductivity of a compressed Li2TiO3 pebble bed, Fusion Engineering and Design 75-79 (2005) 801-805

[8] M. Dalle Donne, G. Sordon, Heat Transfer in Pebble Beds for Fusion Blankets, Fusion Technology 17 (1990) 597-635.

[9] M. Dalle Donne et al. Heat transfer and technological investigations on mixed beds of beryllium and Li4SiO4 pebbles", Journal of Nuclear Materials 212 (1994) 872-876.

[10] M. Dalle Donne, A. Goraieb, G. Piazza, G. Sordon, "Measurements of the effective thermal conductivity of Li4SiO4 pebble bed", Fusion Engineering and Design 49-50 (2000) 513-519.

Southwestern Institute of Physics

Experimental Investigation of Thermal Properties of the Li_4SiO_4 Pebble Beds

Yongjin Feng
(Chinese HCCB TBM Team)

Southwestern Institute of Physics (SWIP),
Chengdu, Sichuan, China

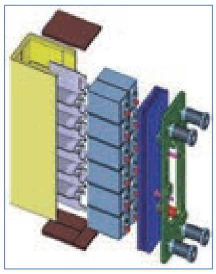

17th Ceramic Breeder Blanket Interactions,12-14 Sep. 2013 Barcelona, Spain

Southwestern Institute of Physics

Outlines

Southwestern Institute of Physics

1. Background

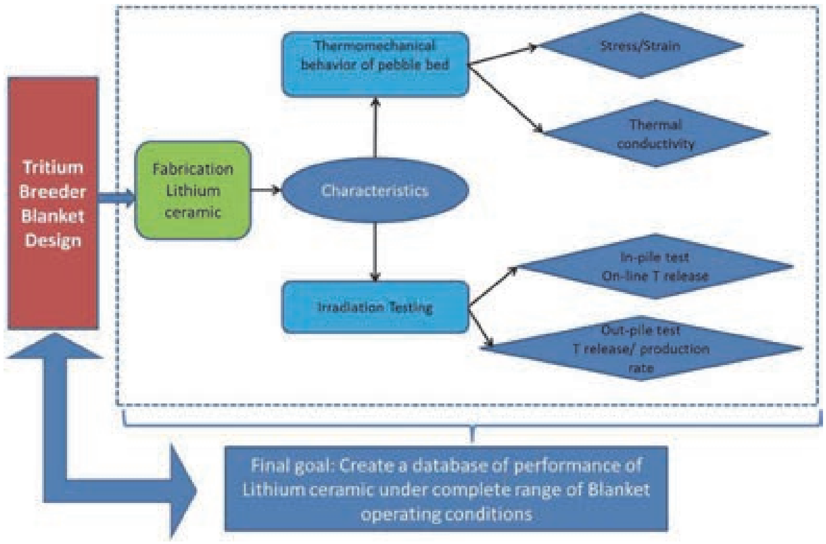

Southwestern Institute of Physics

1. Background (cont.)

Functional requirements Ceramic breeder materials:

- Withstand stresses without excessive fragmentation
- Heat transfer parameters of the pebble beds (temperature control Tmax = 950°C)
- Compatibility between the ceramic and RAFM (max. T~ 550°C)
- Neutron irradiation resistance
- Low tritium residence time in the Li ceramics to minimize tritium inventory
- As low as possible activation under neutron irradiation
- Easy reprocessing capability

Southwestern Institute of Physics

1. Background (cont.)

CN Helium Cooled Ceramic Breeder (HCCB) TBM designs based on the SB/He/FM concept.

Component	Material
Structure	RAFM(CLF-1)
Coolant	He
Purge gas	He+0.1%H_2
Neutron multiplier	Be
Breeder	Li_4SiO_4 , Li_2TiO_3

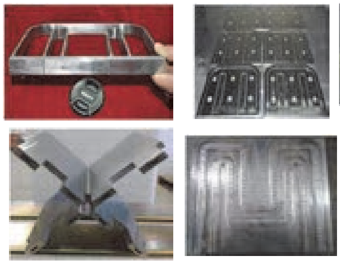

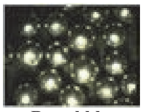

Be pebbles

Li_4SiO_4pebbles

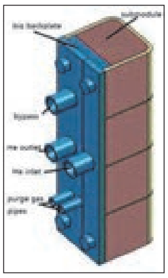

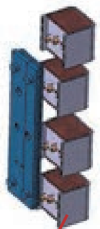

Explosive view of CN HCCB TBM

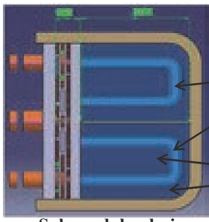

Sub-module design

Southwestern Institute of Physics

1. Background (cont.)

	Li_2O	$LiAlO_2$	Li_2ZrO_3	Li_4SiO_4	Li_2TiO_3
Melting Point / K	1696	1883	1888	1523	1808
Density / g cm^{-3}	2.02	2.55	4.15	2.4	3.43
Li at. density / g cm^{-3}	0.94	0.27	0.38	0.51	0.43
Thermal conductivity (773 K) /W m^{-1} K^{-1}	4.7	2.4	0.75	2.4	1.8
Reactivity with water	large	small	none	small	none
Tritium retention time (713 K) / h	8.0	50	1.1	7.0	2.0
Li Vaporization (in additional H_2)	> 600°C	> 900°C	> 800°C	> 700°C	> 800°C
Long period use (2 years)	Instability (Li vaporization)	Stability	Instability (crack)	Instability (Li vaporization)	Instability (Reduction of Ti)
Tritium release (easy release)	> 400°C	> 400°C	> 400°C	> 350°C	> 300°C
Optimum operating temp.	400 - 600°C	400 - 900°C	400 - 800°C	350 - 700°C	300 - 800°C
Tritium breeding ratio (TBR)	High	Lower	Middle	Middle	Middle
Activation product	^{16}O(n, p) : 7s	^{27}Al (n, 2n) : 4 s ^{27}Al (n, p) : 9.5 m ^{27}Al (n, a) : 15 h	^{90}Zr (n, p) : 64 d ^{91}Zr (n, p) : 57 d ^{94}Zr (n, 2n) : 10^6 y ^{96}Zr (n, 2n) : 64 d	^{28}Si (n, 2n) : 4 s ^{29}Si (n, p) : 6 m ^{30}Si (n, a) : 9 m	^{46}Ti (n, p) : 84 d ^{47}Ti (n, p) : 3.4 d ^{48}Ti (n, p) : 1.8 d

Li_4SiO_4 is considered as reference material and Li_2TiO_3 as alternative material.

Southwestern Institute of Physics

2. Current Fabrication Process and Results

Raw materials: Li_2CO_3 (Purity:99.99%)
SiO_2 (Purity:99.99%)
Li/Si Molar ratio: 4
Melting Pot: Platinum Crucible
The raw materials are melted at temperature of about 1400℃ .
Gas pressure: 1.5 bar,
Gas: Nitrogen,
Falling distance: 3.5 m.

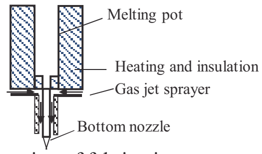

Schematic drawing of fabrication setup


Platinum Crucible


Fabrication facility

Southwestern Institute of Physics

- Shape and surface structure


Optical micrographs

- Most of the pebbles are well spherically shaped, smooth surface.

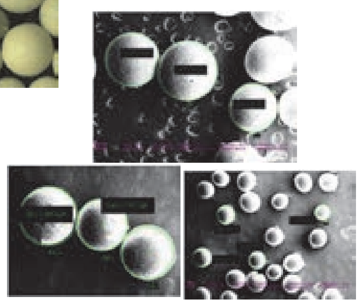
SEM micrographs of the pebbles with different diameter

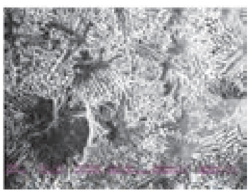
SEM of pebble's surface


SEM of cross section

- The pebbles exhibits the known dendritic solidification microstructure.

Southwestern Institute of Physics

➢ Chemical Composition of pebbles

Elements analysis by ICP-OES

Impurities≈0.4176%

Element	Li	Si	Pt	Na	K	Mg	Ca	Sr	Ba	Ti	Zr
Content (%)	21.24	21.54	0.000934	0.0281	0.0393	0.0011	0.0059	0.0300	0.0023	0.0311	0.0323
Element	V	Cr	Mo	Mn	Fe	Co	Ni	Cu	Zn	Al	
content (%)	0.0239	0.0380	0.0237	0.0183	0.0037	0.0326	0.0334	0.0197	0.0324	0.0218	

➢ Image Analysis

Pebbles Number: 33

Objective Magnification: ×40

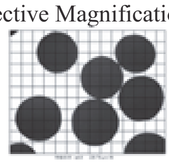

Average sphericity: 0.96

Average Volume diameter: 0.9mm

Average diameter D50:0.889mm

➢ Physical properties

Properties	Values
Density	2.32 g/cm^3 (~96% TD)
Open porosity (%)	~ 5.2
Closed porosity(%)	~ 1.78
Specific surface area (m^2/g)	0.4626
Average pore Radius (nm)	3.674

Southwestern Institute of Physics

➢ Mechanical properties

✓ Mechanical stability analysis by crush load tests.

✓ Single sphere was placed between two parallel plates. A continuously increasing load is imposed by a piston to a single pebble until it breaks.

✓ 20 pebbles with a diameter ~1.0 mm were tested, respectively.

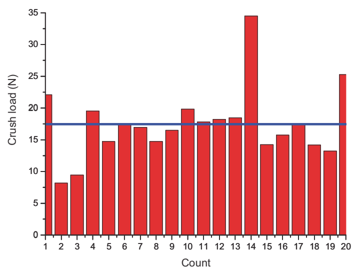

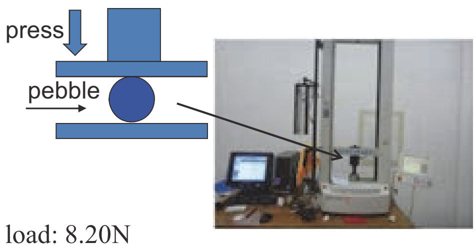

Min. Crush load: 8.20N

Max . Crush load: 34.49N

Ave. Crush load: 17.44 N

Southwestern Institute of Physics

3. Thermal properties of Li_4SiO_4 pellets

Aim: To investigate the density dependence on thermal properties of Li_4SiO_4 pellets

Synthesize Li_4SiO_4 Powder
↓
Pressing: Load: 10-15Mpa
↓
Sintering: 900℃ 2h in air
↓
Li_4SiO_4 pellets

Flow chart on preparation of different density of Li_4SiO_4 pellets

Items	Specimens			
	Sample 1	Sample 2	Sample 3	Sample 4
Dimension (mm)	12.7 ×2.3980	12.7 ×2.5130	12.7 ×2.6750	12.7 ×2.2130
Density (g/cm^3)	1.9422 (80.925% TD)	2.0254 (84.39%TD)	2.0459 (85.25%TD)	2.0633 (85.97%TD)
Specific surface (m^2/g)	0.45	0.36	0.34	0.29

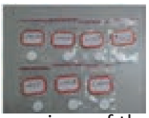

The dimensions of the prepared Li_4SiO_4 pellets were 12.7 mm diameter with 2-2.6mm thickness.

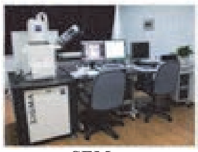

SEM

He-Pycnometry

Laser method thermal conductivity meter measuring device

Southwestern Institute of Physics

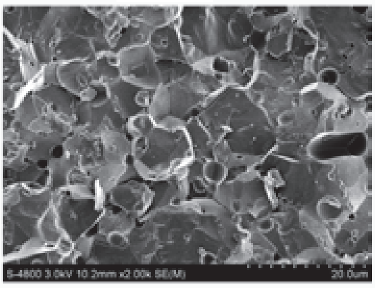

SEM photographs of the cross-section of the Sample 1

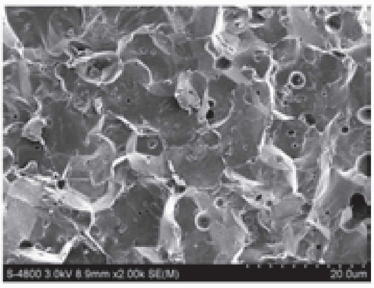

SEM photographs of the cross-section of the Sample 4

Element	wt%
Li	22.3178
Si	24.29
Fe	0.0039
Na	0.024
Cu	0.0048
Ca	0.03
Al	0.0017
Zn	0.0005

Chemical Composition of Sample 1

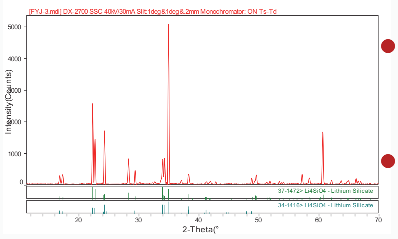

X-ray diffraction patterns of pellet (sample 1)

- The large pores and the amount of pores are decreased with the density increased.
- All of the diffraction peaks that are assigned to Li_4SiO_4

Southwestern Institute of Physics

- **Procedure**
  - ✓ Thermal diffusivity and thermal conductivity of Li_4SiO_4 pellets were measured by laser flash method.
  - ✓ Thermal diffusivity of these pellets was obtained by measuring the temperature elevation on the near surface of the pellets using an infrared temperature sensor and a thermocouple.
  - ✓ Thermal conductivity was calculated from these measurement values and from the density of these pellets.

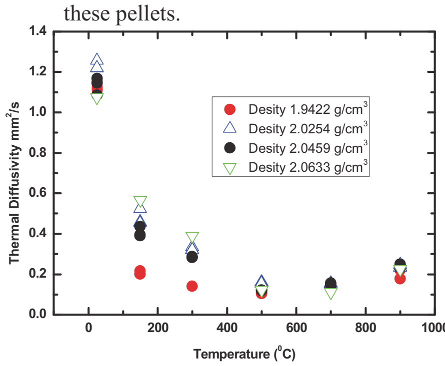

Thermal diffusivity of Li_4SiO_4 pellets

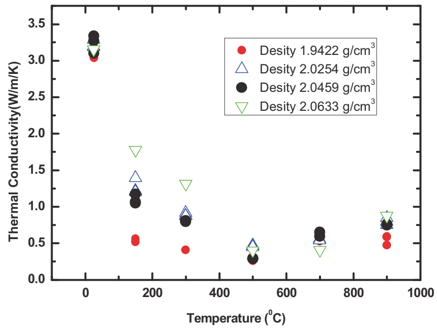

Thermal conductivity of Li_4SiO_4 pellets

- **The thermal diffusivity and thermal conductivity decreased with the temperature.**
- **The density slightly affect the thermal conductivity and thermal diffusivity .**

Southwestern Institute of Physics

4. Thermal properties of non-compressed pebble beds

In development of ceramic breeder blanket, the effective thermal conductivity of pebble beds is an important design parameter. The pebbles-packed bed is considered a heterogeneous solid-gas (two phase) system.

Material:

	Li_4SiO_4 pebbles	Al Alloy pebbles
Ave. diameter (mm)	~1.0	~1.0
Packing factor	60.5%	61%
Process	Melt spraying Method	Rotating Electrode Process

Test temperature range

R.T.- 600℃ (For Li_4SiO_4 pebbles)

R.T.- 500℃ (For Al Alloy pebbles)

Gas He (0.1Mpa)

Pebbles container

Stainless steel (304)

Southwestern Institute of Physics

Method

Transient Plane Source (TPS) Method has been used to measure the thermal conductivity and thermal diffusivity.

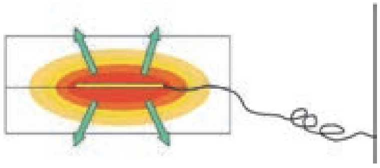

Heater sensor

- The disk sensor serves both as a heater and a temperature detector.
- The disk sensor is embedded in the center of the pebble bed and is heated by a <u>constant electrical current</u> for a <u>short period of time</u>.
- The generated heat dissipates from the sensor into the surrounding pebbles, causing a rise in temperature of the sensor and surrounding pebbles.
- The average transient temperature increase of the sensor is simultaneously measured by monitoring the change in electrical resistance. The temperature coefficient of resistivity of the sensor material correlates the change in resistivity with the corresponding change in temperature.

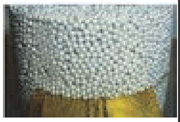

Southwestern Institute of Physics

Experiment results

For Li_4SiO_4 pebble bed

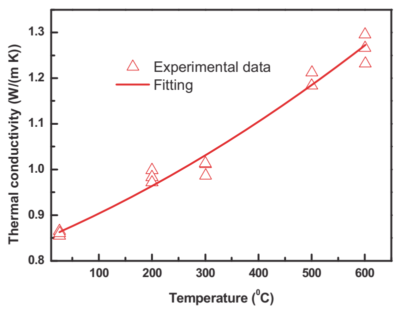

Thermal conductivity of Li_4SiO_4 pebble bed

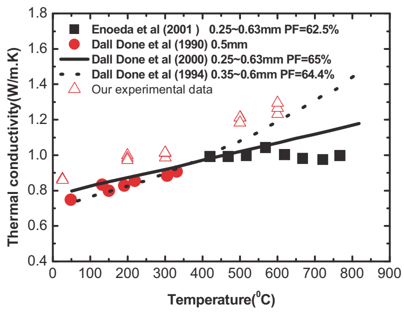

Comparison with the previous data

- The Effective thermal conductivity of the Li_4SiO_4 pebble bed has the tendency to increase with the temperature increase.

The data was correlated in the temperature range of R.T.-600℃ by the following equation:
$\lambda = 0.97198 + 5.04496\times10^{-4}T + 3.30432\times10^{-7}T^2$

The experimental data are higher than the other experimental data. This is because of the different test method. The contact areas between pebbles with sensor using TPS are larger than hot wire method.

*Enoeda et al, Fusion Tech., 39, 612 (2001)
* M. Dalle Done et al, Fusion Tech., 17 (1990)
* M. Dalle Done et al, J. Nuclear Mat. 212 (1994)
* M. Dalle Done et al, Fusion Eng. & Design, 49 (2000)

Southwestern Institute of Physics

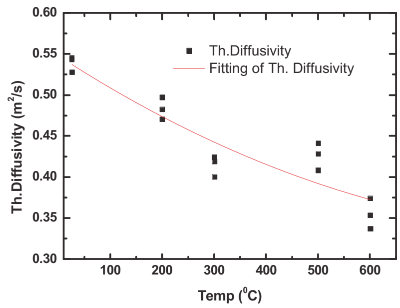

Thermal diffusivity of Li_4SiO_4 pebble bed

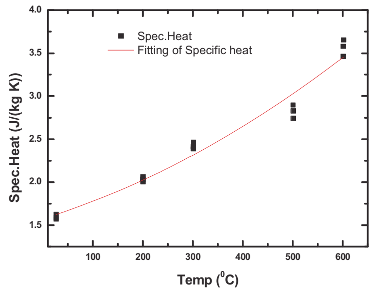

Specific heat of Li_4SiO_4 pebble bed

The thermal diffusivity of the Li_4SiO_4 pebble bed has the tendency to decrease with the temperature increase.

The fitting equation can be obtained,
$\alpha = 0.54761 - 4.08679 \times 10^{-4} T + 1.95265 \times 10^{-7} T^2$

The specific heat of the Li_4SiO_4 pebble bed is increased with the temperature increase.

The fitting equation can be obtained,
$c_p = 1.57753 + 0.00179T + 2.22244 \times 10^{-6} T^2$

Southwestern Institute of Physics

For Al Alloy pebble bed

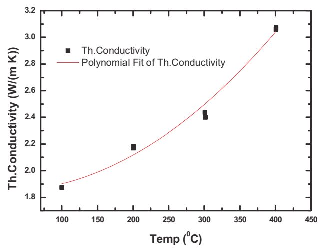

Thermal conductivity of Al alloy pebble bed

$\lambda = 01.85148 - 3.13475 \times 10^{-4} T + 8.20421 \times 10^{-6} T^2$

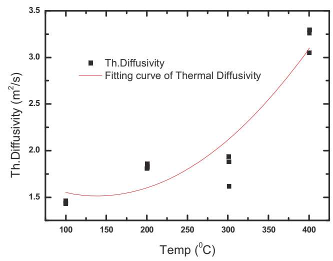

Thermal diffusivity of Al alloy pebble bed

$\alpha = 1.96337 - 0.00646T + 2.32025 \times 10^{-5} T^2$

The thermal conductivity and thermal diffusivity of Al alloy pebble bed is increased with the temperature increase.

The specific heat of the Al alloy pebble bed is decreased with the temperature increase.

$c_p = 1.57753 + 0.00179T + 2.22244 \times 10^{-6} T^2$

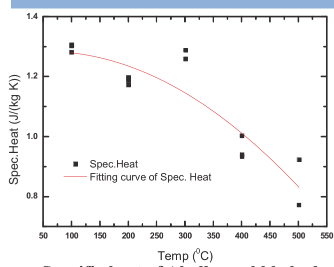

Specific heat of Al alloy pebble bed

5 Summary

- ✓ Li_4SiO_4 pebbles produced by spray of liquid droplets have almost spherical shape, a smooth surface and high density. The pebbles with different size are produced by adjusting the process parameters.
- ✓ The thermal properties of the different density of Li_4SiO_4 pellets were measured. The density slightly affect the thermal conductivity and thermal diffusivity of the pellets.
- ✓ The thermal parameters of Li_4SiO_4 pebble bed are measured by means of TPS method. The effective thermal conductivity and specific heat of pebble bed have the tendency to increase with the temperature increase. The thermal diffusivity of pebble bed are decreased
  with the temperature increase.
- ✓ In order to assess the method using in metal pebble bed, Al alloy pebble bed are substituted by Beryllium pebble bed in this study.
- ✓ More experimental data, with acceptable level of confidence and accuracy, are still required especially for compressed pebble bed.
- ✓ Further work will focus on the tritium release properties and thermal-mechanical of pebble beds.

Pebble bed thermomechanics modeling for solid breeder designs: DEM and FEM development

Jon Van Lew
University of California, Los Angeles (UCLA)
Fusion Science and Technology Center
CBBI-17, Barcelona

In this presentation we discuss the recent progress made in modeling and experimental work at UCLA. The main focus has been on employing the discrete element method (DEM) to study the thermal effects of pebble failure in an ensemble of lithium ceramic spheres. In the model, we homogeneously induced failure and applied nuclear heating until reaching dynamic and thermal steady-states. Conduction between pebbles and from pebbles to the boundary is the only mode of heat transfer presently modeled, though a short introduction was given on the advanced computational fluid dynamics – discrete element method (CFD-DEM) coupling to account for interstitial helium gas in future generations of the model. In the pebble-pebble conduction only model, the effective thermal conductivity was found to decrease rapidly as a function of the percent of failed pebbles in the bed. It was found that the dominant contributor to the reduction was the drop in inter-particle forces as pebbles fail; implying the extent of failure induced may not occur in real pebble beds.

To extend the accuracy of the model, the CFD-DEM coupling was introduced to mainly account for the large influence of energy transport that interstitial helium is known to provide. In the CFD-DEM coupling scheme, the DEM governing equations include a semi-empirical term to account for the energy and momentum transfer between each pebble and the surrounding fluid. Similarly, the computational cells of CFD also include a term for the energy and momentum transfer between the fluid and all the pebbles inside the computational cell. Only some introductory results were presented as the work is ongoing.

We also introduced the finite element method code used at UCLA for modeling the macroscopically observed features of pebble beds. Similar in some respects to the Drucker-Prager Cap model used with ABAQUS by KIT researchers, the FEM model we employ uses a non-linear elasticity, a single unified cap (including the shear failure and cap), volumetric strain, and volumetric strain rate for creep. The model has been used to match simple uniaxial compression experiments with acceptable accuracy. The model was also extended to simulate the conditions in the HELICA experiment and match plastic strain was calculated. The results point to a concern of gap formation between the pebble bed and containing structure. One of the main differences between the UCLA and KIT approaches is the treatment of creep rate. In the model used here, the creep rate is a function of the volumetric strain rather than as a function of time. This approach appears to more realistically represent the behavior of ceramic pebble beds under compression and thermal loads.

Finally, we outlined the test stands now running at UCLA for performing high temperature pebble bed and single pebble experiments. Data from pebble bed experiments will be used to form a material database for constitutive equations and to benchmark the FEM code. The uniaxial compresion tests will provide stress-strain data for initial cap surfaces, cap-hardening correlations, and the pebble bed Young's modulus that are fed into our FEM code. We will also measure the important features of creep-strain of pebble beds at high temperatures. For single pebble experiments we will perform crush load experiments at temperature to observe how the crush distribution evolves at high temperatures.

Pebble bed thermomechanics modeling for solid breeder designs: DEM and FEM development

Jon T. Van Lew

University of California, Los Angeles (UCLA)

Fusion Science and Technology Center

CBBI-17, Barcelona

Thermomechanical issues for ceramic breeders

- Lithium ceramics by their nature, are brittle and prone to cracking under loadings
- Blanket analysis indicates strong mechanical loads will arise from the differential thermal expansion rates between breeder pebbles and container
- Packing states will evolve from both pebble breakages as well as pebble time-dependent deformation.
  - Decrease in effective thermal conductivity raises bed temperature
  - Pebble isolation creates hot spots and sintering – decreasing tritium release rates
  - Gap formation decreases interfacial heat conductance, neutron streaming, etc.
- Evolution of pebble bed thermomechanics is critical to providing confidence in the performance and lifetime of a ceramic breeder blanket design.

From CBBI-16 --Pebble Bed Assemblies irradiation experiment
Lida Magielsen, Sander van Til, Alexander Fedorov

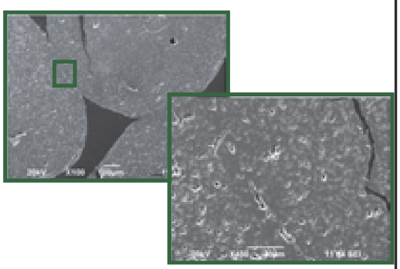

Interactions of multi-scale modeling and experiments

Discrete Element Method

Pebble failure prediction model
- Inter-particle stress giving rise to failure
- Per-particle absorbed thermal energy leading to failure

Failure event model
- Treatment of a failed pebble

Property evolution
- Ensemble response to failed pebbles and rearrangement

Cohesion models
- Treatment of sintering

Finite Element Method

Breeder unit analysis
- Pebble bed interaction with breeder materials
- Stresses expected on the packed bed
- Stress/strain evolution

Pebble Bed Experiments

Ensemble behavior
- Effective thermomechanical properties
- Thermal cycles
- Time-dependent properties

In/out-of-pile
- Benchmarking of code with large-scale or unit-cell experiments

Single Pebble Experiments

Crush load distributions
- Individual pebble strength; temperature and fatigue

Current UCLA Ceramic Breeder Efforts

- **Numerical studies on pebble failure**
  - Thermomechanical changes due to pebble failure via Discrete Element Method (DEM)
  - Enhancing Computational Fluid Dynamics coupling (CFD-DEM)
- **Module-level simulations via Finite Element Method (FEM) tools**
- **Experimental**
  - Constitutive equations for compacted and heated pebble bed
  - Single pebble crushing

UCLA Ceramic Breeder Efforts

- **Numerical studies on pebble failure**
  - Thermomechanical changes due to pebble failure via Discrete Element Method (DEM)
  - Enhancing Computational Fluid Dynamics coupling (CFD-DEM)
- **Module-level simulations via Finite Element Method (FEM) tools**
- **Experimental**
  - Constitutive equations for compacted and heated pebble bed
  - Single pebble crushing

Transient Discrete Element Method

$$\boldsymbol{F}_i = m_i g + \sum_j^N \left(k_n \delta_{n_{ij}} - \gamma_n v_{n_{ij}}\right) + \left(k_t \delta_{t_{ij}} - \gamma_t v_{t_{ij}}\right)$$

- Spring/dashpot coefficients are from Hertz theory for contacting elastic spheres
- based solely on material and geometric properties

A Velocity-Verlet integration algorithm

Heat transfer model captures conduction between particles through contact

$$m_i c_{p_i} \frac{dT_i}{dt} = Q_{\mathrm{nuc}_i} + \sum_j^Z h_{ij}(T_i - T_j)$$

$$h_{ij} = 2k^* \left[\frac{3F_n R^*}{E^*}\right]^{\frac{1}{3}}$$

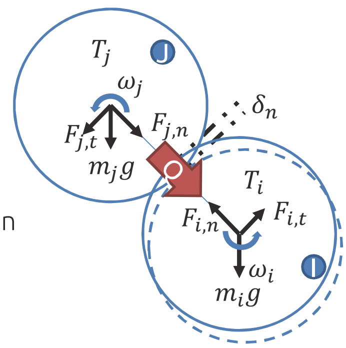

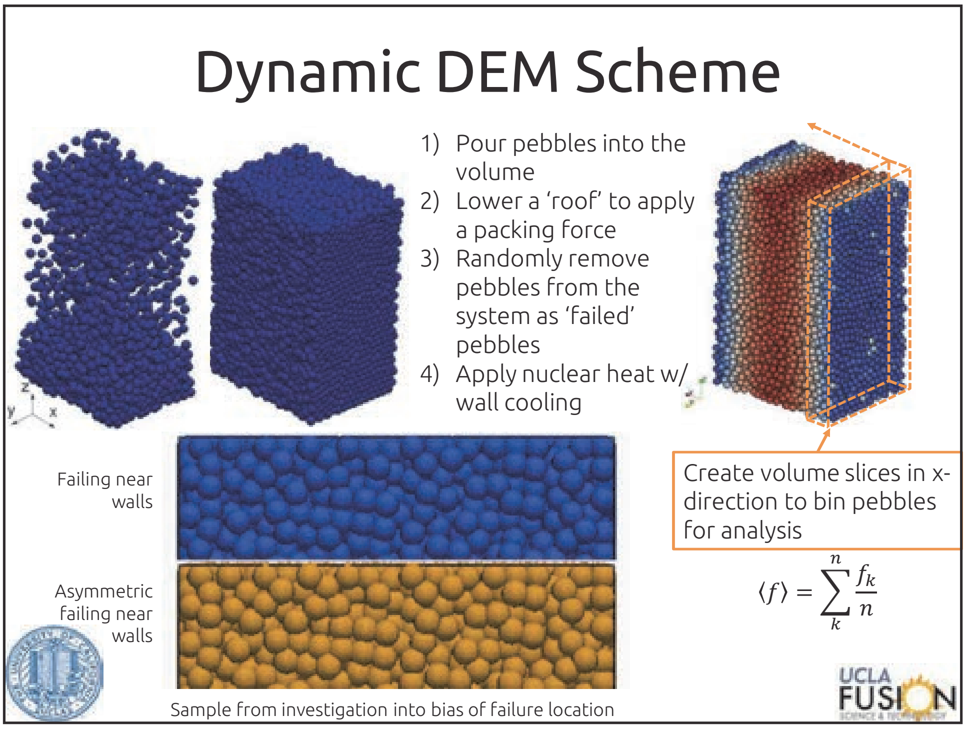

Dynamic DEM Scheme
1) Pour pebbles into the volume
2) Lower a 'roof' to apply a packing force
3) Randomly remove pebbles from the system as 'failed' pebbles
4) Apply nuclear heat w/ wall cooling
Failing near walls
Asymmetric failing near walls
Create volume slices in x-direction to bin pebbles for analysis
$\langle f \rangle = \sum_k^n \frac{f_k}{n}$
Sample from investigation into bias of failure location

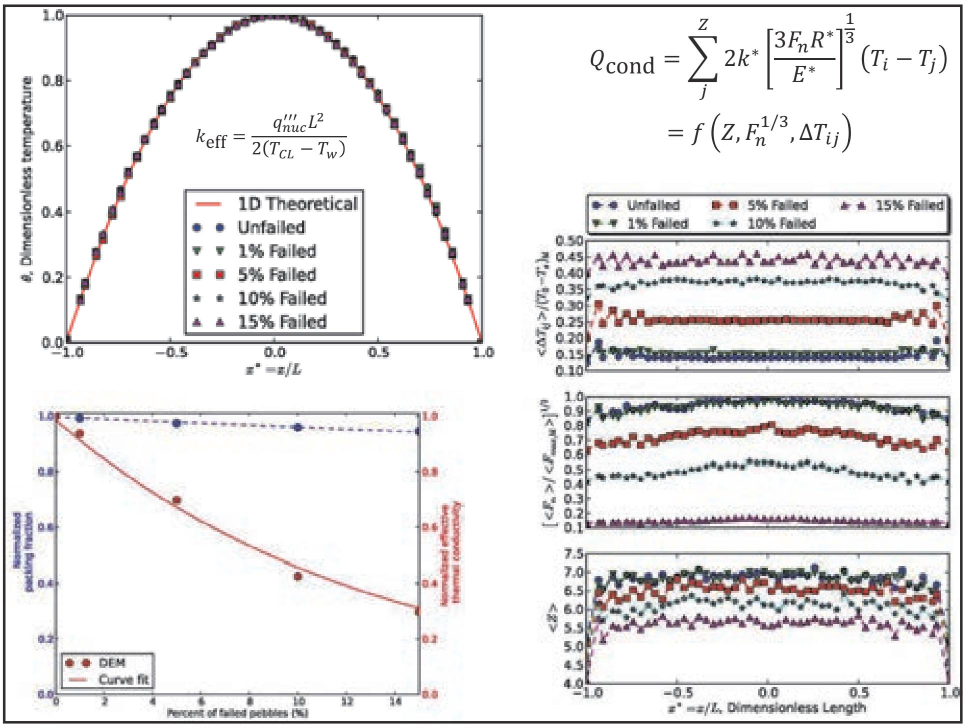

$Q_{cond} = \sum_j^Z 2k^* \left[\frac{3F_n R^*}{E^*}\right]^{\frac{1}{3}} (T_i - T_j)$
$= f\left(Z, F_n^{1/3}, \Delta T_{ij}\right)$
$k_{eff} = \frac{q'''_{nuc} L^2}{2(T_{CL} - T_w)}$
1D Theoretical
Unfailed
1% Failed
5% Failed
10% Failed
15% Failed
θ, Dimensionless temperature
$x^* = x/L$
DEM
Curve fit
Percent of failed pebbles (%)
$x^* = x/L$, Dimensionless Length

Plans for DEM of solid breeders at UCLA

First steps

✓ Found pebble failure dramatically reduced the conductive thermal transport between pebbles

- Next generation model will replace a failed pebble with pebble fragments

- Include multiple thermal cycles to deduce thermal packing influence

Tanigawa, H., Tanaka, Y., & Enoeda, M. (2010)

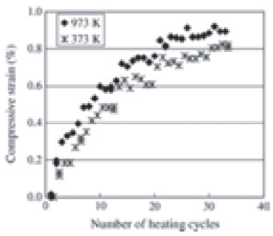

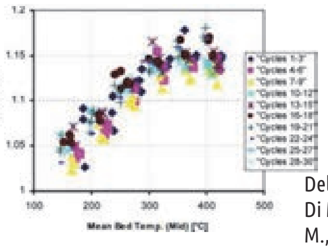

Dell'Orco, G., Ancona, A., Di Maio, F. P., Simoncini, M., & Vella, G. (2004)

CFD-DEM Coupling momentum equations

Pebble bed

Introduce a fluid drag force into the DEM equation

$$F_i = m_i g + (f_n + f_t)_i + \sum_j^N \left(k_n \delta_{n_{ij}} - \gamma_n v_{n_{ij}}\right) + \left(k_t \delta_{t_{ij}} - \gamma_t v_{t_{ij}}\right)$$

Di Felice (1994) gives a semi-empirical relationship

$$\boldsymbol{f}_i = \boldsymbol{f}_{0,i} \epsilon_i^{-\chi}$$

Drag force of a single particle in flow

$$\boldsymbol{f}_{0,i} = \frac{1}{2} C_{d0,i} \rho_f \pi R_i^2 |\boldsymbol{u}_i - \boldsymbol{v}_i| (\boldsymbol{u}_i - \boldsymbol{v}_i)$$

$$C_{d0,i} = \left(0.63 + \frac{4.8}{\mathrm{Re}_p^{1/2}}\right)^2$$

Porosity around particle inside the CFD computational cell

$$\epsilon_i = 1 - \frac{\sum_i^k V_i}{\Delta V}$$

Fluid

Local averaging for mass conservation

$$\frac{\partial(\epsilon_i \rho)}{\partial t} + \nabla \cdot (\epsilon_i \rho \boldsymbol{u}) = 0$$

and Navier-Stokes' with a body force

$$\frac{\partial(\epsilon_i \boldsymbol{u})}{\partial t} + \nabla \cdot (\epsilon_i \boldsymbol{u}\boldsymbol{u}) = -\frac{\epsilon_i}{\rho} \nabla p + \nabla \cdot (\nu \epsilon_i \nabla \boldsymbol{u}) + \frac{\boldsymbol{F}}{\rho}$$

Volume averaged force contribution from all the pebbles in the computational cell

$$\boldsymbol{F} = -\frac{\sum_i^k \boldsymbol{f}_i}{\Delta V}$$

CFD-DEM Coupling energy equations

Pebble bed

$$m_i c_{p_i} \frac{dT_i}{dt} = Q_{\mathrm{nuc}_i} + h_{if} A_i (T_i - T_f) + \sum_j^N h_{ij} (T_i - T_j)$$

Heat transfer coefficient from fluid interaction

$$h_{if} = \frac{\mathrm{Nu}_p k_f}{2 r_i}$$

Li and Mason (2003) provide some correlations for *dilute* gases

Fluid

$$\frac{\partial(\epsilon_i T)}{\partial t} + \nabla \cdot (\epsilon_i \boldsymbol{u} T) - \nabla \cdot (\alpha \epsilon_i \nabla T) = T_{\mathrm{source}}$$

Volume averaged energy contribution of all the pebbles inside the CFD computational cell

$$T_{\mathrm{source}} = -\frac{\sum_i^k h_{if} A_i (T_i - T_f)}{\rho_f C_f \Delta V}$$

Correlation	Valid range
$\mathrm{Nu}_p = 2 + 0.6 \mathrm{Re}_p^{1/2} \mathrm{Pr}^{1/3}$	$\mathrm{Re}_p < 200$
$\mathrm{Nu}_p = 2 + 0.5 \mathrm{Re}_p^{1/2} \mathrm{Pr}^{1/3} + 0.02 \mathrm{Re}_p^{0.8} \mathrm{Pr}^{1/3}$	$200 < \mathrm{Re}_p < 1500$
$\mathrm{Nu}_p = 2 + 0.000045 \mathrm{Re}_p^{1.8}$	$\mathrm{Re}_p > 1500$

Boundary conditions

	Temperature (K)	Velocity (m/s)	Pressure (Pa)
Inlet	Uniform 250 K	Uniform (0 0 0.001)	Zero gradient
Outlet	Inlet-derived	Inlet-derived	Uniform 0
x-wall	Uniform 250 K	No slip (0 0 0)	Zero gradient
y-wall	Cyclic (periodic)	Cyclic (periodic)	Zero gradient

Simulation time: $\tau = \frac{t}{R^2/\alpha} = 0.034$

Load packing state of previous DEM study

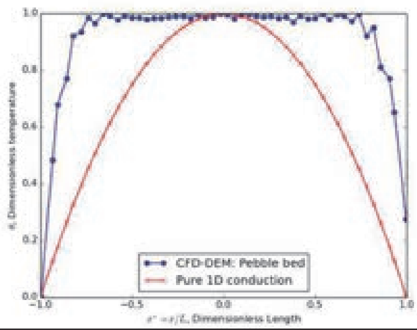

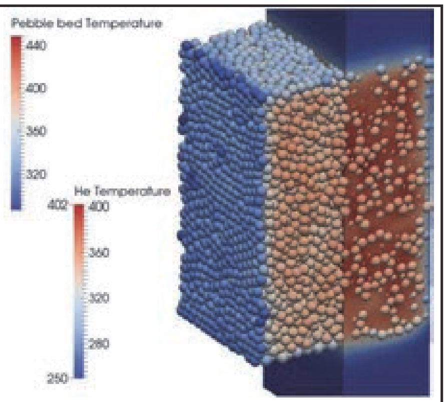

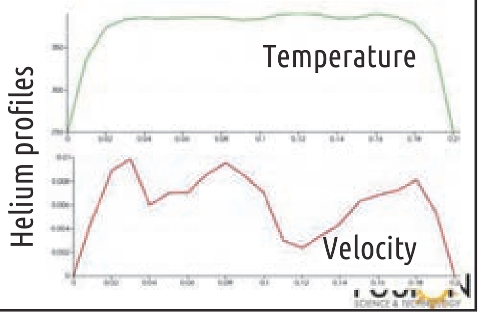

UCLA Ceramic Breeder Efforts

- **Numerical studies on pebble failure**
  - Thermomechanical changes due to pebble failure via Discrete Element Method (DEM)
  - Enhancing Computational Fluid Dynamics coupling (CFD-DEM)
- **Module-level simulations via Finite Element Method (FEM) tools**
- **Experimental**
  - Constitutive equations for compacted and heated pebble bed
  - Single pebble crushing

FEM modeling

Overview of FEM work advanced by Dr. Chunbo Zhang and Justin Tucker

- Continued focus on continuum approach
  - Computational scalability
  - Interfacial effects
- Extant models
  - Drucker-Prager cap in ABAQUS at KIT
  - Hyperelasticity model at ENEA-Brasimone
  - And now… unified cap in ANSYS at UCLA

Model Details – much like the DPC

Example curves

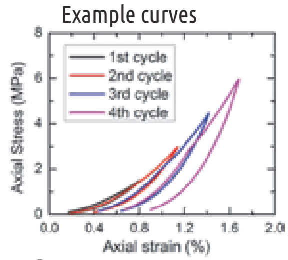

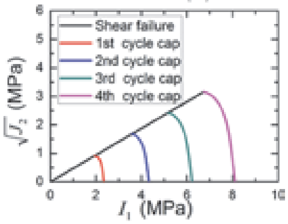

$$E = \left[A_1 + A_2\epsilon_{vol}^p + A_3(\epsilon_{vol}^p)^2\right]\left[(1+v)J_2 + \frac{1-v}{3}I_1^2\right]^{s/2} + E_0$$

$A_{1\text{-}3}$, s, E_0 are empirically derived T-dependent constants

$$Y(I_1, J_2, K, \sigma_0) = J_2 - Y_c(I_1, K, \sigma_0)Y_s^2(I_1, \sigma_0)$$

$$Y_s(I_1, \sigma_0) = \sigma_0 - \alpha I_1$$

R, K_0, σ_0, and α are empirically derived constants

$$Y_c(I_1, K, \sigma_0) = 1 - H(K - I_1)\left[\frac{I_1 - K}{R\,Y_s(K, \sigma_0)}\right]^2$$

$$\epsilon_v^p = W\{e^{(D_1 - D_2(X - X_0))(X - X_0)} - 1\}$$

W, D_1, D_2, and X_0 are empirically derived constants

$$\dot{\epsilon}_{cr} = C_1\sigma^{C_2}\epsilon_{cr}^{C_3}e^{-C_4/T}$$

C_1, C_2, C_3, and C_4 are empirically derived constants

Features:
1) A unified yielding surface for both cap and shear portions;
2) Strain-dependent creep law better reflecting the localized creep behavior of pebble bed.

UCLA FUSION

FEM used to analyze ceramic breeder under prototypical conditions

Temperature distribution (ºC)

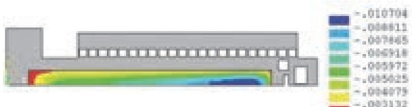

Plastic strain distribution along the Y-direction

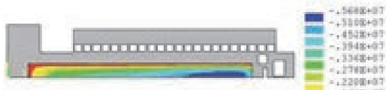

Stress distribution along the Y-direction (Pa)

Analysis: a portion of the bed will undergo time-dependent creep deformation

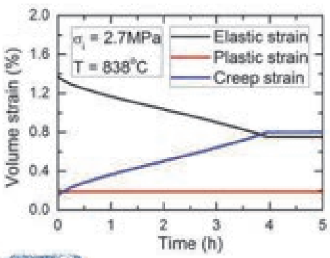

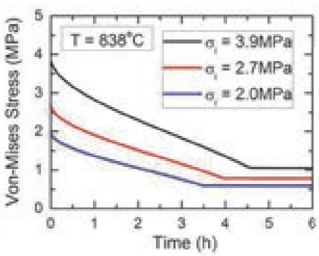

Stress/strain during loading and unloading

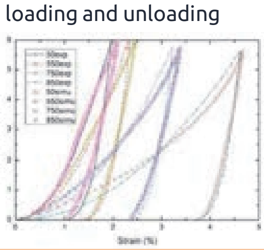

Strain evolution and stress relaxation during time-dependent creep deformation

ANSYS simulation fits experimental curves

FEM coupling with DEM

- Finite element treatment of pebble beds can give advanced understanding of interaction at the outset
- Gap formation from settling and pebble damage still a major issue
- Can FEM simulations integrate with DEM to intermittently provide new packing formations?

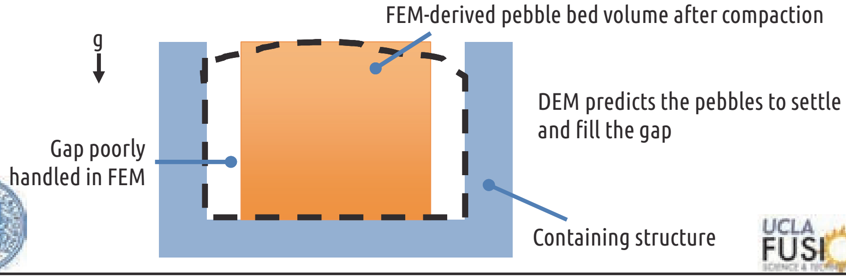

UCLA Ceramic Breeder Efforts

- **Numerical studies on pebble failure**
  - Thermomechanical changes due to pebble failure via Discrete Element Method (DEM)
  - Enhancing Computational Fluid Dynamics coupling (CFD-DEM)
- **Module-level simulations via Finite Element Method (FEM) tools**
- **Experimental**
  - Constitutive equations for compacted and heated pebble bed
  - Single pebble crushing

Experimental interests of UCLA

- Pebble bed
  - Uniaxial compression for stress-strain
  - High temperature stress-strain & creep strain
- Single pebble
  - Crush load distribution
  - High temperature crush load distribution
  - Fatigue load cycle
- Sintered beds
  - Investigations of spark-plasma-sintering (SPS)

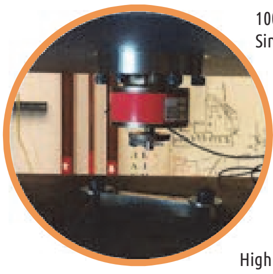

High temperature furnace

50kN Load cell

Dual cross-head test stand for multiple test types (single pebble and pebble bed) with minimal disassembly

- Data used to derive material database constitutive equations and to benchmark FEM code
- Uniaxial compression tests provide stress-strain data used to obtain initial cap surface, cap hardening correlations and Young's modulus
- Creep strain rate data at high temperatures

Li_2ZrO_3 pebbles are used as test pebbles for establishing experimental procedures

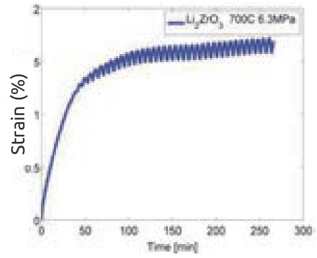

Tests using Canadian-made Li_2ZrO_3

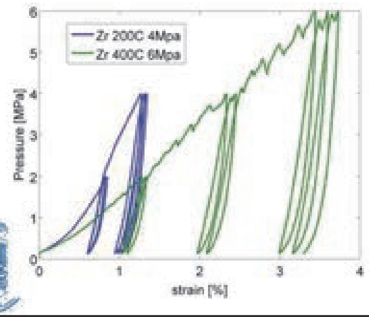

Stress relaxation data for FEM code benchmark

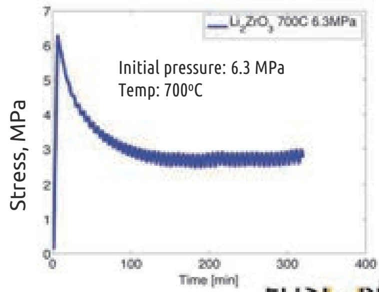

Advanced single pebble crush tests

Get a crush load distribution plot at every temperature, *i.e.* more data points to Papp, et al's work

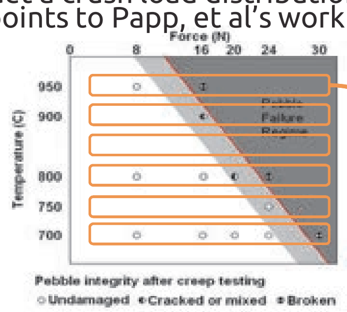

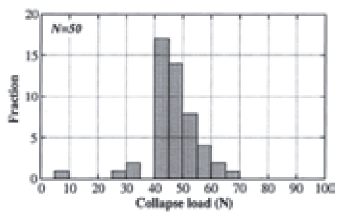

Japanese Li2TiO3
Tsuchiya (1998)

Crushing strength is not constant in time, particles may fatigue under repeat loading

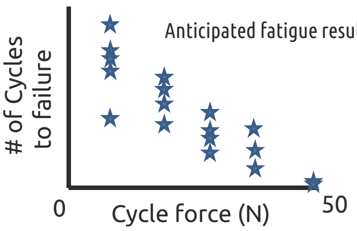

Advanced material investigations

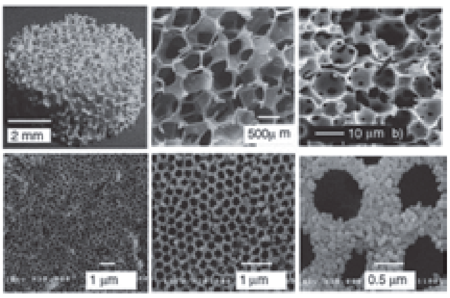

Ceramic foam
Sharafat, S., Ghoniem, N., Sawan, M. E., Ying, A., & Williams, B. (2006)

Spark-plasma Sintering

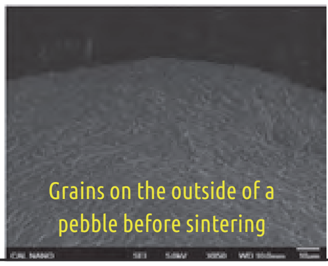

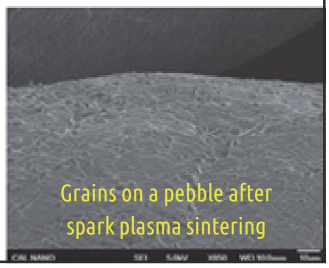

Conclusions

- Basic thermomechanical knowledge of ceramic pebble beds is established
- We are helping to develop models with the foundation of established thermomechanics to investigate the evolving lifecycle of ceramic breeders
- An advanced test stand has revamped UCLA's experimental capabilities

Topic 3: Tritium Release, Extraction and Permeation

Tritium recovery experiment on water cooled ceramic breeder blanket under DT neutron irradiation
K. Ochiai, Y. Kawamura, T. Hoshino, Y.Edao and C. Konno

Examination of tritium release properties of advanced tritium breeders by DT neutron
Tsuyoshi Hoshino*, Kentaro Ochiai, Yuki Edao and Yoshinori Kawamura

Basic studies on new neutron multiplier and breeder materials
Kenzo Munakata, Kohei Wada, Ayano Nakamura, Jae-Hwan Kim, Masaru Nakamichi and Regina Knitter

Advanced tritium extraction process for HCPB breeding blanket
David Demange

Influence of the microstructure on the light species behaviour in ceramic breeder blanket materials
E. Carella, R. Gonzalez-Arrabal, Q. Zhao, A. Ibarra and M. Gonzalez

He thermal-induced diffusion in lithium titanate
M. González, E. Carella, A. Ibarra, B. Courtois, R. Bes and T. Sauvage

Recent progress on the development of erbium oxide coatings for tritium permeation barrier
Takumi Chikada, Akihiro Suzuki, Takayuki Terai and Takeo Muroga

Topical Discussion: Tritium Permeation in the Breeding Zone

Tritium recovery experiment on water cooled ceramic breeder blanket under DT neutron irradiation

K. Ochiai, Y. Kawamura, T. Hoshino, Y.Edao and C. Konno

Japan Atomic Energy Agency, Naka-shi, Ibaraki-ken, 311-0193 Japan

The Li_2TiO_3 breeding material is one of primary candidates of water-cooled solid breeder and Japanese Test Blanket Module (TBM) of ITER. The experimental investigation concerning the tritium recovery ratio of the blanket is one of the urgent technical issues. Therefore, we have performed the tritium recover experiment for the blanket with DT neutrons at the Fusion Neutronics Source (FNS) facility in Japan Atomic Energy Agency (JAEA).

Recently, we conducted an online experiment during DT neutron irradiation in order to clarify detailed temperature dependency of the tritium recovery process. We prepared for a stainless container with a heater. The Li_2TiO_3 pebble of 70g was put into the container and set up it into a beryllium assembly. The Li_2TiO_3 pebble was heated up to a constant temperature (573 or 873 K) and helium sweep gas including H_2 (1%) was flowed before DT neutron irradiation. With the above conditions maintained, the extracted tritium was collected to water bubblers during the irradiation. We also re-arranged the tritium recovery system to measure tritiated water vapor (HTO) and tritium gas (HT), separately. On this WS, we report the present status concerning the experiment.

11th International Symposium on Fusion Nuclear Technology
20 September 2013. Barcelona, Spain

DT Neutron Irradiation Experiment for Tritium Recovery on WCCB Blanket

Kentaro Ochiai, Yoshinori Kawamura,
Tsuyoshi Hoshino, Yuki Edao, Kosuke Takakura,
Masayuki Ohta, Satoshi Sato, Chikara Konno

Japan Atomic Energy Agency

1

Background and objectives

The tritium recovery properties of the WCCB type is not sufficiently investigated.

- A water cooling ceramic breeding (WCCB) blanket is proposed by Japan team and a similar module will be examined on the Test Blanket Module (TBM) program of ITER.
- The Li_2TiO_3 pebble is employed as the prime candidate breeding material in the Japanese TBM.

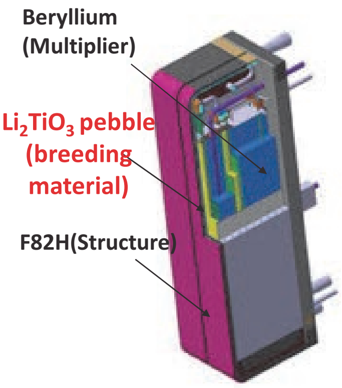

Test Blanket Module
(WCCB-type)

2

- In order to clarify the following properties on the WCCB blanket, we have started the tritium recovery experiment with DT neutrons at the FNS facility of JAEA.

Key issues

1. Recovered tritium quantity
2. Chemical form of recovered tritium
3. Recovery time
4. Temperature dependency
5. Sweep gas dependency

3

- We have gradually performed the following to investigate the above key issues.

- **Offline experiment**
  - Recovered tritium quantity
- **Online experiment-I**
  - Recovery time
  - Chemical form
- **Online experiment-I**
  - Temperature dependency
  - Sweep gas dependency

4

Experimental apparatus

Experiment apparatus is mainly constructed with 4 parts

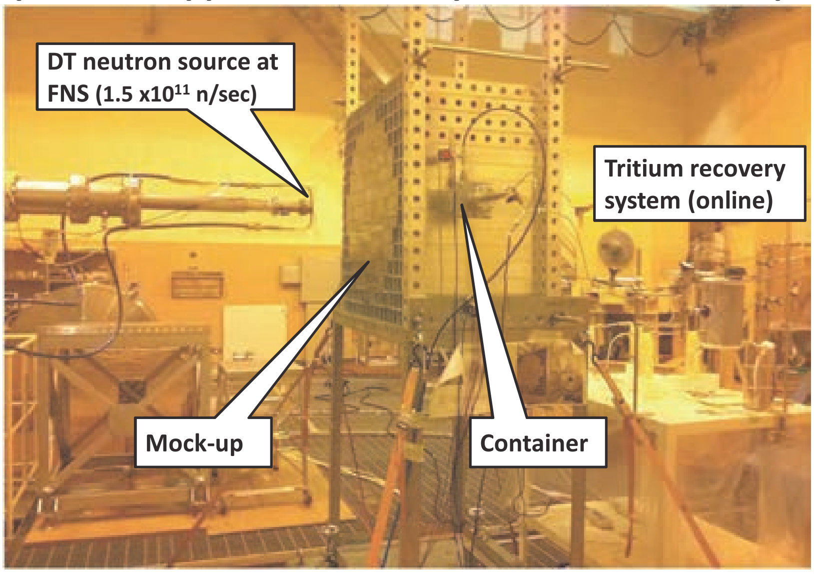

5

Measurement and calculation

DT neutron counting

- Associated 3.5 MeV α particle with Silicon SBD
- Measurement error: < 3 %

Tritium production rate

- LSC measurement with direct dissolution method
  Experimental error: < 10 %
- Calculation with MCNP-5 and FENDL-2.1

Tritium recovery rate

- LSC measurement from bubbler.
- Experimental error : < 10 %.

6

Offline experiment

As our first tritium recovery experiment, we have performed an offline experiment. A beryllium assembly was used to enhance $^{6}Li(n,t)^{4}He$ reaction rate.

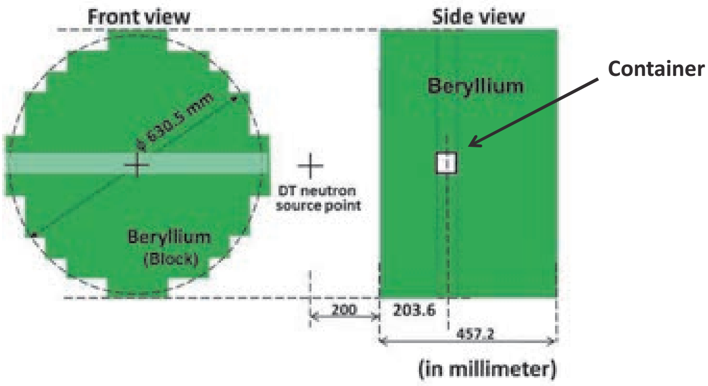

Cross sectional view of assembly for offline experiment

7

Container

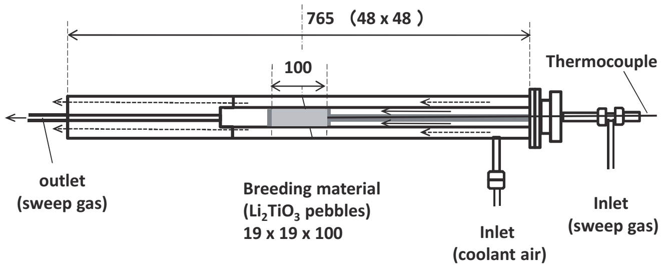

Li_2TiO_3 pebble

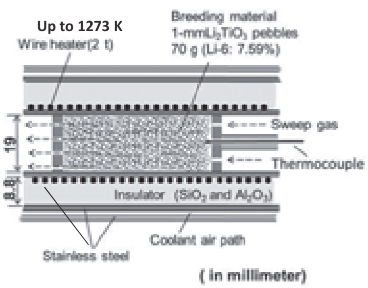

Cross sectional views of container and Li_2TiO_3 pebble.

8

Offline experiment

We have two irradiations for measurements of tritium recovery ratio and tritium production ratio.

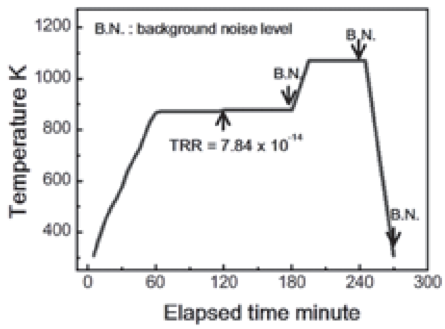

TPR = 7.84 x 10^{-14} Bq/g/S.N.

Tritium recovery with our off line experiment

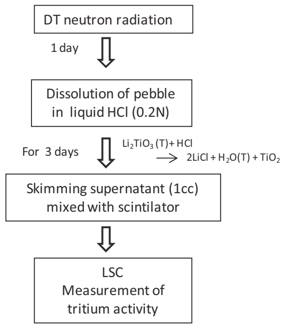

TPR = 7.46 x 10^{-14} Bq/g/S.N.

Chemical procedure of TPR measurement

TRR corresponds with TPR within the experimental error (10%).

Time resolution experiment

- To investigate the time dependency, we have carried out the time resolution experiment.

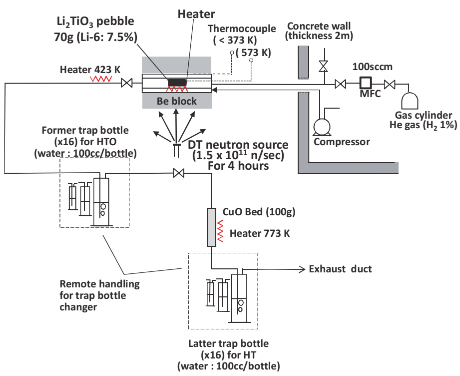

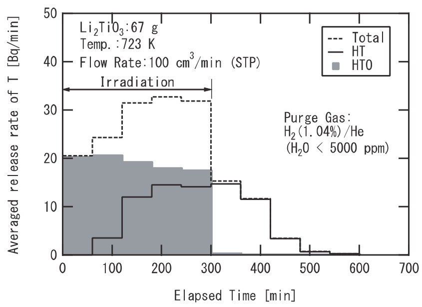

From the result, it was shown that the tritiated water (HTO) was quickly recovered and the recovered tritium gas (HT) had a time gap of several hours.

Integral experiment with blanket mock-up

We have performed an integral experiment for the temperature dependency and the sweep gas dependency with a WCCB blanket mock up.

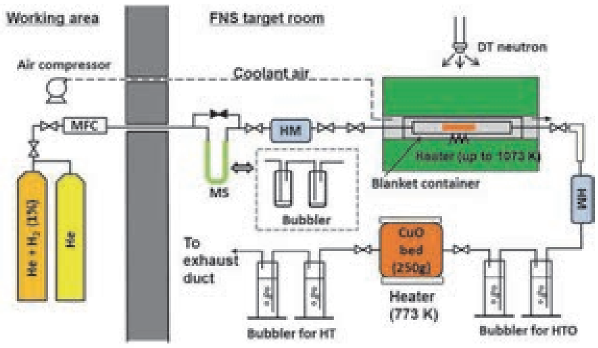

Tritium recovery system of integral experiment at JAEA-FNS

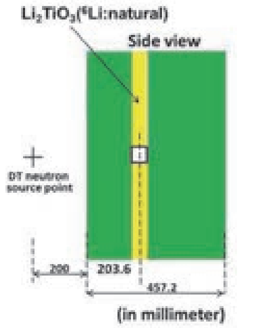

Cross sectional view of WCCB blanket mock-up

11

In case of H_2 sweep gas

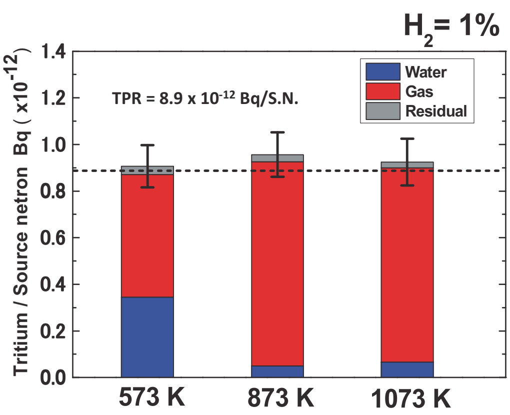

The recovered tritium gas at 573 K is 53% of the whole . In case of more than 873 K, the tritium gas increases up to 90 % of the total recovery.

12

In case of H_2O sweep gas

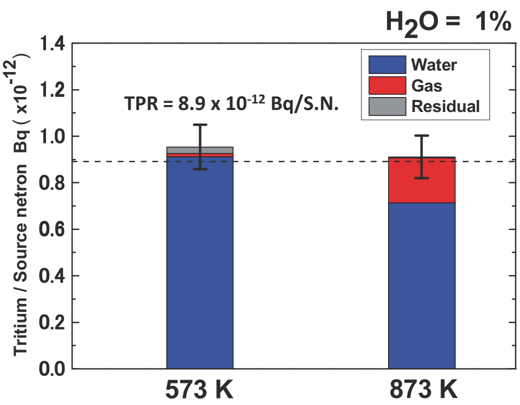

Tritium recovery is collected as tritium gas at 573 K. The tritium gas increases only 20 % of the total recovery at 873 K.

13

In case of H_2O + H_2 sweep gas

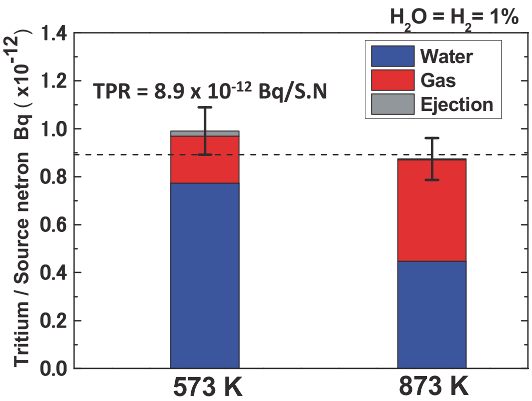

The tritium gas at 573 K is about 20% of the whole. The case of 873 K is about 50 % of the total.

14

Summary

- In order to investigate the tritium recovery properties on WCCB blanket, we have carried out the tritium recovery experiments with DT neutron.
- From our offline experiments, it was shown that the produced tritium certainly was recovered.
- From our online experiment, it was indicated that the tritium produced in the Li_2TiO_3 pebbles easily reacted on water vapor in the sweep gas line and quickly changed to HTO.
- It was also shown that the recovered tritium gas (HT) enhanced at higher temperature and dry hydrogen sweep gas. The cause is thought that the exchange reaction from H_2 to HT was more active than that of tritiated water (HTO).

15

Examination of Tritium Release Properties of Advanced Tritium Breeders by DT Neutron

Tsuyoshi Hoshino[a*], Kentaro Ochiai[b], Yuki Edao[c] and Yoshinori Kawamura[c]

[a]*Breeding Functional Materials Development Group, Fusion Research and Development Directorate, Japan Atomic Energy Agency, 2-166 Obuchi, Omotedate, Rokkasho-mura, Kamikita-gun, Aomori, 039-3212, Japan*
[b]*Fusion Neutronics Group, Fusion Research and Development Directorate, Japan Atomic Energy Agency, 2-4 Shirakata Shirane, Tokai-mura, Naka-gun, Ibaraki 319-1195, Japan*
[c]*Tritium Technology Group, Fusion Research and Development Directorate, Japan Atomic Energy Agency, 2-4 Shirakata Shirane, Tokai-mura, Naka-gun, Ibaraki 319-1195, Japan*

Demonstration power reactors (DEMOs) require advanced tritium breeder materials with high thermal stability. Lithium titanate (Li_2TiO_3) is one of the most promising candidates among tritium breeders because of its tritium release characteristics. However, the mass of Li_2TiO_3 decreases with time in a hydrogen atmosphere because of Li evaporation and Li burn-up. To prevent the reduction in mass at high temperatures, Li_2TiO_3 with additional Li ($Li_{2+x}TiO_{3+y}$) has been developed as an advanced tritium breeder. $Li_{2+x}TiO_{3+y}$ has higher stability at high temperatures in a reducing atmosphere. Although the tritium release properties of tritium breeders are documented in databases for DEMO blanket design, no in-situ examination under fusion neutron (DT neutron) irradiation has been performed. In this study, a preliminary examination of the tritium release properties of advanced tritium breeders was performed.

The $Li_{2+x}TiO_{3+y}$ powders were synthesized by a novel sold phase reaction as an advanced tritium breeder, and the $Li_{2+x}TiO_{3+y}$ pebbles were granulated by the emulsion method. This emulsion method consisted of two syringes arranged in a T-shaped flow path. One syringe was filled with oil, and the other syringe was filled with a $Li_{2+x}TiO_{3+y}$ slurry. The two flow lines from these syringes were connected in a T-shaped flow path. This arrangement allowed the $Li_{2+x}TiO_{3+y}$ slurry flow to be cut by the oil from the oil-filled syringe. The size of the $Li_{2+x}TiO_{3+y}$ gel particles was controlled by the relative flow speeds of the oil and the $Li_{2+x}TiO_{3+y}$ slurry. The gel particles were sintered in a 1% H_2-He atmosphere at 1373 K for 2 h.

DT neutron irradiation experiments were performed at the fusion neutronics source (FNS) facility in JAEA. A bulk cylinder with beryllium blocks as neutron multipliers was used to simulate the neutron spectrum in the Japanese solid breeder blanket design. The tritium breeder was contained in a stainless steel rectangular container. The temperature of the tritium breeder was kept at 723 K using a wire heater. To remove tritium produced by neutron irradiation, 1% H_2–He purge gas was passed from the inlet to the outlet through the tritium breeder pebbles.

The tritium release speed of the $Li_{2+x}TiO_{3+y}$ pebbles in the preliminary fabrication test was slower than that of ordinary Li_2TiO_3 pebbles because the average grain size on the surfaces and cross sections of the $Li_{2+x}TiO_{3+y}$ pebbles was 2–10 μm. Considering the tritium release characteristics, the optimum grain size after sintering is <5 μm. From the results of the optimization of the granulation conditions, prototype $Li_{2+x}TiO_{3+y}$ pebbles with the optimum grain size (<5 μm) were successfully fabricated. The $Li_{2+x}TiO_{3+y}$ pebbles exhibited good tritium release properties similar to the Li_2TiO_3 pebbles. In particular, the released amount of HT gas for easier tritium handling was higher than that of HTO water.

These results show that the $Li_{2+x}TiO_{3+y}$ pebbles improve the DEMOs blanket design and can contribute to early realization of DEMO reactors.

*Corresponding author's email: hoshino.tsuyoshi@jaea.go.jp

Ceramic Breeder Blanket Interactions (CBBI-17)
12-14 September 2013

Examination of Tritium Release Properties of Advanced Tritium Breeders by DT Neutron

Presented by K. Ochiai instead of T. Hoshino
Japan Atomic Energy Agency

Pebble Fabrication of Advanced Tritium Breeder

Comparison of Tritium Breeders

	Li_2O	Li_2AlO_2	Li_2ZrO_3	Li_4SiO_4	Li_2TiO_3
Tritium release (easy release)	> 400°C	> 400°C	> 400°C	> 350°C	> 300°C
Optimum operating temp.	400 - 600°C	400 - 900°C	400 - 800°C	350 - 700°C	300 - 800°C
Tritium breeding ratio (TBR)	High	Lower	Middle	Middle	Middle

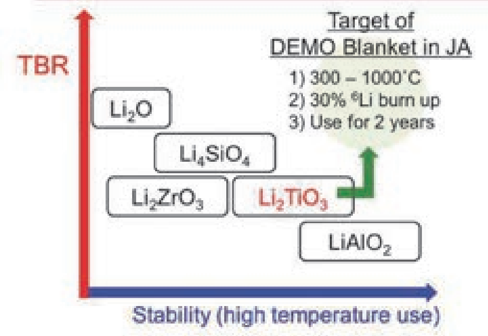

Demonstration power reactor (DEMO) requires "advanced tritium breeders" that have increased stability at high temperatures for getting the higher tritium breeding ratios (TBRs).

Necessity of Advanced Tritium Breeder

Li mass in Li_2TiO_3 decreases with time because of evaporation and burn-up.

The addition of Li into Li_2TiO_3 was invented to make up for these Li loss.

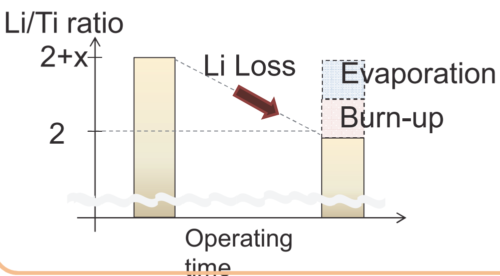

Li_2TiO_3 is non-stoichiometric compound and has the range of Li/Ti ratio from 1.88 to 2.25.

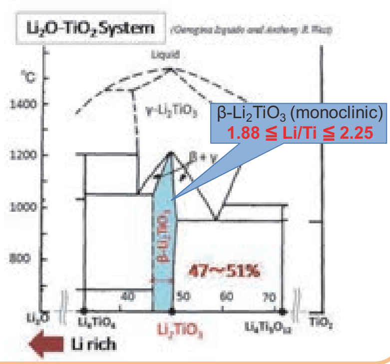

To prevent the these mass decreases, Li_2TiO_3 with additional Li ($Li_{2+x}TiO_{3+y}$) has been developed as an advanced tritium breeder.

Production of Advanced Tritium Breeder

New solid phase reactions

$LiOH \cdot H_2O$ → Precursors mixed in the molecular ratio of Li/Ti = 2.2 ← H_2TiO_3

↓

Mixture rotated at room temperature

↓

Gelation

↓

Calcination

↓

Sintering

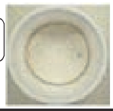

Usually, solid phase reaction of Li2CO3 and TiO2 is used in the synthesis of Li2TiO3.
However, the Li addition by solid phase reaction was found to be difficult.

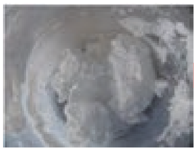

Rotation time: 10h

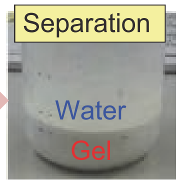

Rotation time: 48h

Powders of $LiOH \cdot H_2O$ and H_2TiO_3 were mixed in a molecular ratio of Li/Ti = 2.2. In addition, the mixture of the starting powders was continuously rotated at room temperature for 48 h in a polyethylene container.
The mixture gradually turned into a gel through a solid phase reaction at room temperature.
After drying, the gel was calcined in air at 873 K for 5 hr and sintered in N_2 at 1373 K for 2 h.

Characterization of Advanced Tritium Breeder

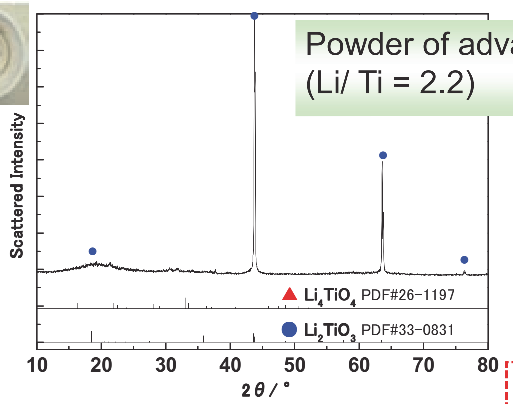

Powder of advanced tritium breeder (Li/ Ti = 2.2)

↓

The molar ratios of reaction products were corresponding well with the original mixing ratio of $LiOH \cdot H_2O$ and H_2TiO_3.

Single phase $Li_{2+x}TiO_{3+y}$

Samples	Molar ratio Li/Ti		Cristal structure	
	At mixing	After sintering (ICP-AES)	XRD measurement	Neutron diffraction
LiTi22-N	2.2	2.2	$Li_{2.2}TiO_{3+x}$ Single phase	$Li_{2.2}TiO_{3+x}$ Single phase

Pebble Fabrication - Emulsion Method -

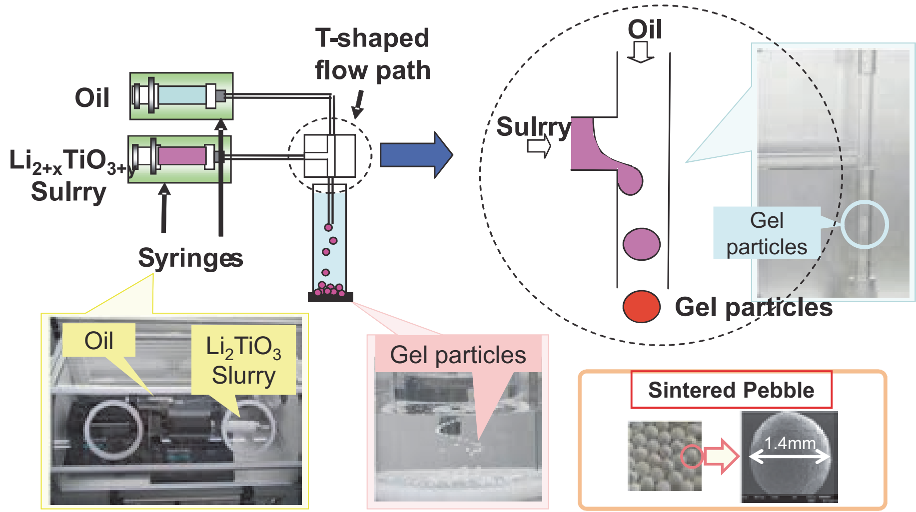

This granulator is composed of two syringes and T-shaped flow path. One syringe is filled with oil. Other syringe is filled with $Li_{2+x}TiO_{3+y}$ slurry. Two flow lines from these syringes are connected in the T-shaped flow path. In this time, $Li_{2+x}TiO_{3+y}$ slurry flow is cut by oil flow from the oil-filled syringe.

Emulsion Method - Video 1 -

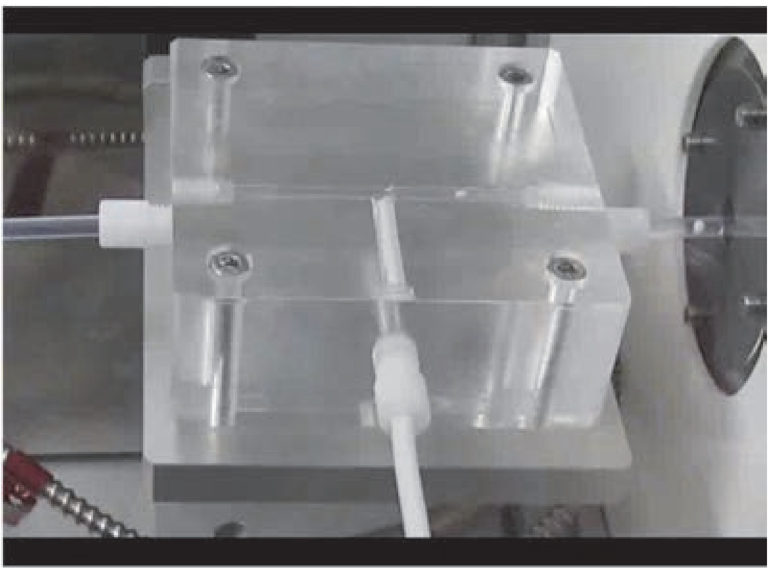

Emulsion Method - Video 2 -

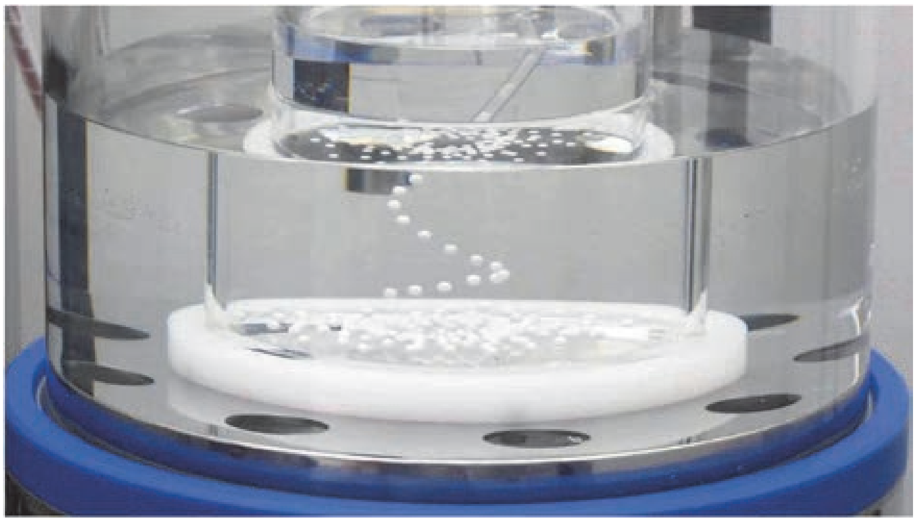

Sintered $Li_{2+x}TiO_{3+y}$ Pebbles

Pebble Fabrication

Slurry ($Li_{2+x}TiO_{3+y}$ with binder)

↓

Emulsion method

↓

Gel-spheres

↓

Calcination — in air at 873 K for 5 h

↓

Sintered pebbles — in 1%H_2-He at 1373 K for 2 h

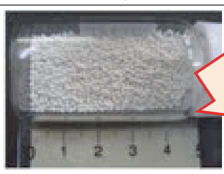

XRD patterns of sintered $Li_{2+x}TiO_{3+y}$ pebbles

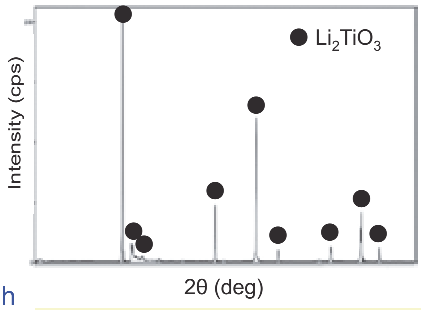

The XRD results of the sintered $Li_{2+x}TiO_{3+y}$ were almost the same as those of the Li_2TiO_3 listed in the JCPDF.
No other phases or impurities were observed.

Single phase $Li_{2+x}TiO_{3+y}$

Grain Size of Sintered $Li_{2+x}TiO_{3+y}$ Pebbles

SEM emages of sintered $Li_{2+x}TiO_{3+y}$ pebbles

(a)Surface

(b)Cross-section

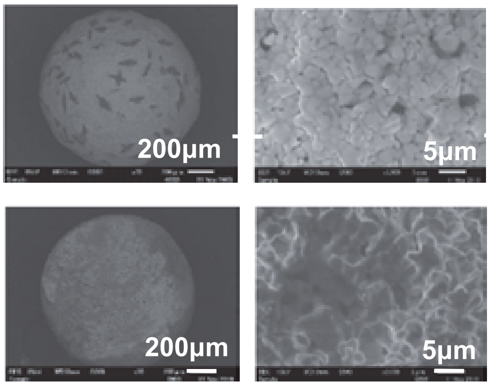

Average grain size on the surface and the cross section was < 5 μm and 5 – 10 μm, respectively.

Tritium Release properties of Advanced Tritium Breeder

Schedule of Tritium release properties

Tritium release properties of the advanced tritium breeder under the DEMO blanket relevant neutron condition is very important for the DEMO blanket design.

Task	2013	2014	2015	2016
Preparation and preliminary examination with neutron source				
Trial examination and analysis with neutron source				

At the Fusion Neutronics Source (FNS) facility in JAEA , preliminary test of tritium release properties from conventional lithium titanate pebbles have been carried out. In this new task, small blanket mockup with $Li_{2+x}TiO_{3+y}$ pebbles is under fabrication.

Preliminary Examinations

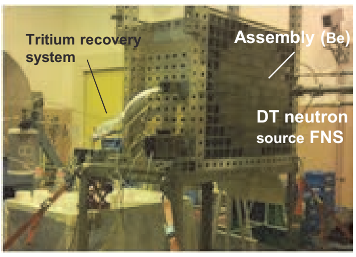

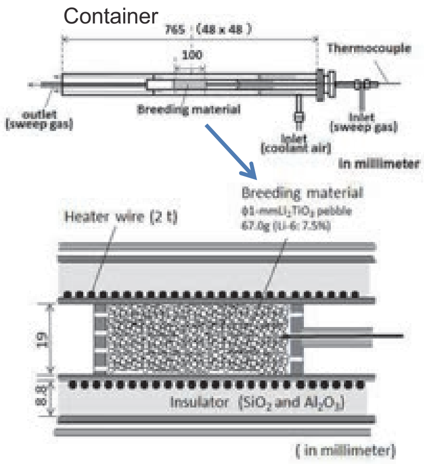

DT neutron source :JAEA-FNS
Neutron intensity: 1.5 x 10^{11}n/sec
Breeding material: Li_2TiO_3 small pebble
Temperature: RT~ 1273 K
Sweep gas: He (H_2, H_2Ovapor)
Recovery system: Water babbler
Detector: Liquid scintillation counter

In 2013: Preparations and preliminary examinations for tritium release properties of advanced tritium breeders was started by DT neutron irradiation as a new task.

Experimental setup

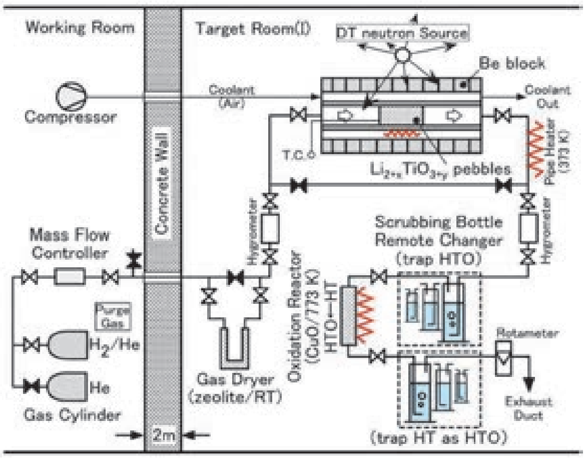

A bulk cylinder with beryllium blocks as neutron multipliers was used to simulate the neutron spectrum in the Japanese solid breeder blanket design. The tritium breeder was contained in a stainless steel rectangular container. The temperature of the tritium breeder was kept at 723 K using a wire heater. To remove tritium produced by neutron irradiation, 1% H_2–He purge gas was passed from the inlet to the outlet through the tritium breeder pebbles.

$Li_{2+x}TiO_{3+y}$ Pebbles

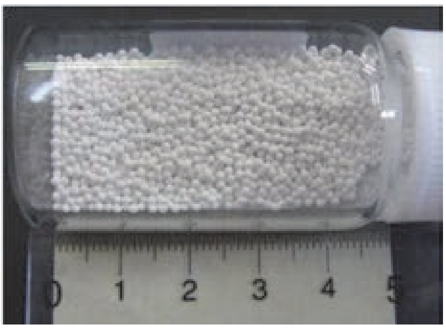

Diameter	1.4 mm
Ratio of Li/Ti	2.16
Grain size	< 5 μm (Surface) **> 2-10 μm (Cross section)**
Sphericity	1.02
Crystal structure	Single phase of $Li_{2+x}TiO_{3+y}$

Tritium release properties of $Li_{2+x}TiO_{3+y}$

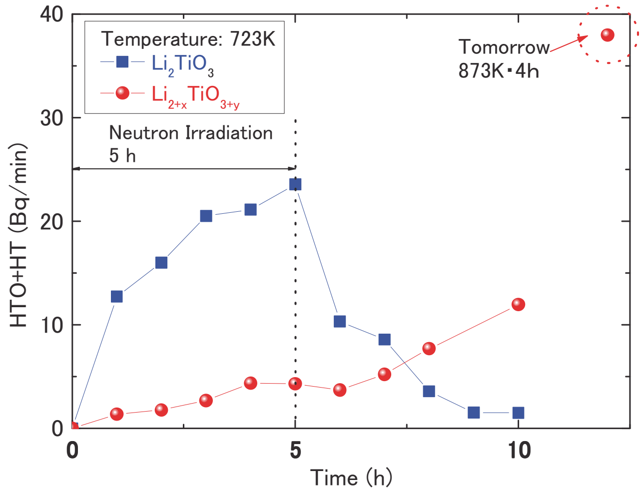

The tritium release speed of the $Li_{2+x}TiO_{3+y}$ pebbles in the preliminary fabrication test was slower than that of ordinary Li_2TiO_3 pebbles.
Considering the tritium release characteristics, the optimum grain size after sintering is <5 μm.

Improvement of the Grain Size

New Pebble ①

Sintering in vacuum atmosphere

Diameter	1.18mm
Sphericity	1.04
Structure	$Li_{2+x}TiO_{3+y}$
Li/Ti	2.11
Grain size	< 5 μm
Density	60% T.D.

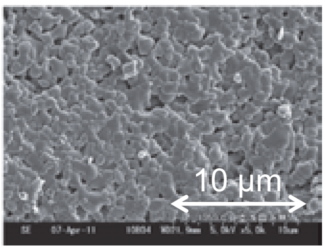

Surface

Good!

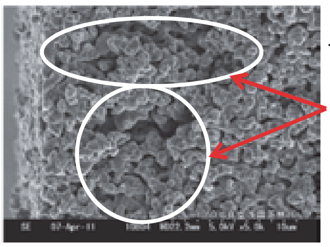

Cross-section

Large pore is observed.

Optimum sintering conditions was surveyed in order to increase the density of advanced breeder pebbles.

Improvement of Density

New Pebble ②

The $Li_{2+x}TiO_{3+y}$ pebbles were sintered at 1073 K for 1 h in vacuum and at 1323 K for 5 h in an argon atmosphere.

Surface

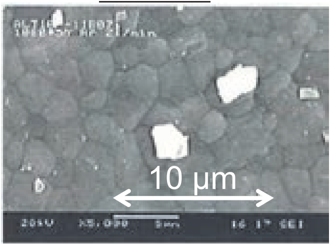

Cross-section

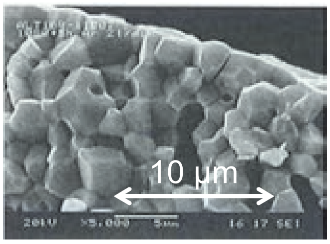

Grain size	< 5 μm
Density	86% T.D.

Good!

To determine whether the emulsion method is suitable for large fabricating $Li_{2+x}TiO_{3+y}$ pebbles.

New $Li_{2+x}TiO_{3+y}$ Pebbles

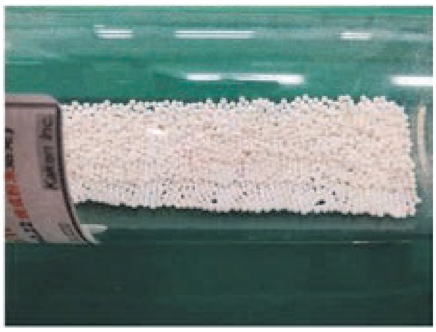

Diameter	1.4 mm
Ratio of Li/Ti	2.15
Grain size	**< 5 μm**
Sphericity	1.02
Crystal structure	Single phase of $Li_{2+x}TiO_{3+y}$

Tritium release properties of New $Li_{2+x}TiO_{3+y}$

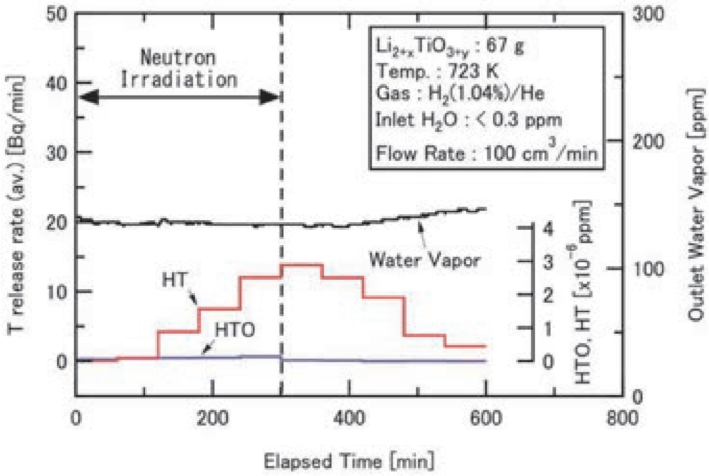

The released amount of HT gas for easier tritium handling was higher than that of HTO water.

Tritium release properties

New $Li_{2+x}TiO_{3+y}$

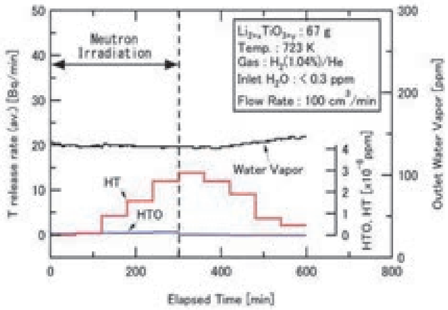

Li_2TiO_3

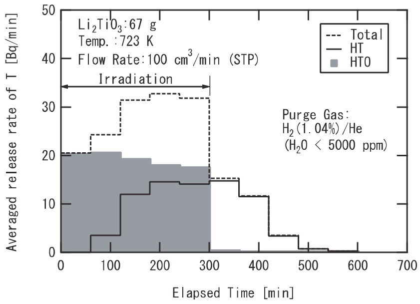

The $Li_{2+x}TiO_{3+y}$ pebbles exhibited good tritium release properties similar to the Li_2TiO_3 pebbles.

Conclusion

The tritium release speed of the $Li_{2+x}TiO_{3+y}$ pebbles in the preliminary fabrication test was slower than that of ordinary Li_2TiO_3 pebbles because the average grain size on the surfaces and cross sections of the $Li_{2+x}TiO_{3+y}$ pebbles was 2–10 μm.

Considering the tritium release characteristics, the optimum grain size after sintering is <5 μm. From the results of the optimization of the granulation conditions, prototype $Li_{2+x}TiO_{3+y}$ pebbles with the optimum grain size (<5 μm) were successfully fabricated.

The $Li_{2+x}TiO_{3+y}$ pebbles exhibited good tritium release properties similar to the Li_2TiO_3 pebbles. In particular, the released amount of HT gas for easier tritium handling was higher than that of HTO water.

Basic Studies on new neutron multiplier and breeder materials

Kenzo Munakata[1], Kohei Wada[1], Ayano Nakamura[1], Jae-Hwan Kim[2], Masaru Nakamichi[2], Regina Knitter[3]

[1]*Faculty of engineering and resource science, Akita university, 1-1, Tegatagakuen-cho, Akita, 010-8502, Japan*
[2]*Fusion Research and Development Directorate, Japan Atomic Energy Agency, 2-166, Omotedate, Obuchi, Rokkasho, Kamikita, Aomori, 039-3212, Japan*
[3]*Karlsruhe Institute of Technology, Institute for Applied Materials (IAM-WPT), Hermann-von- Helmholtz-Platz 1, 76344 Eggenstein-Leopoldshafen*

The neutron multiplier is indispensible for generation of tritium that is a fuel of fusion reactors. Metallic beryllium is considered as a candidate for the neutron multiplier. Titanium beryllide is an alternative of metallic beryllium as the neutron multiplier of the fusion reactor blanket. The authors examined oxidation resistance of the titanium beryllide, $Be_{12}Ti$, samples fabricated by the spark plasma sintering method. The titanium beryllide samples were placed in a reactor. A H_2O/Ar (10,000 ppm) gas was generated by passing a (10,000 ppm) H_2/Ar gas to a copper oxide bed held at 623 K, and then it was introduced to the reactor with the flow rate of 300 cm^3/min. Experimental temperature of test tube was raised up to 1273 K by the constant rate of 5 K/min using a electric furnace. The reactor temperature was held at 1273 K until generation of hydrogen was terminated. The concentrations of hydrogen in the outlet streams of the reactor were measured with gas chromatograph or mass spectrometer. Thermo-gravitational apparatus was also used to examine the oxidation behavior from the viewpoint of weight gain. The state of the sample surface oxidized during exposure to water vapor was characterized by means of the X-ray diffraction analysis (using Ultima IV manufactured by RIGAKU Co. LTD.) and electron probe micro analyzer (using JXA-8230 manufactured by JEOL Co. LTD.).

New breeder materials were supplied by Karlsruhe Institute Technology (KIT). They are complex oxides of Li, Si and Ti. With regards to these breeder samples, the ratio for contents of Si and Ti were varied a bit. The authors had restarted out of pile tritium release experiments on these new breeder materials utilizing the Kyoto University Research Reactor. In the experiments, a 0.1% H_2/Ar gas was used as a sweep gas to avoid chemical interaction of sweep gas and breeder materials (the authors previously used nitrogen as a carrier gas), and two ion chambers were used to separately measure the concentration of molecular form of tritium and tritiated water vapor. Experimental temperature of test tube was raised up to 1173 K by the constant rate of 5 K/min using an electric furnace. The reactor temperature was held at 1173 K until tritium release terminated. At the temperature of 1173 K, the sweep gas was switched to a 0.5% H_2O/Ar gas to ensure whole release of tritium bred in the breeder pebbles.

The summary and more details of the experimental results for neutron multiplier and breeder materials shown above are talked on our presentation.

Basic Studies on new neutron multiplier and breeder materials

Kenzo MUNAKATA[1)], Kohei WADA[1)], Ayano NAKAMURA[1)], Jae-Hwan KIM[2)], Masaru NAKAMICHI[2)], Regina KNITTER[3)]

[1)]*Faculty of engineering and resource science, Akita university, 1-1, Tegatagakuen-cho, Akita, 010-8502, Japan*

[2)]*Fusion Research and Development Directorate, Japan Atomic Energy Agency, 2-166, Omotedate, Obuchi, Rokkasho, Kamikita, Aomori, 039-3212, Japan*

[3)]*Karlsruhe Institute of Technology, Institute for Applied Materials (IAM-WPT), Hermann-von- Helmholtz-Platz 1, 76344 Eggenstein-Leopoldshafen*

Outline of presentation

- *History of the development of intermetallic compounds of beryllium*
- *Experimental study on $Be_{12}Ti$*
- *Introduction of new breeder developed by KIT*
- *Experimental study on complex oxides of Li, Si and Ti.*
- *Modeling*
- *Ab-initio quantum chemistry calculation on $Be_{12}Ti$ and Li_4LiO_4 crystals.*

Neutron multiplier

- The neutron multiplier is indispensable for generation of tritium that is a fuel of fusion reactors.
- Metallic beryllium has been considered as a candidate for the neutron multiplier.
- Titanium beryllide is an alternative of metallic beryllium as the neutron multiplier of the fusion reactor blanket.
- The authors examined oxidation resistance of the titanium beryllide, $Be_{12}Ti$, samples fabricated by the spark plasma sintering method.

Breeder material

- New breeder materials were supplied by Karlsruhe Institute Technology (KIT).
- They are complex oxides of Li, Si and Ti.
- With regards to these breeder samples, the ratio for contents of Si and Ti were varied a bit.
- The authors had restarted out of pile tritium release experiments on these new breeder materials utilizing the Kyoto University Research Reactor.

Why beryllide?

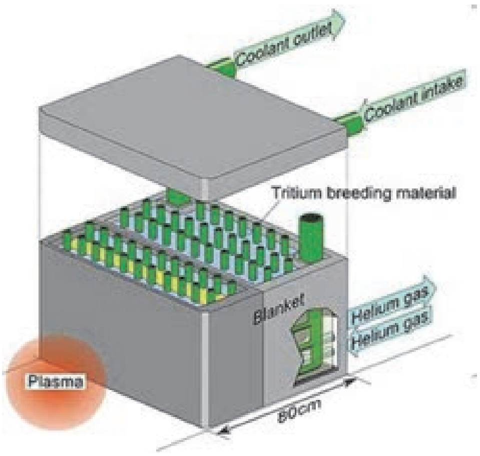

- Beryllium is regarded as a primary candidate material.
- Be is highly reactive with oxygen and water vapor.
- Reaction with water vapor generate hydrogen.
- This problem could be severe in the case of water-cooled blanket.
- More stable neutron multiplier is necessary.

Metallic beryllium contacted with water vapor and breakaway reaction

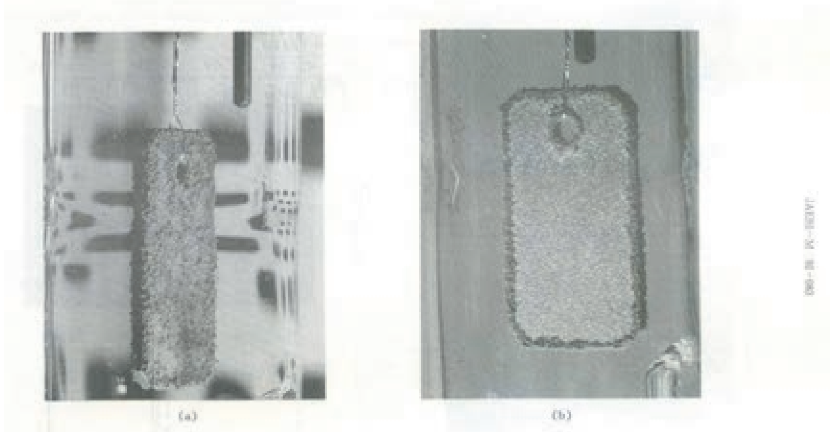

Yoshida et al., JAERI

Mass gain of pure beryllium samples contacted with water vapor

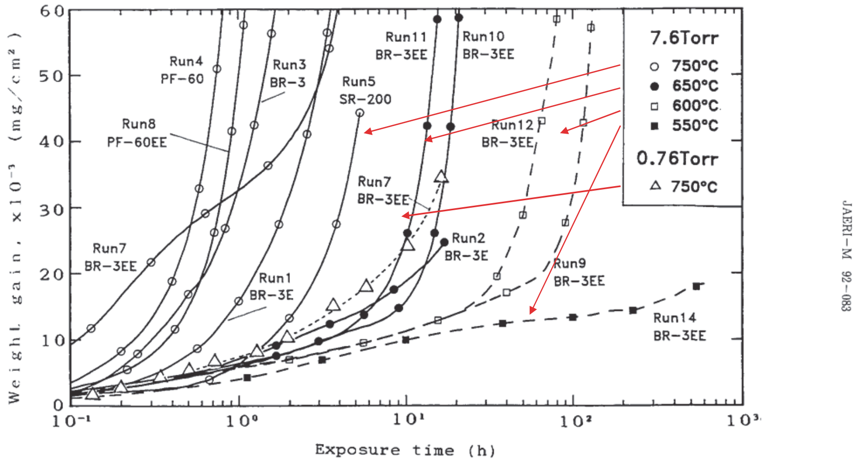

Yoshida et al., JAERI

Comparison of HIP method and plasma-sintering method

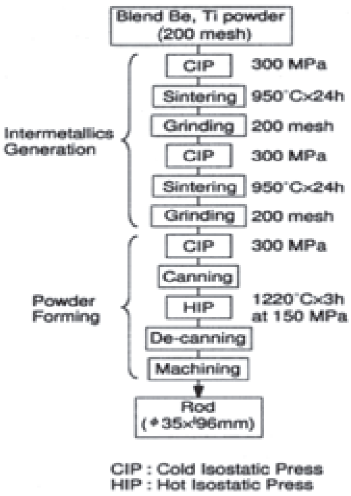

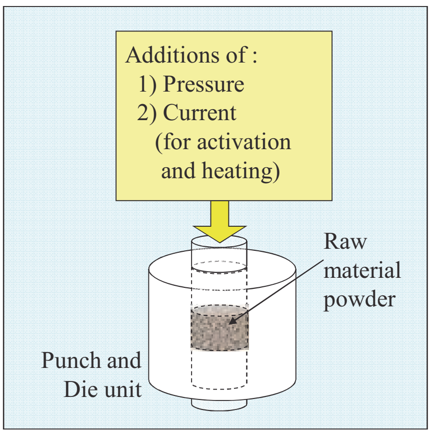

Experiments for hydrogen generation from $Be_{12}Ti$ sample prepared by HIP

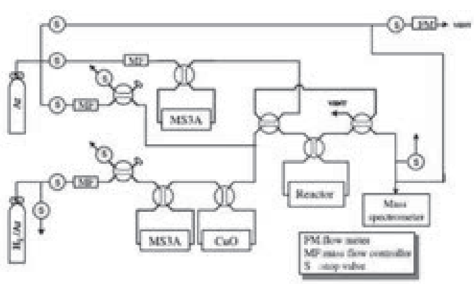

- The sample geometry was 7.9 mm in diameter and 1.4 mm in thickness.
- The flow rate of the gas was 91.6 cm3-STP/min.
- the reactor temperature was held at ambient temperature for 30 min, and then it was raised to 1213~1273 K at the constant rate of 5~10 K/min.

K. Munakata et al., Journal of Nuclear Materials 329–333 (2004) 1357–1360

Hydrogen genertion of the $Be_{12}Ti$ samples fabricated by HIP method

- *Breakaway reaction does not take place on the surface of the Be12Ti disk,*
- *The generation of hydrogen started at a temperature near 873 K, and the concentration of hydrogen in the outlet stream of the reactor reached a peak at 1273 K..*

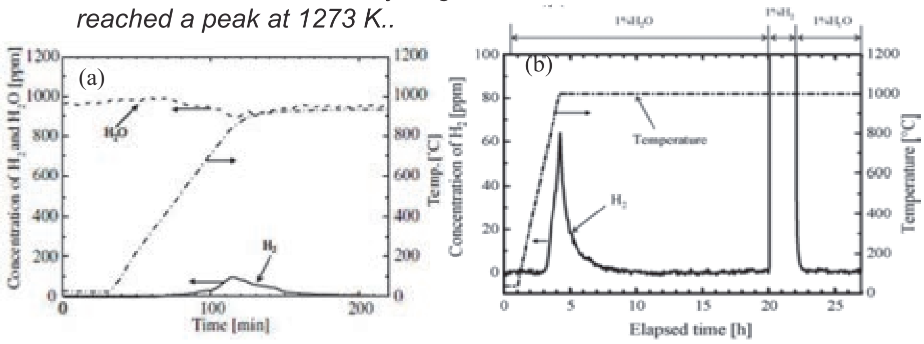

(a) 960 ppm H_2O/Ar gas (b) 10,000 ppm H_2O/Ar.

K. Munakata et al., Journal of Nuclear Materials 329–333 (2004) 1357–1360

X-ray diffraction pattern of the $Be_{12}Ti$ sample fabricated by HIP method before experiment

- (a) before use (as received)
- (b) after exposure to 0.096% H_2O/Ar
- (c) after exposure to 1% of H_2O/Ar

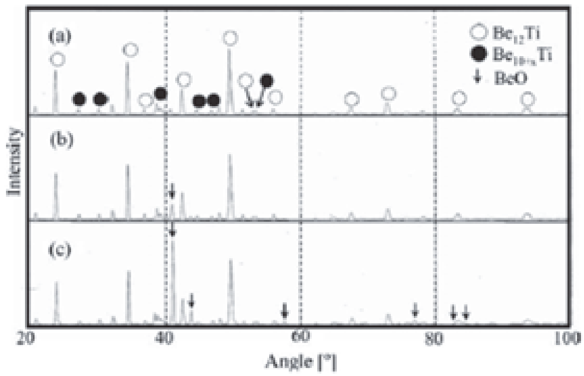

Photographs of the $Be_{12}Ti$ sample fabricated by HIP method contacted with water vapor

- After the experiment, the color of the surface of the sample disk was found to turn to white.
- Yhis could indicate that the surface of the sample was covered by the layer of beryllium oxidized.

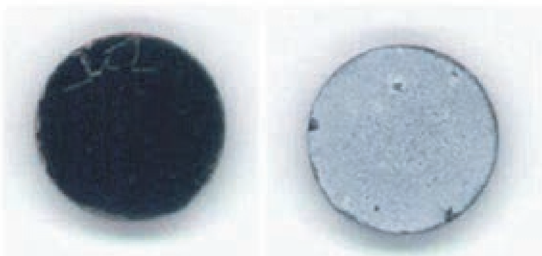

Photographs of a $Be_{12}Ti$ sample: (a) before and (b) after experiment.

K. Munakata et al., Journal of Nuclear Materials 329–333 (2004) 1357–1360

Experimental apparatus for hydrogen generation *from* the $Be_{12}Ti$ sample prepated by the plasma-sintering method

- *The samples were placed under a flow of Ar gas containing 10,000 ppm (1%) water vapor.*
- *The temperature of the samples was raised from 313 K to 1273 K at 5 K/min. After the reactor temperature reached 1273 K, it was held at 1273 K for 24 h. The flow rate of the Ar gas containing 10,000 ppm of water vapor was 300 cm^3/min.*

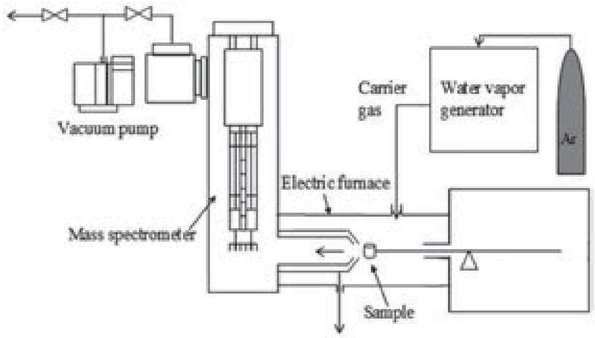

Hydrogen generation from pure beryllium sample

- *The final mass gain of the pure beryllium sample was 21.75 mg, which corresponds to approximately 50 % of its initial weight (44.63 mg).*
- *The amount of hydrogen generated from each 1 cm^2 of the surface of the metallic beryllium sample was 2.78×10^{-3} mol.*

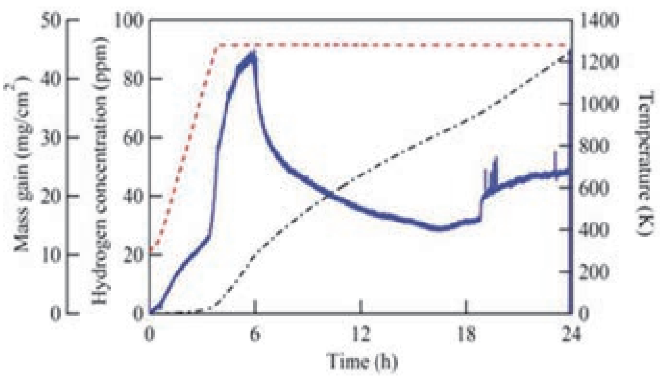

Hydrogen generation from $Be_{12}Ti$ sample prepared by plasma-sintering method

- The final mass gain of the plasma sintered $Be_{12}Ti$ sample was 1.10 mg, approximately 1.7 % of its initial weight (64.18 mg).
- The amount of hydrogen generated from each 1 cm^2 of the surface of the $Be_{12}Ti$ sample was 1.14×10^{-4} mol.

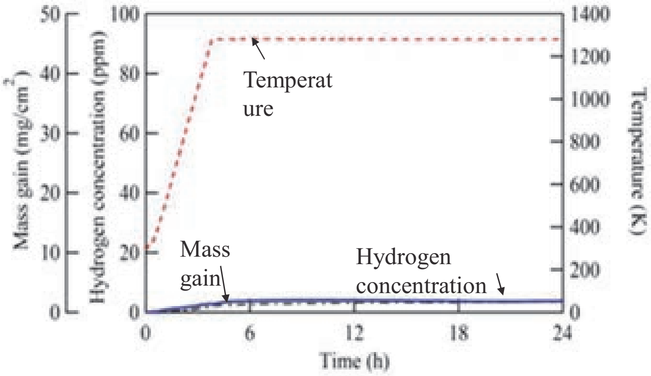

X-ray diffraction pattern of the pure beryllium sample

- *In the sample after exposure to the Ar gas containing 10,000 ppm of water vapor, several diffraction peaks arose, and most of them were attributed to BeO (marked with closed triangle).*
- *After the experiment, a large amount of white product was observed on the surface of the pure beryllium sample. Furthermore, volume expansion and peel-off of this white product was observed.*

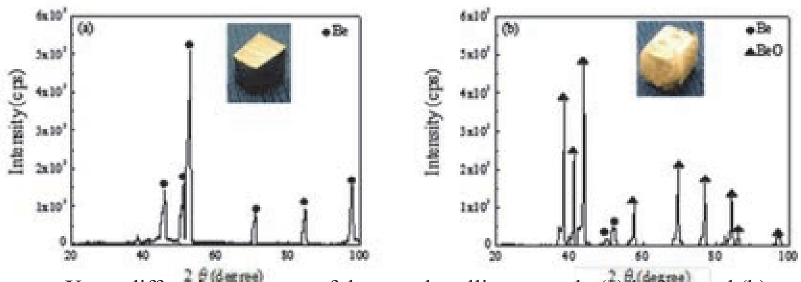

X-ray diffraction patterns of the pure beryllium sample (a) before and (b) after exposure to the Ar gas containing 10,000 ppm of water vapor.

X-ray diffraction pattern of the $Be_{12}Ti$ sample

- White products only appeared as limited spots on the surface, and neither swelling nor peel-off of the surface product was observed.
- Diffraction peaks related to BeO were observed on the sample surface, whereas the intensity of the diffraction peak attributed to BeO was quite

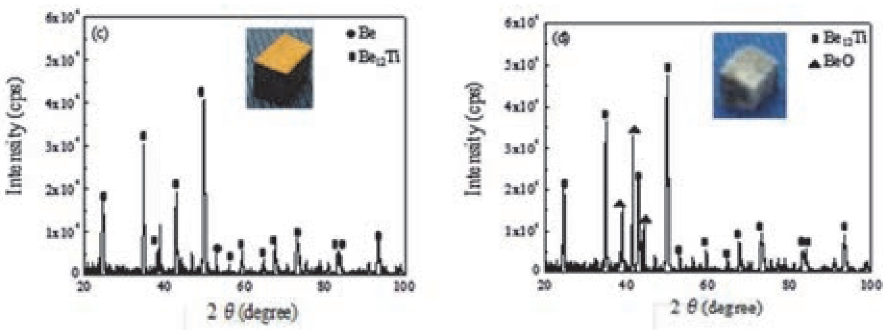

X-ray diffraction patterns of the $Be_{12}Ti$ sample (a) before and (b) after exposure to the Ar gas containing 10,000 ppm of water vapor.

EPMA analysis of pure beryllium sample and $Be_{12}Ti$ sample before exposure to water vapor

- *The results of EPMA analysis demonstrate that the titanium beryllide is composed of four different phases such as Be, $Be_{12}Ti$, $Be_{17}Ti_2$, and Be_2Ti with different fractions small compared with the oxidized metallic beryllium sample.*

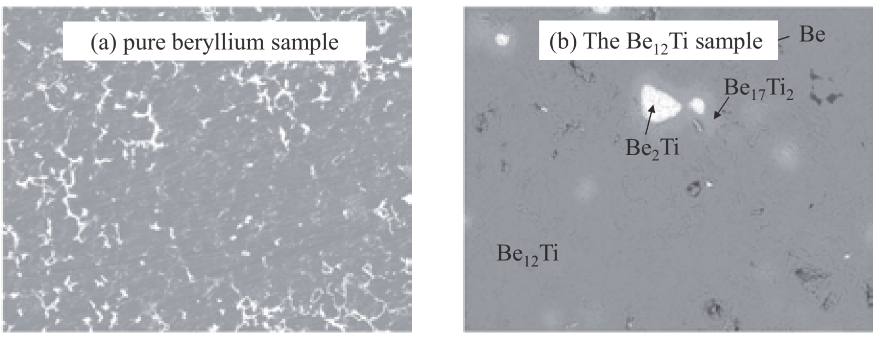

EPMA images of (a) the pure beryllium sample and (b) the $Be_{12}Ti$ sample before exposure to the Ar gas containing 10,000 ppm of water vapor.

EPMA analysis of pure beryllium sample and $Be_{12}Ti$ sample after exposure to water vapor

- BeO generated on the surface of the pure beryllium sample after the experiment had small particle diameter, and it was not protective.
- BeO generated on the surface of the $Be_{12}Ti$ sample after the experiment had large particle diameter, and it was protective.

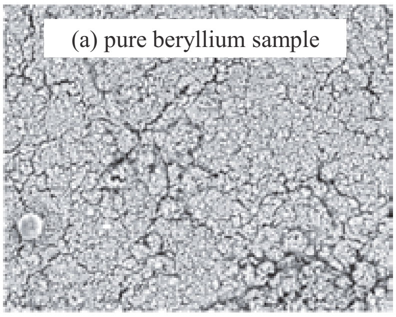

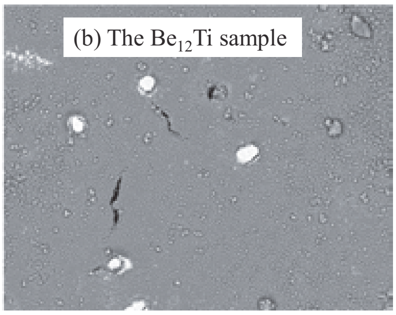

EPMA images of (a) the pure beryllium sample and (b) the $Be_{12}Ti$ sample after exposure to the Ar gas containing 10,000 ppm of water vapor.

New breeder material

- *New breeder materials were developed by Karlsruhe Institute Technology (KIT).*
- *They are complex oxides of Li, Si and Ti.*
- *With regards to these breeder samples, the ratio for contents of Si and Ti were varied a bit.*
- *The authors had restarted out of pile tritium release experiments on these new breeder materials utilizing the Kyoto University Research Reactor.*

Experimental setup

- *A 0.1% H_2/Ar gas was used as a sweep gas to avoid chemical interaction of sweep gas and breeder materials (the authors previously used nitrogen as a carrier gas).*
- *Two ion chambers were used to separately measure the concentration of molecular form of tritium and tritiated water vapor.*

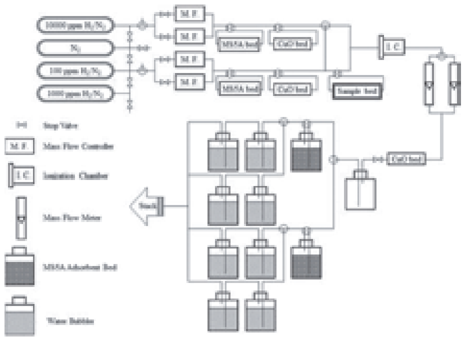

Experimental setup

- *Experimental temperature of test tube was raised up to 1173 K by the constant rate of 5 K/min using an electric furnace.*
- *The reactor temperature was held at 1173 K until tritium release terminated. At the temperature of 1173 K, the sweep gas was switched to a 0.5% H_2O/Ar gas to ensure whole release of tritium bred in the breeder pebbles.*

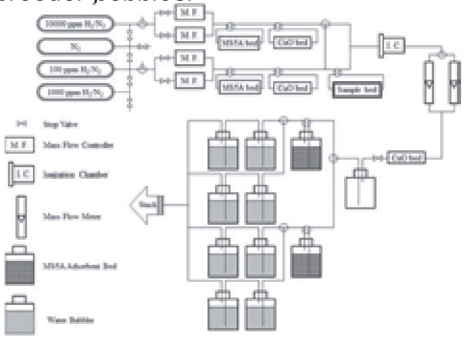

Samples used in experiments

- OSiO7M 800d: Lithium orthosilicate with thermal treatment at 800 ℃
- OSiO7M 900d: Lithium silicate with thermal treatment at 900 ℃
- KALOS31: OSi + 10 mol% MTi
- KALOS33: OSi + 15 mol% MTi
- KALOS34C: OSi + 20 mol% MTi cond.
- KALOS35: OSi + 30 mol% MTi

OSiO7M 800d-2

- Carrier gas: 1,000 ppm H_2/Ar
- Flow rate: 100 cc/min
- Temperature: was raised up to 1173 K at the constant rate of 5 K/min.
- Tritium released: 3.49 μCi

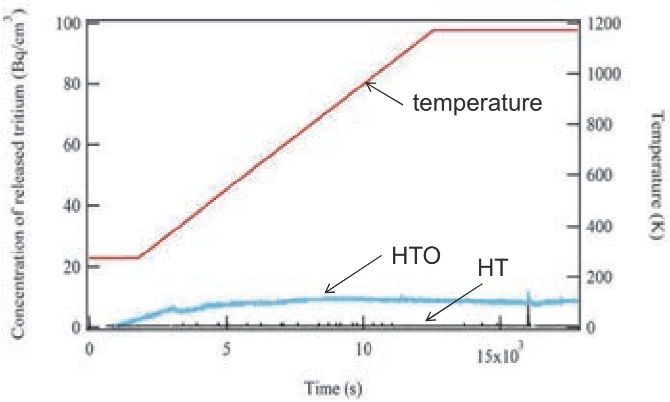

OSiO7M 900d-2

- *Carrier gas: 1,000 ppm H_2/Ar*
- *Flow rate: 100 cc/min*
- *Temperature: was raised up to 1173 K at the constant rate of 5 K/min.*
- *Tritium released: 2.02 μCi*

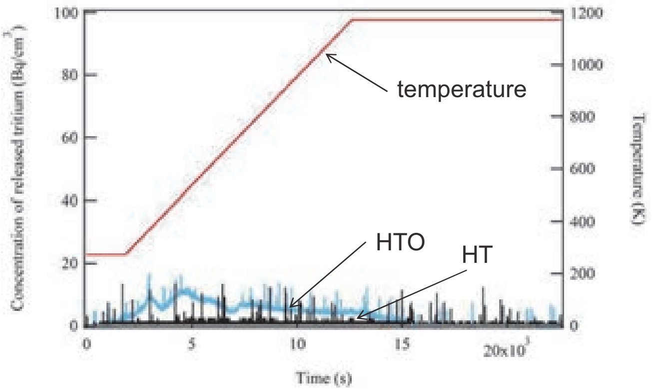

KALOS31 (10 mol% MTi)

- *Carrier gas: 1,000 ppm H_2/Ar*
- *Flow rate: 100 cc/min*
- *Temperature: was raised up to 1173 K at the constant rate of 5 K/min.*
- *Tritium released: 6.03 μCi*

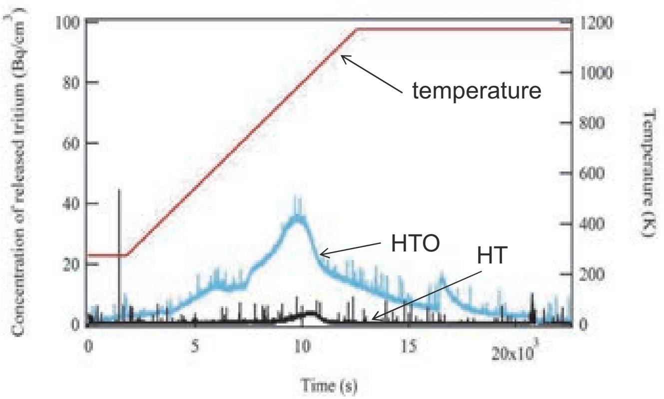

KALOS33 (15 mol% MTi)

- Carrier gas: 1,000 ppm H_2/Ar
- Flow rate: 100 cc/min
- Temperature: was raised up to 1173 K at the constant rate of 5 K/min.
- Tritium released: 6.03 μCi

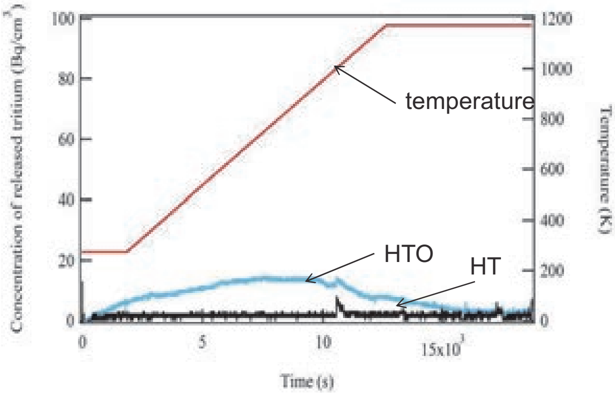

KALOS34C (20 mol% MTi)

- Carrier gas: 1,000 ppm H_2/Ar
- Flow rate: 100 cc/min
- Temperature: was raised up to 1173 K at the constant rate of 5 K/min.
- Tritium released: 5.39 μCi

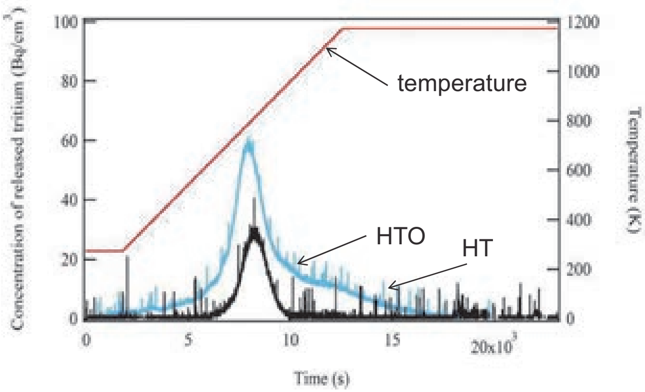

KALOS35 (30 mol% MTi)

- Carrier gas: 1,000 ppm H_2/Ar
- Flow rate: 100 cc/min
- Temperature: was raised up to 1173 K at the constant rate of 5 K/min.
- Tritium released: 6.64 μCi

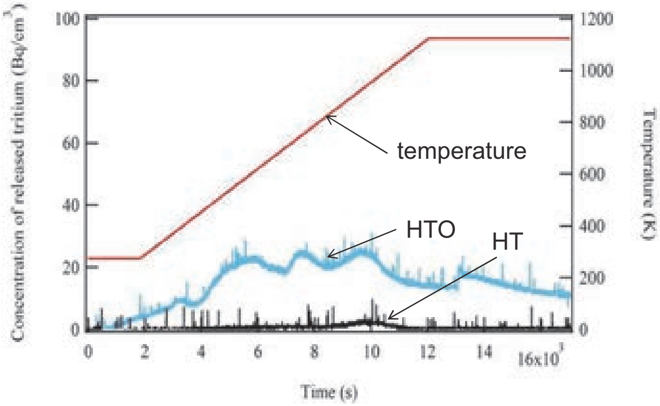

Summary of results

- At present, consistent and systematic discussion is not possible.
- Reproducibility of experimental results should be checked.
- As far as chemical form of tritium, tritiated water is the main from of tritium released from short-irradiated breeder materials regardless of difference in chemical constituents.
- Numerical simulation of tritium release process is planed based on new and more sophisticated mathematical model.

Modelling

- *Modelling of the tritium release behavior from Li_4SiO_4 pebbles were performed.*
- *In the model, surface reaction was eliminated since wet sweep gases were used in the experiment.*
- *However trapping and detrapping of tritium in the crystal was taken into account.*
- *Numerical simulation was based on finite volume discretization and Crank-Nicolson Differential scheme was applied.*
- *Fitting of the parameters were performed by combining the simulation code and an algorithm based Levenberg-Maquartz method (non linear least squares analysis).*

Diffusion Model with Trapping Site Effect

- *The effect of trapping sites was incorporated into diffusion model. The mass balance equation is expressed as*

$$r^2 \frac{\partial q}{\partial t} = \frac{\partial}{\partial r}\left(r^2 D \frac{\partial q}{\partial r} \right) - r^2 k_T q(\boxed{q_{T,0}} - q_T) + r^2 k_D q_T$$

$$r^2 \frac{\partial q_T}{\partial t} = r^2 k_T q(q_{T,0} - q_T) - r^2 k_D q_T$$

$$D = \boxed{D_0} \exp\left(\boxed{-E_{AD}} / RT \right)$$

$$k_T = \boxed{k_{T,0}} \exp\left(\boxed{-E_T} / RT \right)$$

$$k_D = \boxed{k_{D,0}} \exp\left(\boxed{-E_D} / RT \right)$$

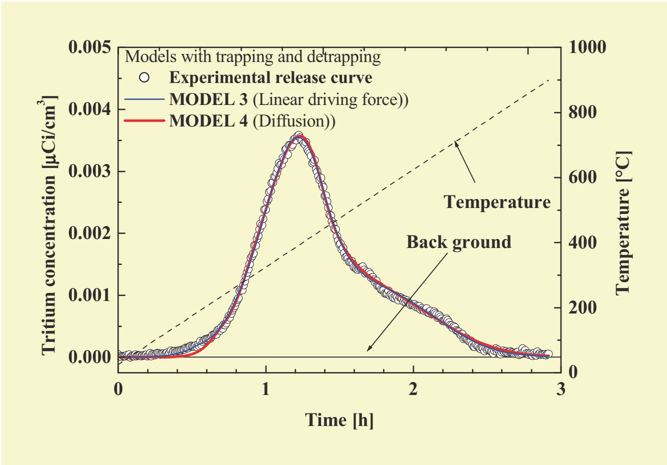

Comparison of experimental release curve and numerical computations by MODEL 3 and MODEL 4 with trapping effect

Ab-initio study on neutron multiplier and breeder materials

- *Electron state in crystal*
- *Prediction of thermodynamic property*
- *Prediction of mechanical property*
- *Effect of vacancy or interstitials*
- *Surface reaction*
- *Molecular dynamics calculation by Car-Parrinello method based on Lagrangian formulation and density functional theory*

CRYSTAL code

- *CRYSTAL has been developed by Torino University.*
- *CRYSTAL which can be used for the linear combination of atomic orbital and Hartree-Fock (LCAO-HF) ab initio electron calculation in periodic systems.*
- *This code utilizes the linear combination of Bloch function defined in terms of local functions.*

Crystal structure of $Be_{12}Ti$

- *Precise crystal structure of $Be_{12}Ti$ has not been known.*
- *Gillam et al. have reported that $Be_{12}Ti$ and $Be_{12}V$ have crystal structures similar to that of $Mn_{12}Th$ with the space group of I4/mmm.*
- *The crystal structure of $Be_{12}Mo$ is hexagonal with a unit cell a = 7.271 Å and c = 4.234, and its space group is also I4/mmm.*

Lattice parameter and basis function

- *In ab initio calculation, the authors used the lattice parameters (a = 7.35 Å and c = 4.19 Å) reported by Zalkin et al. With regard to the positional parameters of atoms, those reported for $Mn_{12}Th$ and $Be_{12}Mo$ are first tested.*
- *For the local functions, the Gaussian type functions were used. The Gaussian basis set used for Be was a 5-111G contraction and for Ti a 8-6-411G contraction reported in a literature was used.*
- *The version restricted Hartree-Fock was used for SCF calculation.*

Optimization of crystal structure

- *The positional parameters for $Be_{12}Mo$ resulted in a lower energy state and a more stable structure.*
- *Next, the structure optimization was attempted with LoptCG that is a korn-shell script for performing a geometry optimization with CRYSTAL package.*
- *The script employs the steepest descent and conjugate gradient approaches.*

Initial crystal sturcture

- *The crystal structure of $Be_{12}Mo$ was used as the initial structure of $Be_{12}Ti$. The optimized structure gave the total energy of -1023.43 hartree (-27849.0 eV), which is lower than the total energy calculated based on the crystal structure of $Be_{12}Mo$. The positional parameters obtained are x = 0.3465 (Be-II) and x = 0.2994 (Be-III).*

$Mn_{12}Th$ (I4/mmm)				
Th	2a	x = 0	y = 0	z = 0
Mn-I	8f	x = 1/4	y = 1/4	z = 1/4
Mn-II	8i	x = 0.361	y = 0	z = 0
Mn-III	8j	x = 0.277	y = 1/2	z = 0
$Be_{12}Mo$ (I4/mmm)				
Mo	2a	x = 0	y = 0	z = 0
Be-I	8f	x = 1/4	y = 1/4	z = 1/4
Be-II	8i	x = 0.344	y = 0	z = 0
Be-III	8j	x = 0.284	y = 1/2	z = 0

Electron density map for $Be_{12}Ti$

- *Figure A shows the electron density map on the (0,0,1) plane. Contours are increased logarithmically. Electron densities around Be atoms appears to be almost same despite of difference in location.*

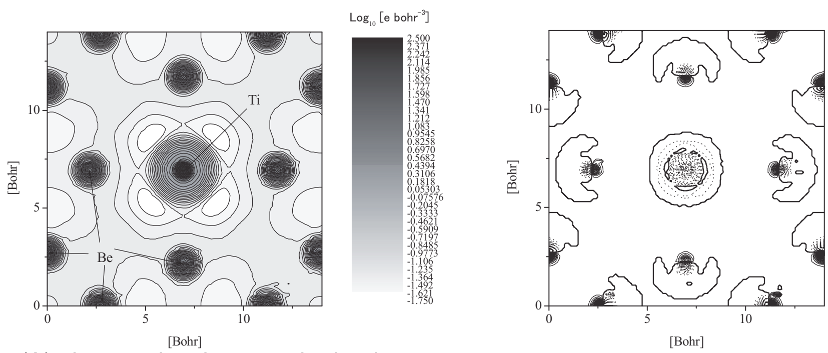

(A) electron density map obtained in SCF calculation

(B) electron density difference map

Electron density map for $Be_{12}Ti$

- *Figure B shows the electron density difference map. In this case, contours are increased linearly and the electron density spacing is 0.1 electrons bohr^{-3}. The electron density difference was computed by subtracting the superposition of the electron density of isolated atoms located in the $Be_{12}Ti$ crystal structure from the electron density obtained in the SCF calculation.*

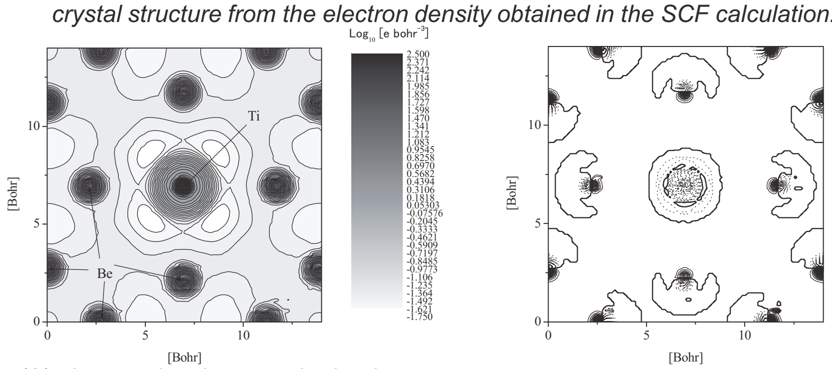

(A) electron density map obtained in SCF calculation

(B) electron density difference map

Ab-initio study on Li_4SiO_4 crystal

- *Tranqui et al. defined the structure of Li_4SiO_4 crystal by analyzing their X-ray diffraction data. The reported structure is also monoclinic with space group $P2_1/m$, but the unit cell is a = 11.546 Å, b = 6.090 Å, c = 16.645 Å and β = 99.5 °.*
- *The structure is considerably lager than that reported by Völlekle et al. They call it "super structure", which contains 14 formula units (seven different units) and is seven times as large as the cell described by Völlekle et al.*

Ab-initio study on Li_4SiO_4 crystal

- *The Gaussian basis set used for O was the Pople 6-21G* contraction, and for Si the standard 6-21G contraction was modified; the 4sp exponent for Si was 0.13 bohr^{-2} and the 3d shell with the exponent of 0.5 bohr^{-2} was added to this contraction.*
- *The authors also confirmed that the energy state of the Li_4SiO_4 crystal obtained with the basis set for Si is lower than that obtained with the Pople standard 6-21G contraction.*
- *With regard to Li, the 6-1G basis set was used with a modification for the 2sp exponent (= 0.53 bohr^{-2}), which was optimized for the Li_2O crystal.*

Density of state

- *Density of state as function of Energy (The Fermi level is assumed to be zero.)*

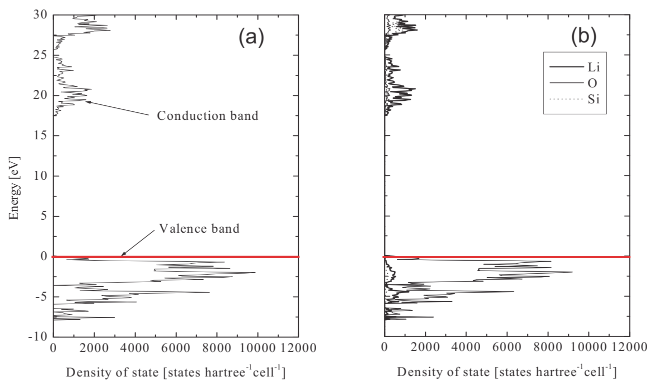

(a) total density of state, (b) density of state projected on to Li, O and Si

Electron density map for Li_4SiO4

- Electron density map on (0,1/3,0) plain (most densely populated)

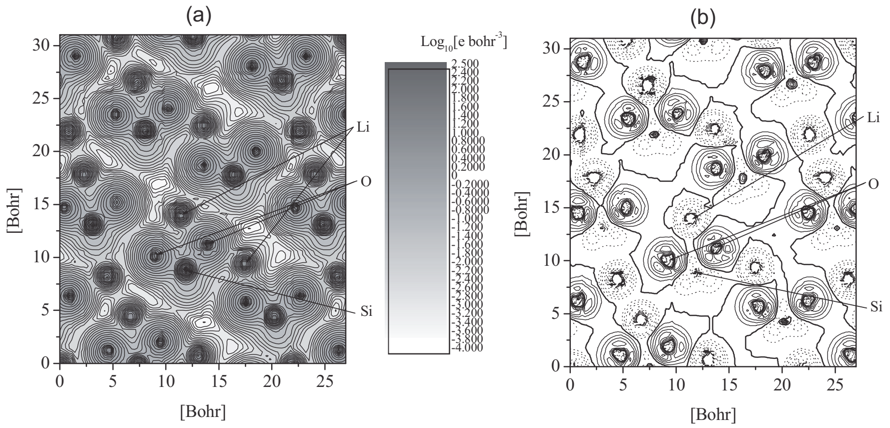

(a) electron density map obtained in SCF (b) electron density difference map

Future plan

- *Application of density functional theory for CRYSTAL*
- *Ab initio study with VASP and SIESTA for electron state and crystal structure*
- *Effect of vacancy and interstitials (larger super cell)*
- *First principle calculations at real operational temperatures*
- *5 PC cluster (20 cores, 40 sleds, 120 GBytes memory space, CentOS (RedHat)), Super computer in IFERC*
- *PGI, IFORT, GFORTRAN, G95*

Advanced tritium extraction process for HCPB breeding blanket

D. Demange

Karlsruhe Institute of Technology, Institute for Technical Physics, Tritium Laboratory Karlsruhe, Germany
Corresponding author: david.demange@kit.edu

Many issues will arise from the unprecedented amounts of tritium handled in the breeding blankets of future fusion reactors. For operation, tritium self-sufficiency will be required during the overall life-time of the breeding blanket. Major issues for licensing will concern tritium inventories and releases; both will have to be kept as low as reasonably achievable [1]. A reliable and effective tritium management will be based on i) efficient tritium extraction processes, and ii) irreproachable tritium tracking and accountancy [2].

For HCPB blanket, tritium is extracted from the breeding material by a helium purge gas doped with 0.1% H_2 as reference. Tritium extraction processes as presently foreseen for ITER-TBMs and DEMO mostly rely on packed bed columns operated in adsorption / regeneration cycles, and packed bed reactors for chemical transformations (HTO to HT, and vice versa). This approach has intrinsically some disadvantages, mainly tritium inventories build-up, and cycling operation with transients in tritium flows.

An alternative fully continuous approach has been recently proposed based on advanced membrane and membrane reactor technologies [4]. The objective is to improve the overall tritium management, i.e. to reduce inventories in the processes and to facilitate tritium accountancy at the extraction system outlet. Zeolite membranes have been selected as front-end process to produce from the purge gas at the breeder zone outlet: i) a tritium enriched stream to be routed to the tritium recovery step, and ii) a tritium depleted stream to be returned to the breeder zone. The 2nd step is acting as tritium recovery stage using a catalytic membrane rector able to recover simultaneously tritium in various chemical forms.

First material screening tests to evaluate the performances of potential zeolite membrane candidates revealed that the HT/He separation will be very challenging due to the limited membrane selectivity around 2. It will necessitate a large total membrane area and a multi-stage permeation cascade to reach sufficiently high tritium recovery fraction and tritium enrichment factor. If the purge gas would be doped with water vapor instead of molecular hydrogen, the HTO/He membrane selectivity is expected to be around 2 orders of magnitude higher than for HT/He. This would greatly relax the zeolite membrane pre-concentration step, and would also be of great advantage to reduce the tritium permeation towards the coolant.

[1] B. Bornschein, C. Day, D. Demange, T. Pinna "Tritium management and safety issues in ITER and DEMO breeding blankets" Fusion Eng. Des. (2013) in press.
[2] D. Demange, et al. "Overview of R&D at TLK for process and analytical issues on tritium management in breeder blankets of ITER and DEMO" Fusion Eng. Des. 87 (2012) 1206.
[3] D. Demange, S. Stämmler, M. Kind "A new combination of membranes and membrane reactors for improved tritium management in breeder blanket of fusion machines" Fusion Eng. Des. 86 (2011) 2312.

Advanced tritium extraction process(es) for HCPB breeding blanket

David DEMANGE, Olga BORISEVICH, Stefan WELTE

INSTITUTE OF TECHNICAL PHYSICS, TRITIUM LABORATORY KARLSRUHE

Content

1) Short introduction to TLK
2) Tritium management and issues in breeding blankets of ITER and DEMO (synergies and gaps)
3) Conventional tritium processes HCPB – TES / CPS
4) Advanced / alternative tritium processes in BB

1) Tritium Laboratory Karlsruhe

Campus North of KIT
(Karlsruhe Institute for Technology)

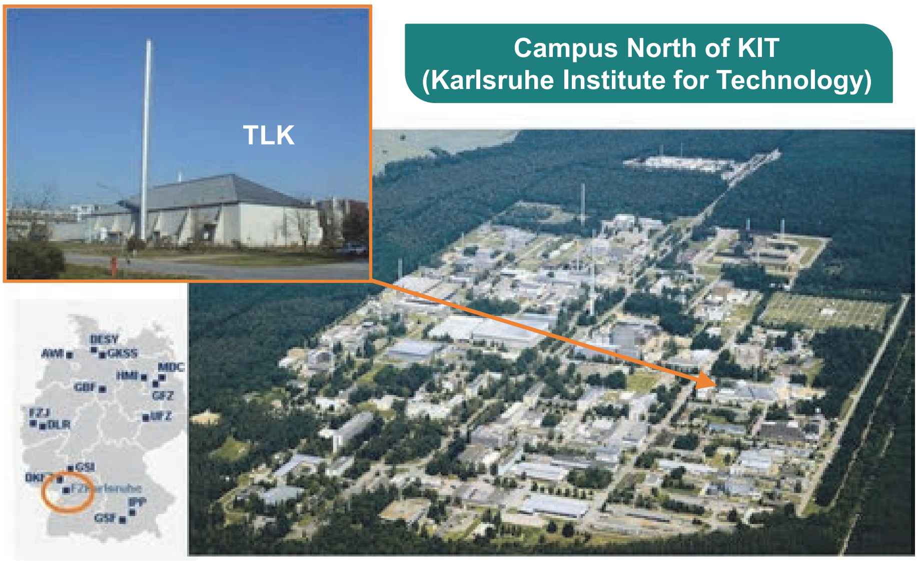

1) Tritium Laboratory Karlsruhe

- 2 major missions
  - Development of DT fuel cycle for fusion
  - Measurement of neutrino mass via beta decay
- 3 R&D groups
  (+ 3 support groups)
  - Inner fuel cycle
    (mostly ITER WDS & ISS)
  - Blanket & tritium technology
    (for ITER TBM and DEMO)
  - KATRIN & Analytics

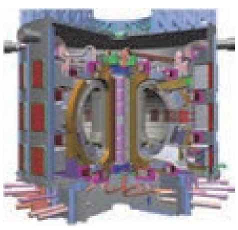

ITER

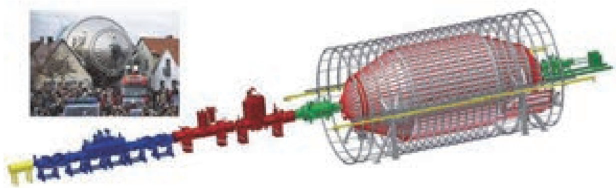

KATRIN

1) Tritium Laboratory Karlsruhe

- Almost unique semi-technical facility (closed loop)
  - 13 glove box systems (volume 125 m³, supervised area ~1450 m²)
- Long experience in tritium handling
  - License: for 10 g (1993), and 40 g in (1996)
  - Inventory: 3.5 g (1993), currently ~20 g
- About 30 permanent staff (+ 15-25 students)

CAPER facility for tritium recovery (TEP)

Analytical system using gas chromatography

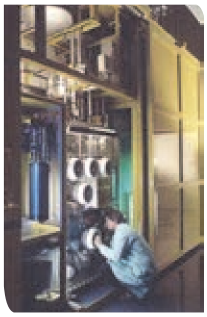

Central tritium retention system (DS)

2) Tritium fuel cycle for DT fusion machine

Outer fuel cycle *Inner fuel cycle* *Infrastructure*

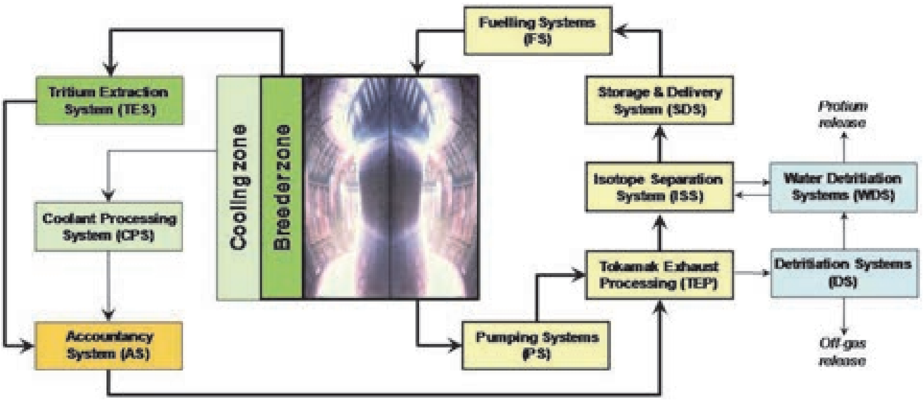

Simplified inner & outer fuel cycle considering ITER & TBM

…could be slightly different in DEMO

2) How much tritium is needed for DEMO?

- 2.7 GW fusion (1 GW electricity @ 37% efficiency) for 1 day continuous operation (full power day)

  $2.7 \cdot 10^{9} \times 86400 = 2.33 \cdot 10^{14}$ J (energy per day)

- D + T $\Rightarrow$ He + n + 17.6 MeV

  $17.6 \cdot 10^{6} \times 1.602 \cdot 10^{-19} = 2.82 \cdot 10^{-12}$ J (energy per tritium atom)

- Tritium consumption

  $2.33 \cdot 10^{14} / 2.82 \cdot 10^{-12} = 8.27 \cdot 10^{25}$ at. T

  $8.27 \cdot 10^{25} / 2 / 6.02 \cdot 10^{23} \times 6 = 412$ g

- Tritium production (@TBR = 1.1) is 453 g/d (136 kg/y) !!!

2) Fuelling rate and burn-up fraction

Parameters	ITER	DEMO
Fusion power [MW]	500	2700 ?
Tritium consumption [g/d]	76.4	412 ?
Tritium burn-up fraction [no dim]	0.3%	1.5% ??
Tritium fuelling rate [kg/h]	1.06	1.15 ??

Unprecedented tritium throughputs
Higher BUF can compensate higher fuelling rates

2) Gap between ITER & DEMO in BB

Parameter	ITER	DEMO	Gap
Tritium production [g/d]	~ 2 - 5 x 10^{-3} (1 TBM)	~ 500 (machine)	2 x 10^{4}
He flow rate in TES [m^3/h]	8 - 40	~ 10 000	~10^{3}
Tritium permeation [g/d]	~ 10^{-2}	~ 10	~10^{3}
He flow rate in CPS [m^3/h]	75	~ 50 000	~10^{3}

Extrapolation from TBM to DEMO very difficult: huge gap in size and time schedule discrepancy

2) Tritium release from Li-ceramics

1. Inter-granular diffusion
2. Grain boundary diffusion
3. Surface adsorption/desorption
4. Pore diffusion
5. Purge flow convection

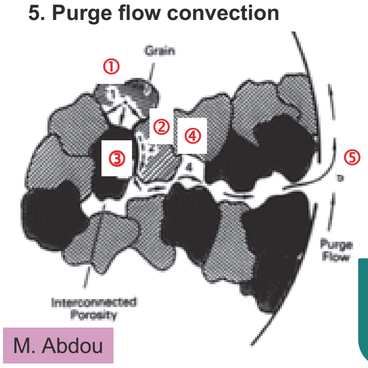

M. Abdou

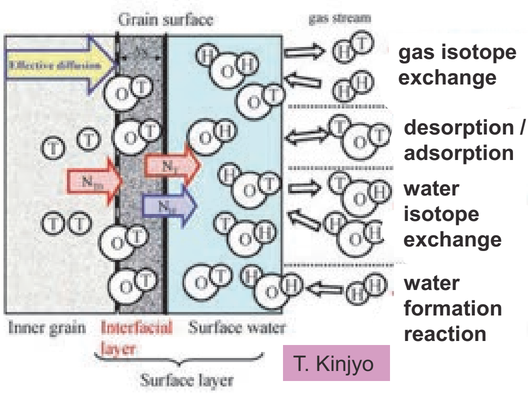

T. Kinjyo

Complex mechanism with T release as HT & HTO; HT/HTO ratio depends on material, temperature & purge gas chemistry

2) Tritium management issues in BB

- In general, for any breeder blanket concept
  - Processes: Tritium as traces in helium, HT & HTO, efficiency
  - Accountancy: procedures, analytics, accuracy
  - Inventories and releases (=> Permeation barrier needed !?)
- For solid breeder blanket
  - HT / HTO ratio
  - Purge gas chemistry
  - Inventory in Be (up to kg!)
- For liquid breeder blanket
  - Solubility (Sievert's constant)
  - Permeator vs. contactor
  - Permeation into coolant

To be solved before completion of DEMO design…or big risk to fail!

3) Conventional tritium processes

- Different approaches for HCPB TES (from last century…)

	Method/origin	Main components
1	Pressure swing adsorption (PSA) AECL, Canada [3]	Compressor (0.1 → 1 MPa), MSB (−195°C), vacuum pump/compressor, Pd/Ag diffuser
2	Thermally coupled pressure swing adsorption (TCPSA) Canada [4]	Cold trap (−195°C), several compressor units, several adsorber units, several MSBs (−195°C), Pd/Ag diffuser
3	Tritium recovery system ANL, USA [5]	Cold trap (−100°C), several MSBs (−195/+25°C), electrolytic cells, Pd/Ag diffuser
4	JAERI, option A, Japan [6]	MSB (20°C), Pd/Ag diffuser, MSB (−195°C), electrolytic cell
5	JAERI, option B, Japan [7]	Oxidizer MSB, WGSR Pd/Ag diffuser
6	ENEA-Option A Italy [8]	Oxidizer (2), Cold trap or cryosorber, WGSR, Pd/Ag diffuser, MSB (2)
7	ENEA, option B, Italy [8]	Oxidizer, cold trap or cryosorber, WGSR, MSB, CO_2 adsorber, Pd/Ag diffuser
8	ENEA, option C, Italy [9]	Oxidizer, cryotrap, WGSR, Pd/Ag diffuser
9	Sulzer, option A, Switzerland [10]	Compressor (→ 10 bar), cold trap (−100°C), MSB (−195°C), cryogenic freezer (−263°C)
10	Sulzer, option B, Switzerland [11]	Oxidizer compressor (→ 6 bar), MSB, condenser, water processor

[a] MSB, molecular sieve bed; WGSR, water gas shift reactor.

H. Albrecht

3) Conventional tritium processes (TLK option)

H. Albrecht

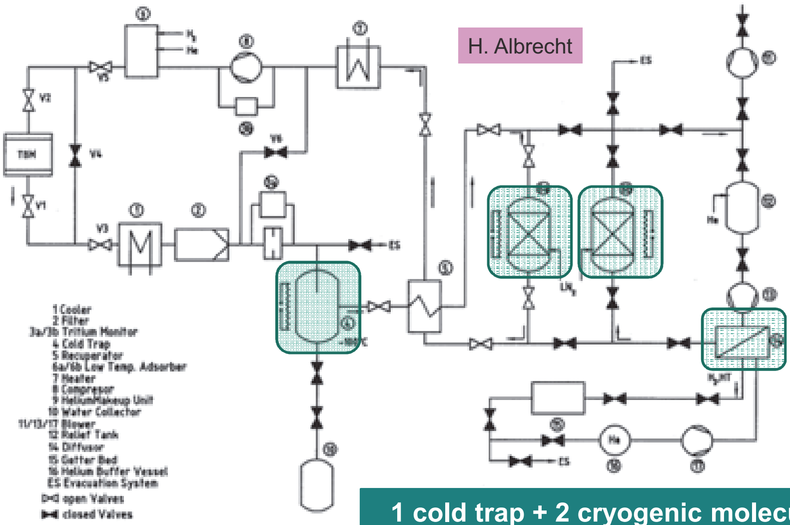

1 cold trap + 2 cryogenic molecular sieve beds + Pd/Ag permeator

3) Cold trap / cryogenic molecular sieve bed

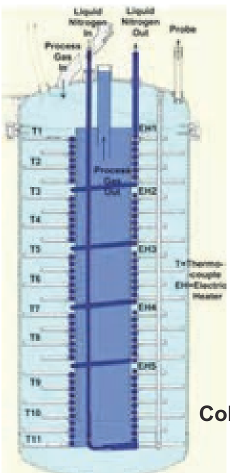

Cold Trap @ 173K

N. Bekris

Cryogenic Molecular Sieve Bed @ 77K

S. Beloglazov

Both successfully demonstrated @ TLK for 2 m^3/h (~1/6th ITER scale)

3) Design review & process selection (TBM)

I. Ricapito A. Ciampichetti

	Original (TLK)	Revisited (ENEA)
Process for HTO	- Cold trap @ 173K - HTO recovered as liquid	- Adsorption column @ RT - Water recovered as vapour - Reducing bed (PERMCAT)
Process for HT	- Cryogenic molecular sieve bed @ 77K	- Getter bed @ RT
Accountancy	- HTO & HT	- HT (after chemistry)

Cryogenic temperatures abandoned, but still semi ("quasi") continuous process with "traps"

4) Advanced T process(es) for DEMO

- T process(es) selection for TBM
  - Conceptual Design Review ongoing not driven by DEMO relevancy
  - More importance given on reliability, simplicity, and maturity
- Synergy with downstream T process(es), especially T accountancy stage never considered (still not, even for TBM!)
- Ideal T processes for DEMO BB should have
  - Short residence time (to relax tritium start-up inventory)
  - Low inventory (according to ALARA, beneficial for safety)
  - Adequate stream for accurate accountancy & good synergy with the inner-fuel cycle (i.e. avoid too high dilution with He and H_2)
  - High efficiency, if possible at low energy consumption

4) Alternative TES for HCPB DEMO

- Fully continuous at constant non-cryogenic temperatures
- Tritium removal and pre-concentration using inorganic zeolite membranes
- Tritium recovery from HTO using PERMCAT (catalytic membrane reactor)
- Water vapour in purge gas
  - Facilitates tritium release
  - Improves separation
  - Reduces permeation

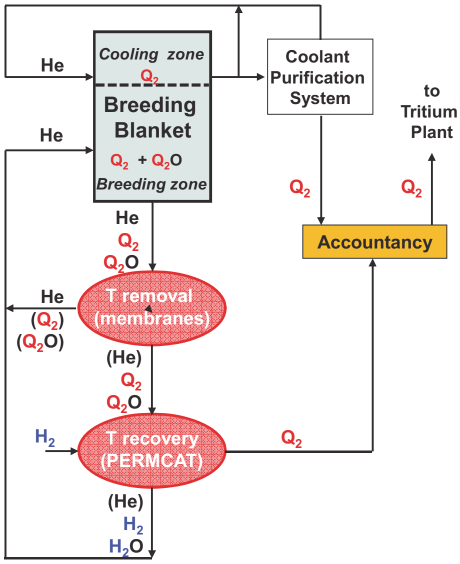

4) T recovery with PERMCAT

- PERMCAT = catalytic Pd-membrane reactor using counter-current isotope swamping technique
- Developed & demonstrated for Tokamak Exhaust Processing
  1) H_2 permeation
  2) Isotope exchange reactions
     $H_2 + Q_2O \leftrightarrow H_2O + Q_2$
  3) Q_2 back permeation

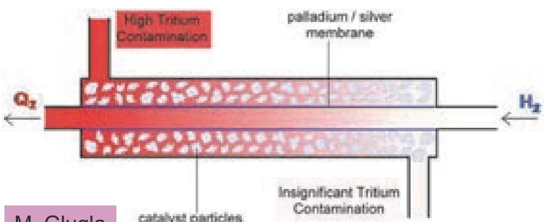

M. Glugla

- Swamping ratio governs tritium recovery fraction & enrichment factor
- Recovers tritium from all molecules simultaneously
- Produces enriched & pure molecular tritium (HT)

Very attractive as interface with accountancy stage & tritium plant

4) R&D on PERMCAT mechanical design

- Prototypes reactors (single-tube)
  - Finger-type membrane (old)

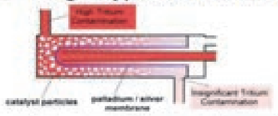

  - Corrugated membrane (new)

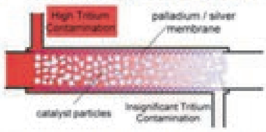

  - Edge-welded bellow (new)

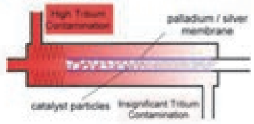

S. Welte

- Technical reactors (multi-tube)
  - Bundle of single-tube units (old)

masse: 46 kg
volume: 43 L
Pd/Ag: 320 cm^2
catalyst: 36 g

  - Multi-tube in single bed (new)

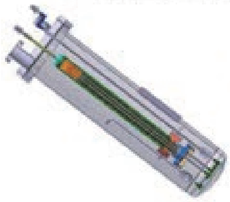

masse: 20 kg
volume: 11 L
Pd/Ag: 460 cm^2
catalyst: 95 g

R. Wagner

Tritium Laboratory Karlsruhe

4) R&D on PERMCAT simulation

K. Munakata

- 1D model (validated) considers
  - All possible chemical species
  - Isotope exchange reactions
  - Chemical side reactions
  - Q2 permeation
  - Permcat process design
- 2D model (in validation) considers
  - Velocity profile
  - Axial & radial diffusion
  - Permcat reactor design
- Final developments (ongoing)
  - Integration of kinetics for isotope exchange reactions

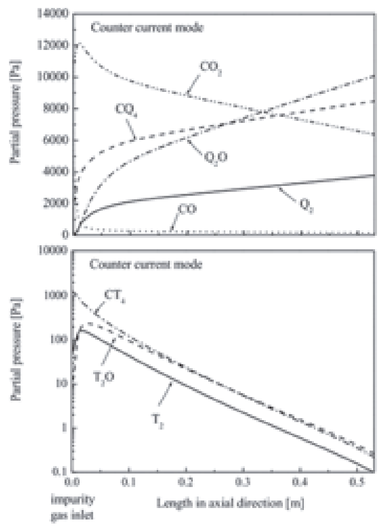

Tritium Laboratory Karlsruhe

4) Pre-concentration stage with membrane(s)?

- Membranes other than…
  - Pd-alloys used in Tokamak Exhaust Processing (too selective, cannot recover HTO, expensive)
  - Polymers proposed in glove boxes and atmosphere detritiation (not primary tritium compatible, tritium contamination & inventory)

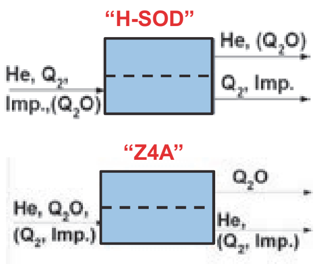

Zeolite membranes are new but promising

- ☺ Tuneable materials in pore size & chemical affinity
- ☺ Chemically & thermally resistant
- ☺ Primarily tritium compatible
- ☺ Unprecedented dehydration performances

S. Stämmler

21 12.09.2013 D. DEMANGE - CBBI 17 - Barcelona

Tritium Laboratory Karlsruhe

4) Experiments on MFI zeolite membrane

- MFI (pore size 5.1×5.5 Å)

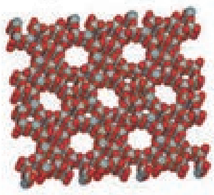

- Membrane: hollow fiber (hosted in porous holder) provided by IRCELYON

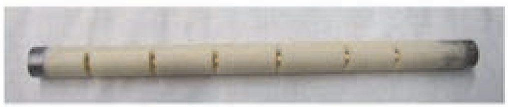

- "pore-plugging" synthesis

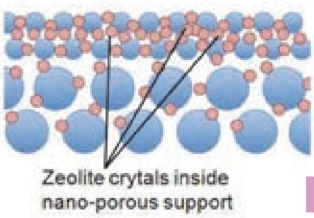

M. Pera-Titus

Parameter	Value
Length	130 mm
Outer diameter	1.65 mm
Surface area	497 mm²
Thickness	< 1 µm

22 12.09.2013 D. DEMANGE - CBBI 17 - Barcelona

Tritium Laboratory Karlsruhe

4) Experiments on zeolite membrane(s)

- Single gas experiments "dead end mode"
  - $\Delta P \sim 0.5$ bar
  - Permeation flow measured

- Results @ RT
  - High permeance 1.3 µmol/m²sPa (for H_2)
  - Limited selectivity $H_2/He = 2.2$

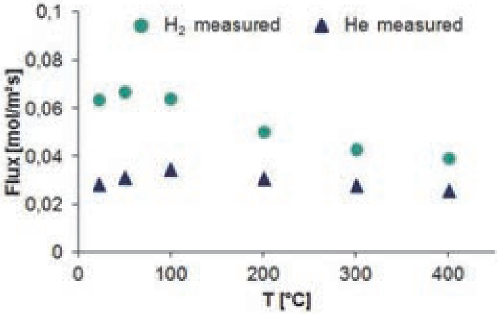

O. Borisevich

4) Simulation of a membrane cascade

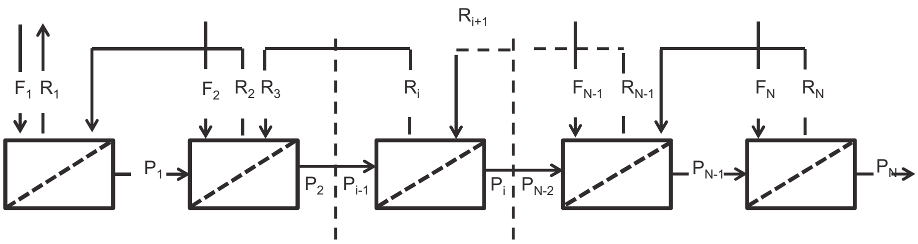

- Inputs
  - Feed composition
  - Pressures
  - Membrane cut
  - Selectivity (from expt.)
  - Enrichment factor
  - Recovery factor
- Outputs
  - Number of stage
  - Feed position
  - Permeate and retentate compositions
  - Membrane areas

4) Simulation of a membrane cascade

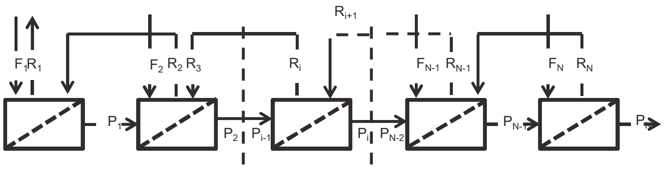

Selectivity (no dim)	Stage N_{min}	Injection position	Optimized cut range (no dim)
2	16	7	0.41-0.42
2.5	12	6	0.37-0.39
3	10	5	0.35-0.38
5	7	4	0.26-0.32
10	5	3	0.17-0.27

Numbers for 90% removal efficiency & 20 times enrichment factor

Summary & outlook

- Tritium management in Breeding Blanket is very challenging
  - Tritium as Q_2 & Q_2O traces, diluted in huge helium flows
  - Tritium inventory and processing time must be minimised
  - Downstream accountancy must be very accurate
- Conventional Tritium extraction from He
  - Tritium “immobilised” in several (Q_2 & Q_2O dedicated) traps
  - 2 reactors in //, thermal cycles, transients & dilutions
- Advanced Tritium processes for blanket
  - PERMCAT for T recovery (=> catalyst and sizing issues)
  - Zeolite membrane for pre-concentration (=> selectivity issue)
  - R&D efforts for experiments & simulation of both stages

Influence of the microstructure on the light species behaviour in ceramic breeder blanket materials

E. Carella[1*], R. Gonzalez-Arrabal[2], Q.Zhao[3], A.Ibarra[1], M.Gonzalez[1].
[1]LNF-CIEMAT, Materials for Fusion Group, Madrid, Spain
[2] IFN-ETSII, Universidad Politécnica de Madrid, Spain
[3] K.U.Leuven, Belgium
*elisabettacarella@gmail.com

The study and understanding of the diffusion and retention processes relatives to light atoms (H, D, He) produced by transmutation in the Breeder Blanket ceramics, is crucial in order to develop materials with improved properties. Therefore, the role of the microstructure is here discussed, the radiation-induced damage being an additional factor.

Previous experimental and simulated results [i] evidence that both Tritium transport and release in Li-based ceramics are complex processes involving, among others: grain boundary and inter-granular diffusion, absorption and desorption at the gas/solid interfaces, diffusion along the interconnected porous, surface reactions, etc. Moreover an additional factor, which has to be considered when studying T behaviour in irradiated materials, is the evolution of the microstructure during irradiation with energetic ions, neutrons and electrons [ii].

Since the operational temperature of a solid breeding material has been estimated to be in the range from 300ºC to 900ºC [iii], and in an attempt to simulate the tritium transport during operation with the help of a comparable H isotope as a trace, this work compares the D thermal behaviour implanted in two different orthosilicates (with a Li:Si proportion of 2:1 and 3:1) and in a metatitanate ceramic breeder candidate.

The D desorption profiles were studied from RT to 200 °C by Resonance Nuclear Reaction Analysis (RNRA), using the D (^{3}He, p) ^{4}He nuclear reaction up to the D total outgas being the implanted fluence of about 3×10^{17} cm^{-2}. Using the obtained experimental densities, the maximum depths for the implanted ions were calculated by the SRIM Monte Carlo code [iv] to be 1.32 µm for 2Li:Si, 1.1 µm for 3Li:Si and 0.96 µm for 1Li:Ti.
The D depth profiles were RNRA characterised at the KUL-Leuven tandem accelerator facility by the D (^{3}He, p) ^{4}He [v] nuclear reaction. Measurements were carried out with a ^{3}He ion beam impinging the sample surface at normal incidence.

The estimated (implantation fluence) and measured (RNRA) total amount of D in as-implanted samples is almost the same, which indicates that, even when D diffusion occurs at RT, it does not significantly release.

Concerning the D concentration, it generally results to be higher at the surface region than deeper into the bulk, which indicates the influence of surface on D retention. Annealing at T> 125 ºC promotes a change in the D release from all ceramics. For annealing temperatures ≥ 150ºC, the D concentration is negligible and a quite complete outgas is observed at 200 ºC for all the specimens.

Since in the actual breeder-blanket design (i.e the European HCPB concept) the operational temperature will be limited to 900ºC [[iii]], the presented results indicate that Li-based ceramics are very promising candidates for breeder applications.

For the titanate composition (1Li:Ti), irradiation damage using Ti^{4+} ions and/or gamma rays is used to further discuss the effect of a pre-damaged target on the D distribution in the bulk. The Ti^{4+} irradiation took place in the UCM (Madrid) with a 150 keV beam and a fluence of 10^{15} ions/cm^2 to a depth of 500 nm, while gamma irradiation took place in the CIEMAT (Spain) by a ^{60}Co source in the Nayade pool-facility, at 6Gy/sec to a total dose of 7,3 MGy.

The presence of two annihilation processes of the radiation effect, working as light ion trapping sites is identified, resulting in a really fast release-rate in the case of the ceramic previously damaged by Ti^{4+} and a higher D adsortion when both damages are combined.
The nature of insulating materials makes them highly sensitive to electrical damage, ionization and displacement damage. This implies a degradation and loss of oxygen from the surface due to a radiolityc anion sputtering of the implanted/irradiated zone with a consequent reduction of Ti from Ti^{4+} to Ti^{3+}. The effect is a modification of diffusion/release rate of the light ion implanted from the solid BB structure. The confirmation of the present results are been found in other works effectuated on the same ceramic structure implanted with others light ions [[vi]].

On the other side the porous size distribution and the grain boundary density are identified as the principal factors for diffusion mechanism, thus the first part of the study is focused on the comparison between different microstructures. Our preliminary conclusions point out that the behaviour of the studied ion is strongly dominated by the density of grain boundaries (GBs). They seem to act (i) as annihilation centre for Frenkel pairs (self-healing behaviour) and (ii) as pinning centres for light ions. Moreover, since the trap energy for light species at the grain boundaries is smaller than that at the radiation-induced defects, GBs may favour their release, performing as the effective diffusion paths. Finally, the fabrication of polycrystalline ceramics with small grain sizes is here emphasized to achieve the best light ion performances as breeding blanket candidates [[vii]].

---

[i] R.E. Avila, J.C. Jiménez, J. Nucl. Mat. 405(2010) 244-251.

ii J.Vanderlaan et al., J. Nucl. Mat. 283-287 (2000) 99-109.

iii T. Hino, H. Shibata, Y. Yamauchi, Y. Nobuta, S. Suzuki, M. Akiba, J. Nucl. Mat. 417 (2011) 713-717.

iv J.F. Ziegler, M.D. Ziegler, J.P. Biersack, SRIM -2006.02

v V.Kh. Alimov, M. Mayer, J. Roth, Nucl. Inst. Meth. Phys. Res.B. 234 (2005) 169-175.

vi E.Carella, T.Sauvage, R.Bes, B.Courtois, M.González, Nucl.Inst. Meth. Phys. Res.B, *In Press.*

vii E.Carella,M.Gonzalez, R.Gonzalez-Arrabal, J.Nucl.Mat. 438 (2013)193-198.

Ceramic Breeder Blanket Interactions 12-14 September 2013, Barcelona, Spain

Influence of the microstructure on the light species behaviour in ceramic breeder blanket materials

E. Carella[1], A.Ibarra[1], M.Gonzalez[1]
R. Gonzalez-Arrabal[2],Q.Zhao[3]

[1]LNF-CIEMAT, Materials for Fusion Group, Madrid, Spain
[2] IFN-ETSII, Universidad Politécnica de Madrid, Spain
[3] K.U.Leuven, Belgium

Introduction

To establish a secure and efficient fuel cycle in fusion reactors

- The behavior of tritium in the blanket breeding materials
- The surface process (one of the factors controlling the tritium release rate) (Avila 2010, Bertone 1988)

The present work is focused on the desorption behavior of the implanted deuterium in as-implanted and damaged ceramics with different microstructures.

BB candidate ceramics

Li_4SiO_4 (2Li:Si) and Li_2TiO_3 (Li:Ti)

+

a third ceramic candidate with higher Li:Si proportion (3:1)

Compositions	1Li:Ti	2Li:Si	3Li:Si
Sintering temperature/dwell time (ºC/h)	1150/2	950/2	1000/2
Present phases	(100%) Li_2TiO_3	(47.8%) Li_2SiO_3, (23.4%) Li_4SiO_4, (3%) SiO_2 *	(59.4%) Li_4SiO_4, (38.8%) Li_2SiO_3 and (1.8%) SiO_2

* other phases (crystalline and amorphous) and secondary reaction products.

elisabettacarella@gmail.com

Microstructure

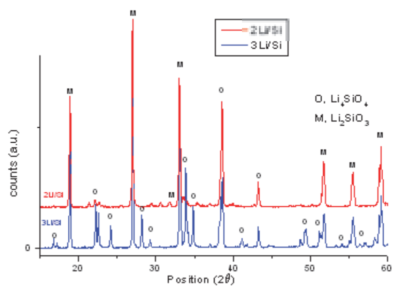

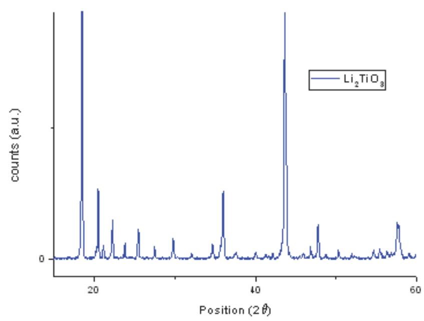

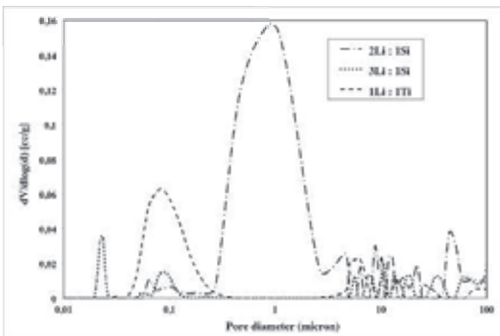

Material	1Li:Ti	2Li:Si	3Li:Si
D_{th}: theoretical density (gr/cc)	3.43	2.24	2.17
D_{exp}: experimental density (gr/cc)	2.7	1.6	2.05
Density (% T.D.)	78	73	94.5
Porosity (%)	**22**	**27**	**5.5**
Main open pore diameters (µm)	**0.08**	**0.9**	**0.1; 0.025**
Grain size (µm)	**3**	**2**	**0.15 & 6 (bimodal)**

elisabettacarella@gmail.com

Microstructure

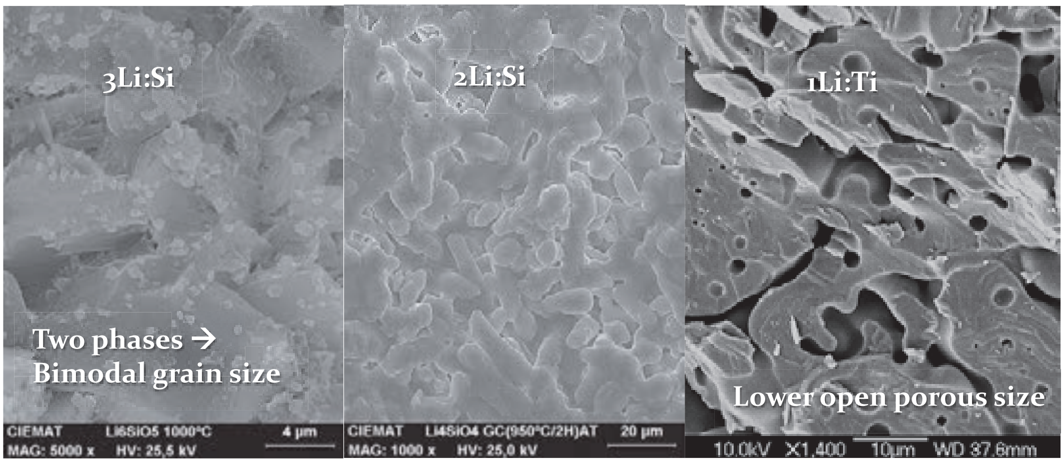

SEM micrographs of the polished and thermally etched surfaces of the three lithium-based ceramic pellets

Ceramic Breeder Blanket Interactions 12-14 September 2013, Barcelona, Spain

Why Nuclear Reaction Analysis?

Methods for light ion detection:
- ✓ spectrometry-based technique (SIMS, TDS)
- ✓ resonance based technique (NMR, EES, absorption spectrosopy)
- ✓ indirect techniques (neutron scattering, small-angle X-ray..)
- ✓ accelerator – based techniques (ERDA, p-RBS, NRA)

Several authors (among others Paszti 1992) emphasized the sensitivity of nuclear reaction analysis in the case of light ions profiling.

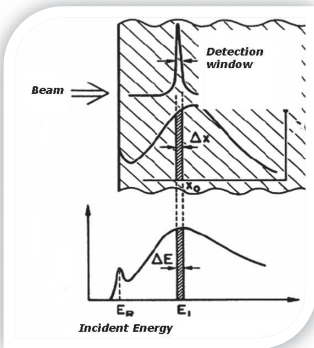

D-implantation + NRA characterization

Implantion in UCM accelerator facility, (Madrid) at Room T at an energy of 100keV with a deuterium beam to a fluence of $3{*}10^{17}$ D_2^+ /cm².

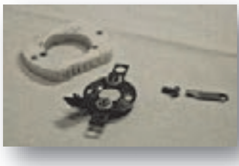

Characterized by the D(³He,p)⁴He nuclear reaction in Leuven KUL's laboratories, Belgium.

1 PIPS detector at 142º.
Absorber foil technique (13 µm Mylar foil).
In-situ thermal annealing at 100ºC, 150 ºC and 200ºC during NRA measurements.

NRA characterization with temperature variation

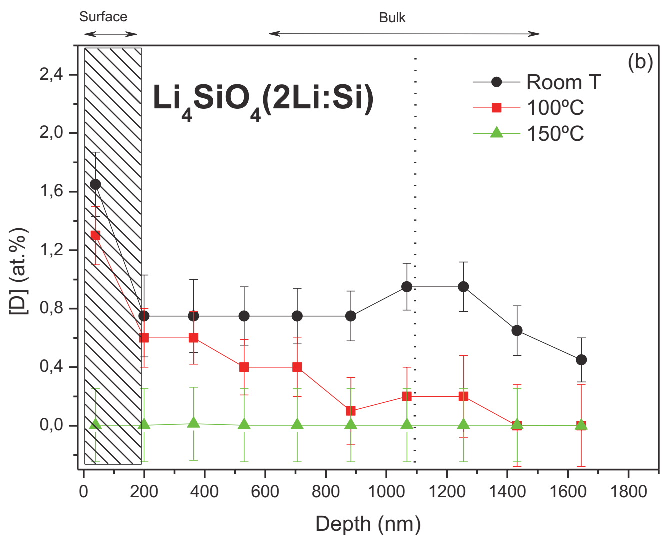

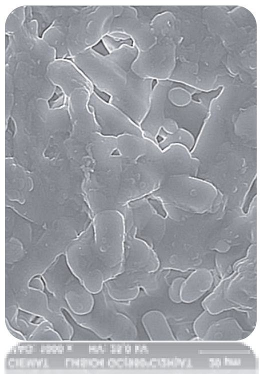

Porosity: 27%
Main porous ø: 1 µm
Mean Grain size: 2µm

Constant diffusion along the depth

NRA characterization with temperature variation

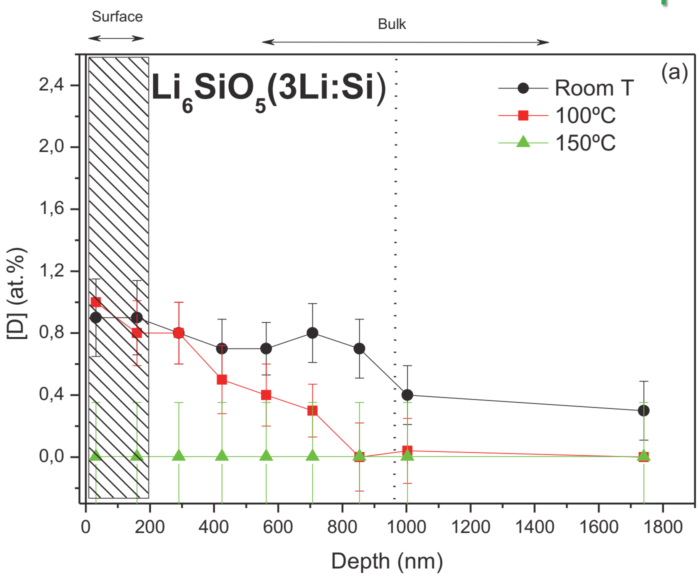

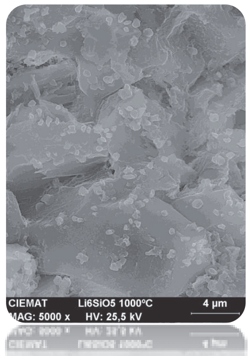

Porosity: 6%
Main porous ø: 0,02&0,1 µm
MeanGrain size: 0,15µm and 6 µm
BIMODAL!

Lowest [D] concentration, lowest barrier effect of the surface

Ceramic Breeder Blanket Interactions 12-14 September 2013, Barcelona, Spain

NRA characterization with temperature variation

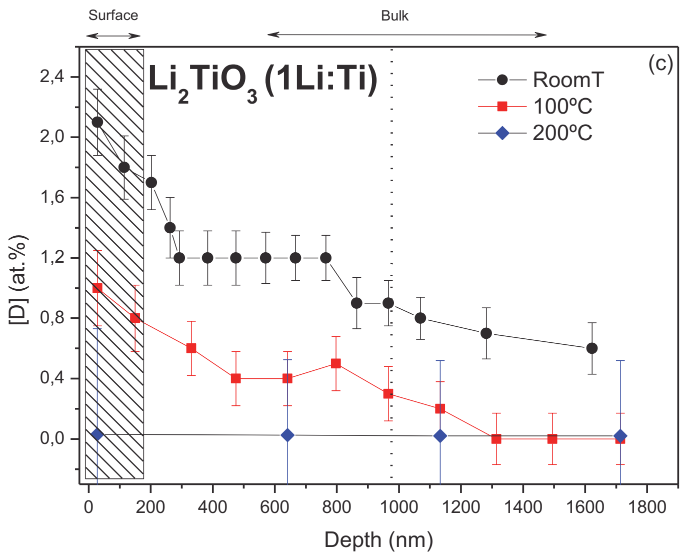

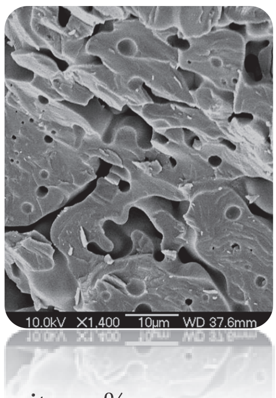

Porosity: 22%
Main porous ø: 1&10 µm
MeanGrain size: 3µm

Highest [D] concentration, highest barrier effect of the surface

NRA characterization with temperature variation

Grain Boundaries seem to act as:

1. annihilation centre for Frenkel pairs (self-healing behaviour)
2. pinning centres for light ions.

The main mechanism of release is diffusion/migration within the implantation plane and certainly at the neighboring of grain boundaries, performing as the effective diffusion paths.

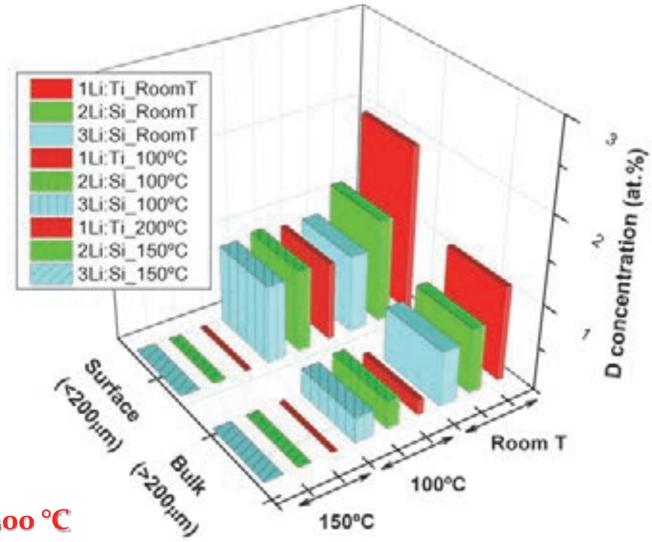

D totally outgas at 200 °C

Ceramic Breeder Blanket Interactions 12-14 September 2013, Barcelona, Spain

First Results


Journal of Nuclear Materials 438 (2013) 193–198

Contents lists available at SciVerse ScienceDirect

Journal of Nuclear Materials

journal homepage: www.elsevier.com/locate/jnucmat

ELSEVIER

Review

D-depth profiling in as-implanted and annealed Li-based breeder blanket ceramics

Elisabetta Carella [a,*], Maria Gonzalez [a], Raquel Gonzalez-Arrabal [b]

[a] LNF-CIEMAT, Avda Complutense 40, 28040 Madrid, Spain
[b] IFN-ETSII, Universidad Politécnica de Madrid, C/José Gutiérrez Abascal 2, 28006 Madrid, Spain

These results agree with those previously reported by Federici et al. and by Bertone et al. who model the T transport in lithium ceramics by assuming a rather favourable and not rate controlling grain boundary diffusion.

G. Federici, A.R. Raffray, M.A. Abdou, J. Nucl. Mater. 173 (1990) 185-213.
P. Bertone, J. Nucl. Mat. 151 (1988) 281-292.

New experiments

1 BB ceramic: Li_2TiO_3
D-implanted at $1*10^{17}$ D^+/cm^2 with a 70 keV beam to a depth of 700 nm

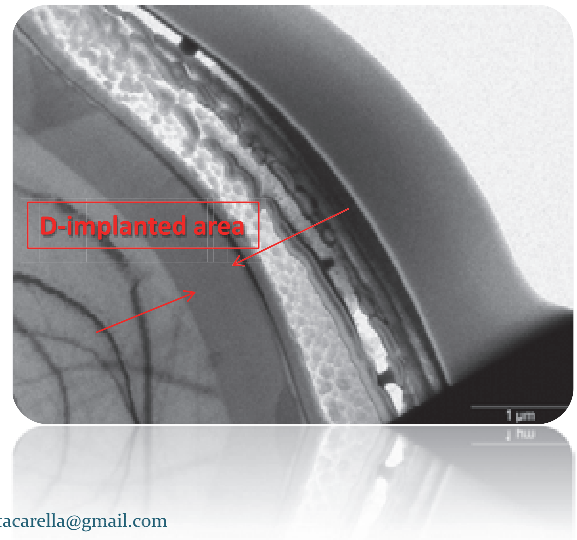

Ceramic Breeder Blanket Interactions 12-14 September 2013, Barcelona, Spain

NRA characterization with temperature variation

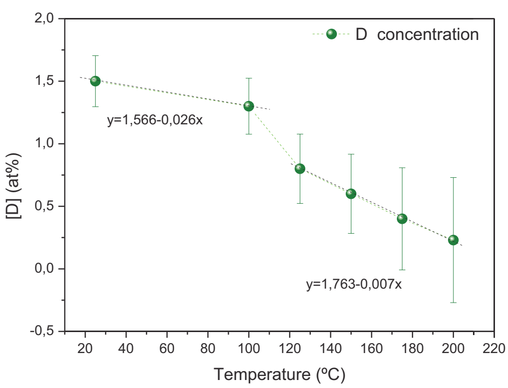

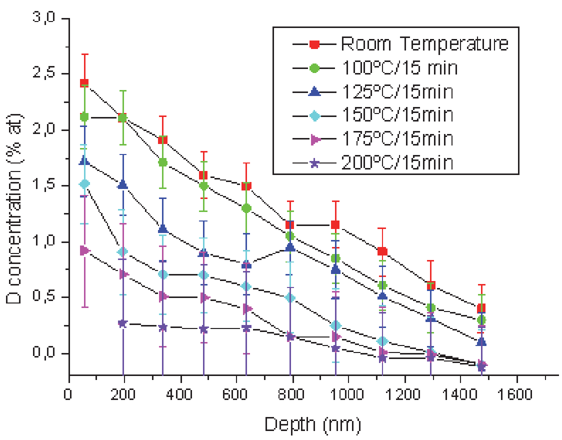

D has completely outgased at 200ºC

Barrier effect of the surface

Time-dependence of D-release during thermal treatments

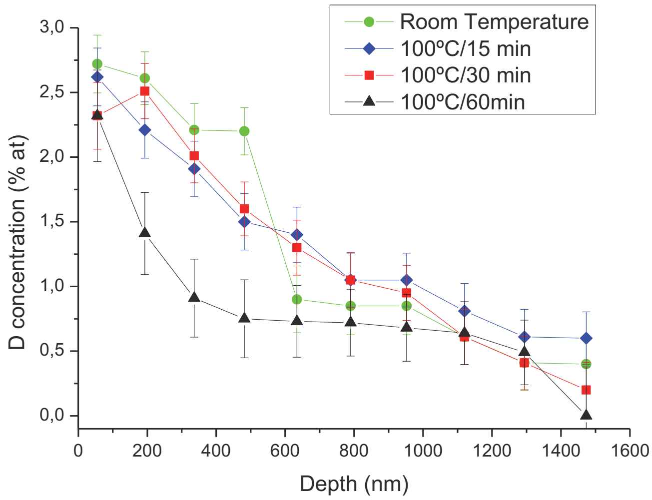

Deuterium migrates towards the surface even with high annealing times

Ceramic Breeder Blanket Interactions 12-14 September 2013, Barcelona, Spain

Different Kind of Damage

- Heavy ion implantation

The Ti^{4+} irradiation took place in the UCM (Madrid) with a 150 keV beam and a fluence of 10^{15} ions/cm² to a depth of 500 nm.

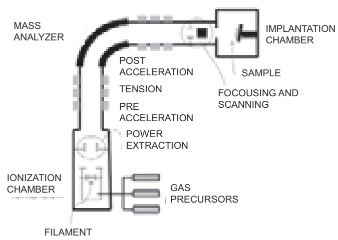

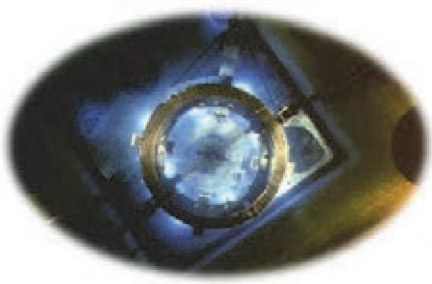

- γ-ray irradiation

Gamma irradiation took place in the CIEMAT (Spain) by a ^{60}Co source in the Nayade pool-facility, at 6Gy/sec to a total dose of 7,3 MGy.

D- release in damaged sample

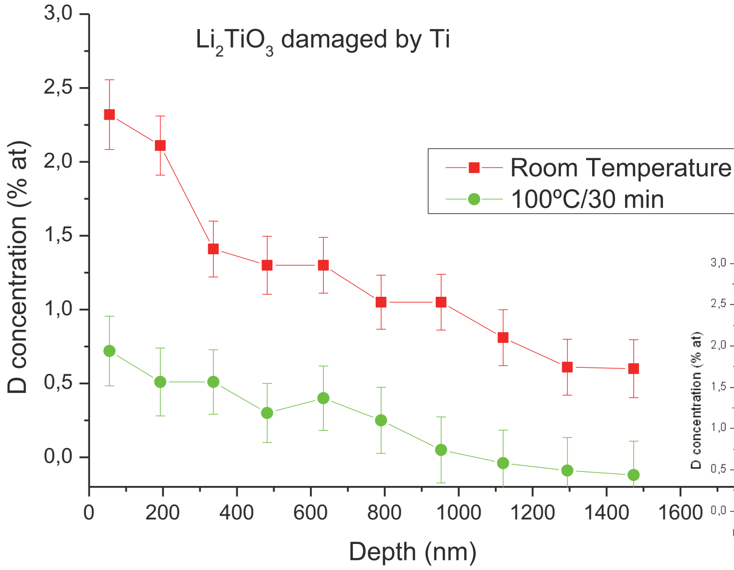

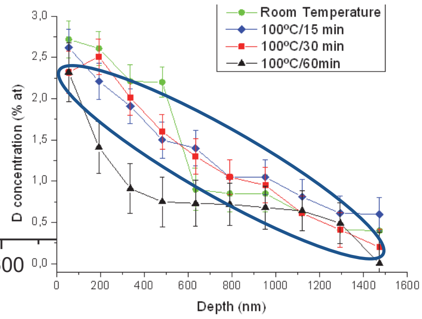

Ceramic Breeder Blanket Interactions 12-14 September 2013, Barcelona, Spain

D- release in damaged sample

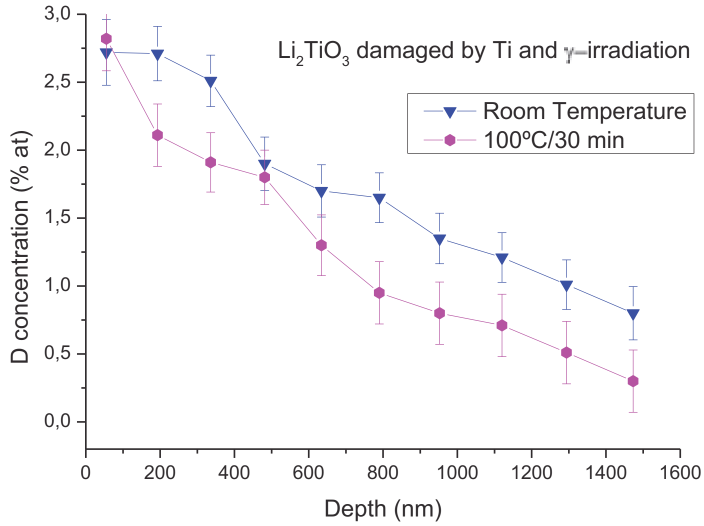

Higher [D] concentration
even an room T.
Small release at 100 ºC.

D- release in damaged sample

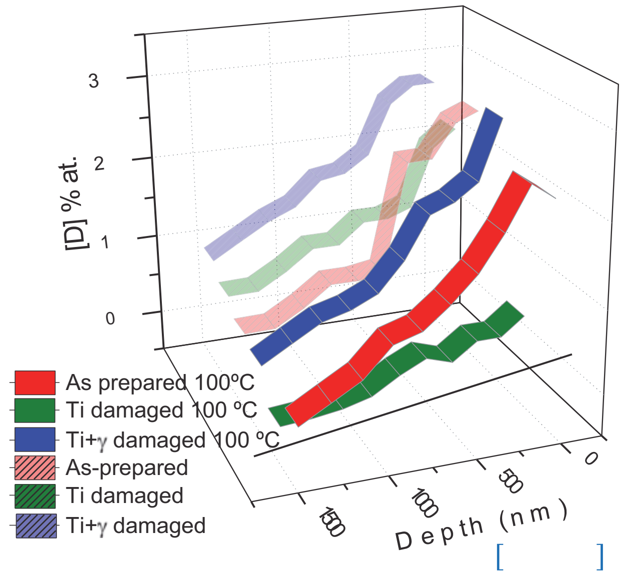

Presence of two annihilation processes of the radiation effect (fast and slow), working as light ion trapping sites.

Damage effect on D-release

The nature of insulating materials makes them highly sensitive as to electrical damage, as to ionization and displacement damage.

→ Degradation and loss of oxygen due to a radiolityc anion sputtering of the <u>surface</u>

→ Anihilation of E' centres by recovering O vacancies or by the reduction of Ti from Ti^{4+} to Ti^{3+}

→ Recombination and diffusion of trapped electrons by thermal activation

Correlation between diffusion/release process of the light ions and annihilation of defects

Conclusions

- The porous size distribution and the grain boundary density are identified as the principal factors for diffusion mechanism.
- The complete outgas of D was observed at T ≥ 200ºC.
- Surface plays a crucial role for the release kinetics and grain boundaries are confirmed as an alternative path to porous for diffusion.
- The fabrication of polycrystalline ceramics with bi-modal grain sizes is emphasized to achieve the best light ion performances in lithium-based breeding blanket candidates (new concept of solid BB).
- Both diffusion/release processes and annihilation of defects are temperature dependent.

Rate-controlling mechanisms depend on the release temperature and the structural and microstructural characteristics of the crystal.

Ceramic Breeder Blanket Interactions 12-14 September 2013, Barcelona, Spain

Proposal for the future

A model for tritium production in solid breeder blanket toghether with the modelization of its kinetics under degradation processes.

These informations would contribute to support the experimental results yet obtained and for taken a concious decision on the best TBM conditions and operational limits for the future breeder systems.

He thermal-induced diffusion in lithium titanate

M. González[1], E. Carella[1], A. Ibarra[1], B. Courtois[2], R. Bes[2], T. Sauvage[2]

[1]LNF-CIEMAT, Materials for Fusion Group, Spain

[2]CNRS, CEMHTI UPR3079, Univ. Orléans, F-45071 Orléans, France

The breeder (or breeder blanket) is a key component of the future deuterium-tritium fusion reactors performing the triple function of (1) tritium breeding base on the nuclear reaction: $^{6}Li + {}^{1}n \rightarrow T + {}^{4}He + 4,8$ MeV, (2) heat conversion and removal and (3) neutron and radiation shielding.

Since ^{4}He will be one of the products of the Li transmutation reaction and considering possible similarities with tritium, a double interest in studying the thermal evolution and transport mechanisms of ^{3}He was found. The aim of this work was then to understand the mechanisms for the ^{3}He thermal-induced release inside of a porous lithium metatitanate ceramic, a solid candidate for some breeding blanket concepts. ^{3}He ions were then implanted at room temperature and the remaining concentration and its depth distribution followed at different thermal annealings using an IBA technique. Finally its correlation with the material microstructure was determined using transmission electron microscopy.

1. Sample preparation and characterization techniques

Lithium metatitanate (Li_2TiO_3) ceramic samples, with porosity of about 15% of the theoretical density, were implanted at room temperature with a 600 keV ^{3}He ion beam up to a fluence of 10^{17} ions/cm^2.

Nuclear Reaction Analysis (NRA) in the coincidence mode was used to study the He profiles before and after isothermal annealing treatments. He depth profiles were measured by using a ^{2}H ion beam at energy of 900 keV. NRA was also the ion beam technique used to register the He desorption as a function of increasing temperature from room temperature to 900ºC at constant time.

FESEM and TEM microstructural techniques were applied to cross sections samples, where the implanted surface was protected during ion beam milling.

2. He release and depth profiling analysis by NRA

Both helium depth profiles and the helium release as a function of the temperature were investigate by means of NRA technique based on the ^{2}H (^{3}He, α) ^{1}H nuclear reaction. The analysis was performed on a dedicated apparatus DIADDHEM at the CEMHTI-Cyclotron laboratory, Orleans [1].

Release results with temperature indicate that the ^{3}He gas trapped inside grains starts to leave the metatitanate polycrystalline structure at about 200ºC (Figure 1). For breeding applications in a fusion reactor environment, this fact is an advantage, considering the operational temperature of actual lithium ceramic

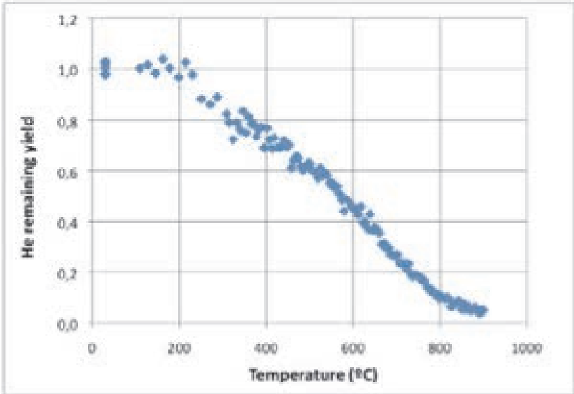

Figure 1. Gas release experimental data registered during isochronal thermal annealings of a ^{3}He-implanted lithium metatitanate ceramic implanted at 600keV to a fluence of 1x 10^{17} ions/cm^2.

breeder concepts [2]. Gas release is temperature dependent, the curve presenting two different releasing rates with temperature. Temperatures higher than 500ºC give rise to a more efficient outgas process, indicating that a fraction of He needs higher activation energies to release.

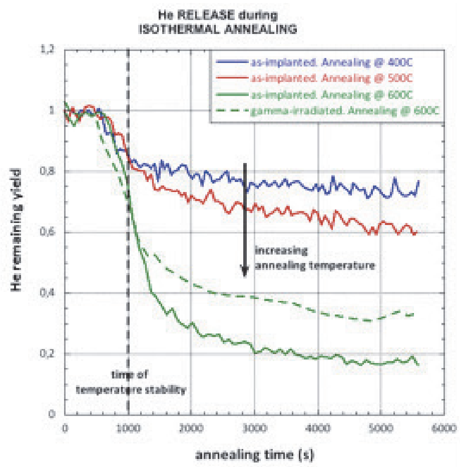

Figure 2. Isothermal annealings as a function of time of ^{3}He-implanted lithium metatitanate ceramic samples implanted at 600keV to a fluence of 1x 10^{17} ions/cm^2.

The He-remaining yield was registered as a function of time during isothermal annealings at 400, 500 and 600ºC (figure 2). Few minutes after achieving the thermal equilibrium, the gas concentration inside the material tends asymptotically to a value, which decreases with annealing temperature, as expected for a thermally stimulated process. The releasing rate seems to be higher for the annealing above 500ºC. It must be pointed out the good agreement between the isochronal and the isothermal release experiments since both indicate a different outgas dynamic for the release process in the vicinity of 500ºC.

After isothermal annealings, the remaining gas depth distributions were determined using the NR analysis at room temperature (figure 3). For comparison, a reference sample was used to measure the depth profile of the as-implanted material. The implantation depth maximum was measured at 1.7 microns. He depth profiles indicate the insignificant diffusion of ^{3}He towards surface. This experimental observation suggest that the release mechanism for the trapped He gas maybe diffusion/migration within the implantation plane forward the reaching of easier ways (as grain boundaries or pores) to complete the outgas process.

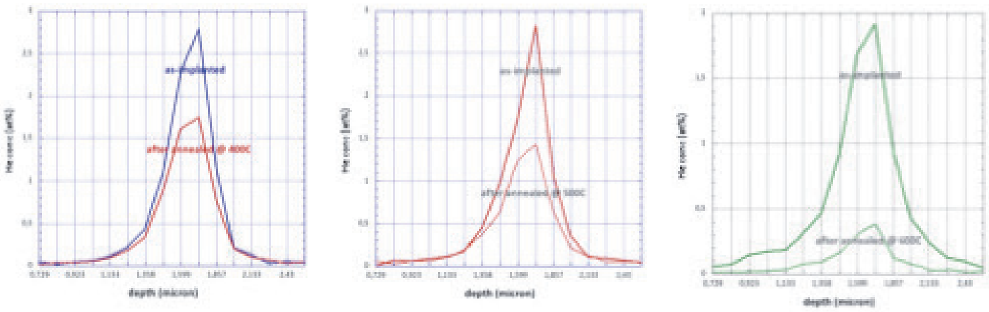

Figure 3. Depth profiles of the ^{3}He remaining concentration obtained at room temperature using the NRA technique before and after thermal annealings at 400 (left), 500 (center) and 600ºC (right).

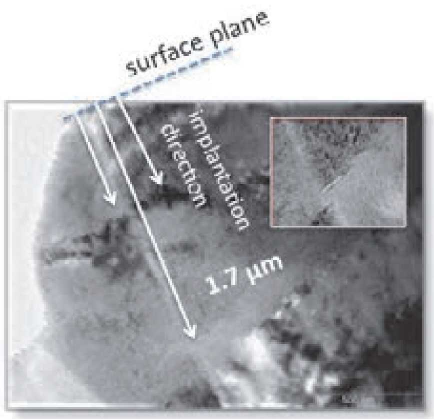

Figure 4. Cross-section TEM microstructure of a lithium metatitanate lamella after ^{3}He-implantation (600keV; 1x 10^{17} ions/cm^2) and 400ºC/5000s thermal treatment. The protected original implanted surface is located to the top left of the micrograph. The ion implantation direction and the implantation range are indicated in the micrograph. The inset shows a higher magnification of the microcracked planes of microcavities accumulation.

3. TEM studies on cross section samples

The microstructure of implanted and thermal annealed samples was studied by TEM in surface protected cross section samples [3]. The micrograph in figure 4 shows a cross section TEM lamella obtained from a surface protected He-implanted sample. A region (300nm width) of interconnected microcavities, arranged perpendicular to the implanted direction, are located at a depth of 1.7 ± 0.2 μm. Microcracking also occurred within the implanted region. The magnified picture shows the microstructure of these cavity planes located at a depth of 1.5 to 1.9 micron. Smaller cavities are rarely presented at irradiated depths lower than the implantation peak. As expected, the more probable association of He atoms at this depth gives rise to their arrangement into bigger cavities and the increase of cavity density. The so-called trapped helium having a higher release rate during the thermal desorption experiments could be then associated to that presented in these grain interior cavities whose escaping path are grain boundaries and/or pores.

4. Summary and conclusion

Small cavities and few extended microcracks planes, located at the implantation range (1.7 ± 0.2 μm) and running parallel to the irradiated surface have been identified in TEM images of lithium metatitanate cross section lamellas.

The formation of a great density region of interconnected nanocavities within the ion-damaged plane is consistent with the experimental NRA He depth profiles, which points out the stability of the He gas distribution in depth with temperature. The no broadening of depth profiles suggests the occurrence of no diffusion of He or He-vacancy complexes inside grains.

^{3}He gas associations are here proposed to diffuse or migrate within the ion-damaged plane and along the cavity planes towards grain boundaries or pore surfaces, where an easier path for the gas to release is found.

Acknowledgements

The authors wish to thank the EMIR – French national network under the project ID 10-12-3469 for supporting the He implantation experiments and NR analysis. TEM observations were performed using funding provided by the Spanish National Government under the contract ENE2011-30118-C06-00.

References

[1].- Lhuillier P.E. , B. T., Desgardin P., Courtois B., Sauvage T., Barthe M.F., Tessier Y.. "Helium retention and early stages of helium-vacancy complexes formation in low energy helium-implanted tungsten." J. Nucl. Mater., 433 (2013) 305–313.

[2].- Raffray A.R. et al., "Breeding blanket concepts for fusion and materials requirements", Nucl. Mater., 307–311 (2002) 21–30.

[3].- Zinkle, S., "Effect of H and He irradiation on cavity formation and blistering in ceramics." Nucl. Instrum. Meth. B, 286 (2012) 4-19.

He thermal-induced diffusion in lithium titanate

M. González, E. Carella, A. Ibarra

LNF_CIEMAT, Madrid, Spain

T. Sauvage, R.Bès, B.Courtois

CEMTHI-CNRS, Orléans, France

Work was supported by the EMIR French National Network (project ID 10-12-3469) and the Spanish National Government (project ENE2011-30118-c06-00

Objective

In the framework of a Spanish National Project
"to understand the effects of ions and radiation
in the ions transport mechanisms of material for fusion"

**Thermal-induced release of implanted He
inside porous lithium metatitanate ceramics,
to elucidate the mechanisms of gas release**

Spanish – French collaboration

- CEMTHI-CNRS, Orléans, France: **Ion implantation and analysis**, supported by the EMIR French National Network
- LNF_CIEMAT, Madrid, Spain: **Sample fabrication and TEM microstructural studies**, using the Spanish National Government funding.

Workshop CBBI_17, 12-14 Septembre 2013, Barcelona

OUTLINE

Objective

Sample preparation. Implantation. Characterization techniques. Experimental set ups.

Results.
- He release with temperature
- Isothermal He behaviour
- Implantation damage and He distribution in depth through TEM microstructure

Summary and conclusions

Some studies to achieve in the near future

Workshop CBBI_17, 12-14 Septembre 2013, Barcelona

Experimental (1/3)

1. Classical ceramic method for fabrication of lithium metatitanate (Li_2TiO_3) pellets from commercial powders. Porosities of about 15% TD after ceramic sintering.

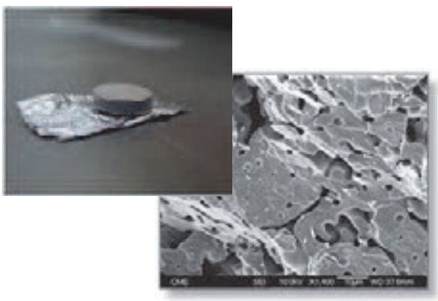

FESEM fresh fracture microstructure of a sintered Li_2TiO_3 ceramic:

Transgranular fracture of a matrix of monophasic polygonal grains (mean size about 20 μm) surrended by open and closed porosity (pore size from 0.1 μm to 10 μm).

2. ^{3}He implantation on ceramic targets at the CEMHTI-Cyclotron laboratory, Orleans. At room temperature. 600 keV ion beam (depth maximum aprox 1.8 μm was, SRIM calculated). Up to a fluence of 10^{17} ions/cm^2.

Workshop CBBI_17, 12-14 Septembre 2013, Barcelona

Experimental (2/3)

3. He behaviour was studied by Nuclear Reaction Analysis (NRA, an IBA technique) through:

   a) He release curve registration up to 900ºC; plus
   b) He depth profiling after increasing in-situ temperature treatments.

He release and depth profiles determinations were performed by energy spectrometry of protons and α-particles emitted from the

$$^{3}He + {}^{2}H \rightarrow {}^{1}H + {}^{4}He$$

nuclear reaction using a 900 keV deuteron analysis beam.

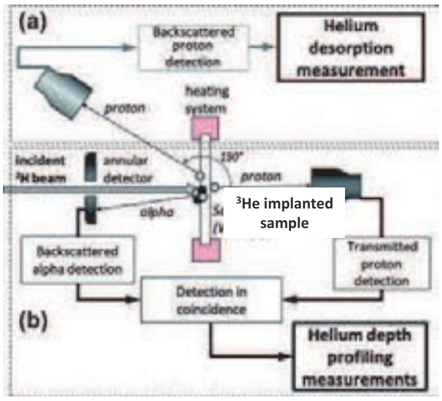

Scheme of the experimental set up.
DIADDHEM apparatus at the CEMHTI-Cyclotron laboratory, Orleans.
From P.E. Lhuillier et al., JNM 433, 2013

Experimental (3/3)

4. TEM was applied to study the microstructure of cross sectional samples. The implanted surface was protected before ion beam milling.

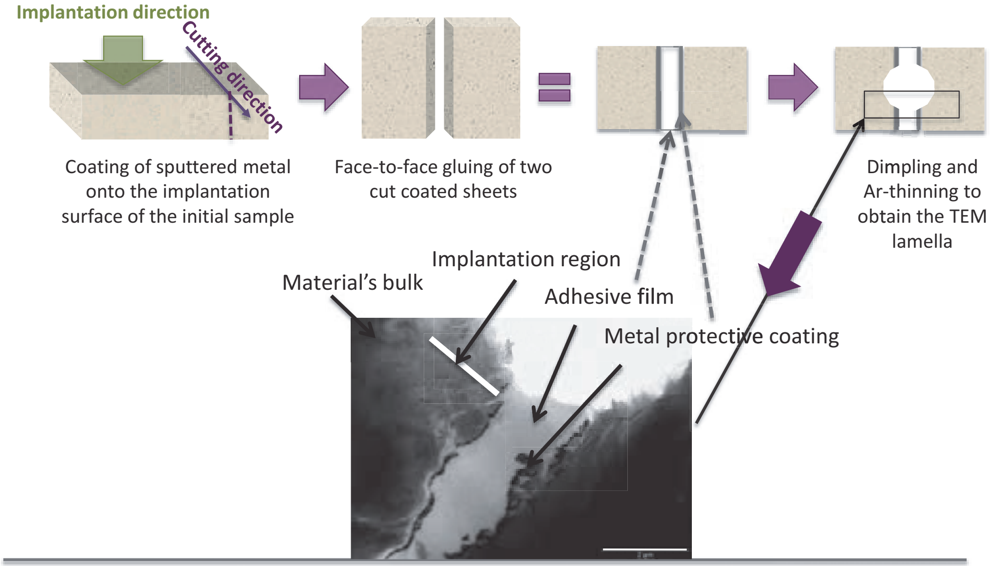

OUTLINE

Objective

Sample preparation. Implantation. Characterization techniques. Experimental set ups.

Results.

- **He release with temperature**
- **Isothermal He behaviour**
- **Implantation damage and He distribution in depth through TEM microstructure**

Summary and conclusions

Some studies to achieve in the near future

Results (1/4)

He RELEASE OR ISOCHRONAL DESORPTION CURVE

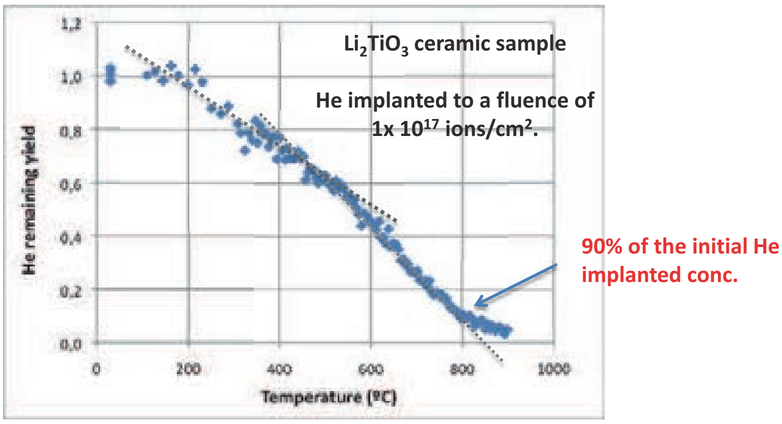

- The He gas starts to release at a very low temperature.
- 500ºC seems to be an inflexion point for the He release kinetics.

OUTLINE

Objective

Sample preparation. Implantation. Characterization techniques. Experimental set ups.

Results.

- **He release with temperature**
- **He isothermal annealing behaviour**
- **Implantation damage and He distribution in depth through TEM microstructure**

Summary and conclusions

Some studies to achieve in the near future

Results (2/4)

ISOTHERMAL ANNEALING TREATMENTS

Li_2TiO_3 ceramic sample.
He implanted to
a fluence of 1x 10^{17} ions/cm^2.

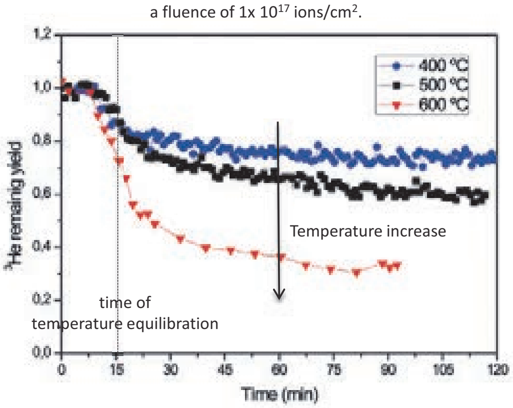

$$N(t)/N(t=o)= [1- N(t=\infty)/N(t=o)]\ e^{-K(T).t} + N(t=\infty)/N(t=o)]$$

K(T) ---- helium loss term

Annealing temperature (ºC)	K (T) factor (±0.01)
400	0,068
500	0,065
600	0,100

- gas remaining concentration decreases with annealing temperature.
- a different outgas dynamics for the release process in the vicinity of 500ºC.

OUTLINE

Objective

Sample preparation. Implantation. Characterization techniques.
Experimental set ups.

Results.

- **He release with temperature**
- **Isothermal He behaviour**
- **He depth profiling**
- **Implantation damage and He distribution in depth through the TEM microstructure**

Summary and conclusions

Some studies to achieve in the near future

Results (3/4)

He DEPTH DISTRIBUTIONS

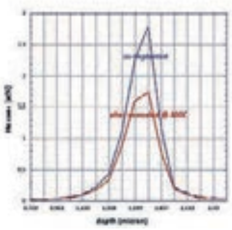

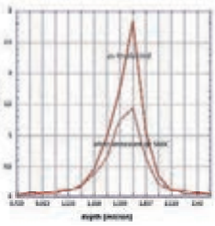

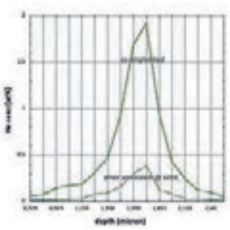

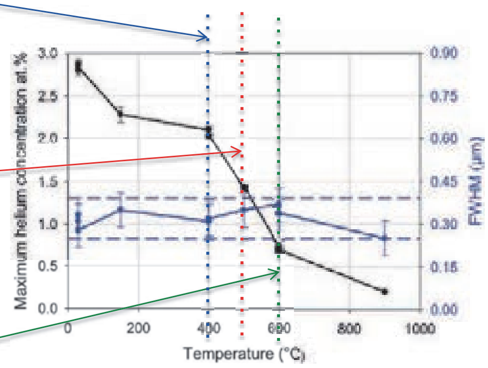

At any temperature,
insignificant diffusion of ^{3}He towards surface
while the loss of gas is once more corroborated.

OUTLINE

Objective

Sample preparation. Implantation. Characterization techniques. Experimental set ups.

Results.

- **He release with temperature**
- **Isothermal He behaviour**
- **Implantation damage and He distribution in depth through the TEM microstructure**

Summary and conclusions

Some studies to achieve in the near future

Results (4/4)

He DEPTH DISTRIBUTION ASSESMENT USING TEM

Region of maximum cavity density and extended microcracking. Coincident with implantation peak.

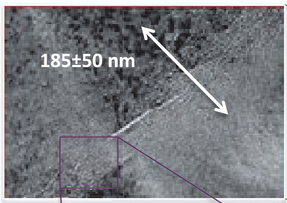

Cross section TEM lamellas preparations. Implantation surface specially protected to damage and thinning

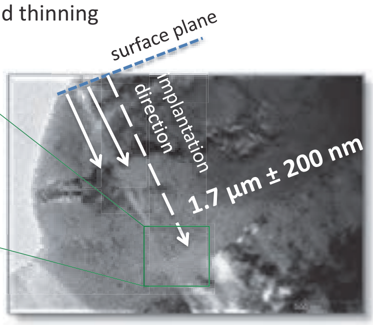

Individual and interconnected cavities

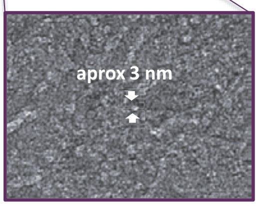

Planes of nanocracks and interconnected nanocavities are observed at the implantation peak (1.7 ± 0.2 µm) running parallel to the surface plane.

OUTLINE

Objective

Sample preparation. Implantation. Characterization techniques.
Experimental set ups.

Results.
- He release with temperature
- Isothermal He behaviour
- Implantation damage and He distribution in depth through the TEM microstructure

Summary and conclusions

Some studies to achieve in the near future

SUMMARY ….

In a He-implanted monoclinic lithium titanate matrix,

✓ the outgas starts at very low temperatures. An enhancement of the release dynamics is registered in the vicinity of 500ºC.

✓ isochronal and isothermal desorption processes indicate a deeply trapped fraction of He.

✓ 3nm in diameter He cavities and few extended cracks are visible at a depth of about 1.7 micron within a 200 nm band. No diffusion of He and or He-vacancy complexes towards surface is observed.

✓ He distribution in depth have been corroborated experimentally using the NRA technique and TEM.

…. AND CONCLUSIONS

This analytical work suggests that diffusion of the deeply trapped fraction of He takes place along the plane of high cavities density towards easier paths (grain boundaries or pores) for the gas to release.

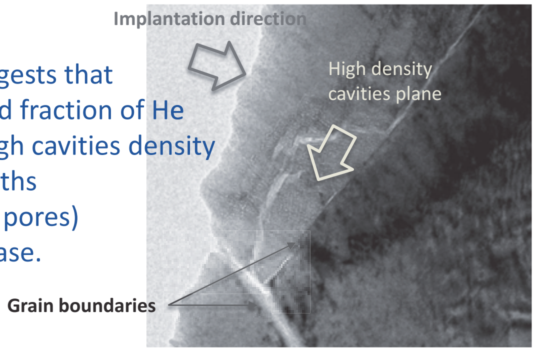

The low temperatures for the Helium release is an advantage considering the operational temperature range of actual lithium ceramic breeder concepts.

OUTLINE

Objective

Sample preparation. Implantation. Characterization techniques. Experimental set ups.

Results.
- He release with temperature
- Isothermal He behaviour
- Implantation damage and He distribution in depth through the TEM microstructure

Summary and conclusions

Some studies to achieve in the near future

Some studies to achieve in the near future

• Study light ion behaviour inside damaged solid breeders. Damaged due to gamma-ray and / or heavy ions.

• Make use of the CIEMAT's new equipment to characterize breeder ceramic materials: a FESEM+FIB microscope (including thermal microtensile-compresion testing platform) or the dynamic SIMS.

• Progressing into modeling and simulation of D and He gas diffusion processes in lithium ceramics.

Recent progress on the development of erbium oxide coatings for tritium permeation barrier

Takumi Chikada[1], Akihiro Suzuki[2], Takayuki Terai[1], and Takeo Muroga[3]

[1] Institute of Engineering Innovation, School of Engineering, The University of Tokyo, 2-11-16 Yayoi, Bunkyo-ku, Tokyo 113-8656, Japan

[2] Nuclear Professional School, School of Engineering, The University of Tokyo, 2-22 Shirakata-shirane, Tokai, Naka, Ibaraki 319-1188, Japan

[3] Fusion Systems Research Division, Department of Helical Plasma Research, National Institute for Fusion Science, 322-6 Oroshi, Toki, Gifu 509-5292, Japan

1. Introduction

Establishing an efficient tritium breeding/recovering system is one of the main issues of D-T fusion blanket systems. Structural materials for DEMO reactors, such as reduced activation ferritic/martensitic (RAFM) steels, have high permeability for hydrogen isotopes in the operational temperature range. To mitigate tritium permeation to an acceptable level, the fabrication of a thin ceramic film as a tritium permeation barrier (TPB) has been studied over several decades. In recent years, erbium oxide (Er_2O_3) coatings have been assessed as being a promising candidate for a TPB [1]. In this report, results and future challenges related to Er_2O_3 coatings as promising TPBs are reviewed. In addition, issues and perspectives on the application to ceramic breeder blanket concepts are discussed.

2. Experimental details

Er_2O_3 coatings were prepared on RAFM steels by gas-phase and liquid-phase methods: vacuum arc deposition (VAD) and metal-organic decomposition (MOD) described in detail in Ref. [2,3]. Characterizations of the coatings were carried out mainly using scanning electron microscopy (SEM), transmission electron microscopy (TEM), and X-ray diffraction (XRD). Hydrogen isotope permeation behaviors of the coated samples were examined using gas-driven deuterium permeation apparatus described in Ref. [4]. Permeation phenomena of hydrogen are represented by the following equation [5]:

$$J = P\, p^n / d, \qquad (1)$$

where J is the permeation flux, P is named permeability which is intrinsic parameter for the sample, p is the driving pressure introduced into the upstream, and d is the thickness of the sample. The exponent n represents permeation regime: diffusion limited and surface limited when n = 0.5 and 1, respectively.

3. Achievements

3.1. Permeation properties

The coated samples fabricated by the VAD at room temperature decreased deuterium permeation to the close level in spite of different permeability of the substrates. The pressure exponent *n* indicated the diffusion-limited regime, and the surface effects is small [4]. The crystal phase of the coatings transformed from the monoclinic B-phase to the cubic C-phase during the permeation measurements at 500–700 ºC. The average grain size of the coating increased after the permeation measurements at up to 700 ºC from 20 to 280 nm. The grain growth caused the enhancement of the suppression property, indicating deuterium permeation in the coating is dominated by diffusion along grain boundaries [6]. The both-side-coated samples showed over one order of magnitude higher TPB efficiency than those of the one-side-coated samples with the same total coating thickness. The 2.6 μm-thick coating on both sides reduced the permeability to $1/10^5$ in comparison with the bare RAFM steel at 600 ºC [6].

Regarding the coated samples fabricated by MOD, the samples heat-treated in high-purity argon produced a rough surface that was caused by the Fe–Cr–O layer and degradation during deuterium permeation measurements at 500–600 ºC. A uniformly coated surface with a high sufficiency of deuterium permeation was achieved by the heat treatment in high-purity hydrogen with 0.6% moisture. A 0.3-μm-thick coating yielded reduction factors of more than 500 and data reproducibility at 500–700 ºC, which is comparable in terms of efficiency to the coatings fabricated by the VAD. Additionally, it is expected that higher PRFs can be obtained by repeating the coating process as per the requirements of blanket systems [3].

3.2. Modeling of tritium permeation

The surface-coverage model describes the degradation of a TPB by the formation of pores and cracks in the coatings fabricated by different coating methods. The grain-boundary-diffusion model agrees with the grain growth of the coating with a columnar structure. However, large errors derived from the contributions of different coating structure are suggested for the MOD coatings. The energy-barrier model explains the relationship between the contributions to the permeation reduction and the activation energy of permeation and diffusion for the multilayer coatings [7].

3.3. Development of Er_2O_3-metal multilayer coatings

Two-layer Er_2O_3-Fe coatings were fabricated using the VAD and magnetron sputtering. The outer Fe layer deposited by the RF-magnetron sputtering had a smooth surface and good integration to the inner Er_2O_3 layer. The Fe layer was oxidized during the deuterium permeation experiment at 700 ºC, resulting in a measurable surface effect and a more than 10^3 increase of the permeation reduction factor. Thus a surface-oxidized metal layer has been proven to influence permeability, indicating that higher PRFs and reliability can be obtained by layering ceramic-metal structures. The notion of the multilayer coatings can be also extended to other combinations of ceramic-metal materials [8]. Li-Pb compatibility tests of Er_2O_3 and Er_2O_3-Fe two-layer coatings showed that deuterium permeability of the Er_2O_3 coatings after static Li-Pb immersion at 500 ºC for 500 h showed comparable permeation reduction factor with as-deposited coatings, and seriously degraded after immersion at 500 ºC for 1505 h. The corrosion rate of the Er_2O_3-Fe coatings was lower than that of the Er_2O_3 coatings.

4. Discussion regarding ceramic breeder blankets

Low concentration tritium permeation experiments have been performed on uncoated F82H and Er_2O_3-coated tubular samples. The uncoated sample tested with 1.2 ppm tritium showed one order of magnitude lower permeability than that of a plate sample with 100% deuterium. The Er_2O_3-coated sample with 1.2 ppm tritium showed two orders of magnitude lower permeability than the uncoated sample, and less permeability than that of the coated plate sample with 100% deuterium. That suggests that the tritium permeation under a practical blanket condition might be overestimated when using the permeation data at high partial pressure.

5. Summary

A series of studies achieved precise deuterium permeation behaviors, such as effects of surface coverage, grain size, multilayer structure, and etc., through high-purity Er_2O_3 coatings deposited on RAFM steel substrates as well as PRFs of up to 10^5 at 600 °C. The development of fabrication process toward plant-scale fabrication without restriction of substrate geometry has progressed using the MOD method. Tritium permeation measurements revealed that the permeability under a low tritium partial pressure condition was approximately one order of magnitude lower than that measured with 100% deuterium.

Reference

[1] D. Levchuk *et al.*, J. Nucl. Mater. 367–370 (2007) 1033–1037.
[2] F. Koch *et al.*, J. Nucl. Mater. 329–333 (2004) 1403–1406.
[3] T. Chikada *et al.*, Fusion Eng. Des. 85 (2010) 1537–1541.
[4] T. Chikada *et al.*, Fusion Eng. Des. 84 (2009) 590–592.
[5] K.S. Forcey, J. Nucl. Mater. 160 (1988) 117–124.
[6] T. Chikada *et al.*, Nucl. Fusion 51 (2012) 063023.
[7] T. Chikada *et al.*, Fusion Sci. Technol. 60 (2011) 389–393.
[8] T. Chikada *et al.*, J. Nucl. Mater. 442 Suppl. 1 (2013) S592–S596.

17th IEA International Workshop on the Ceramic Breeder Blankets:
Ceramic Breeder Blanket Interactions

13th September, 2013

Recent progress on the development of erbium oxide coatings for tritium permeation barrier

Takumi Chikada[1], Akihiro Suzuki[1], Takayuki Terai[1], Takeo Muroga[2]

[1]School of Engineering, The University of Tokyo, Tokyo, Japan
[2]National Institute for Fusion Science, Toki, Japan

Email: chikada@nuclear.jp

THE UNIVERSITY OF TOKYO

Outline

1. Introduction
   - Tritium in fusion blankets
   - Tritium permeation barriers (TPBs)
2. Experimental details
   - Preparation of Er_2O_3 coatings
   - Deuterium permeation setup
3. Achievements
   - Permeation properties of Er_2O_3 coatings
   - Modeling of tritium permeation
   - Study on Er_2O_3-metal multilayer coatings
4. In the case of ceramic breeder blankets
   - Will tritium permeation be crucial?
5. Summary

1. Introduction
   - Tritium in fusion blankets
   - Tritium permeation barriers (TPBs)
2. Experimental details
   - Preparation of Er_2O_3 coatings
   - Deuterium permeation setup
3. Achievements
   - Permeation properties of Er_2O_3 coatings
   - Modeling of tritium permeation
   - Study on Er_2O_3-metal multilayer coatings
4. In the case of ceramic breeder blankets
   - Will tritium permeation be crucial?
5. Summary

Tritium in fusion blankets

4

Toward DEMO and commercial D-T fusion reactors

In a GW-class fusion reactor, a blanket system must produce and recover ~100 kg/yr tritium

→ The establishment of **an integrated tritium production/recovery system** is crucial in order to secure TBR

Interaction between tritium and blanket materials

1) Structural material
   - T permeation
   - T accumulation (inventory)

2) Solid breeder (Li_2TiO_3, Li_4SiO_4 etc.)
   - T release behavior

3) Liquid breeder (Li, Pb-Li, 2LiF-BeF_2)
   - Dynamic transfer in flowing conditions
   - T recovery (Li)
   - T release behavior (Pb-Li, Flibe)

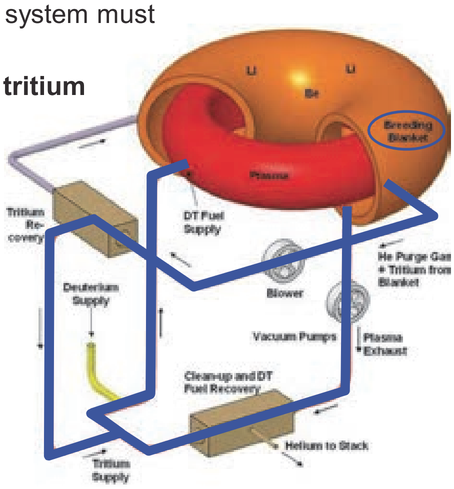

http://www.iter.org/doc/www/edit/Lists/WebsiteText/Attachments/16/fueling_5.jpg

Development of tritium permeation barrier

5

Main metals for structural materials of fusion blankets (Fe, V, Ti, etc.) has high permeability of hydrogen isotopes

→ Tritium permeation through structural materials at blanket sections causes: crucial fuel loss / radiological problems

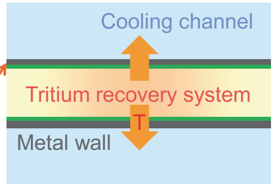

Tritium Permeation Barrier (TPB)

TPB coatings have been investigated for several decades with ceramics

Investigated TPB materials and their PRFs (until 2007) [1]

Material	Permeation Reduction Factor	Number of papers
Al_2O_3	10∼>10000	~30
TiC/TiN	<10∼>10000	~5
Cr_2O_3	10	~5
BN	100	3
Er_2O_3	800	2

Requirements:

- ◆ High permeation reduction factor (PRF) PRF = $J_{uncoated}/J_{coated}$ >10^2-10^3
- ◆ Compatibility with blanket materials especially corrosive breeding materials
- ◆ Tolerance for thermal cycles, irradiation etc.

[1] G.W. Hollenberg, *et al.*, *Fusion Engineering and Design* 28 (1995) 190–208.

Problems and possibilities of TPB coatings

6

Ceramic coatings (Al_2O_3 etc.) reduced hydrogen permeation to 1/10-1/10^4 compared with structural materials

However,

- less than 1/10^6 by the bulk ceramics
- 4 orders of magnitude scattered data

Clarification of hydrogen permeation mechanism through the coatings is of great importance for a plant design!

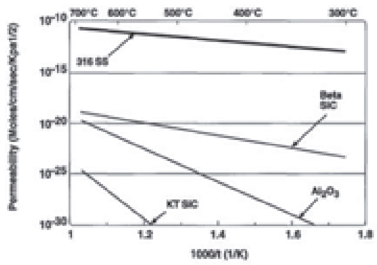

Permeabilities of SiC and Al_2O_3 bulk samples [1]

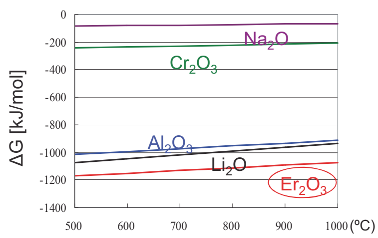

Gibbs free energy of oxides

Coating material: Erbium Oxide (Er_2O_3)

- Originally selected as an insulating coating
- High thermodynamic stability
- Compatibility with liquid lithium [2]
- Lower crystallization temperature (< Al_2O_3)

[1] G.W. Hollenberg, *et al.*, *Fusion Engineering and Design* 28 (1995) 190–208.
[2] A. Sawada, *et al.*, *Fusion Engineering and Design* 75–79 (2005) 737–740.

1. Introduction
- Tritium in fusion blankets
- Tritium permeation barriers (TPBs)

2. Experimental details
- Preparation of Er_2O_3 coatings
- Deuterium permeation setup

3. Achievements
- Permeation properties of Er_2O_3 coatings
- Modeling of tritium permeation
- Study on Er_2O_3-metal multilayer coatings

4. In the case of ceramic breeder blankets
- Will tritium permeation be crucial?

5. Summary

Coating methods

8

(1) Filtered arc deposition
A physical vapor deposition (PVD) method
Good adhesion on substrates
Low impurity
→ Clarification of precise permeation behaviors

Substrate: SS316, SS430, JLF-1, F82H
Substrate temperature: room temp. (R.T.), 700 ºC
Coating thickness: 0.3–2.6 μm

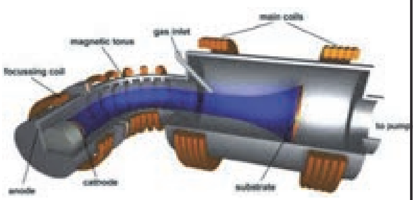

Vacuum arc deposition device (IPP-Garching)

(2) Metal-organic decomposition (MOD)
Ability to coat on complex-shape substrates
Potential to apply plant-scale fabrication

Substrate: JLF-1, F82H
Coating precursor: Er-03® (Er content 3%)
Coating method: spin coating / dip coating
Heat-treatment temperature: 600–700 ºC
atmosphere: Ar, H_2+0.6%H_2O
Coating thickness : 0.1–0.3 μm

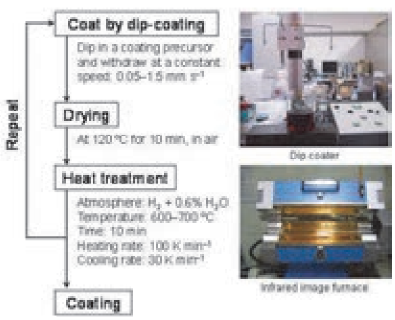

MOD process (dip coating)

Deuterium permeation experiment

9

Gas-driven permeation formula

$$J = SD\frac{\Delta p^{n}}{d} \;\Rightarrow\; \boxed{J = P\frac{p^{n}}{d}}$$

(Richardson's law)

J : Permeation flux
P : Permeability
p : D_2 pressure of upstream
d : Sample thickness

n = 0.5 limited by diffusion of hydrogen atoms
1.0 limited by surface reactions
(absorption, desorption)

Energy barrier of permeation

$$P = P_0 \exp\left(-\frac{E_P}{RT}\right) \qquad E_P = \Delta H_S + E_D$$

E_P : Activation energy of permeation
ΔH_S : Enthalpy difference
E_D : Activation energy of diffusion
R : Gas constant
T : Temperature

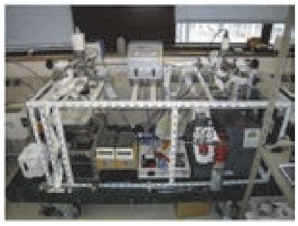

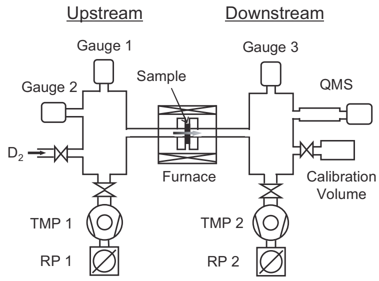

Schematic view of deuterium permeation apparatus

1. Introduction
- Tritium in fusion blankets
- Tritium permeation barriers (TPBs)

2. Experimental details
- Preparation of Er_2O_3 coatings
- Deuterium permeation setup

3. Achievements
- Permeation properties of Er_2O_3 coatings
- Modeling of tritium permeation
- Study on Er_2O_3-metal multilayer coatings

4. In the case of ceramic breeder blankets
- Will tritium permeation be crucial?

5. Summary

Permeation regimes of Er_2O_3 coatings

11

PVD

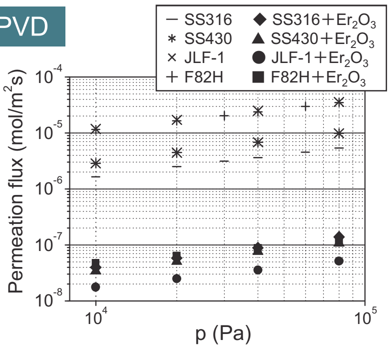

Driving pressure dependence of bare and coated samples at 773 K (no heating during deposition, 1 μm-thick)

- Similar permeation flux for coated samples
- Permeation regime of the coating

$J = P\,p^n/d$ n = 0.45–0.61

Deuterium dissociated in the coating

MOD

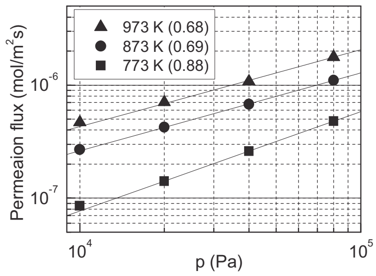

Driving pressure dependence of coated samples by the MOD method (on RAFM, coating thickness ~0.2 μm)

- Permeation regime n = 0.68–0.88

→ Surface effects by impurities, surface roughness, oxide layer, etc.

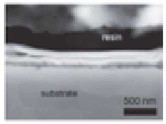

Permeation mechanism in Er_2O_3 coating (PVD)

12

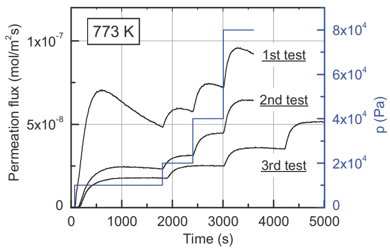

Temporal change of deuterium permeation flux of PVD-Er_2O_3 coating deposited at R.T.

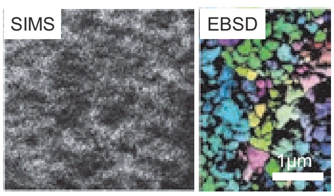

Deuterium distribution of the coating surface after deuterium introduction (left) and grain structure of the coating (right)

Will be presented by R. Sato at 11th ISFNT

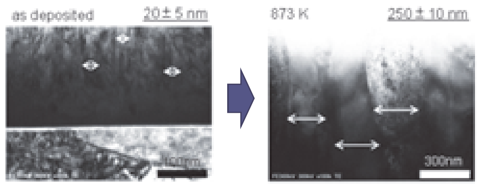

Cross-sectional bright field TEM images before and after permeation tests

- In spite of fixed driving pressures, deuterium permeation flux decreased at the beginning of the permeation tests
- The crystal grain of the coating grew depending on the test temperature

Grain growth ⇔ High TPB efficiency

Deuterium permeation through the coating is dominated by grain boundary diffusion rather than lattice diffusion

Permeation mechanism in Er_2O_3 coating (PVD)

13

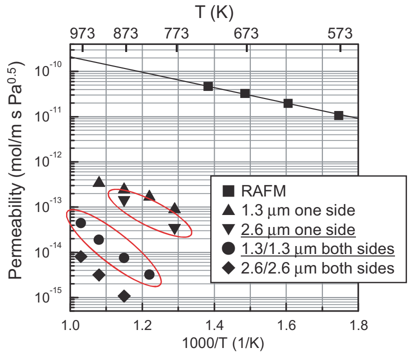

Arrhenius plots of permeability of one/both-side-coated samples

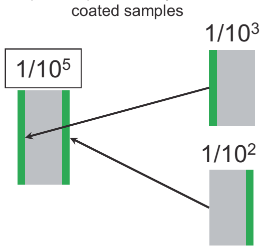

- Permeability of both sides coated samples showed one order of magnitude lower than those of one side coated samples with the same total thickness
- PRFs: 20000–100000
- No degradation during measurements

Activation energies of permeation E_P

one side: 75±5 kJ/mol

both sides: 130±10 kJ/mol

Activation energies of diffusion E_D

one side: 20±5 kJ/mol

both sides: 47±5 kJ/mol → Almost twice

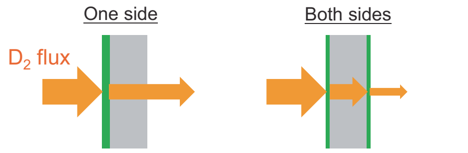

One-side-coated samples can be approximated by permeation through only the coating

A contribution of backside exists → not single layer and E_D and E_P show apparent values

Permeation mechanism in Er_2O_3 coating (MOD-dip)

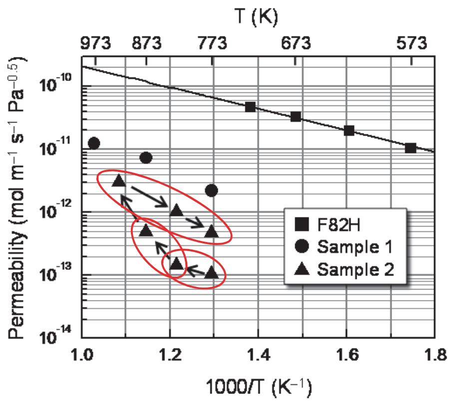

Arrhenius plots of deuterium permeability of Sample 1 and 2

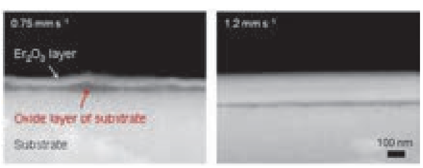

Sample 1 Sample 2

Sample 1 (withdrawal speed: 0.75 mm s^{-1})

- PRF: 20–30 (0.1 µm on both sides)

→ Probably because the uneven structure of the coating easily generated pores and cracks

Sample 2 (withdrawal speed: 1.2 mm s^{-1})

- PRF: 600–700 (0.2 µm on both sides)
  → ~100 after the test at 650 °C
- Several stages of permeation behaviors
  1) 500–550 °C: Crystallizing
     Gentle slope of temperature dependence due to the continuous decrease of permeation flux during the measurement
  2) 550–600 °C: Crystallized/Stable
     Steeper slope of temperature dependence (reproducible)
  3) 650 °C and later: Crack formation
     Gentle slope (≈ Sample 1)

Comparison of permeation reduction factors

15

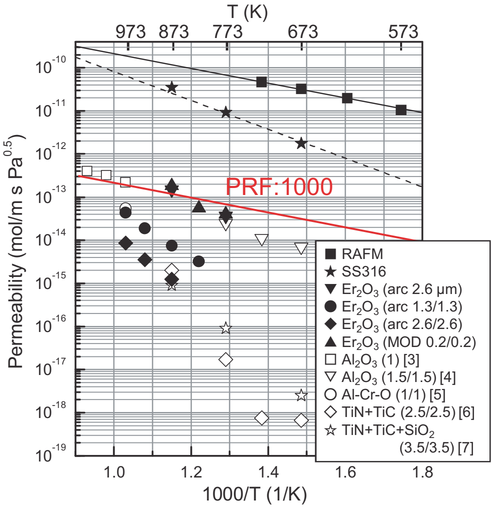

Comparison of permeabilities obtained in this study (filled) and references [3–7] (open)

[3] D. Levchuk, *et al.*, *Journal of Nuclear Materials* 328 (2004) 103–106.
[4] E. Serra, *et al.*, *Journal of Nuclear Materials* 257 (1998) 194–198.
[5] D. Levchuk, *et al.*, *Surface & Coatings Technology* 202 (2008) 5043–5047.
[6] C. Shan, *et al.*, *Journal of Nuclear Materials* 191–194 (1992) 221–225.
[7] Z. Yao, *et al.*, *Journal of Nuclear Materials* 283–287 (2000) 1287–1291.

A series of experiments achieved not only various permeation behaviors (surface coverage, grain diffusion etc.) but also the world largest PRF (10^5) by both-side-coated samples

Toward DEMO plant design

- Necessary to confirm reliability of TPBs in blanket conditions

→ Compatibility with breeder/coolant
Irradiation tests
Heat cycle resistance, etc.

- Need to enlarge application range both nano and macro scales

→ Atomic-scale simulation (nano)
Fabrication on complex-shape substrates (tube etc.) (macro)

Modeling of tritium permeation through Er_2O_3 coatings

16

Combining two models (peeling/crack model and grain diffusion model) and evaluating response to each parameter

$$J(\theta, S_a) = \left(P_{gb}\frac{S_a}{d_p}\right)\frac{p^{0.5}}{d_{coat}}\theta + P_{sub}\frac{p^{0.5}}{d_{sub}}(1-\theta)$$

The lower the rate of surface coverage, the smaller change the permeation flux shows according to grain growth

→ Large permeation reduction cannot be expected by the coatings with large crystal grain if surface coverage is low

First priority is surface coverage

→ Materials and fabrication methods with lower S_a and P_{gb} should be selected afterwards

P_{coat} : permeability of coating
d_{coat} : thickness of coating
P_{sub} : permeability of substrate
d_{sub} : thickness of substrate
p : driving pressure
($P_{coat} \ll P_{sub}$)

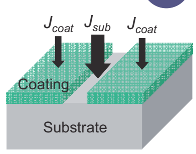

P_{gb} : permeability through grain boundary
S_a : grain density
d_p : effective distance factor

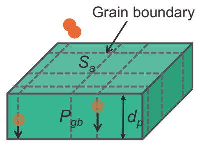

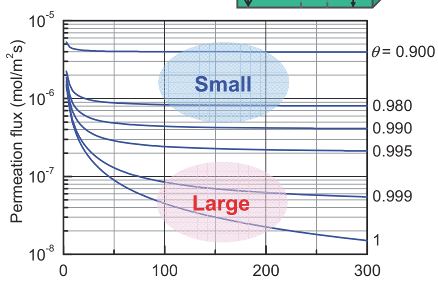

Relationship between permeation flux and grain size of the PVD coatings with different surface coverage
(calculated with 773 K, 1.3 μm-thick, 8.00 × 10^4 Pa)

Modeling of tritium permeation through Er_2O_3 coatings

Microscopic behavior of hydrogen migration in Er_2O_3 is investigated using first-principles calculation (density functional theory, molecular dynamics)

- Elemental steps in hydrogen permeation were simulated: dissociation, adsorption, penetration into Er_2O_3 bulk, trapping, and grain boundary diffusion
- Energetic values such as activation energy of diffusion and heat of solution were calculated on Er_2O_3 with/without defects and grain boundaries
- Although several modifications remain in calculation methods and interatomic potentials, experimental results are being reconstructed by computational simulations

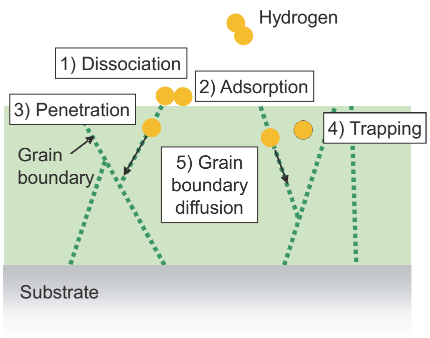

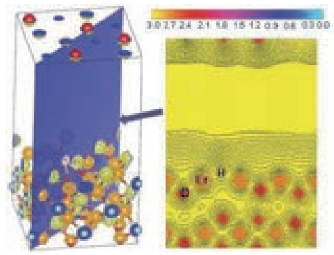

Charge density plot in logarithmic scale for one hydrogen adatom penetrated into Er_2O_3 subsurface .

Potential of multi-layer coatings

18

Er_2O_3-Fe two-layer coatings have been fabricated successfully, and shown comparable PFRs (~5000) with Er_2O_3 single layer coatings (~1000)

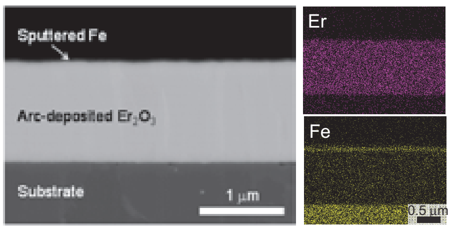

Cross-sectional SEM image of Er_2O_3-Fe two-layer coating

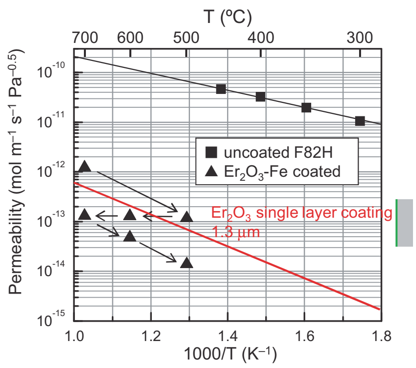

Arrhenius plots of deuterium permeability of F82H and Er_2O_3-Fe coating measured at up to 700 ºC

The important findings are:

- The outer metal layer was not peeled off after permeation tests at up to 700 ºC
- Each layer in the multi-layer coatings contributes to the permeation independently

An optimum coating may be designed with multi-layer structure (materials, number of layers, thickness) depending on blanket concepts

Potential of multi-layer coatings

19

Li-Pb compatibility of Er_2O_3 and Er_2O_3-Fe coatings were investigated
(Static immersion tests in $Li_{15.7}Pb_{84.3}$ for 1505 h at 550 ºC)

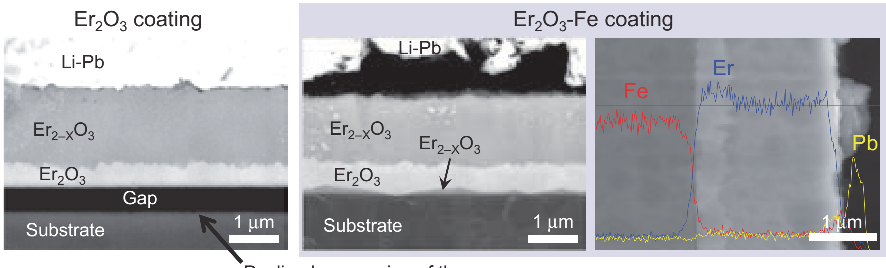

Peeling by corrosion of the interface and thermal stress

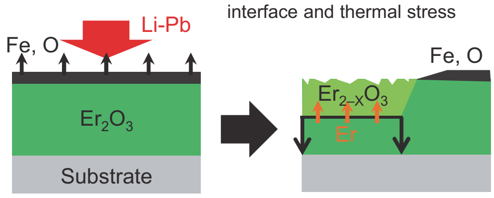

Oxidation of the outer Fe layer
→ Li-Pb corrosion

Formation of non-stoichiometric layer
→ Li-Pb corrosion

- Loss of coating thickness:
  Er_2O_3: 1 μm
  Er_2O_3-Fe: 0.5 μm

→ The Fe outer layer reduced the corrosion rate

- To keep the outer Fe layer unoxidized is very important in order to control the corrosion

Potential of multi-layer coatings

20

- Since independent contributions of two-layer coatings have been verified, schemes of layer structure can be optimized depending on blanket concepts
- Compatibility with blanket materials and tolerance for thermal cycles should be discussed for further investigations

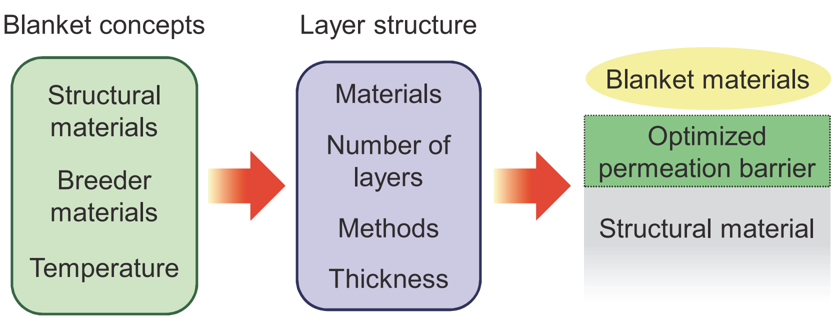

1. Introduction
- Tritium in fusion blankets
- Tritium permeation barriers (TPBs)

2. Experimental details
- Preparation of Er_2O_3 coatings
- Deuterium permeation setup

3. Achievements
- Permeation properties of Er_2O_3 coatings
- Modeling of tritium permeation
- Study on Er_2O_3-metal multilayer coatings

4. In the case of ceramic breeder blankets
- Will tritium permeation be crucial?

5. Summary

Tritium permeation in ceramic breeder blankets

22

Tritium permeation experiments on F82H and Er_2O_3-coated F82H <u>tubular samples</u> were carried out with low partial pressure tritium (1–100 ppm / 0.1–10 Pa) in the framework of Japan-US TITAN collaborative program

→ The condition was partly corresponding to solid breeder blanket concepts (HCPB, HCCR, WCSB etc.) ex.) 0.8–3.9 vppm HT, 0.03–0.13 vppm HTO [8]

Sample assembly (Er_2O_3-coated)

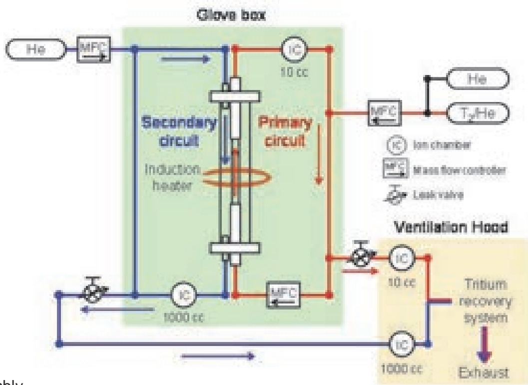

Tritium permeation system

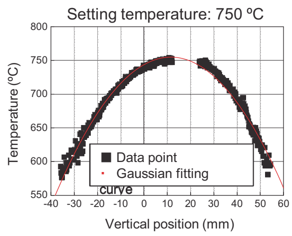

$$\bar{P} = \frac{1}{L}\int_0^L P_0 \exp\left(-Q_p \middle/ R\underbrace{\left(a\exp\left(-\frac{(x-b)^2}{2c^2}\right)\right)}_{\text{Gaussian function}}\right)dx$$

Temperature profile

[8] A. Ciampichetti, *et al.*, *Fusion Engineering and Design* 87 (2012) 620–624.

Tritium permeation in ceramic breeder blankets

23

- ◆ Uncoated F82H showed approximately one order of magnitude lower permeability than a previous data with 100% deuterium possibly because of surface effects (adsorption etc.)
- → Tritium permeation might be overestimated when high pressure data is extrapolated [9]
- ◆ A 0.2 μm-thick Er_2O_3 coating on F82H tube showed PRF of ~400 at 650–700 ºC. In addition, a memory effect of ion chambers was observed due to the formation of HTO
- ◆ In water-cooled solid breeder (WCSB) blanket concept, tritium leakage in cooling water is assumed to be 370 GBq/kg (1 ppmT_2), and tritium permeation rate to the coolant water of ~1/10 would be permissible [10]
- → Er_2O_3 coatings would be applicable as a tritium permeation barrier at blanket cassette, pipe walls, and heat exchanger with great care for HTO

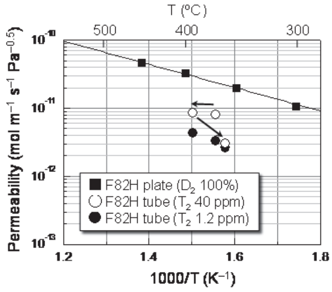

Arrhenius plots of tritium/deuterium permeability of F82H plates and tubes

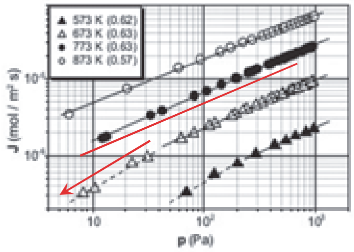

Partial pressure dependence of deuterium permeation flux through EUROFER plates [9]

[9] D. Levchuk, *et al.*, *Journal of Nuclear Materials* 328 (2004) 103–106.
[10] T. Yamanishi, *et al.*, *Fusion Engineering and Design* 81 (2006) 797–802.

1. Introduction
   - Tritium in fusion blankets
   - Tritium permeation barriers (TPBs)
2. Experimental details
   - Preparation of Er_2O_3 coatings
   - Deuterium permeation setup
3. Achievements
   - Permeation properties of Er_2O_3 coatings
   - Modeling of tritium permeation
   - Study on Er_2O_3-metal multilayer coatings
4. In the case of ceramic breeder blankets
   - Will tritium permeation be crucial?
5. Summary

Summary

25

A series of investigations on erbium oxide coatings as a tritium permeation barrier have been overviewed:

- Methodology for the fabrication of high-quality Er_2O_3 coatings has been established using gas/liquid phase methods

→ PRFs of 10^3–10^5 were achieved (world record at high temperatures)

- Various permeation behaviors have been found by microstructural analysis and deuterium permeation measurements

→ Effects of grain growth, surface effects, layer structure, and corrosion by Li-Pb

- Modeling of tritium permeation through the coating provides microscopic/macroscopic information on permeation mechanism

→ Computational approaches enlarge the application range

- Contributions to ceramic breeder blankets have been introduced

→ Considering effects of tritiated water and isotopic reactions, permeation behavior in practical tritium partial pressure range should be carefully evaluated for the blanket design

TOPICAL DISCUSSION: TRITIUM PERMEATION IN THE BREEDING ZONE

(summarized by D. Demange)

Before starting the discussions, a short presentation was given to recall the permeation issue, which was subsequently presented at ISFNT (ISFNT 2013 P3-050) “Tritium management issues and anti-permeation strategies for different DEMO breeder blanket options“. Since the breeding blankets (and steam generators) operate at rather high temperatures (> 400°C), are made of thin walls (few mm) for thermal efficiency, and use RAFM steels that have rather high permeability (about 10 times higher than standard stainless steel), tritium permeation and consecutive losses are significant (likely too high). Permeation mitigation strategies are required as a trade-off between very efficient and large tritium extractions in TES & CPS, and reliability and efficiency of anti-permeation barriers made of coatings or chemically assisted self-healing oxide layers.

The following points were afterwards discussed under this topic:

(1) How much tritium is permeating?

Actually the amount of tritium permeating towards the coolant is extremely difficult to quantify, since most of the key parameters are suffering from large uncertainties. A recent European study using the FUS-TPC code showed tritium permeation from the breeding zone towards the coolant ranging between 3-10% of the tritium produced for HCPB DEMO case. The simulation used a very simple model. Additional efforts are needed to develop more complex models taking into account profiles in temperature and tritium generation rates, also considering the gas flowing conditions that impact the tritium behaviour and migration in the breeding zone.

(2) Can coatings withstand severe conditions?

Along the life time of the breeding blanket, not only the neutron irradiation but also the temperature gradients and cycles might significantly damage coatings. After a certain operation time, the permeation reduction factor would likely dramatically be worsened. However, it seems not possible at this moment to quantify this effect (insufficient experiments on coatings under irradiation). This is exactly the critical issue of considering such anti-permeation barriers as main mitigation strategy if it appears that these coatings may not provide constant permeation reduction factor. Additional efforts are needed to investigate coatings under irradiation.

(3) Are coating materials a compatibility issue?

Likely yes, for Li-ceramics and for Be, so that only very a limited range of materials might be appropriate. The usually proposed oxide ceramics for permeation barriers will most probably react with beryllium as well as with the tritium breeder ceramics. From this point of view a coating on the cooling channel side is preferable. (4) What are the requirements for APB in term of permeation reduction factor?

Since the permeation issue is not well substantiated yet, establishing requirements for permeation reduction factor is not possible at this stage. However, qualitatively, any benefit of permeation reduction is welcome so that barriers with only moderate effects could be of interest to reduce the load on tritium systems. A meticulous trade-off study is required to analyse the efforts and benefits for using barriers with regards to the size and operation of the tritium systems.

(5) Is water vapour doping in He purge gas a possible (reasonable) mitigation?

Addition of 0.1% H_2 in the He purge gas is the reference (historical) option, arguing it enhance tritium release from the ceramics, thus helping to reduce inventory and residence time. Also, it can shift the tritium into its molecular form, which is more suitable for reuse, however, able to permeate, and does not prevent to get a significant amount of tritium in HTO form. Alternatively, one could imagine (propose) to replace H_2 with H_2O, which is known to enhance the tritium release even better, while it would reduce permeation. Recently developed tritium processes seem capable of handling this HTO. It is discussed that a too high water level should be avoided with respect to the corrosion issue, and also that the He purge, even without addition already contains moisture. More efforts are necessary to define what could be the maximum partial pressure of water vapour to be used as alternative to H_2.

(6) Any other (good) ideas?

No other idea for mitigating permeation was suggested

TOPIC 4: STATUS OF BREEDER BLANKETS

Development and qualification of ceramic breeder materials for the EU Test Blanket Module: Strategy and R&D achievements

M. Zmitko[1], Y. Poitevin[1], R. Knitter[2], L. Magielsen[3], S. van Til[3]

[1] *Fusion for Energy, Barcelona, Spain*
[2] *Karlsruhe Institute of Technology, Postfach 3640, Karlsruhe, Germany*
[3] *NRG Petten, Petten, The Netherlands*

Europe has developed two reference tritium Breeder Blankets concepts that will be tested in ITER under the form of Test Blanket Modules (TBMs): i) the Helium-Cooled Lithium-Lead (HCLL) which uses the liquid Pb-16Li as both breeder and neutron multiplier, ii) the Helium-Cooled Pebble-Bed (HCPB) with lithiated ceramic pebbles as breeder and beryllium pebbles as neutron multiplier. Both concepts are using the EUROFER reduced activation ferritic-martensitic (RAFM) steel as structural material and pressurized Helium technology for heat extraction (8 MPa, 300-500ºC).

The paper reviews the current status of development and qualification of the EU TBMs functional materials; namely ceramic solid breeder materials (Li-orthosilicate and Li-metatitanate). The main functional requirements are listed with the selection/acceptance criteria. The EU development and qualification strategy is presented. Also, the current status of the R&D activities with the main achievements is overviewed.

Corresponding Author:
Milan Zmitko
Fusion for Energy, Josep Pla 2, Torres Diagonal Litoral B3, 08019 Barcelona, Spain
Tel. +34 93 320 1824
E-mail: milan.zmitko@f4e.europa.eu

FUSION FOR ENERGY

17th IEA Int. Workshop on Ceramic Breeder Blanket Interactions (CBBI-17)

Barcelona, Spain
September 12-14, 2013

Development and Qualification of Ceramic Breeder Materials for the EU Test Blanket Module: Strategy and R&D Achievements

M. Zmitko
TBM & MD Project Team, Fusion for Energy (F4E), Barcelona, Spain

FUSION FOR ENERGY

Presentation Outline

- The European Breeder Blanket concepts
- Test Blanket Modules (TBMs) in ITER
  - Technical information
  - Time schedule
- Ceramic breeder materials for HCPB
  - Requirements & open issues
  - Development and procurement strategy
  - On-going CB materials related activities
  - Some R&D achievements
- Conclusions

ITER, a unique opportunity to test Breeder Blanket mock-ups:

‘Test Blanket Modules’ (TBMs)

ITER TBM project mission

“The TBM project provides test blankets to test and validate design concepts of tritium breeding blankets relevant to a power-producing reactor.”

ITER Project Requirements (*27ZRW8)*

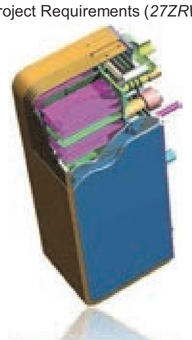

- Europe is currently developing two reference breeder blankets concepts for DEMO to be tested in ITER under the form of Test Blanket Modules (TBMs) Systems:
  - Helium-Cooled Lithium-Lead (**HCLL**)
  - Helium-Cooled Pebble-Bed (**HCPB**)

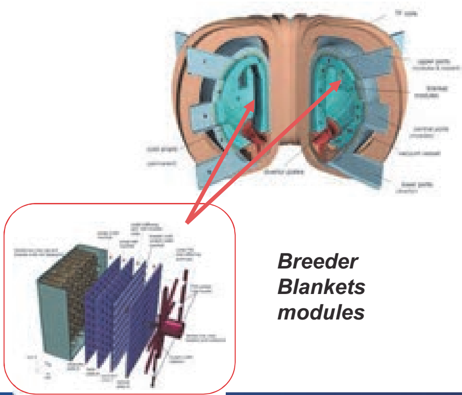

Breeder Blankets modules

FUSION FOR ENERGY

The TBM program in ITER

"Council Decision on the Establishment of the Test Blanket Module (TBM) Program", IC-3, Nov. 2008; TBM Port Allocation endorsed by the IC-5, 2009

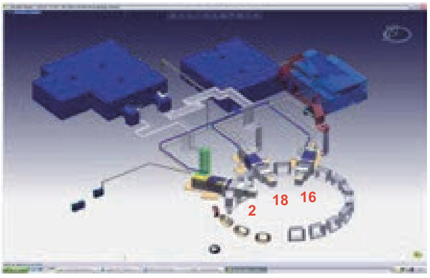

European TBM concepts

	HCPB He-Cooled Pebble-Bed	HCLL He-Cooled lithium-Lead
Structural material	EUROFER (RAFM steel)	
Coolant	Helium (8 MPa, 300-500°C)	
Tritium breeder, neutron multiplier	Solid pebbles Li_2TiO_3 / Li_4SiO_4, Be	Liquid Pb-16Li
Sub-systems	HCS, CPS, TES	HCS, CPS, TES, PbLi loop

ITER Port # ('Port Master', PM)	TBM Concept 1	TBM Concept 2
#16 (PM: EU)	HCLL (He-Cooled Lithium-Lead) (TBM Leader: EU)	HCPB (He-Cooled Pebble Bed) (TBM Leader: EU)
#18 (PM: JA)	WCCB (Water-Cooled Ceramic Breeder) (TBM Leader: JA)	HCCB (He-Coolant Ceramic Breeder) (TBM Leader: KO)
#2 (PM : CN)	HCCB (He-Cooled Ceramic Breeder) (TBM Leader: CN)	LLCB (Lithium-Lead Ceramic Breeder) (TBM Leader : IN)

5

FUSION FOR ENERGY

The TBM systems extend from Vacuum Vessel to Port Cell and buildings

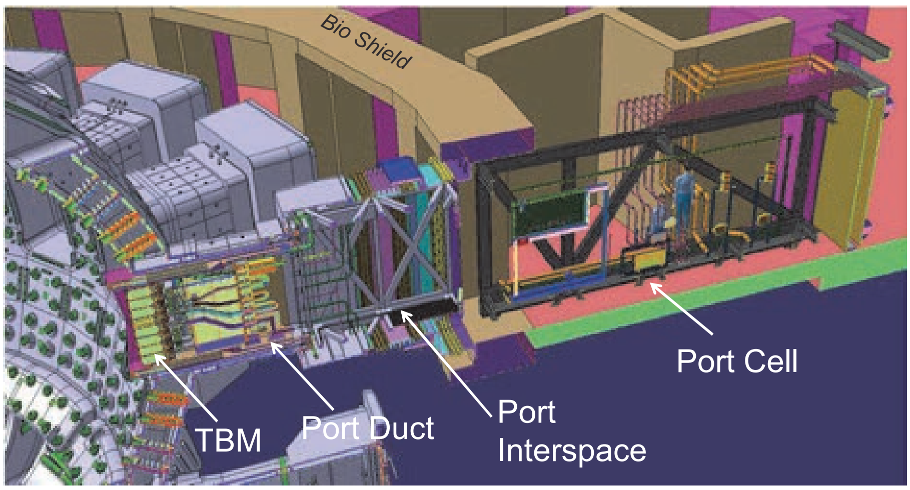

– From L.V. Boccaccini , SOFT-2010

6

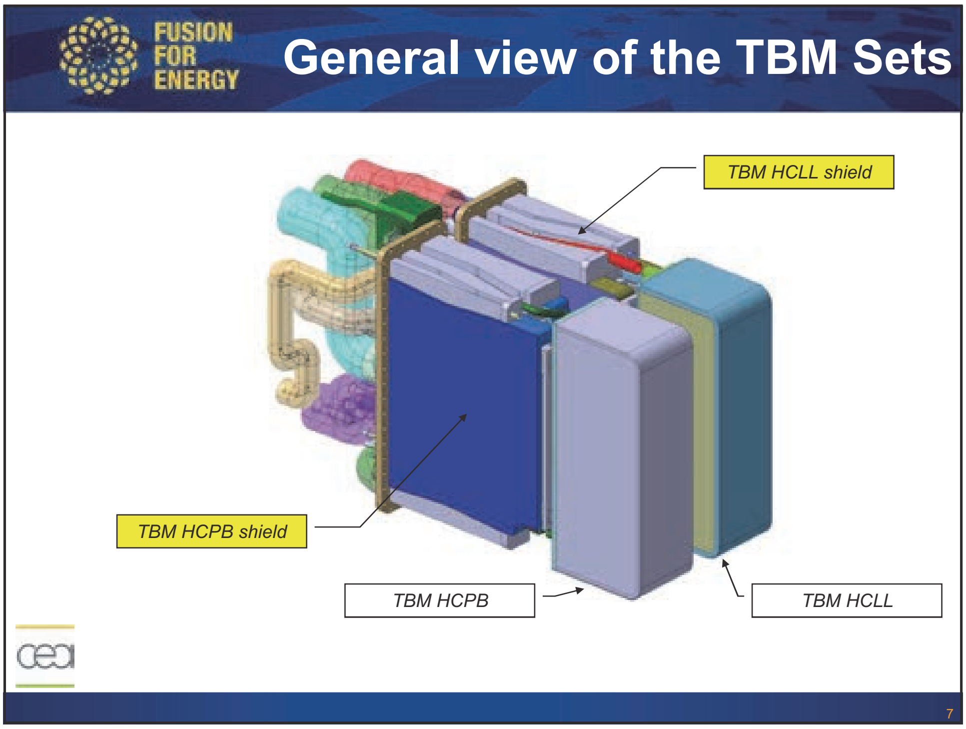
FUSION FOR ENERGY
General view of the TBM Sets
TBM HCLL shield
TBM HCPB shield
TBM HCPB
TBM HCLL
cea
7

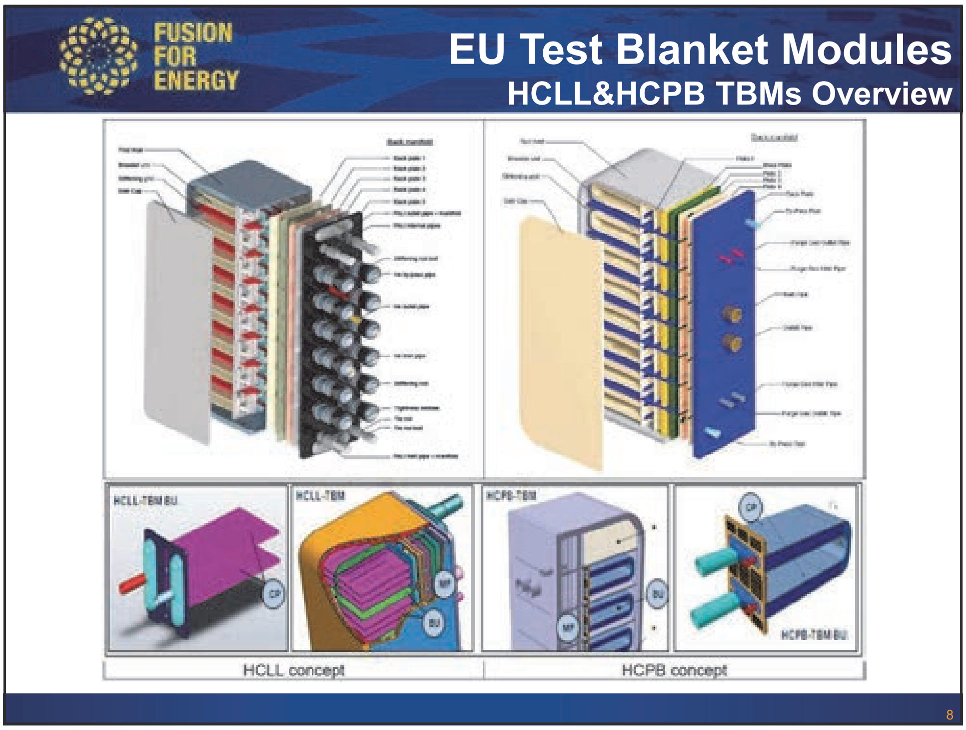
FUSION FOR ENERGY
EU Test Blanket Modules
HCLL&HCPB TBMs Overview
HCLL concept
HCPB concept
8

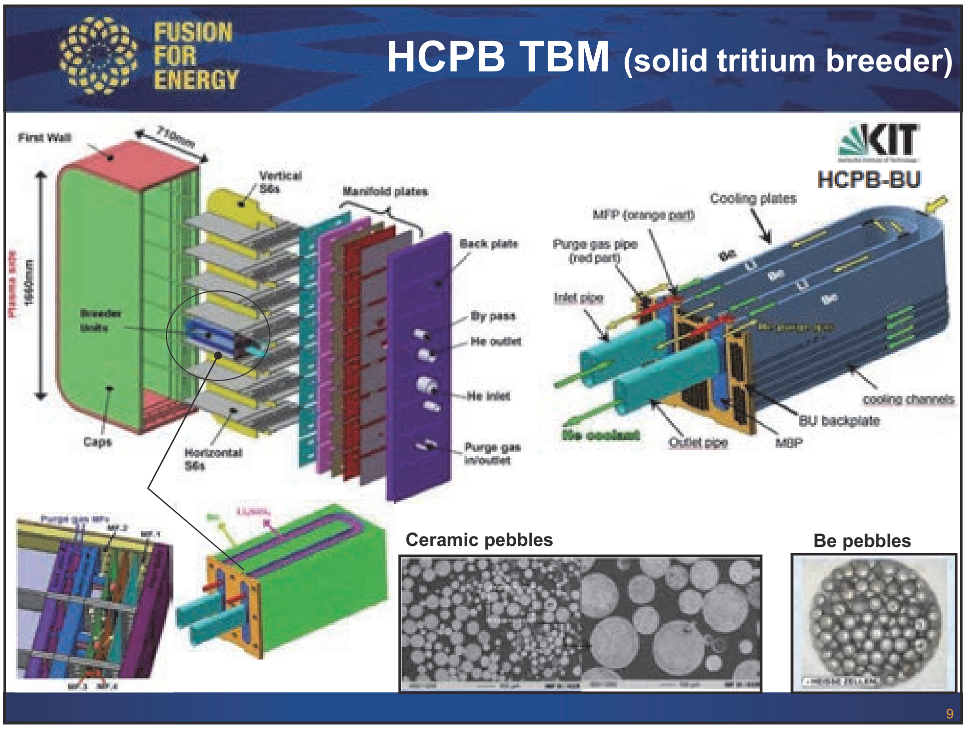
FUSION FOR ENERGY
HCPB TBM (solid tritium breeder)
KIT
HCPB-BU
First Wall
710mm
1660mm
Plasma side
Vertical SGs
Manifold plates
Back plate
By pass
He outlet
He inlet
Purge gas in/outlet
Breeder Units
Caps
Horizontal SGs
Cooling plates
MFP (orange part)
Purge gas pipe (red part)
Inlet pipe
Be
Li
cooling channels
BU backplate
He coolant
Outlet pipe
MBP
Ceramic pebbles
Be pebbles
9

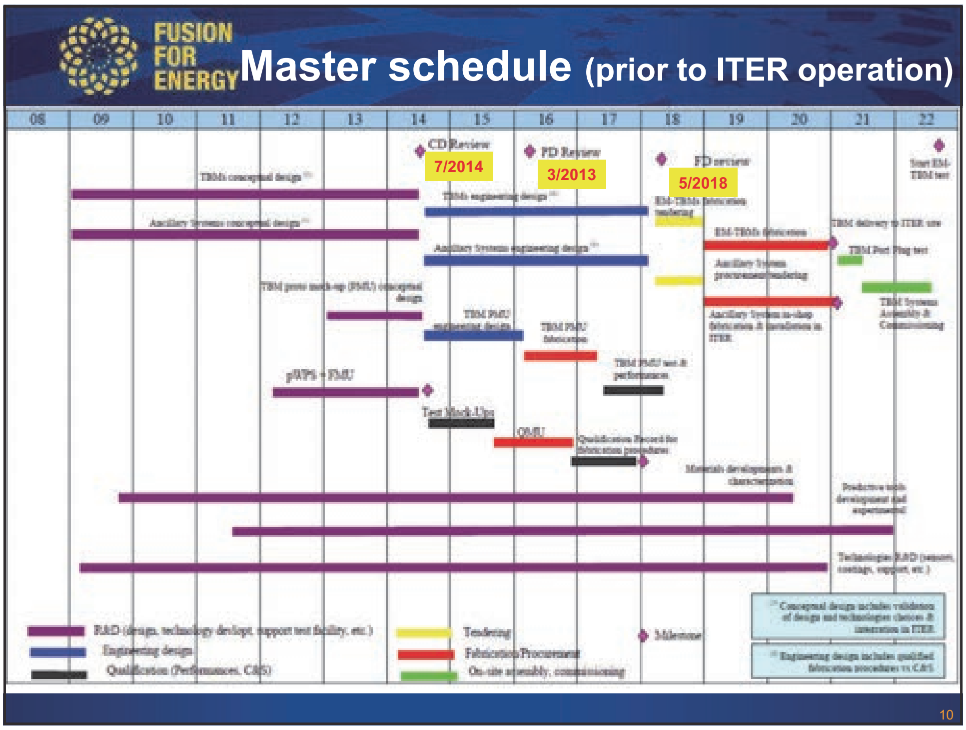
FUSION FOR ENERGY
Master schedule (prior to ITER operation)
08 09 10 11 12 13 14 15 16 17 18 19 20 21 22
CD Review
7/2014
PD Review
3/2013
FD review
5/2018
Start EM-TBM test
TBMs conceptual design
TBMs engineering design
Ancillary Systems conceptual design
Ancillary Systems engineering design
EM-TBMs fabrication
TBM delivery to ITER site
TBM Port Plug test
Ancillary System procurement/tendering
TBM Systems Assembly & Commissioning
TBM proto mock-up (PMU) conceptual design
TBM PMU engineering design
TBM PMU fabrication
TBM PMU test & performances
pWPS + FMU
Test Mock-Ups
QMU
Qualification Record for fabrication procedures
Materials developments & characterization
Technologies R&D (sensors, coatings, support, etc.)
R&D (design, technology develpt, support test facility, etc.)
Engineering design
Qualification (Performances, C&S)
Tendering
Fabrication/Procurement
On-site assembly, commissioning
Milestone
10

FUSION FOR ENERGY

HCPB Ceramic Breeder Materials - Development and Qualification

11

FUSION FOR ENERGY

Ceramic Breeder Materials

- Tritium breeding material of the EU HCPB breeder blanket concept is a ceramic breeder in the form of pebble beds
- Reference option: Lithium Orthosilicate (Li4SiO4; OSi); ~0.25-0.63 mm pebbles produced by melt-spraying process and containing a surplus of 2.5 wt% of SiO2; KIT & SCHOTT
- Back-up option: Lithium Metatitanate (Li2TiO3; MTi); pebbles produced by extrusion-spheronisation-sintering process at different nominal diameters in the range of 0.6-1.2 mm; CEA & CTI
- For TBM → Li-6 enrichment of 90 at%

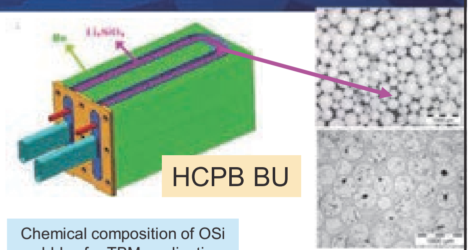

Chemical composition of OSi pebbles for TBM application

Elements	Specific content (in wt %)
Li_2O	48.4±0.2
SiO_2	51.2±0.2
Li	22.498
Si	23.923
O	53.458
Al	≤0.003
C	≤0.100
Ca	≤0.002
Co	≤0.0001
Cr	≤0.0001
Cu	≤0.0001
Fe	≤0.0004
K	≤0.001
Mg	≤0.0002
Mn	≤0.0002
Pt	≤0.009
Na	≤0.002
Ni	≤0.0002
Ti	≤0.0004
Zn	≤0.0002
Zr	≤0.001

Data from EU HCPB PrSR v2.0

Chemical composition of MTi pebbles for TBM application

Elements	Specific content (in wt %)
Li	12.648
Ti	43.615
O	43.736
Al	≤0.0003
B	≤0.001
C	≤0.005
Ca	≤0.001
Cr	≤0.0003
Fe	≤0.0005
P	≤0.0001
K	≤0.001
Na	≤0.002
S	≤0.0001
Ni	≤0.0002
Si	≤0.001

12

Ceramic Breeder Materials
Functional Requirements

FUSION FOR ENERGY

General requirements come from DEMO objectives with a short-term objective to characterize & qualify Functional Materials (Li-ceramics, Be) for a use in the ITER TBM

- Neutronic performances for T self-sufficiency (TBR ≥ 1.1)
- Temperature control of the pebble beds during operation in the temperature window of ~400-920ºC (PBTM issues/aspects)
- Sufficient long lifetime → (i) neutron irradiation resistance without significant changes of thermo-physical and mechanical properties; (ii) to withstand stresses induced under DEMO-relevant operating conditions without excessive fragmentation
- Material compatibility between the ceramic breeder and EUROFER (up to max. T~ 550ºC)
- Low tritium residence time/tritium retention in the Li-ceramics pebbles; efficient tritium extraction → purge gas chemistry optimization
- As low as possible activation under neutron irradiation (impurities level control; e.g. Co, Ni, Al, Fe,…)
- Easy reprocessing capability (in the view of DEMO/future FPR)

Lithium Orthosilicate (OSi)
Li_4SiO_4
(FZK-Schott, melt-spray process)
Ø = [0.25 - 0.63] mm

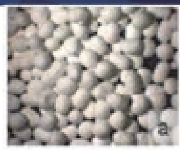

Lithium Metatitanate (MTi)
Li_2TiO_3
(CEA-CTI, extrusion-spheronisation-sintering)
Ø = [0.6 – 1.2] mm

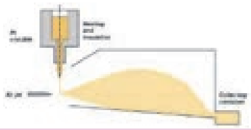

Schematic representation of melt-spray process for OSi

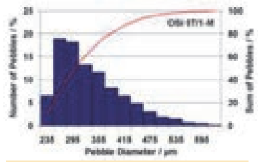

Typical pebble size distribution of OSi

Ceramic Breeder Materials
Open technical issues

FUSION FOR ENERGY

Development and further optimization of fabrication routes

- Optimization of the OSi fabrication route aimed at enhancing mechanical properties of the pebbles, yield of the process and controlling size distribution of the pebbles
- Development of a modified melt-based process to enhance the mechanical properties of OSi pebbles by additions of titania (TiO2) in order to obtain pebbles with MTi as a secondary phase
- Control of undesired impurities level in the CB materials (e.g. Co, Cr, Ni, Al, Fe,…); Standardization (i.e. elaboration of standard procedures) to be used for characterization of the produced materials
- Li-6 enrichment of ceramic breeder (e.g. availability of enriched Li-6 in a proper chemical form, procurement of a sufficient amount of Li-6, dual use material issue)
- In general, reprocessing capability of CB materials in the view of DEMO and FPR

Availability of the materials properties needed for a proper TBMs design

- Effect of neutron irradiation on thermo-mechanical properties of CB pebbles and CB pebble bed as function of irradiation temperature and neutron dose taking into account material degradation under irradiation
- Tritium retention/release characteristics as a function of irradiation temperature, neutron dose, purge gas chemistry, material properties/microstructure
- Compatibility with structure material under neutron irradiation
- Thermal conductivity in pebble beds under compressive loads

Functional Materials Development Strategy

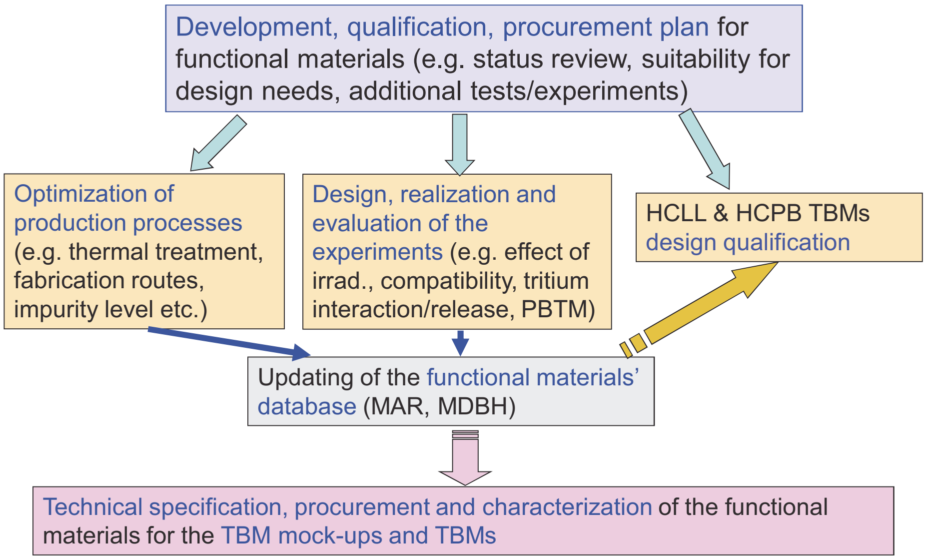

Ceramic breeder related activities (1/3)

TBMs functional materials (Be, ceramic breeder, Pb-Li) development/qualification [grant F4E-2009-GRT-030]:

- **Action 1:** Elaboration of the Development /qualification /procurement plan for functional materials
  - review the current status of development, including fabrication process and its drawbacks, further optimization needs and commercial applicability,
  - summarize the achieved characteristics/properties and their suitability in the view of TBMs design needs,
  - define a roadmap for further development, including identification of additional tests/experiments to be performed in order to qualify the materials for TBMs application,
  - define, in terms of quantity and quality, the materials' procurement plan for various steps/phases of the TBM project
- **Activities completed/achieved**

Ceramic breeder related activities (2/3)

Framework Partnership Agreement for the Activities in support of the conceptual and preliminary design of the European Test Blanket Systems (F4E-FPA-380)

- **Action 3: Qualification of Functional Materials for TBM Applications →** duration 48 months; implementation through Specific grants – **ONGOING**
  - Optimization/adjustment of the production processes/routes for Functional Materials → properties/characteristics improvement; scalability to an industrial application level
  - Characterization of the newly produced FMs (geometrical characteristics, chemical and phase composition, porosity, density, microstructure, mechanical properties, pebble bed characteristics, interaction with air/steam and tritium release characteristics)
  - Preliminary qualification of the FMs under TBM-relevant operative conditions → design and realization of newly identified tests/experiments (determination of missing properties and characteristics, FMs performance)
  - Evaluation of the performed tests/experiments (e.g. PIE of HIDOBE, HICU campaigns performed under the past EFDA framework) → determination of the FMs properties and characteristics after neutron irradiation
  - Update of the existing materials' properties database (MDBRs & MAR to be used for TBMs design qualification)

17

Ceramic breeder related activities (3/3)

1st Specific Grant of the Framework Partnership Agreement F4E-FPA-380-A3 (IMPLEMENTATION TO BE STARTED)

- Service S2: Post-irradiation examination of specimens from HICU irradiation
  - PIE Plan definition (geometrical characteristics, morphology & microstructure, chemical & phase composition, Li burn-up, mechanical properties, tritium release/retention,…); PIE realization
  - Activity duration: 24 months
- Service S3: Development and characterization of Li-ceramic pebbles/pebble beds
  - Optimization/improvement of OSi pebbles properties and quality for TBM application (MTi phase intro.)
  - Characterization of the newly produced improved OSi pebbles: geometrical characteristics, morphology/microstructure, chemical & phase composition, mechanical properties,…
  - Activity duration: 18 months
- Service S5: Design of irradiation rig for Functional Materials new irradiation test
  - Definition of the new irradiation test objectives/goals & test matrix, specification of the experimental conditions and irradiation requirements
  - Design of the new irradiation rig incl. supporting analyses; preliminary cost and time schedule estimation for the manufacturing, irradiation and PIE
  - Activity duration: 12 months
- Service S6: Update of the existing FMs properties database for CDR
  - In the form of MDBR & MAR
  - Incorporation of available new data (e.g. HICU, PBA, EXOTIC,…)
  - Activity duration: by March-2014

18

FUSION FOR ENERGY

F4E-FPA-380/A3 Specific Grants planning

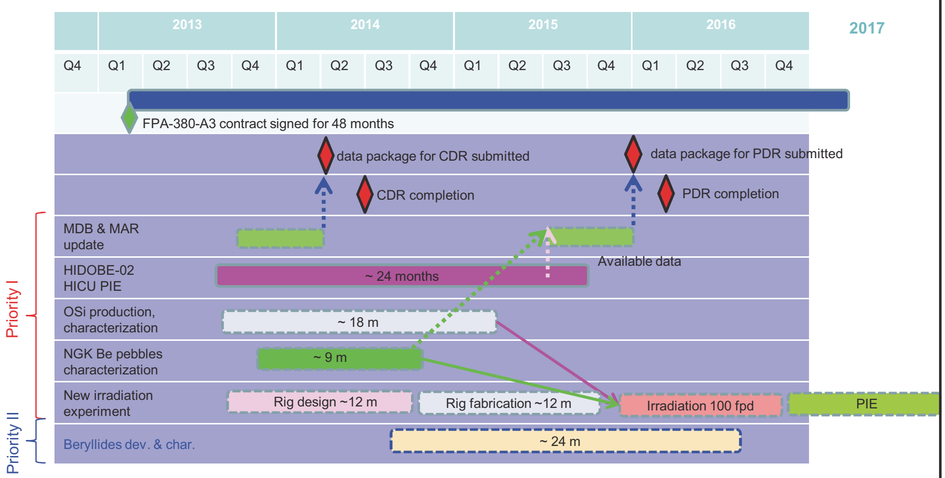

FUSION FOR ENERGY

Ceramic breeder materials - Main R&D Achievements

PIE of OSi & MTi irradiated in PBA & EXOTIC-9/1 campaigns

Optical Microscopy

OSi

before irradiation

PBA #1 T_{irr} = 600 C

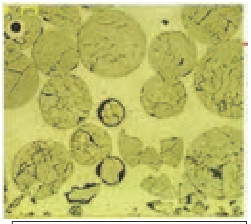

PBA #4 T_{irr} = 750 C

MTi

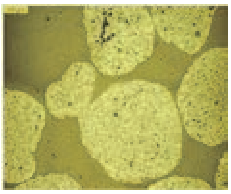

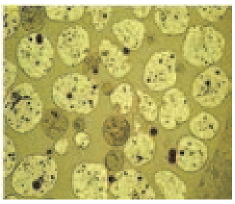

EXOTIC-9/1 T_{irr} = 500 C

OSi
Crack along grain boundaries
Fragmentation
MTi
High internal porosity

NRG

Tritium release from OSi & MTi irradiated at PBA & EXOTIC-9/1

On-line tritium release measurements

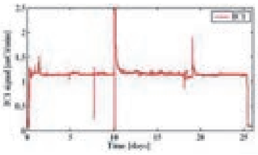

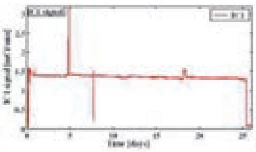

MTi (PBA #2)
700-740 C

OSi (PBA #4)
750-770 C

MTi and OSi exhibit a similar behavior

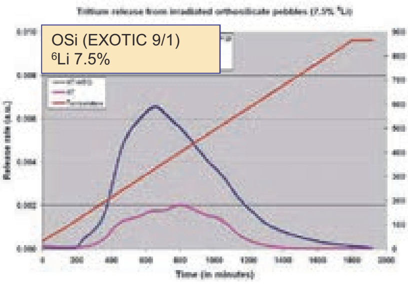

Out of pile Tritium release (TPD)

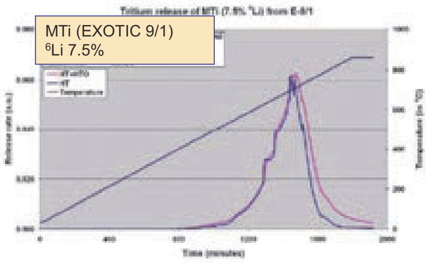

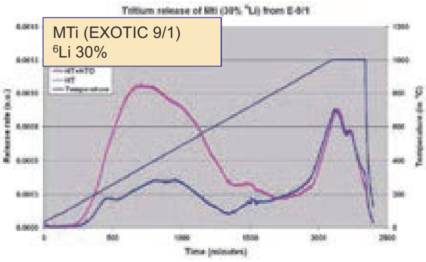

NRG

HICU irradiation program & PIE

Irr. Exp.	Irradiation duration: Runtime	Cycles	FPD	(nominal) Pebble bed Temperature range	Target (range): foreseen	achieved	
HICU	2-2008 – 11-2010	15	440	650- 850	2.2 - 5.7	2.7 - 7.6 *	dpa/%BU

* need confirmation from metrology

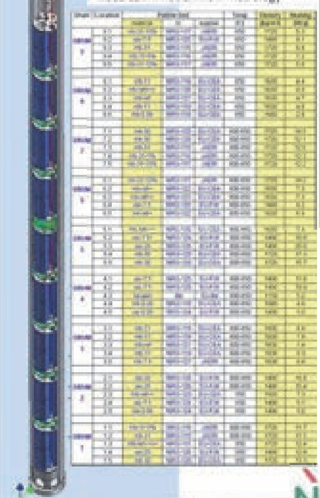

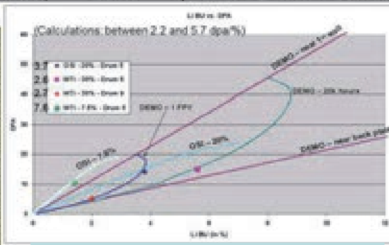

Neutron displacement damage versus Li burn-up with respect to DEMO representative dpa/burn-up values

Post Irradiation Examination:
(PIE planned for 2013-15)
- Geometrical characteristics
- Open/closed porosity, density
- Morphology & microstructure
- Chemical & phase composition
- Li burn-up level and 6Li/7Li ratio
- Tritium residence time
- Mechanical properties
- Interaction with EUROFER

HICU Objectives :
To perform irradiation tests and to study irradiation behaviour of different types of Li ceramic materials (OSi & MTi) at high neutron fluence and Li burn-up.

9 drums with CB samples at 800-850ºC and 600-650ºC.

4 different types of lithium OSi pebbles from KIT, 4 types of MTi from JAEA and 8 types of MTi from CEA. In total 44 different irradiated samples available.

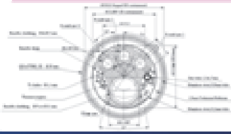

NRG

23

Fabrication of Advanced Tritium Breeder

Modified melt-based process to achieve:
- a controlled droplet generation
- a high yield
- a high crush load
- a low porosity
- a close process control
- LiOH, SiO_2 and TiO_2 as a raw material → formation of two- or three-phase breeder pebbles Li_4SiO_4, (Li_2SiO_3) and Li_2TiO_3

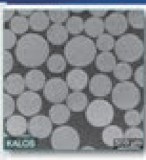

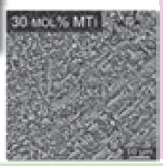

- The fabricated two-phase pebbles exhibit a fine-grained microstructure and increased crush loads.
- The optimum MTi content has yet to be evaluated.

The closed porosity increases with increasing Li2TiO3 content

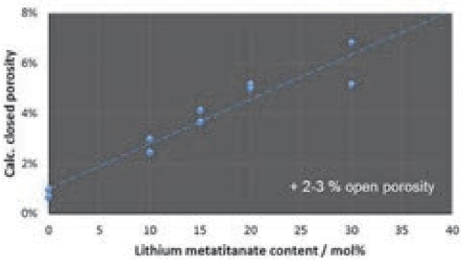

The addition of metatitanate has a strong effect on the crush load

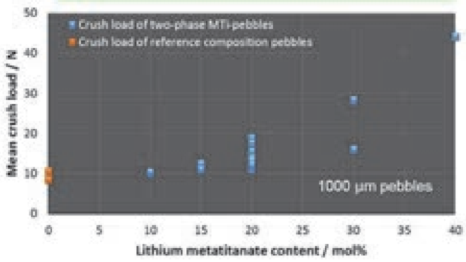

24

Summary

- **Ceramic breeder materials**
  - At present, two ceramic breeder materials available, OSi (reference) and MTi (back-up); minor differences in certain physical parameters but no critical issue exists
  - Further development of two-phase CB pebbles may have the potential to combine the advantages of both, lithium OSi and MTi breeder ceramics
  - HICU irradiation results → an important milestone for the characterization & qualification of the CB materials; a new irradiation experiment foreseen in order to characterize recently developed CB
  - Further development and qualification of the ceramic breeder materials in the view of CDR (07/2014) and PDR (03/2016) with ITER IO
  - Update of MDBR and MAR
  - Later on, finalization of the Technical Specification for Functional Materials (incl. CB pebbles) procurement
  - Procurement and supply of Functional Materials (incl. CB pebbles) for TBM prototypical mock-up (2016-17) and for the 1st EM-TBM (2019-20)

25

Initial design and test of the tritium breeder monitoring system for the Test Breeder Module of the ITER

V.Kapyshev, I. Danilov, I. Kartashev, V.Kovalenko, Yu.Strebkov, and N. Vladimirova

Federal State Unitary Enterprise "Dollezhal Research and Development Institute of Power Engineering", PO Box 788, Moscow 101000, Russian Federation

Demonstration of a tritium breeder is a goal of an ITER mission. A concept of experimental estimation of the tritium-breeding dynamics in test breeder module (TBM) of the ITER has been developed. A system for the experimental estimation of the values is based on tritium breeder and neutron flux measurements under ITER plasma D-T experiments and the use of lithium solid breeder sensors and the neutron detectors. A design of a container with the sensors and detectors is presented. Neutron calculation is performed to estimate the tritium content in the samples under reactor irradiation. The container model with the samples was proposed to test on the nuclear reactor IVV2-M. The post-irradiation results of the tritium measurements in the solid breeder sensors and an activation of the neutron detectors are discussed.

For delivery/withdrawal of the containers into/from the TBM a pneumatic concept is suggested with use a monitor channel connecting the TBM and an operating zone for conveying of the containers in the TBM before a pulse and extraction after the pulse. The laboratory facility for investigation of the pneumatic parameters and the container move in the channel is proposed. Results of the container move parameter measurements are discussed.

НИКИЭТ им.Н.А.Доллежаля

N.A.DOLLEZHAL RESEARCH AND DEVELOPMENT INSTITUTE OF POWER ENGINEERING (NIKIET)

Initial design and test of the tritium breeder monitoring system for the Test Breeder Module of the ITER

presented V.K. Kapyshev

17th IEA International Workshop: Ceramic Breeder Blanket Interactions (CBBI-17)
Barcelona, 12-14 September 2013

OUTLINE

1. Tritium Breeding Ratio (TBR) monitoring for TBM ITER
2. Out-pile activity for Tritium Breeder Monitoring
3. Laboratory device for researches of pneumatic method
4. R&D

Problem of TBR Measurement

TBR = Qr / Qpl

Q_r – *tritium amount breaded in reactor blanket and plasma*

Q_{pl} - *tritium amount burned-up in plasma*.

Error (Δ) of TBR measurement is:

$$\Delta_{TBR} = \Delta Q_r + \Delta Q_{pl}$$

The most accuracy measurements can be done in case of sample location in TBZ for a plasma pulse and follow remove of its from TBZ after the pulse, delivery to an analytical laboratory for analyzing.

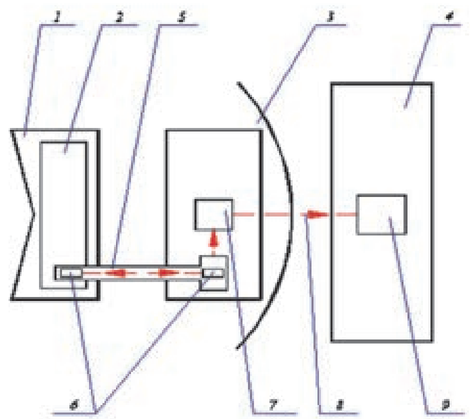

Fig. 1- Diagram of the TBMS in the ITER

1-TBM, 2- TBZ, 3-reactor building, 4-Tririum Plant, 5-TMC, 6- casks with samples, 7-transporter cask, 8-transport way, 9-tritium laboratory

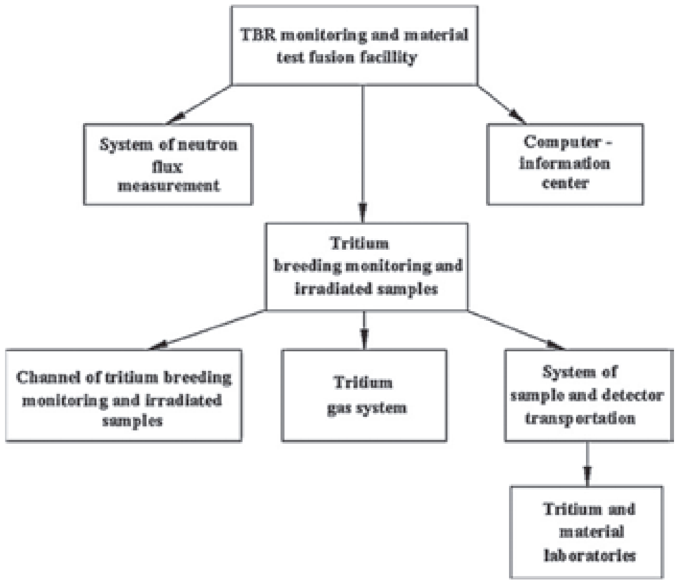

Fig. 2. Conceptual diagram of the TBR monitoring in a fusion reactor

Design of Pneumatic Tritium Breeding Channel (TBC)

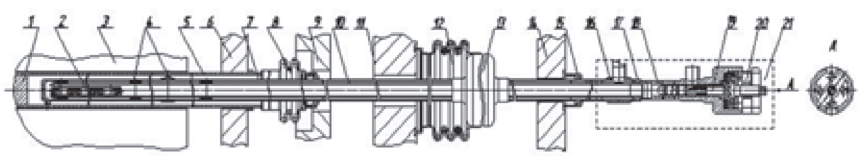

Fig. 3. Longitudinal section of TBC

1-plug, 2-container, 3-eutectic, 4-separation elements, 5-rib of TBM case, 6-back plate of TBM case, 7-out side of channel pipe, 8-bellow, 9-frame, 10-inner pipe of channel, 11-shield plug, 12-armored bellows, 13-heat shield, 14-biological shield, 15-fastening unit of channel,16-union, 17-adapter, 18-load chamber, 19-fingered bushing, 20-bolt, 21-transporter.

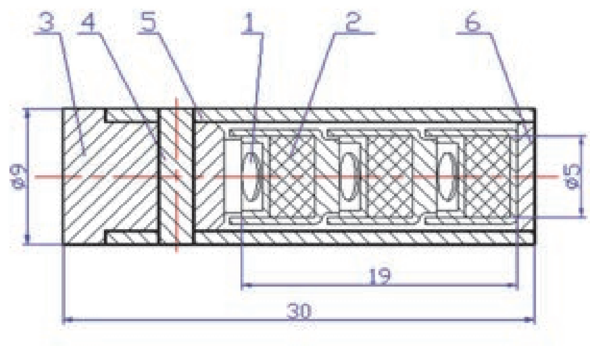

Fig. 4. Location of capsules with material samples in the cask

1- neutron detector, 2- material sample, 1-container, 2- capsule, 3- plug, 4- shift, 5-container, 6- end plug

Table 1. Content of the samples in the capsules

№ cask	Tritium breeder material	Isotope ratio(^6Li / ^7Li) for Li_2CO_3
1	Co	
2	ceramic/Li_2CO_3	natural
3	Co	
4	ceramic/Li_2CO_3	~ 1
5	Co	
6	ceramic/Li_2CO_3	~ 9

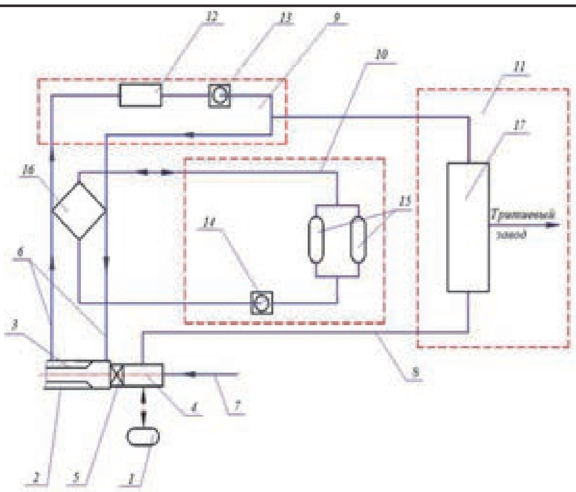

Fig. 5 Conceptual diagram of the tritium-breeder monitoring system with a closed gas circulator.

1- cask, 2- out-side wall of the TMC, 3- inner side of the TMC, 4,- load chamber, 5- channel valve, 6- technology valves, 7- air pipe, 8- tritium pipe, 9- first technology loop, 10- second technology loop , 11- third technology loop, 12- heat exchanger, 13- circulator pump, 14-compressor, 15- tanks, 16- gas flow commutate, 17- tritium technology system of the TBMS

Fig. 6. Lead-Lithium cooled Ceramic Breeder (LLCB) module of the ITER.

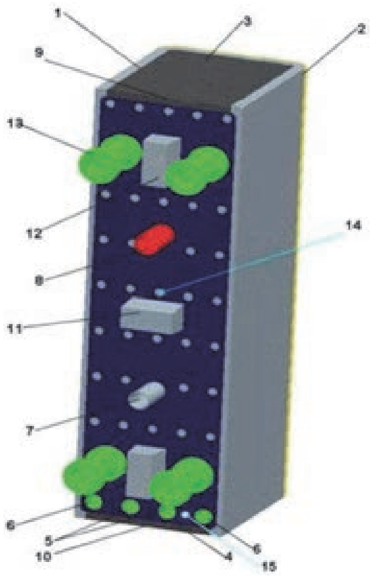

1 - FW cramp; 2 - Be-armour; 3 - upper lid of the TBM casing; 4 - lower lid of the TBM casing; 5 - PbLi inlet branch pipes;

6 - PbLi outlet branch pipes; 7 - He coolant inlet branch pipe; 8 - He coolant outlet branch pipe; 9 - purge gas inlet branch-pipe; 10 - purge gas outlet branch pipe; 11 - toroidal shear key; 12 - poloidal shear key; 13 - flexible cartridge; 14 – hypothetical tritium breeder monitoring canals; 15 – site of TMC

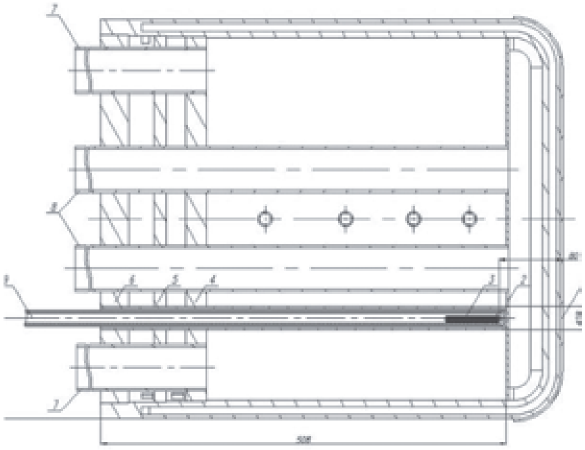

Fig. 7 – Location of the TMC in the LLCB TBM.
1 – first wall; 2 - division walls in an eutectic flow; 3 - cask; 4,5 – division walls; 6 – back plate of the TBM; 7 - PbLi inlet branch pipes; 8 - PbLi outlet branc pipes; 9 - TMC

Table 2 – Specific rate of tritium production, 1/(cm^3·s) and tritium activity (Bq/s) in the CMTB

Capsule number	Specific rate of tritium production	Activity (Bq/s/pellet)
1-st position		
1-st capsule	4,39E+11	4,6E+01
2-nd capsule	1,57E+12	1,60E+02
3-rd capsule	2,85E+12	3,00E+02
2-nd position		
1-st capsule	1,06E+10	1,2E+01
2-nd capsule	5,41E+10	3,4E+01
3-rd capsule	9,50E+10	7,0E+01
3-rd position (1-st cask)		
1-st capsule	4,82E+09	3,6E+00
2-nd capsule	2,85E+10	3,9E+01
3-rd capsule	5,08E+10	7,5E+01

Fig. 8. The reactor assemble for cask irradiation in the nuclear reactor

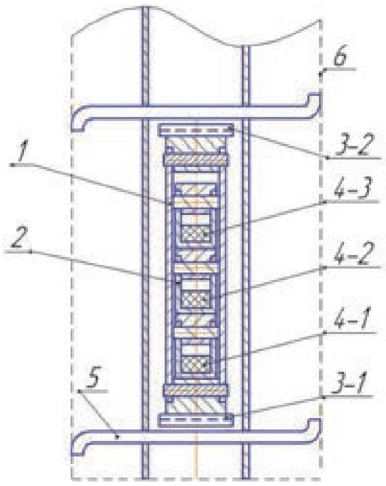

1 – mock-up of the cask, 2 – the capsule with lithium carbonate pellet, 3-1, 3-2 – thermal neutron detectors (Co) in alumina allow, 4-1, 4-2, 4-3 – the lithium carbonate pellets, 5 – spacer, 6 – reactor channel.

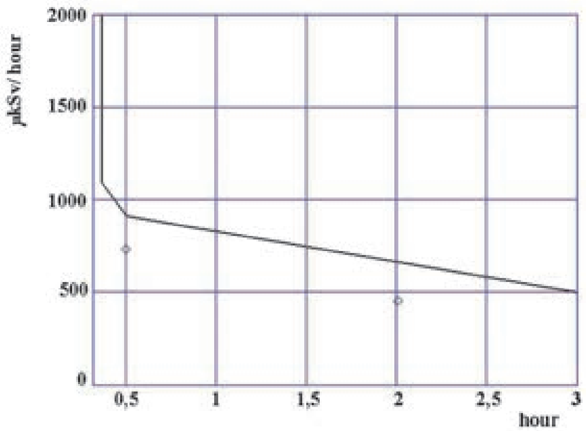

Fig. 9 – Time dependence of radiation dose at 10 cm distance from the reactor assemble

Table 3 - Container dose exposure (μGy/hour) to 10 cm distance from container

Container material	Time of exposure, min				
	0	1	10	30	60
Allow АД31	$2.2 \cdot 10^5$	$1.4 \cdot 10^4$	772	139	91
Allow АД1	$2.2 \cdot 10^5$	$1.4 \cdot 10^4$	639	6.9	0.45

Table 4 - Radioactivity of the Co-detector

Detector number*	weight, мг	Radio-activity Bq	Neutron flux, n/(см^2·s) $\times 10^{-12}$
3-1	27.5	4231	1,254
3-2	27.6	4244	1,253
3-3	23.9	2968	0,879

*Detector number corresponds to Fig. 8

Table 5 – Measurement and calculation tritium radioactivity in the irradiated pellets

Comment 1): 1 – Verzilov's dissolution method, 2 – Dierckx' dissolution method

№ pellet	Method 1)	Tritium radioactivity, Bq		Calculation radioactivity A_{calc}, Bq	(A-Acl)/Acl	(B-Acl)/Acl
		measurement A	Average B		%	%
4-1	1	12658 11917 11125	11900	13420	-11	17
4-3	2	13398 14932	14165		+6	11

Development and test of Tritium Breeding Ratio (TBR) system monitoring (pneumatic)

Development of nuclear reactor facility for TBR system monitoring test (T=200°C, neutron flux ~ 2*10^{14} n/sm^2, t (neutron irradiation)~10min)

Table 6 – Parameters of the CMTB mock-up.

Parameter	Value
Length, m	8
Diameter of the inner transport cask pipe, mm	12
Diameter of the outside pipe, mm	30
Maximum pressure, MPa	1
Temperature of the channel active part, ºC	600
Piped gas for pressure at the channel entrance, 0,5 MPa, m^3/h	21

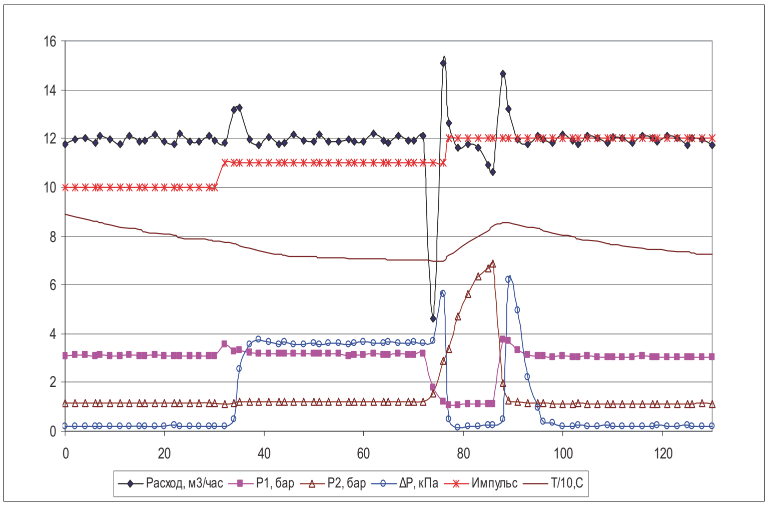

Fig 11. Measurement of pneumatic parameters under container move

Conclusion

1. The design of the sample systems for the tritium breeding monitoring by the irradiation of the samples has been proposed for ITER.

2. The neutron calculations performed for simulating the LLCB TBM show that the tritium breed in the lithium carbonate samples can be measured with the accuracy 7%.

3. At present stage of a measurement accuracy investigation of the tritium content in the carbonate samples irradiated in the LCCB TBM by neutrons during one plasma pulse can approach 17% for all process tritium measurement.

4. The mock-up of the channel system has been fabricated to test of the pneumatic method at the reactor IVV-2M for delivery of the casks to the TBZ of the TBM.

5. The developed nuclear reactor assemble offers an opportunity of a tritium breed simulation under a reactor neutron irradiation and measurement of the tritium content in the irradiated samples.

6. The reactor assemble was irradiated in the reactor IVV-2M during 80 s. After irradiation the doses of γ – irradiation of the container, Co- detector radioactivity and tritium content in the pellets were measured. Manual operations with the casks is possibly after 60 min after the reactor irradiation.

R&D

1. Reactor devices for investigation of pneumatic systems

2. Selection and irradiation of neutron detectors in IVV-2M nuclear reactor

3. Irradiation of the cask and capsule in nuclear reactor IVV-2M

Current Status of Design and Accident Analysis for Korean HCCR TBS

Mu-Young Ahn[1], Seungyon Cho[1], Dong Won Lee[2], Hyung Gon Jin[2],
Eo Hwak Lee[2], Cheol Woo Lee[2], Duck Young Ku[1], Yi-Hyun Park[1], Chang-Shuk Kim[1]

[1]*National Fusion Research Institute, Daejeon, Republic of Korea*
[2]*Korea Atomic Energy Research Institute, Daejeon, Republic of Korea*

Recently Korea has decided to test Helium Cooled Ceramic Reflector (HCCR) Test Blanket Module (TBM) in ITER and design of the TBM with its ancillary systems, i.e. Test Blanket System (TBS), is under progress. Since the TBM is operated at elevated temperature with high heat load, safety consideration is essential in design procedure. In this paper, current status of the HCCR TBS design is briefly introduced and then preliminary accident analysis results on selected scenarios are presented as an important part of safety assessments. To simulate transient thermo-hydraulic behavior, GAMMA-FR code which has been developed in Korea for fusion applications was used. The main cooling and tritium extraction circuit systems, as well as the TBM, were simulated and the main components in the TBS were modeled as the associated heat structures. The important accident scenarios were produced and summarized in the paper considering the HCCR TBS design and ITER conditions, which cover in-vessel Loss Of Coolant Accident (LOCA), in-box LOCA, ex-vessel LOCA, Loss Of Flow Accident (LOFA) and Loss Of heat Sink Accident (LOSA). The accident analysis based on the selected scenarios was performed and it was found that the current design of the HCCR TBS meets the thermo-hydraulic safety requirements while it is envisaged to need more precise model for some components such as circulator, cooler, etc. for future works.

17th IEA International Workshop :
Ceramic Breeder Blanket Interactions (CBBI-17)
Barcelona, Spain, 12 - 14 Sep. 2013

Current Status of Design & Accident Analysis for Korean HCCR TBS

Mu-Young Ahn[1], Seungyon Cho[1], Dong Won Lee[2], Hyung Gon Jin[2], Eo Hwak Lee[2], Cheol Woo Lee[2], Duck Young Ku[1], Yi-Hyun Park[1], Chang-Shuk Kim[1], Youngmin Lee[1]

[1] National Fusion Research Institute, Daejeon, Korea
[2] Korea Atomic Energy Research Institute, Daejeon, Korea

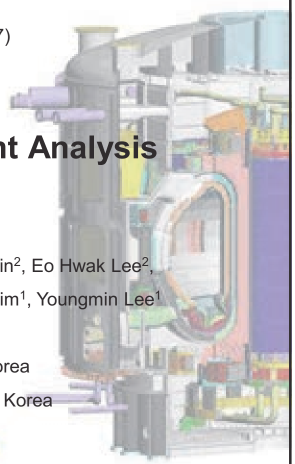

Contents

- HCCR TBS Design
- Accident Analysis
- Summary

HCCR TBS schematic

- Helium Cooled Ceramic Reflector (HCCR) TBS
  - TBM
    - Solid type with helium coolant
    - Graphite reflector adopted to reduce amount of beryllium multiplier
  - Ancillary systems
    - Helium Cooling System (HCS), Coolant Purification System (CPS), Tritium Extraction System (TES), etc

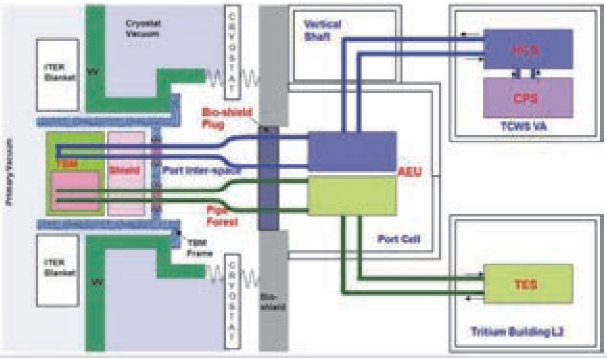

TBM design (1)

- Current TBM design
  - 4 sub-modules
  - Main components with First Wall (FW), Breeding Zone (BZ), Side Wall (SW), Back Manifold (BM)

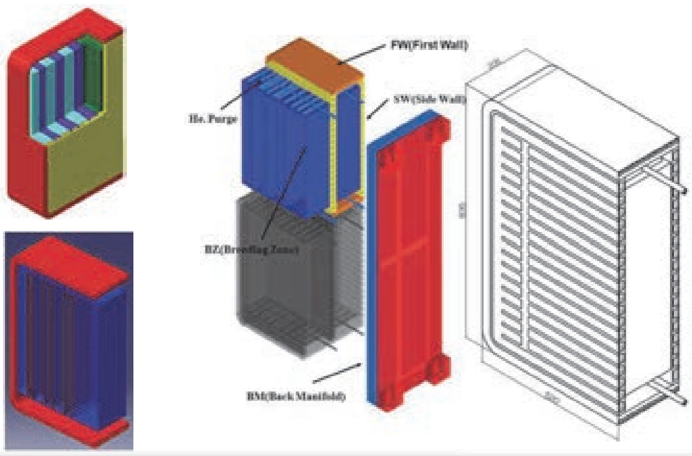

TBM design (2)

- Nuclear analysis
  - Neutronics with MCNP5 & FENDL 2.1
    - Detailed tally regions in the radial direction for more realistic TH calculation

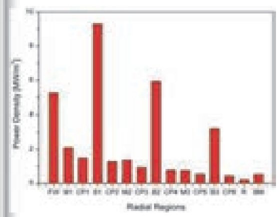

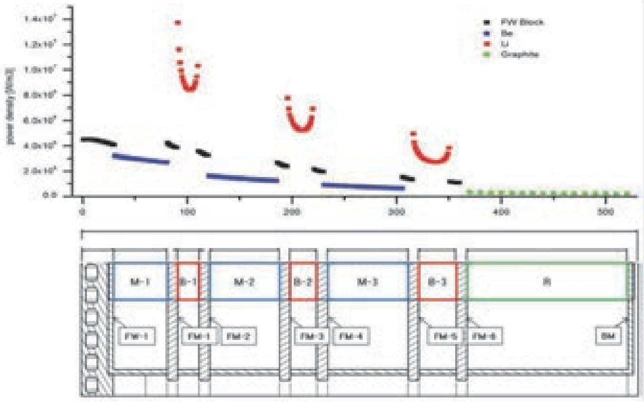

TBM design (3)

- Nuclear analysis
  - Activation analysis performed with global model based on B-lite
    - B-lite modified with two HCCR TBM-Sets, dog-legs, PF, bio-shield, AEU, etc
    - SA2 scenario for irradiation history

Total activity of HCCR TBM

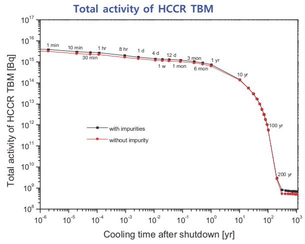

Total activities of the pipes in the port inter-space & port cell

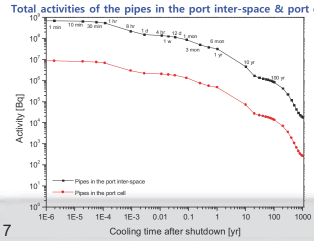

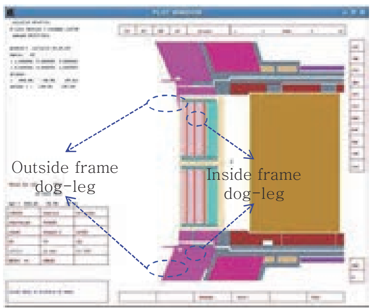

Shutdown dose rate after 12 days in the port inter-space & port cell

Region	Through equatorial port and upper & lower port	Through only equatorial port without upper & lower port
Port inter-space	2.58E+2 μSv/hr	8.93E+01 μSv/hr
Port cell	2.42E+0 μSv/hr	Not performed yet

TBM design (4)

- Thermo-hydraulic analysis
  - TH analysis performed for FW+BZ with updated neutronics data
  - Temperature distribution is in overall below the limit while still minor geometric changes might be needed for the BZ

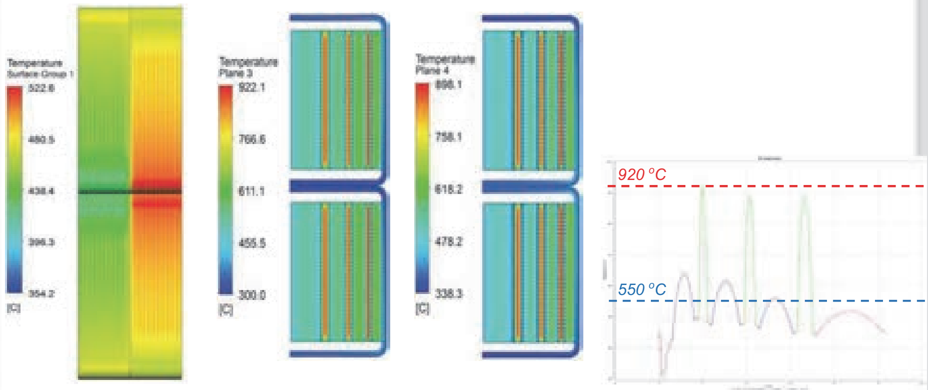

Group A Group B Group A Group B

CBBI-17 6 KOREA DOMESTIC AGENCY

TBM design (5)

- Structural & thermo-mechanical analysis
  - Analysis performed for FW & SW, respectively

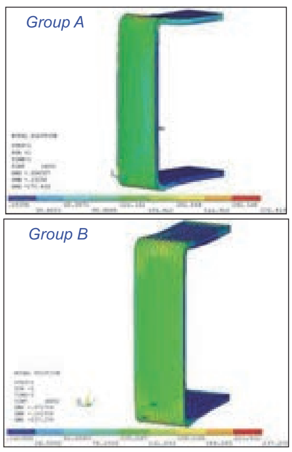

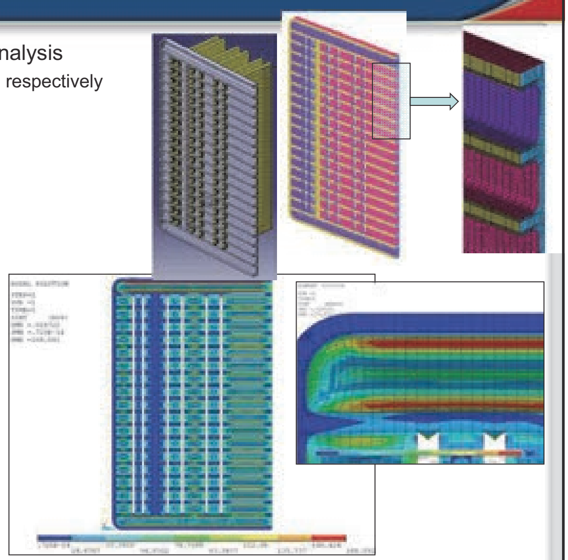

Sum of primary & secondary stress < 3 Sm

Primary stress due to internal pressurization < 1.5 Sm

CBBI-17 7 KOREA DOMESTIC AGENCY

TBM design (6)

- Flow analysis
  - Various options are being explored for flow distribution in manifolds
    - Not only performance such as equal distribution, low pressure drop, etc, but also manufacturing feasibility should be taken into account

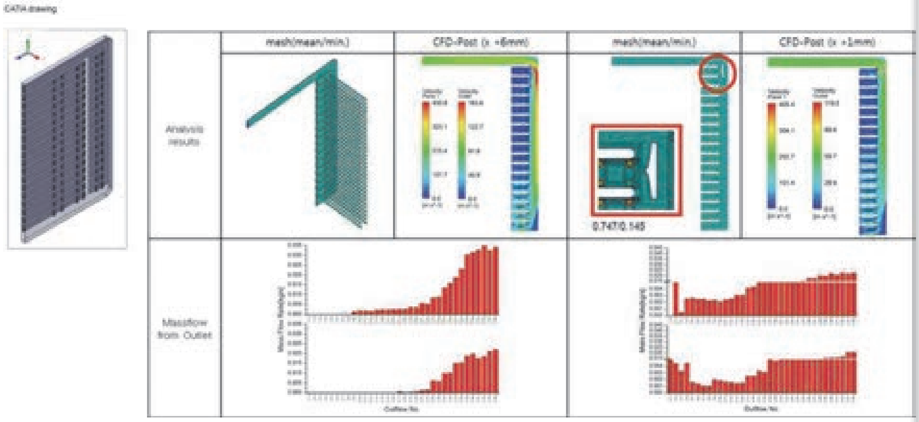

TBM design (7)

- Flow analysis
  - Various options are being explored for flow distribution in manifolds
    - Not only performance such as equal distribution, low pressure drop, etc, but also manufacturing feasibility should be taken into account

Cases	BM to FW (ZX plane)	Interface (BM, FW)	YZ plane	Velocity and Mass flow (1.14kg/s all ch.)	ΔP(kPa)
case00	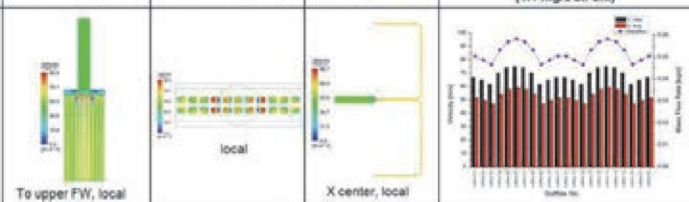 To upper FW, local	local	X center, local		40.627
case03	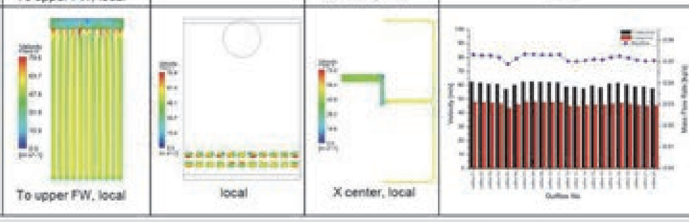 To upper FW, local	local	X center, local		38.568

TBM design (8)

- EM analysis started
  - 20 degree sector modeling for ANSYS
  - DINA input for the plasma and magnet currents
  - Plasma disruption scenario : downward major disruption with 16ms exp. decay

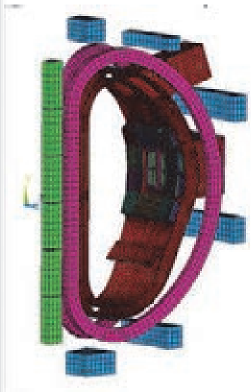

EM global model

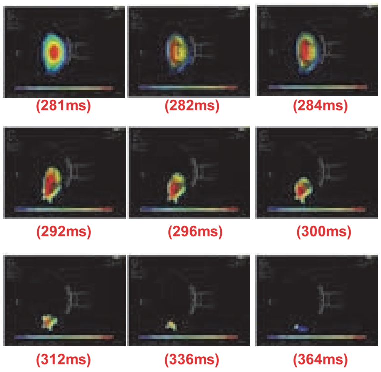

Plasma current distribution applied during plasma disruption

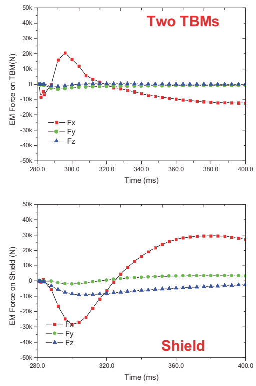

EM Force

HCS & CPS design (1)

- Helium Cooling System
  - Helium flow conditions: 1.15 kg/s, 8 MPa, 300℃ (@HCCR inlet)
  - Main components
    - Helium Circulator (Pressure ratio = more than 1.1)
    - Recuperator (PCHE type, η=0.92)
    - Helium Pre-heater (500 kW)

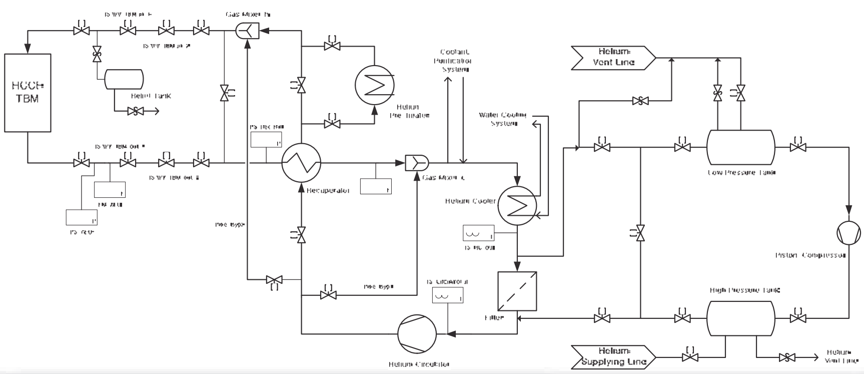

HCS & CPS design (2)

- Coolant Purification System
  - Sampling rate: 11.5 g/s (1% of HCS flow rate)
  - Main components
    - Catalytic Oxidizer (CuO, Cu2O)
    - Molecular Sieve Beds (5A zeolite)

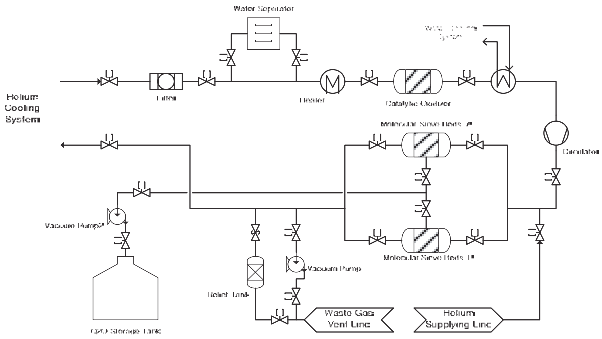

HCS & CPS design (3)

- Preliminary HCS+CPS arrangement
  - Space allocation in TCWS Vault Annex in L4 of Tritium Building

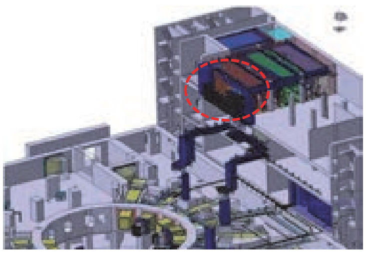

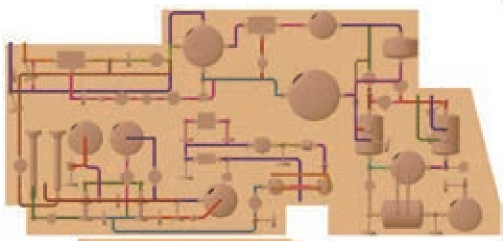

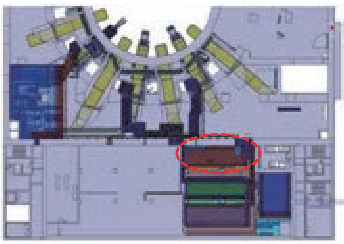

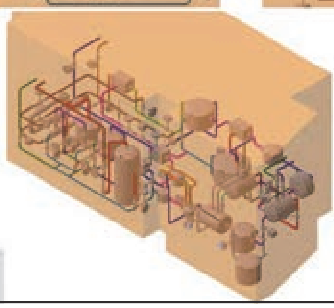

TES design (1)

- Tritium Extraction System
  - Purge gas conditions: 101 kPa He with 0.1% H_2 (> 0.1 g/s)
  - Main components
    - RT & Cryogenic Molecular Sieve Beds (5A zeolite)
    - Circulator, diffuser, filters, valves, et

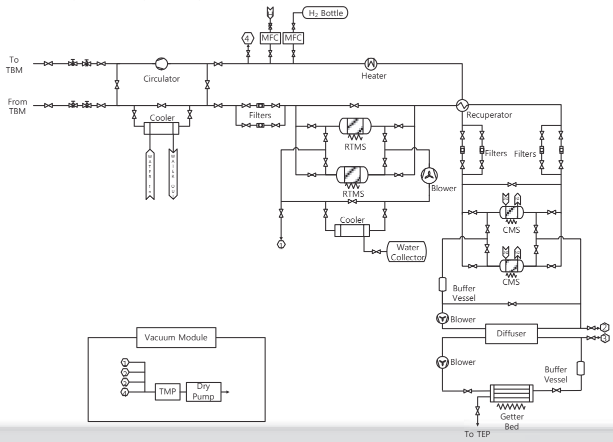

TES design (2)

- Preliminary TES arrangement
  - Space allocation in L2 of Tritium Building

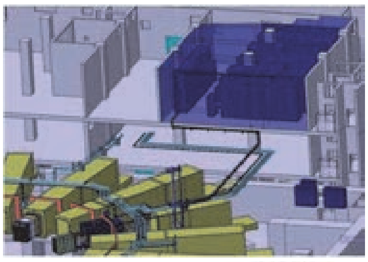

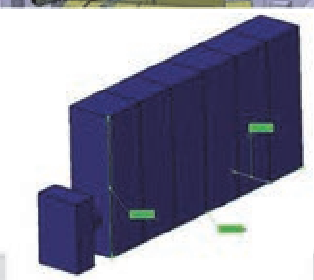

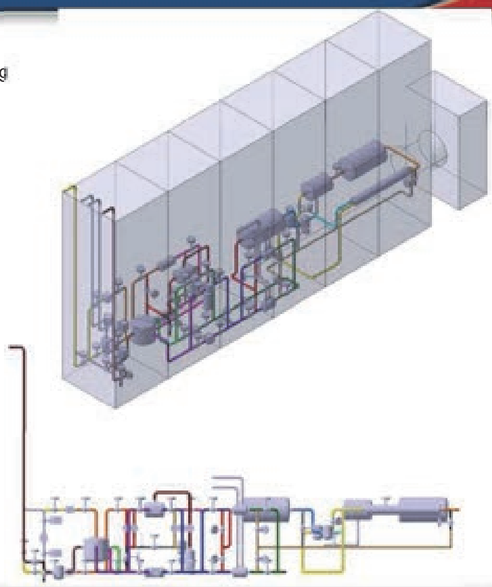

Contents

- HCCR TBS Design
- Accident Analysis
- Summary

CBBI-17 16 KOREA DOMESTIC AGENCY

Objectives

- Safety consideration is essential in HCCR TBS design procedure
  - HCCR TBS is operated at elevated temperature with high-pressure helium coolant
  - HCCR TBS should not adversely affect the safety, reliability and availability of ITER machine
- As an essential part of PrSR, accident analysis has been performed on the HCCR TBS
  - To investigate safety features of the HCCR TBS during accidental conditions
  - To demonstrate that the HCCR TBS is designed to follow the safety requirements and guidelines of ITER

CBBI-17 17 KOREA DOMESTIC AGENCY

Reference accidents (1)

- Total 9 reference accidents were derived from FMEA

Accident #	Initiating Event	Accident Description
Reference Accident 1	In-vessel LOCA (ivc)	This accident is initiated by **one or multiple rupture of TBM FW cooling channels**, causing a **plasma disruption and pressurization of VV.** At the same time, it is postulated that the site electrical power supply is lost at the beginning of the event for up to 32 hours.
Reference Accident 2	In-box LOCA (ibc)	This accident starts with **rupture of cooling plates in the Breeding Zone** (BZ) pressurizing the BZ box structure, thus subsequent **pressurization of the Tritium Extraction System** (TES). When the accident detected, PSS isolates the HCS & TES and requests **Plasma Shutdown** to FPSS. TBM FW channels might break but there is **neither box structure failure nor spill of pebbles**.
Reference Accident 3	Ex-vessel LOCA (xvc)	This accident is initiated by **rupture of TBM coolant pipe in Port Interspace or Port Cell**, causing **radioactive release and pressurization in Port Interspace and Port Cell**. When the accident detected, PSS isolates the HCS and requests **Plasma Shutdown** to FPSS. TBM FW channels might break but there is **neither box structure failure nor spill of pebbles**.
Reference Accident 4	Ex-vessel LOCA (xvc)	This accident is initiated by **rupture of TBM coolant pipe in TCWS VA** where major components of HCS are located, causing **radioactive release and pressurization in TCWS VA**. When the accident detected, PSS isolates the HCS and requests **Plasma Shutdown** to FPSS. TBM FW channels might break but there is **neither box structure failure nor spill of pebbles**.

Reference accidents (2)

- Total 9 reference accidents were derived from FMEA

Accident #	Initiating Event	Accident Description
Reference Accident 5	LOFA (lfc)	This accident is a **loss of flow caused by failure of cooling circuit circulator** leading to a temperature excursion of the TBM FW and pressurization of the coolant in the TBM FW. When the accident detected, PSS (isolates the HCS and) requests **Plasma Shutdown** to FPSS. TBM FW channels might break but there is **neither box structure failure nor spill of pebbles**.
Reference Accident 6	LOHSA (hb)	This accident is a **loss of heat sink caused by housing rupture of cooling circuit heat exchanger**, leading to a temperature excursion of the TBM FW due to heat sink loss and pressurization of the coolant in the TBM FW. When the accident detected, PSS (isolates the HCS and) requests **Plasma Shutdown** to FPSS. TBM FW channels might break but there is **neither box structure failure nor spill of pebbles**.
Reference Accident 7	TES pipe rupture in PC (xvg)	This accident is initiated by **purge pipe rupture at upstream position of the TES circulator inside port cell**. Due to suction pressure, air ingress with moisture discharges to TBM Breeding Zone followed by **reaction with beryllium and graphite**.
Reference Accident 8	Accidents in Tritium System Room (xvg)	Accidents include rupture of TES components inside or outside of Glove Box in Tritium Building. These are considered to be enveloped in general Tritium Systems accident analysis.
Reference Accident 9	Accidents in Hot Cell	Accidents include radioactive release in Hot Cell by dropping of TBM, etc. These are considered to be enveloped in general Hot Cell accident analysis

Safety Function

- Safety function of the HCCR TBS
  - Two Plant Safety Systems (PSSs) exist for redundancy
  - PSS is activated based on 2 out of 3 logic, i.e., two safety devices among three of them detecting accidental conditions
  - Then safety function is activated accordingly

Accidents	Actuating Signal	Action
In-vessel LOCA	NA	NA
In-box LOCA	$p_{\_TES}$ > 0.4 MPa (TBD)	PSS isolates HCS & TES loops PSS sends plasma-off request to CSS
Ex-vessel LOCA	$p_{\_HCS}$ < 4 MPa (TBD)	PSS isolates HCS loop PSS sends plasma-off request to CSS
LOFA	Flow-rate$_{_HCS}$ < 50% of initial (TBD)	PSS isolates HCS loop PSS sends plasma-off request to CSS
LOHSA	60% of $dT_{\_nominal}$ at HX (TBD)	PSS isolates HCS loop PSS sends plasma-off request to CSS
TES pipe rupture in PC	TBD	TBD

Modeling (1)

- GAMMA-FR code was used to simulate transient behavior of the TBS during accidents
  - GAMMA is a KO domestic code mainly used for High Temperature Gas Cooled Reactor
  - GAMMA-FR has been developed for fusion applications to predict thermo-hydraulic and chemical reaction phenomena during thermo-fluid transients

- Fluid transport and material properties
- Multi-dimensional heat conduction
- Multi-dimensional fluid flow
- Chemical reactions for graphite oxidation
- Multi-component molecular diffusion
- Radiation heat transfer
- Critical flow for blow-down phase

Modeling (2)

- HCCR TBS was nodalized
  - Each TBM sub-module was modeled with 15 layers of heat structure and cooling channels
  - To deal with one sided heat load from the plasma, 3D wall model with McEligot correlation is adopted
  - Main components of the HCS & TES were modeled
  - For simulation of accidents, corresponding volumes were added

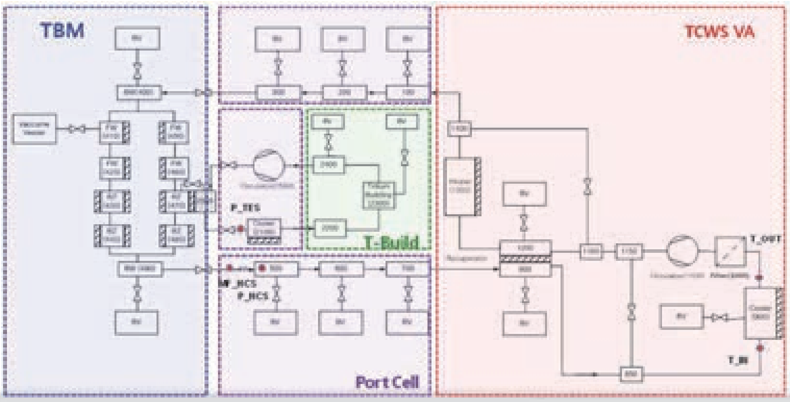

In-vessel LOCA (1)

- Event sequence

Parameter	Specification
Definition of initiating event	1. Double-ended break of a FW coolant channel
Transient sequence	2. Plasma disruption (t=0) 3. LOOP (t=0) 4. 100% volume & surface power with additional disruption load 0.3 GW/m2 (until t=0.001) 5. 100% volume & surface power with additional disruption load 0.3 MW/m2 (until t=1.001) 6. Decay heat cooled only by radiation heat transfer (t>1.001)
Aggravating failures	- None
Loss of power	- A 32 hour loss of off-site power is assumed
Parameter studies	- Hypothetical Accident: Event is further aggravated by complete damage of the TBM FW and ITER FW by disruption, as a common cause failure, thus spill of helium coolant of the TBM and water coolant of ITER Shield Blanket into VV. However, Breeding Zone (BZ) box structure which contains the functional pebbles inside is not assumed to fail.

In-vessel LOCA (2)

- Results
  - The maximum pressure in VV reaches 15.9 kPa (< 200 kPa) at t=71 s
  - The helium spill into VV is 20.7 kg (< 45 kg)
  - The maximum temperature of the FW reaches 572.7 °C at t=1.0 s and then decreases

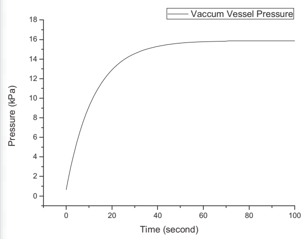

Pressure transient in VV

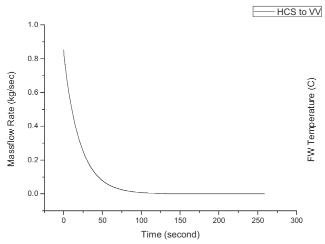

He ingress to VV

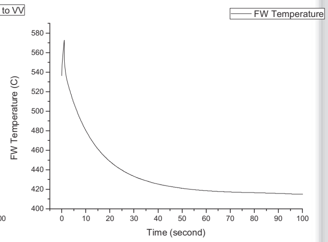

Temperature transient in FW

In-box LOCA (1)

- Event sequence

Parameter	Specification
Definition of initiating event	1. Double-ended break of a coolant pipe in BZ
Possible transient sequence	2. TBM box & TES pressurized 3. 100% volume & surface power until t=4.5 s when the accident detected 4. HCS & TES isolated 5. FPSS requested and fast plasma shutdown follows at t=7.5 s 6.100% volume & surface power with additional disruption load 0.3 GW/m2until t=7.501 s 7.100% volume & surface power with additional disruption load 0.3 MW/m2 until t=8.501 s 8. Decay heat cooled only by radiation heat transfer (t >8.501 s)
Aggravating failures	- None
Loss of power	- None
Parameter studies	- Hypothetical Accident: Event is further aggravated by failure of FPSS and TBM FW melting causes large plasma disruption, thus complete damage of the ITER FW. Steam from ITER Blankets ingresses to BZ, then reacts with the functional pebbles.

In-box LOCA (2)

- Results
  - The accident is detected at 4.5 s as the TES pressure increases to 0.4 MPa
  - The pressure in TES remains steady at 0.39 MPa (< 0.5 MPa)
  - The temperature of the FW reaches the maximum 626.0 °C at t=8.5 s and then decreases

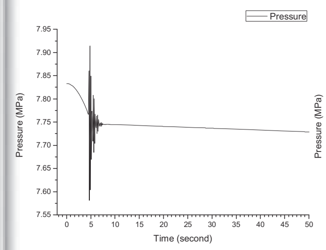

Pressure transient in HCS

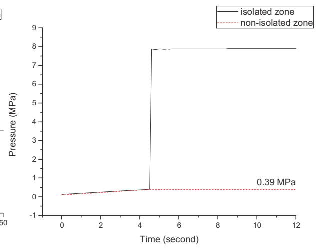

Pressure transient in TES

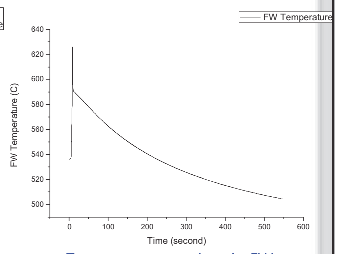

Temperature transient in FW

Ex-vessel LOCA to PI/PC (1)

- Event sequence

Parameter	Specification
Definition of Initiating event	1. Double-ended coolant pipe break inside Port Interspace or Port Cell
Possible transient	2. Port Interspace / Port Cell pressurized 3. Pressure reaches 120 kPa at t=0.1 s and the relief panel opens to TCWS VA 4. 100% volume & surface power until t=0.36 s when detected 5. HCS isolated 6. FPSS requested and fast plasma shutdown follows at t=3.36 s 7.100% volume & surface power with additional disruption load 0.3 GW/m2 until t=3.361 s 8.100% volume & surface power with additional disruption load 0.3 MW/m2 until t=4.361 s 9. Decay heat cooled only by radiation heat transfer (t>4.361)
AF	- None
LOOP	- None
Parameter studies	- Hypothetical Accident: Event is further aggravated by failure of FPSS and TBM FW melting causes large plasma disruption, thus complete damage of the ITER FW. Steam from ITER Blankets ingresses to BZ, then reacts with the functional pebbles.

Ex-vessel LOCA to PI/PC (2)

- Results
  - The accident is detected at 0.4 s as the HCS pressure decreases below 4.0 MPa
  - The maximum pressure of PI/PC is kept below 160 kPa due to the panel opening to TCWS VA
  - The temperature of the FW reaches the maximum 612.6 ^{o}C at t=4.4 s and then decreases

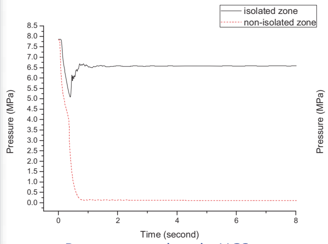

Pressure transient in HCS

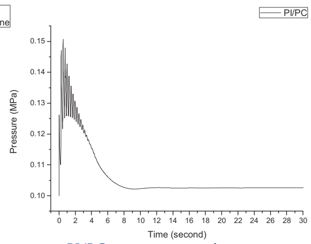

PI/PC pressure transient

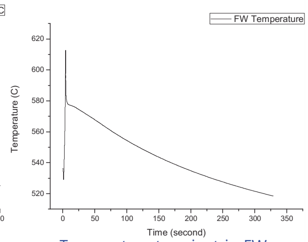

Temperature transient in FW

LOFA (1)

- Event sequence

Parameter	Specification
Definition of initiating event	1. Circulator fails to operate
Possible transient sequence	2. TBM over-heated and pressurized 3. 100% volume & surface power until t=0.1 s when detected 4. HCS isolated 5. FPSS requested and fast plasma shutdown follows at t=3.1 6.100% volume & surface power with additional disruption load 0.3 GW/m2 until t3=3.101 7.100% volume & surface power with additional disruption load 0.3 MW/m2 until t4=4.101 8. Decay heat cooled only by radiation heat transfer (t>4.101)
Aggravating failures	- None
Loss of power	- None
Parameter studies	- Hypothetical Accident: Event is further aggravated by failure of FPSS and TBM FW melting causes large plasma disruption, thus complete damage of the ITER FW. Steam from ITER Blankets ingresses to BZ, then reacts with the functional pebbles.

LOFA (2)

- Results
  - The accident is detected at 0.1 s as the coolant mass flow rate decreases to 50% of initial value
  - Pressurization of the TBM is negligible
  - The temperature of the FW reaches the maximum 626.0 ^{o}C at t=4.1 s and then decreases

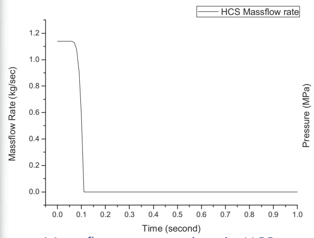

Mass flow rate transient in HCS

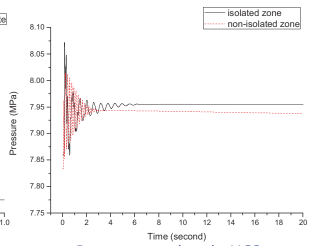

Pressure transient in HCS

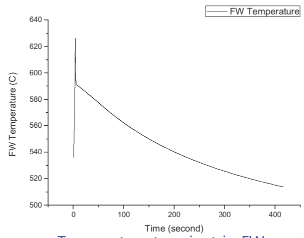

Temperature transient in FW

LOHSA (1)

- Event sequence

Parameter	Specification
Definition of initiating event	1. Shell rupture in HX releasing secondary coolant into TCWS VA
Possible transient sequence	2. TBM over-heated and pressurized 3. 100% volume & surface power until t=1.9 s when detected 4. HCS isolated 5. FPSS requested and fast plasma shutdown follows at t=4.9 6.100% volume & surface power with additional disruption load 0.3 GW/m2 until t3=4.901 7.100% volume & surface power with additional disruption load 0.3 MW/m2 until t4=5.901 8. Decay heat cooled only by radiation heat transfer (t>5.901)
Aggravating failures	- None
Loss of power	- None
Parameter studies	- Hypothetical Accident: Event is further aggravated by failure of FPSS and TBM FW melting causes large plasma disruption, thus complete damage of the ITER FW. Steam from ITER Blankets ingresses to BZ, then reacts with the functional pebbles.

LOHSA (2)

- Results
  - The accident is detected at 1.9 s as the temperature difference before & after the HX decrease to 60% of the nominal condition
  - Pressurization of the TBM is negligible
  - The temperature of the FW reaches the maximum 624.5 ^{o}C at t=5.9 s and then decreases

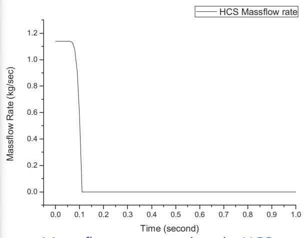

Mass flow rate transient in HCS

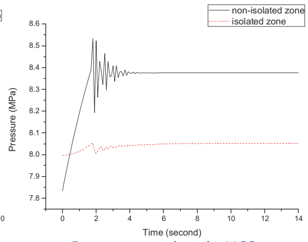

Pressure transient in HCS

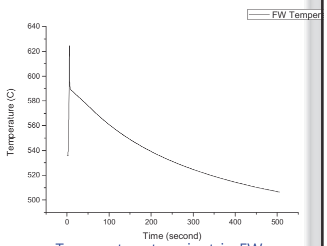

Temperature transient in FW

Contents

Summary

- HCCR TBS design
  - Pre-conceptual design for the TBM components is on-going
  - Various analyses have been performed to demonstrate performance of the TBM
  - PFD and preliminary component arrangement have been prepared for the ancillary systems

- Accident analysis
  - Accident scenarios for the current HCCR TBS design were produced
  - Preliminary accident analysis has been performed for the accidents covering most part of design based accidents
  - It is found that the current design meets the thermo-hydraulic safety requirements

Status of Development of Water Cooled Ceramic Breeder Test Blanket

Mikio Enoeda, Hisashi Tanigawa, Takanori Hirose, Satoshi Sato, Kentaro Ochiai, Chikara Konno, Yoshinori Kawamura, Takumi Hayashi, Toshihiko Yamanishi, Tsuyoshi Hoshino, Masaru Nakamichi, Hiroyasu Tanigawa, Hiroshi Nishi, Satoshi Suzuki, Koichiro Ezato, Yohji Seki, Kenji Yokoyama

Japan Atomic Energy Agency, Naka-shi, Ibaraki-ken, 311-0193 Japan

1. Introduction

Japan Atomic Energy Agency (JAEA) is performing the development of the WCCB blanket as the candidate breeding blanket of Japan. Regarding the TBM development, the engineering R&Ds are ongoing, aiming at the demonstration of fabrication technology and structural integrity of the full size mockup of the WCCB TBM. Regarding the test blanket module fabrication technology development, the real scale back wall mockup was successfully fabricated. Also, the design activities are being performed to show the soundness under various loading conditions of electromagnetic force and thermo-mechanical loading. The evaluation of shutdown dose rate behind the TBM test port is also carried out as one of most important design requirement. Furthermore, key technologies toward DEMO blanket, such as, the development of advanced breeder and multiplier pebbles for DEMO blanket, fabrication technology development of Li rich Li_2TiO_3 pebble and BeTi pebble was performed. Regarding the research activity on the evaluation technology on blanket performance, the experiments of on-line tritium production and recovery using D-T neutron in the Fusion Neutronics Source (FNS) facility has been performed for the purpose of the development of advanced evaluation technology for tritium production performance of DEMO blanket. For the technology development of the tritium behavior simulation in the blanket, the multi-physics and multi-scale integrated tritium performance evaluation code for the breeding blanket has been started and shown the progress. This paper is an overview of recent achievements of blanket development in JAEA.

2. Fabrication technology development for the blanket module by reduced activation ferritic martensitic steel

2.1 Real scale Back Wall mockup fabrication

JAEA has performed the fabrication technology development for the breeding blanket using reduced activation ferritic martensitic steel, F82H [1]. Recently the real scale TBM Back Wall mockup was fabricated by using F82H. Original F82H thick plate with 90 mm thickness with 40 mm share key base part was made by forging. Coolant channels were formed by drilling with the location accuracy of 1mm.

2.2 Cooling pipe penetration through thin plate of breeder box

Inside the blanket module, breeder pebble is contained in the breeder box made by thin plates of F82H. The front and back wall of the breeder box need to have built-in cooling channel for temperature control of the breeder pebble bed. Therefore, the cooling pipes need to penetrate through the top and bottom plate of the breeder box. Fabrication of such sophisticated structure needs careful welding technique. Trial fabrication of such penetration parts was performed by laser welding and TIG welding. For the fabricated mockups by both welding technique, post welding heat treatment was also performed. The final angular deformation of the pipes was within 0.16 degree for both welding technique.

3. Design activity

3.1 Electro-magnetic analysis

Regarding the design of the TBM, primarily the TBM structure is designed to withstand the electro-magnetic force, the internal pressure of coolant and the heat loads of the surface heat flux and volumetric heating by nuclear heating. In the justification of the structural design, load combination will be considered to achieve the possible events during ITER operation. Thus, electro-magnetic analysis was performed to clarify the basic loading conditions due to disruption cases for the future design justification analysis. The modeling was done for 40 m x 40m, 10 degree space including the vacuum vessel, port extension structures, center solenoid and poloidal field coils, shield blankets, TBM's and shields. toroidal magnetic field was simulated by electrical current value. Assumed disruption cases were downward vertical displacement event (VDE) with linear time dependence in 36ms and exponential time dependence in 16 ms, upward VDE with exponential time dependence in 16 ms and upward major disruption (MD) with linear time dependence in 36 ms and exponential time dependence in 16 ms. From preliminary results, it was observed that the deformation seems enough small compared with the tolerance between the surrounding structures.

3.2 Thermo-mechanical analysis for heating

author's email:enoeda.mikio@jaea.go.jp

Thermo-mechanical analysis was performed to identify the loading conditions of surface heat flux and nuclear heating. Surface heat flux on the first wall was assumed 0.5 MW/m^2 as the highest value. Distribution of nuclear heating rate was evaluated by 2D nutronics analysis using DOHEAT2. Using the estimated heating conditions for the input conditions, thermo-mechanical analysis was performed by ANSYS. Using symmetrical conditions, one quarter part of the TBM module was converted to the model. Configuration of coolant channels were also incorporated in the geometry model. Transient analysis are planned on the assumption that the operation sequence follows 30 s of lump-up, 400 s of flat top plasma operation and 90 s lump-down. It was observed that maximum temperature of the first wall surface was 550 ^{o}C and the peaking of the von Mises stress was 580 MPa at the corner of the cooling channels. Further evaluation is needed.

3.3 Reduction of ferritic steel mass and mechanical analysis of box structure for coolant water ingress

The reduction of ferritic steel mass to 1300 kg is important to reduce the fero-magnetic effect to ITER plasma. To achieve this limitation of ferritic steel mass, the reduction of the WCCB TBM box size was studied. It was identified that the mass of ferritic steel of the TBM can be reduced to 1300 kg, in case the radial thickness of the box was reduced from original thickness of 600 mm to 375 mm. At the same time, such reduction of the box size enhances the durability of the box structure in case of ingress of 15.5 MPa coolant water. The mechanical analysis of the reduced size box was performed to examine this point. The box dimension is 232 (Toloidal) x 1660 (Poloidal) x 375 (Radial) mm. FW thickness is 25 mm. Built-in cooling channels of 8 x 8 mm are located at 10mm from the outer surface of the FW. Pitch of the channels is 11mm. Side wall thickness is 45 mm and diameter of its cooling channels is 10mm. Back wall thickness is 90 mm and diameter of its cooling channels 30 mm. It was observed that the stress peak appears at the FW internal corner of the box and it exceeds yield stress of F82H, however, such high stress only appears at the surface of the structure and major part of the FW cross section shows lower stress. This shows that the instantaneous collapse will be avoided.

3.4 Neutronics analysis for the evaluation of shutdown dose rate

Shielding analyses have been performed on the latest TBM port plug design including water and helium gas pipes with the Monte Carlo code MCNP5.14 [2], activation code ACT-4 [3] and Fusion Evaluated Nuclear Data Library FENDL-2.1 [4]. MCNP geometry input data of the TBM is created from CAD data with the CAD/MCNP automatic conversion code GEOMIT [5], and other geometry input data is created manually. A special "Direct 1-step Monte Carlo" method is adopted for the decay gamma-ray dose rate calculation [6]. There are dogleg gaps of 1.5 – 3 cm in width between the TBM and flame and between the flame and equatorial port extension. Dose rates behind the flange in 10^6 seconds after shutdown are 50 – 80 μSv/h in the latest TBM design with the dogleg gap structures, and they are lower than the upper value of 100 μSv/h to allow hands-on access of radiation workers in maintenance. Dose rates behind the bio-shield in one day after shutdown are around 0.2 μSv/h, and they are much lower than the upper value of 10 μSv/h to allow radiation workers unlimited access to those areas.

4. Advanced neutron multiplier

Beryllium metal as a single substance, which is a conventional material for the neutron multiplier, has a drawback of chemical instability at high temperatures. This has led to development of fabrication technology of more stable beryllium intermetallic compounds (beryllides). However, only very hard beryllide material having difficulty in processing was available in conventional powder metallurgy methods, due to its highly reactive nature with oxygen on the surface. Therefore, the plasma sintering method was recognized, in which the synthesis is conducted after the surface of the raw-material powder is cleaned up by electric discharge. And this synthesis method have been optimized in the DEMO R&D building at the International Fusion Energy Research Centre (IFERC) site in Rokksho-mura, Aomori-ken as a series of the Broader Approach activities. As a consequence, beryllide rod with a good capability for processing was successfully fabricated by the plasma sintering method. Furthermore, using the beryllide rod as an electrode in the rotating electrode method, beryllide pebbles of 1 mm in diameter were successfully fabricated.

5. Advanced tritium breeder pebble

Lithium titanate (Li_2TiO_3) pebble has been recognized as a prominent candidate material because of its chemical stability, good tritium release, and low-activation characteristics [7-8]. However, the mass of Li_2TiO_3 decreased with time because of Li evaporation in a H_2 atmosphere and Li burnup [9]. To prevent this mass decrease at high temperatures, Li_2TiO_3 with excess Li (Li_2+xTiO_3+y) has been developed as an advanced tritium breeder [10-11]. The pebble fabrication by the emulsion method is one of the promising techniques for the mass production of advanced tritium breeder pebbles. The granulator consisted of two syringes arranged in a T-shaped flow path. One syringe was filled with oil, and the other syringe was filled with a Li_2+xTiO_3+y slurry. The two flow lines from these syringes were connected in a T-shaped flow path. This arrangement allowed the Li_2+xTiO_3+y slurry flow to be cut by the oil from the oil-filled syringe. The size of the Li_2+xTiO_3+y gel particles was controlled by the relative flow speeds of the oil and the Li_2+xTiO_3+y slurry. The Li_2+xTiO_3+y gel particles were kept in a container filled with oil. In a previous study, the average grain size on the surface and cross sections of sintered $Li_{2+x}TiO_{3+y}$ pebbles was 2–10 μm. Considering the tritium release characteristics, the optimum grain size after sintering was less than 5 μm [12]. Therefore, the next step in the development of the fabrication technique was to optimize the granulation conditions to reach the target value.

6. Evaluation of tritium production and recovery performance by experiments with DT Neutrons

Tritium generation and recovery experiments by DT neutron irradiation of the simulated blanket mockup are conducted continuously [13-14] by using Fusion Neutron Source facility (FNS) of JAEA. The simulated blanket is composed with a capsule of a packed bed of Li_2TiO_3 pebbles (67g), Li_2TiO_3 blocks and Be blocks. The simulated blanket was irradiated by DT neutron for 5 hours. The capsule was kept at 573 K or 873 K, and purged by sweep gas based on helium for 10 hours including 5 hours irradiation. Total amount of produced tritium contained in the He sweep gas in the form of HT and HTO was measured. The ration to the calculated tritium generation amount was evaluated to identify the effect of ingredients of the sweep gas were varied such as (1) dry He, (2) wet He, (3) wet H_2/He and (4) dry H_2/He. It was observed that most of generated tritium were recovered within 10 hours purge and additional 5 hours purge. And, it has been clearly indicated that addition of H_2O or H_2 to the sweep gas is necessary to release tritium faster even at 873 K[15].

7. Conclusions

(1) A full scale TBM Back Wall mock-up has been successfully fabricated. Coolant channels were formed by drilling with the location accuracy of 1mm. also, as the trial fabrication of the most difficult part of breeder box structure, the cooling pipe penetration through the top or bottom plate of the breeder box was successfully fabricated by laser welding and TIG welding within the angular deformation of 0.16 degree

(2) Regarding the design activity, electromagnetic analysis under disruption events, thermo-mechanical analysis under normal ITER operation and neutronics analysis for shutdown dose rate evaluation have been performed. By the preliminary results, the soundness of the module structure was observed.

(3) High quality beryllide rod was successfully fabricated. By using fabricated beryllide rod as an electrode in the rotating electrode method, beryllide pebbles of 1 mm in diameter were successfully fabricated. The fabrication process pebbles of Li_2TiO_3 with excess Li composition was successfully improved to avoid the excess grain growth during sintering. The appropriate grain size of pebbles of Li_2TiO_3 with excess Li composition was achieved.

(4) Evaluation of tritium production and recovery rate by Fusion Neutron Source was performed. The effect of ingredients of the sweep gas was clarified. It has been clearly indicated that addition of H_2O or H_2 to the sweep gas is necessary to release tritium faster even at 873 K.

References

[1] M. Enoeda, Fusion Engineering and Design 87 (2012) 1363– 1369

[2] X-5 Monte Carlo Team, MCNP – A General Monte Carlo N-Particle Transport Code, Version 5, LA-UR-03-1987, Los Alamos National Laboratory, 2003.

[3] Y. Seki et al., THIDA-2: An Advanced Code System for Transmutation, Activation, Decay Heat and Dose Rate, JAERI1301, Japan Atomic Energy Research Institute, 1986.

[4] L. Al-dama et al., FENDL-2.1, Update of an evaluated nuclear data library for fusion application, IAEA Report INDC(NDS)-467, International Atomic Energy Agency, 2004.

[5] S. Sato et al., Development of CAD-TO-MCNP model conversion system and its application to ITER, Nuclear Technology 168 (2009) 843-847.

[6] D. Valenza et al., Proposal of shutdown dose estimation method by Monte Carlo code, Fusion Engineering Design 55 (2001) 411-418.

[7] N. Roux, J. Avon, A. Floreancig, J. Mougin, B. Rasneur, S. Ravel, J. Nucl. Mater., 233-237 (1996) 1431-1435.

[8] N. Roux, S. Tanaka, C. Johnson, R. Verrall, Fusion Eng. and Des., 41 (1998) 31-38.

[9] T. Hoshino, M. Dokiya, T. Terai, Y. Takahashi, M. Yamawaki, Fusion Eng. and Des., 61-62 (2002) 353-360.

[10] T. Hoshino, M. Yasumoto, K. Tsuchiya, K. Hayashi, H. Nishimura, A. Suzuki, T. Terai, Fusion Eng. and Des., 82 (2007) 2269-2273.

[11] T. Hoshino, K. Kato, Y. Natori, M. Nakamura, K. Sasaki, K. Hayashi, T. Terai, K. Tatenuma, Fusion Eng. and Des., 84 (2009) 956-959.

[12] T. Hoshino, M. Nakamichi, Fusion Eng. and Des., 87 (2012) 486-492.

[13] K. Ochiai, T, Hoshino, Y. Kawamura et al., "Tritium recovery experiment from Li ceramic breeding material irradiated with DT neutrons", in: Contributed papers of 23rd IAEA Fusion Energy Conference, Daejon, Republic of Korea, 2010.

[14] Y. Kawamura, K. Ochiai, T. Hoshino et al., "Effect of sweep gas species on tritium release behavior from lithium titanate packed bed during 14 MeV neutron irradiation", Fusion Eng. Des. 87 (2012) 1253-1257.

[15] K. Ochiai, Y. Kawamura, T. Hoshino et al. "DT neutron irradiation experiment for tritium recovery on WCCB blanket", in this workshop.

17th International Workshop of Ceramic Breeder Blanket Interactions (CBBI-17)
Barcelona, Spain, 12-14, September, 2013

Status of Development of Water Cooled Ceramic Breeder Test Blanket

M. Enoeda, Hisashi Tanigawa, Takanori Hirose, Satoshi Sato, Kentaro Ochiai, Chikara Konno, Yoshinori Kawamura, Takumi Hayashi, Toshihiko Yamanishi, Tsuyoshi Hoshino, Masaru Nakamichi, Hiroyasu Tanigawa, Hiroshi Nishi, Satoshi Suzuki, Koichiro Ezato, Yohji Seki, Daigo Tsuru, Kenji Yokoyama

JAPAN ATOMIC ENERGY AGENCY

Contents

1. Blanket and Test Blanket Module (TBM) development schedule in near term
2. Fabrication technology development for TBM
3. Electro-magnetic and thermo-mechanical analysis of TBM
4. Shutdown dose rate analysis around TBM port
5. Advanced Breeder development for DEMO blanket
6. Advanced multiplier development for DEMO blanket
7. Evaluation of Tritium Production Rate of Li_2TiO_3 pebble bed by DT neutron irradiation

ITER Test Blanket Module and Blanket Development

- ITER Test Blanket Module (TBM) Program is to test essential functions of DEMO Blanket in the real fusion environment with scalable module.
- ITER TBM Program is one of the most important development steps.

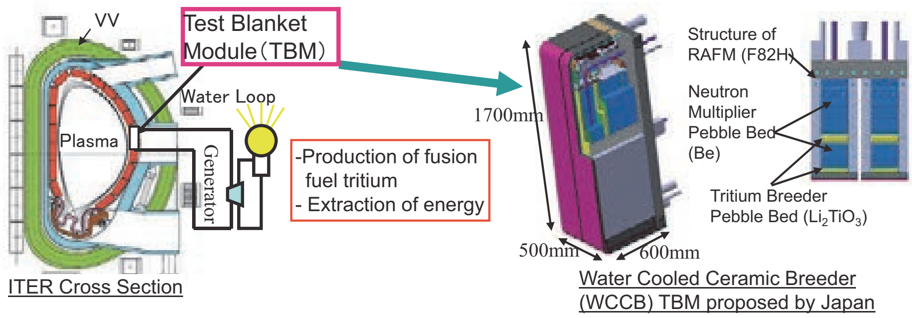

Japan is performing Water Cooled Ceramic Breeder (WCCB) TBM development as one of the most important milestones to DEMO. Also, development of DEMO blanket technology is performed intensively mainly in Rokkasho site. Blanket development program in Japan is envisaged to be expanded based on these activities.

Near Term Schedule of TBM and Blanket development

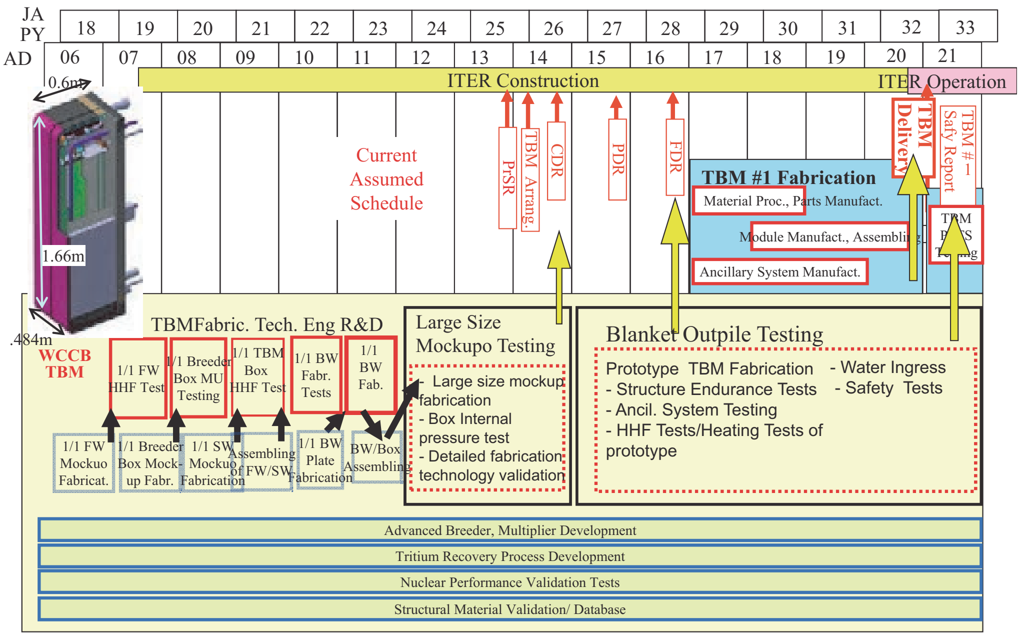

Detailed Design for Manufacturability

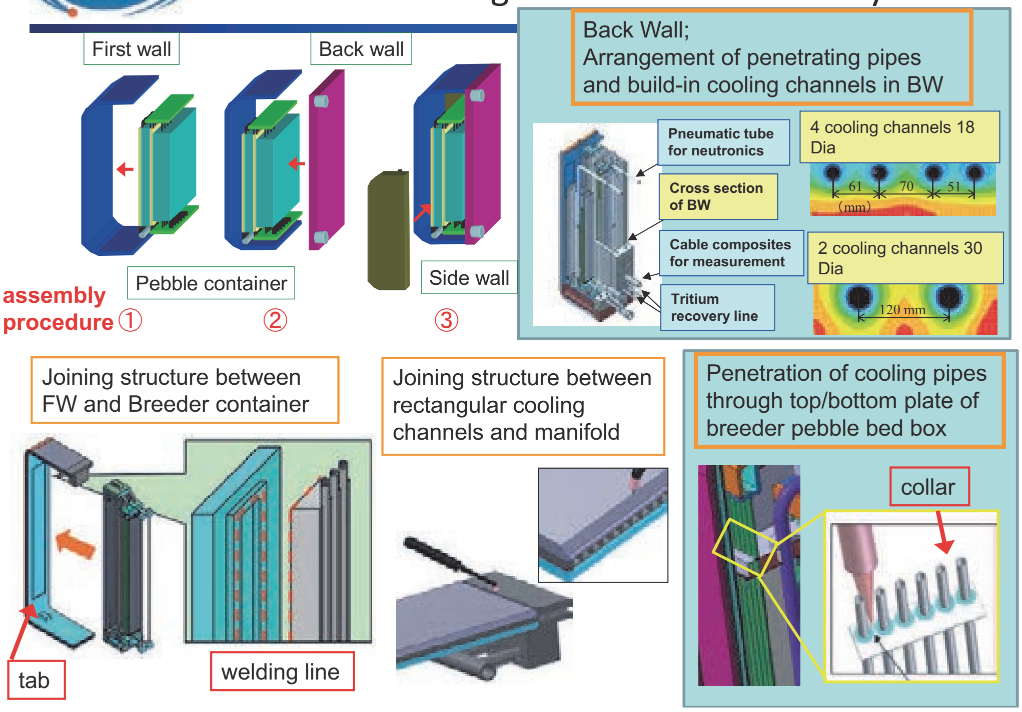

Fabrication of TBM Real Scale Back Wall Mockup

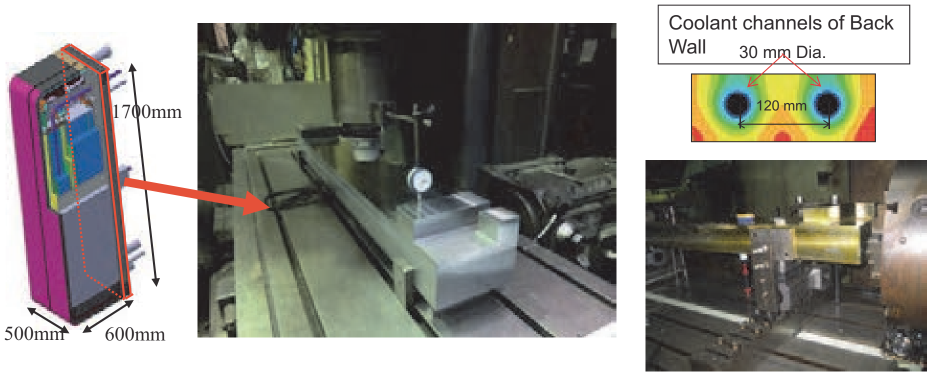

Real Scale TBM Back Wall Mockup

Drilling of coolant channel

Real scale TBM Back Wall fabrication was demonstrated using F82H.
- Shear keys were formed in the forging process of a plate. Final shape was machined to target dimension.
- Coolant channels were formed by drilling, according to the optimized design. Pressure test was performed to coolant channels and headers.

Fabrication of Breeder/Multiplier Pebble Bed Box

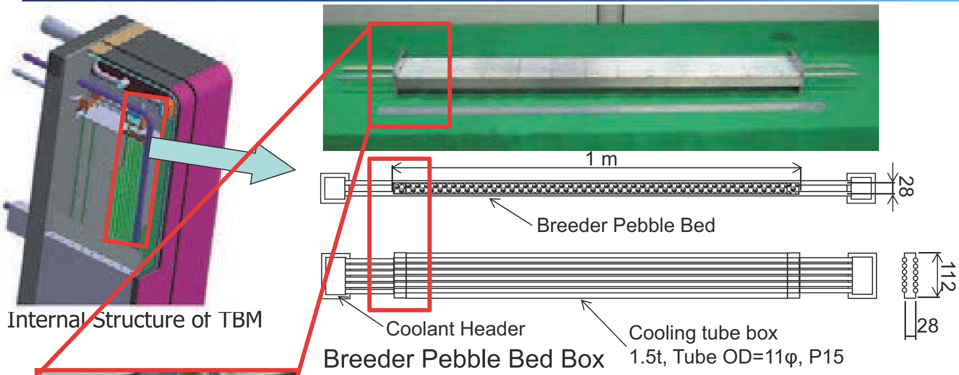

Thin plate – thin tube welding technique was successfully applied to the fabrication of pebble box.

Fabrication of penetration of coolant pipes through top/bottom plate was not yet completed.

Fabrication of penetration of coolant pipes through top/bottom plate

LASER welding: 1 path with no filler, power 0.18 kJ/cm
TIG welding: 2 path with filler, power 3.8 kJ/cm)

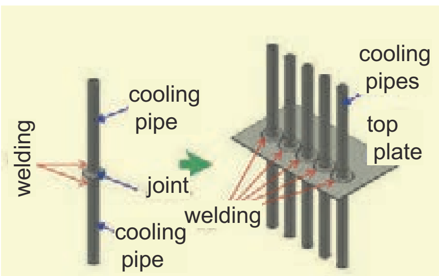

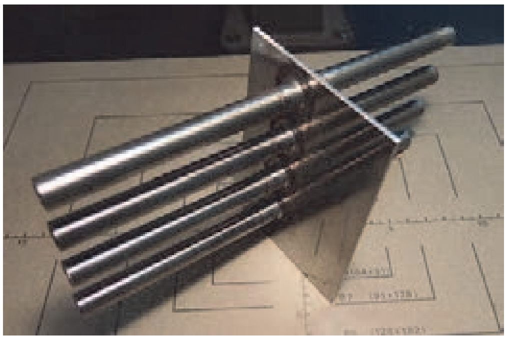

Fabricated coolant pipe penetration part of pebble box

(1) In both welding technique, deformation could be controlled by constraint. Angular deformation was no more than 0.6 degree in TIG case.
(2) It was observed that the deformation by welding process can be corrected by post welding heat treatment.

Structure Feasibility Analysis of TBM

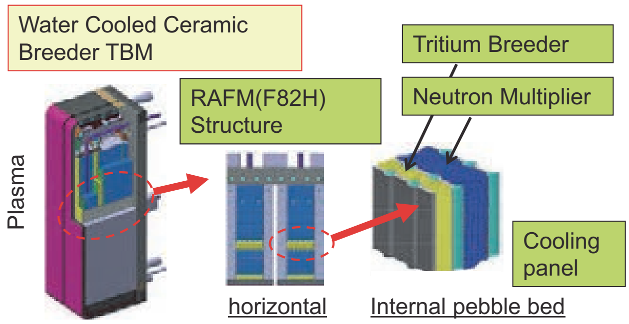

Design Condition

Surface Heat Flux	0.35 MW/m^2
Neutron Wall Loading	0.78 MW/m^2
Coolant Pressure	17.1 MW/m^2

(1) As a part of TBM design activity, analysis of TBM structure feasibility is performed.
(2) Loads to TBM are surface heat flux, nuclear heating by neutron wall loading, coolant water pressure.
(3) In case of plasma disruption, electro-magnetic force is induced.
(4) As an emergency case, coolant ingress in the TBM box is assumed.
(5) By ANSYS code, electro-magnetic analysis and stress analysis, thermo-mechanical analysis under surface heat flux, nuclear heating and coolant pressure.

Thermo-mechanical Analysis of TBM box

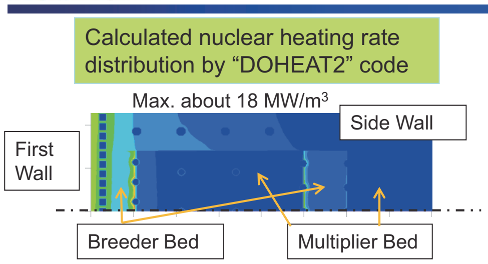

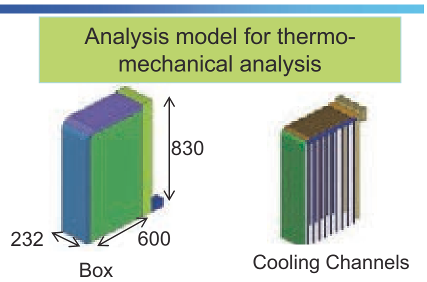

(a) Input data of nuclear heating rate distribution was calculated by 2D nuclear-temperature analysis code "DOHEAT2".
(b) Temperature increase of coolant and heat transfer coefficient was incorporated.
(c) Transient analysis of plasma lump-up and down was performed and compared with steady state analysis.

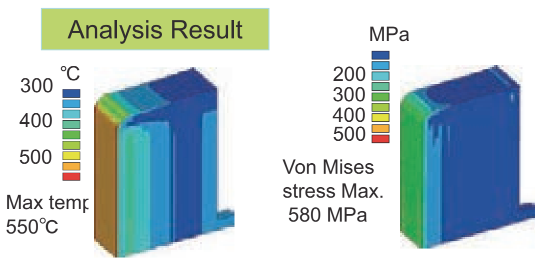

(1) Stress in transient analysis did not exceed that in steady state analysis.
(2) Feasibility of the structure was observed.

Electro-magnetic and Stress Analysis of TBM Box

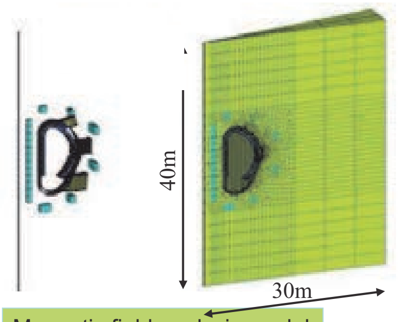

Magnetic field analysis model (VV 10º sector)

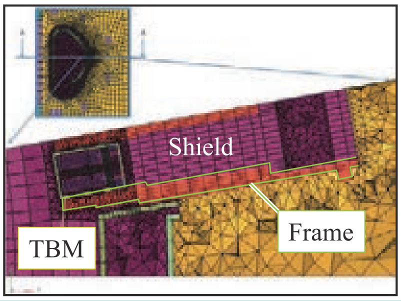

Magnetic field analysis (horizontal cross section around TBM port)

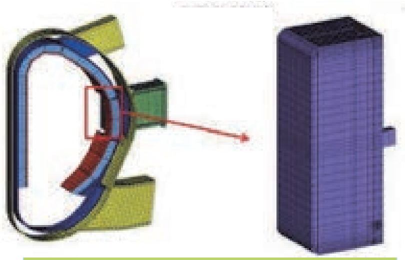

WCCB-TBM stress analysis model

(a) ANSYS was used.
(b) Consistency was checked by E-M analysis benchmarking procedure for shield blankets.
(c) The following 6 cases of disruption scenario were analyzed. Additional 3 cases are on-going.

Disruption scenario

Case	Event / DINA file
1	VDE_DW_lin_36ms
2	VDE_UP_lin_ 36ms
3	MD_UP_lin_ 36ms
4	VDE_DW_exp_16ms
5	VDE_UP_exp_ 16ms
6	MD_UP_exp_ 16ms

Results of Stress Analysis based on Electro-magnetic Analysis

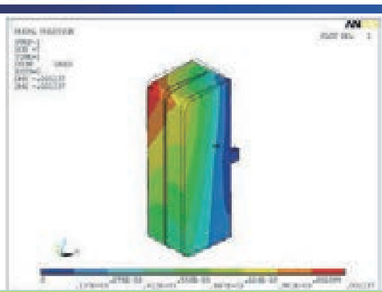

Deformation (MD_UP_exp16ms)

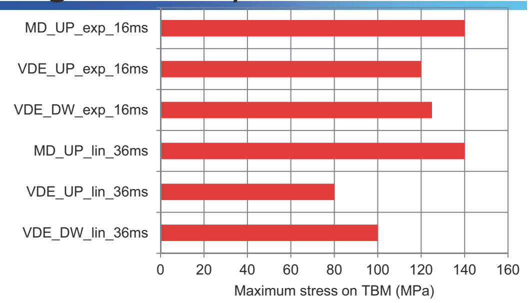

Maximum Stress on TBM Structure

(1) Deformation was small and there is no interference with surrounding structure. Maximum stress was less than 140MPa.
(2) Margin was observed to the acceptable stress of Grade 91 steel, which is similar or lower than F82H.

Mises Stress (MD_UP_exp16ms)

(1) Basic feasibility of structure against electro-magnetic loads was observed.
(2) Further analysis will be performed for shield structure analysis.

TBM Box Dimension and Ferritic Steel Weight

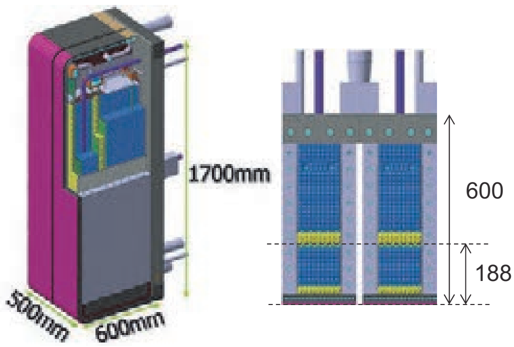

- Ferritic stell mass of TBM is required not to exceed 1300 kg.
- To meet this, reduction of radial thickness was considered.
- TBM Box is required to withstand internal pressure in case of coolant ingress.
➔ Stress analysis of the box was performed to evaluate the impact to the box structure.

Radial dimension / mm	600	375
Total RAFM weight / kg	1800	1300

Tentative survey cases in this analysis

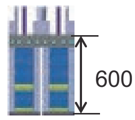

Feritic steel 1800 kg

original case

→

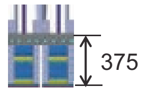

Feritic steel 1300 kg

Breeder zone = about 54%

- ANSYS mechanical APDL ver 14, 3D analysis with SOLID186 elements
- Uniform temperature: 300°C, 15MPa of uniform pressure was applied to internal surface of the box and cooling channels.

Stress Analysis Results of TBM Box in Case of Coolant Ingress (Von Mises Stress)

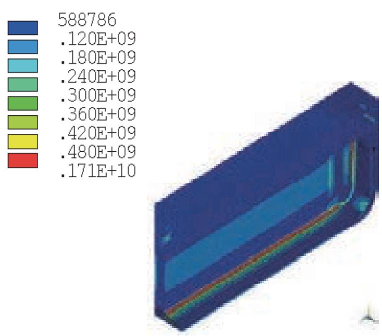

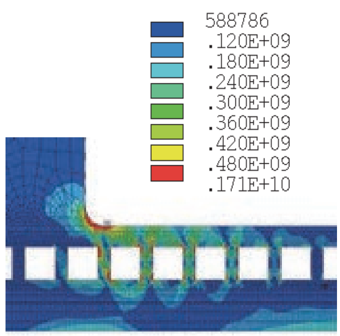

Breeder zone = 54% thickness of the reference design
- Dimension: 232 (Toloidal) x 1660 (Poloidal) x 375 (Radial) mm^3
- FW thickness is 25 mm. 8 x 8 mm^2 cooling channels are located 10mm from the outer surface of the FW. Pitch of the channels is 11mm.
- 45T mm SW with Φ10 mm cooling channels. 90T mm BW with Φ30 mm cooling channels

(1) Red area shows above $\sigma_{0.2}$ at 300 °C.
(2) The red area around corners should be moderated with an appropriate curvature.
(3) There is no part whose total area exceeds $\sigma_{0.2}$.

Effective Dose Rates 1 d after Shutdown

Shutdown dose rates have been evaluated on the latest Japanese TBM port plug design by D1S(Direct 1 Step MCNP) and FENDL-2.1. Dose rates behind the bio-shield in one day after shutdown are around 0.2 μSv/h, which are much lower than the upper value of 10 μSv/h to allow radiation workers unlimited access to those areas.

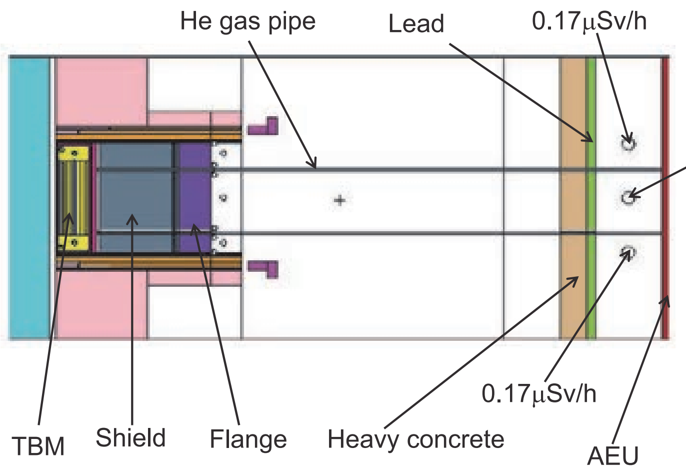

Nuclide	Half-life	Dose rate (μSv/h)
^{24}Na	15 h	8.1E-06
^{92m}Nb	10d	3.0E-06
^{51}Cr	28 d	3.7E-03
^{54}Mn	312 d	5.8E-03
^{56}Mn	2.6 h	1.4E-03
^{58}Co	71 d	1.9E-02
^{59}Fe	44 d	3.6E-03
^{60}Co	5.3 y	1.2E-01
^{64}Cu	13 h	7.1E-04
^{182}Ta	114 d	1.2E-02
Total		1.7E-01

Effective Dose Rates 10^6 s after Shutdown

Dose rates behind the flange in 10^6 seconds after shutdown are 50 – 80 μSv/h, which are lower than the upper value of 100 μSv/h to allow hands-on access of radiation workers in maintenance.

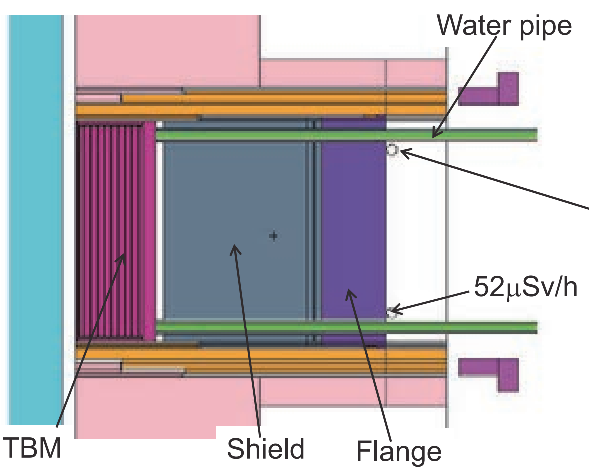

Nuclide	Half-life	Dose rate (μSv/h)
^{51}Cr	28 d	1
^{54}Mn	312 d	3
^{58}Co	71 d	9
^{59}Fe	44 d	2
^{60}Co	5.3 y	24
^{182}Ta	114 d	11
Total		51

Pebble Fabrication of Li_2TiO_3 with Excess Li

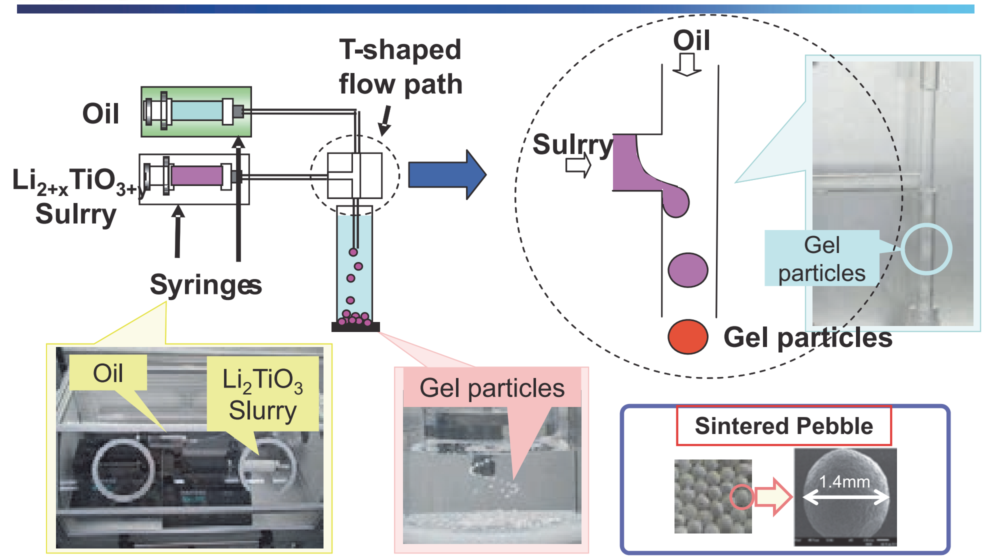

This granulator is composed of two syringes and T-shaped flow path. One syringe is filled with oil. Other syringe is filled with $Li_{2+x}TiO_{3+y}$ slurry. Two flow lines from these syringes are connected in the T-shaped flow path. In this time, $Li_{2+x}TiO_{3+y}$ slurry flow is cut by oil flow from the oil-filled syringe.

Characterizations of Advanced Tritium Breeder

Sintering in vacuum atmosphere

Diameter	1.18mm
Sphericity	1.04
Structure	$Li_{2+x}TiO_{3+y}$
Li/Ti	2.11
Grain size	$< 5\,\mu m$
Density	60% T.D.

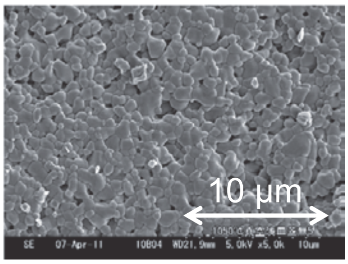

Surface
Good!

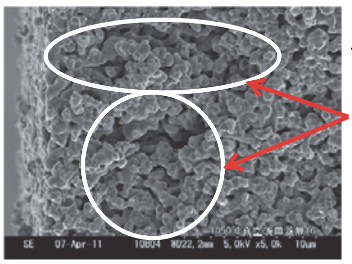

Cross-section

Large pore is observed.

Optimum sintering conditions was surveyed in order to increase the density of advanced breeder pebbles.

Improvement of Density

The $Li_{2+x}TiO_{3+y}$ pebbles were sintered at 1073 K for 1 h in vacuum and at 1323 K for 5 h in an argon atmosphere.

Surface

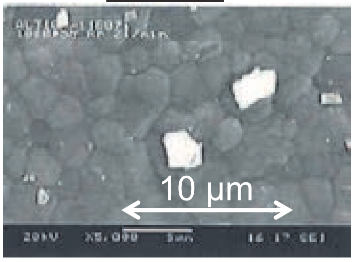

Cross-section

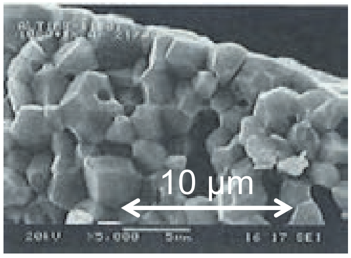

Grain size	＜5 μm
Density	86% T.D.

Good!

Application of the emulsion method to mass production of $Li_{2+x}TiO_{3+y}$ pebbles, is the next development step.

Progress of Beryllide Pebble Development

Fabrication technology for Beryllide pebble was demonstrated by both of Plasma Sintering method and Rotating Electrode method.

Plasma sintering method

This method results in powder surface activation that enhances powder particle sinterability.

1) Uniaxial pressure
2) Plasma generation for powder surface activation
3) Resistance heating

Sintering conditions

Raw material	: Be & Ti(7.7at.%)
Purities	: >99 wt.%
Particle size	: <45 μm
Sintering time	: 20 min
Pressure	: 50 MPa
Temperature	: 1273 K

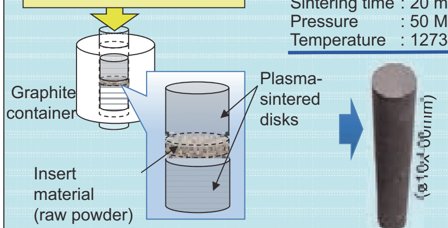

Beryllide could be simultaneously synthesized and jointed.

Rotating electrode method

1) Rotation of beryllide electrode
2) Discharge between beryllide & W electrodes
3) Centrifugally ejection of molten berylldie

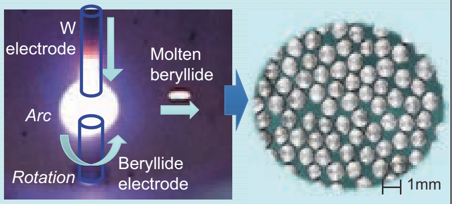

Prototypic pebbles of beryllide with 1mm in diameter were successfully fabricated.

Evaluation of tritium production and recovery performance by experiments with DT Neutrons

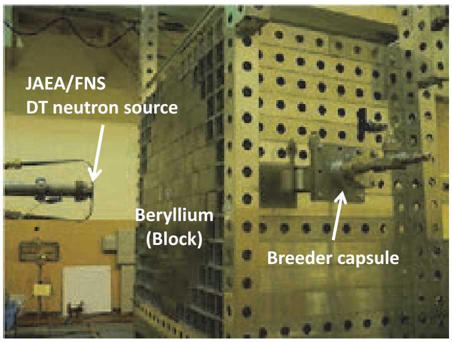

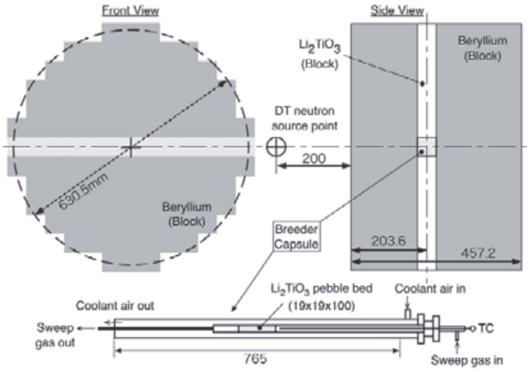

Simulated blanket arrangement for DT neutron irradiation experiment.

(1) Fusion Neutron Source (FNS) facility was used. The DT neutron intensity was 7.7×10^{10} - 1.2×10^{11} neutron/sec.

(2) The breeder capsule within 67 g of Li_2TiO_3 (natural Li) pebble bed was inserted in Be and Li_2TiO_3 blocks assembly, and irradiated by DT neutron for 5 hours.
The capsule was kept at 573 K or 873 K, and purged by He sweep gas with <u>various ingredients (① dry He, ② wet He, ③ wet H2/He and ④ dry H2/He)</u>
for 10 hours including 5 hours irradiation. The flow rate is 100 standard cm^3/min .

Evaluation of tritium production and recovery performance by experiments with DT Neutrons

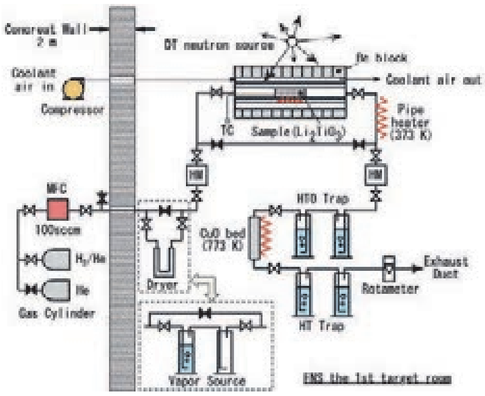

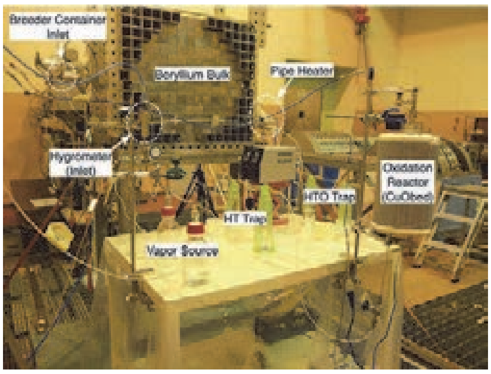

Tritium recovery system arrangement for DT neutron irradiation experiment.

(3) The effluent gas was first introduced to gas-washing bottles to capture HTO, then introduced to a CuO for conversion of HT in sweep gas to HTO, and finally introduced to second gas-bubbling bottles to capture HT as HTO.

(4) Tritium concentration of 1 cm^3 water samples of gas bubbling bottles was measured with a liquid scintillation counter (LSC), which was calibrated with a standard HTO (50 Bq/cc) sample within 2 % accuracy.

(5) <u>Measured value of tritium production was compared with calculated value of MCNP.</u>

Evaluation of tritium production and recovery performance by experiments with DT Neutrons

The effect of various ingredients,
(1) dry He,
(2) wet He,
(3) wet H2/He and
(4) dry H2/He)
in He sweep gas on tritium release was tested.

The ratio of measured value of recovered tritium and tritium generation calculated by MCNP was evaluated.

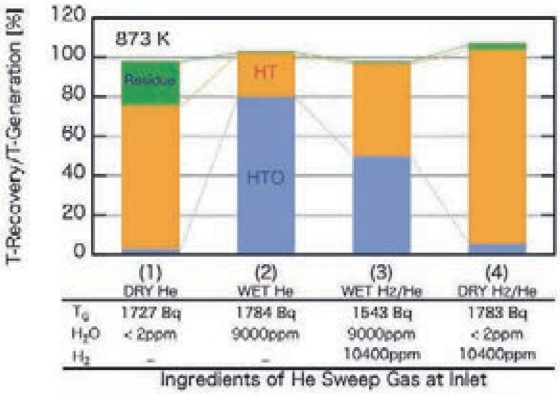

The ratio of tritium recovery to tritium generation for various sweep gases at 873 K.

(1) Most of generated tritium were recovered within 10 hours purge and additional 5 hours purge.
(2) H_2 or H_2O need to be added to enhance tritium recovery from the breeder pebble bed at 873K.

Conclusions

1. Fabrication of real scale Back Wall and cooling channel penetration of breeder pebble box were demonstrated.
2. Electro-magnetic, thermo-mechanical and stress analysis showed important progress to show the feasibility of structure.
3. Shutdown dose rate analysis around TBM port showed good prospect to achieve lower than 100 microSv/h behind the flange in 10^6 seconds after shutdown.
4. In advanced breeder development for DEMO blanket, pebble fabrication of Li_2TiO_3 with excess Li content was principally demonstrated by Emulsion method.
5. In advanced multiplier development for DEMO blanket, fabrication of Beryllide pebble was demonstrated by both of Plasma Sintering method and Rotating Electrode method.
6. By evaluation of tritium production rate of Li_2TiO_3 pebble bed in Fusion Neutron Source facility, the effect of ingredients in He sweep gas was tested. It was clarified that that H_2 or H_2O need to be added for in-situ tritium recovery from the breeder pebble bed at 873K in 10 h.

<u>Disclaimer</u>
The views and opinions expressed herein do not necessarily reflect those of the ITER Organization.

Recent developments of the design of the EU solid breeder blanket for DEMO

L.V. Boccaccini, D. Carloni, S. Kecskes, Q.L. Kang

Karlsruhe Institute of Technology, Institute for Neutron Physics and Reactor Technology, 76021 Karlsruhe, Germany

In year 2011 a new study in EU started with the goal to design a DEMO reactor able to deliver electrical energy in grid in 2050. The blanket technology, key issue for the development of the fusion breeder reactor, is an important part of this study. According to the EU DEMO roadmap, 4 different blankets are considered and assessed for this DEMO. First of all the two concepts that are at the present reference ones for DEMO and for the test in ITER, namely, namely the Helium Cooled Pebble Bed (HCPB) and Lithium lead (HCLL), will be considered. In addition the study will assess also a water cooled concept with PbLi and the more advanced Dual Coolant as possible back-up solutions.

In the frame of the this new European DEMO Breeder Blanket Programme, the Karlsruhe Institute of Technology (KIT) is supporting the design and qualification of the solid breeder blanket (HCPB). The aim of these studies is to adapt the existing concept of the HCPB blanket to the new DEMO configuration, loadings and geometry. In the frame of these activities, previous studies have been revised and a new set of boundary conditions has been elaborated to guide the new conceptual design.

This paper aims to give an overview on these ongoing activities presenting the new CAD design and the assessment done to validate this concept. results of the thermo hydraulic and thermo mechanical investigations performed for its validation. The CAD design presents a proposal of segmentation for an inboard and an outboard blanket segment arranged according to the Vertical Maintenance System. The design of the blanket for a reference equatorial box have been developed including First wall, Breeding zone, internal stiffening Grid and Manifold system. . All of these components have to withstand different typologies of loads, as thermal and pressure loads, during both normal and off-normal operation, e.g. LOCA (Loss of Coolant Accident).

Recent developments of the design of the EU solid breeder blanket for DEMO

L.V. Boccaccini, D. Carloni, S. Kecskes, Q.L. Kang,
Karlsruhe Institute of Technology, KIT

CBBI-17, 12–14 September 2013. Barcelona, Spain

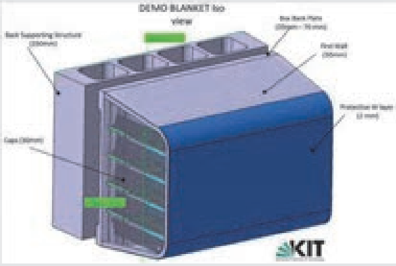

Presentation Outline

Introduction

The EU Roadmap 2013 and Blankets
- Requirements for the PPP&T DEMO Blanket

The EU Blanket Concept development:
- The HCLL and HCPB blankets
- The WCLL blanket
- The DCLL blanket

The new design of the HCPB Blanket

Conclusions

Acknowledgment:
This presentation refers to work performed by several EURATOM associations in projects of the EU Programme under leadership of F4E (TBM Project) and EFDA (DEMO Project). However, the views and opinions expressed herein reflect only the author ones.

1 L.V. Boccaccini

1. Introduction

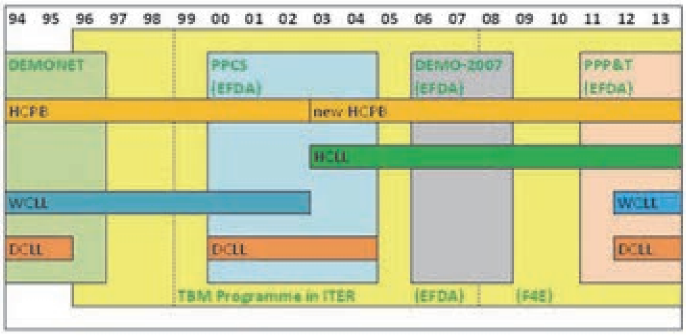

- **HCPB:** Helium Cooled Pebble Bed Blanket
- **HCLL:** Helium Cooled Lithium Lead Blanket
- **WCLL:** Water Cooled Lithium Lead Blanket
- **DCLL:** Dual Coolant Lithium Lead Blanket

- EU is developing since the 80-ties blanket concepts based on liquid and solid breeder blankets.
- DEMONET specification were use in 1995 for the selection of concept to test in ITER.
- The Power Plant Conceptual Study (PPCS) considered plant model for a future Fusion Power Plant (FPP), assessing cost of energy and safety.
- In 2003 the HCLL replaced the WCLL. A new design architecture was proposed for the HCPB and HCLL. The two helium cooled blankets was selected for test the TBM programme.
- In the short DEMO-2007 study possible DEMO configuration were assessed for HCLL and HCPB.

The EU Roadmap 2013 and blanket development

- EU has started in 2011 a new DEMO study under the new EFDA department Power Plant Physic and Technology (PPP&T).
- Objective of the programme is a fusion reactor able to deliver few hundreds MW of electrical power in grid already in 2050 (start construction 2030).
- An Early DEMO seems possible only if it can relay to a pulse tokamak physic that is the present ITER physics basis and to technology and materials with modest extrapolations from present levels of development.
- Also if “the demonstrating all the technologies for the construction of a commercial Fusion Power Plant (FPP) remain in the scope”, the short timeframe suggests that to build the Early DEMO compromises could be done in term of “FPP performances” (e.g. reduced lifetime, efficiency or waste reduction requirements).
- As the blanket is a key technology for DEMO, this choice has direct consequences in the future development strategy.

Performances of the PPP&T DEMO

	units	PPCS-2004(2)	DEMO-2007	PPP&T DEMO(3)
Reactor parameters				
Neutron wall load (av)	MW/m²	2.1	1.6	1.3
Cumulative max fluence at FW	MWa/m²	100	28	9
Effective lifetime	FPY	40	15	6
Lifetime	year	53	40	30
Average availability	%	75	36	20
Pulse length (4)	h	Ss	Ss or lp	2.5
Blanket parameters				
Lifetime (in max damages in steel) (1)	dpa	150	75	20/50(6)
Neutron wall load (max)	MW/m²	2.5	1.9	1.5
Surface Heating (max)	MW/m²	0.5	0.5	0.5(5)
Pulse number	-	n/a	tbd	5800/14500(6)

(1) Irradiation damage in steel is considered the limiting factor for blanket (~75 dpa in steel for DEMO and ~150 dpa in steel for FPP). 1 MWa/m² is equivalent to ~10 dpa in steel at FW.
(2) FPP (Fusion Power Plant) defined as 10th-of-a-kind plant.
(3) Parameters used in 2013 design work.
(4) Ss : steady state; lp: long pulses.
(5) Excluding possible plasma flux interaction
(6) If a strategy of two sets of blankets is confirmed

Helium Cooled Blanket Systems: HCPB and HCLL

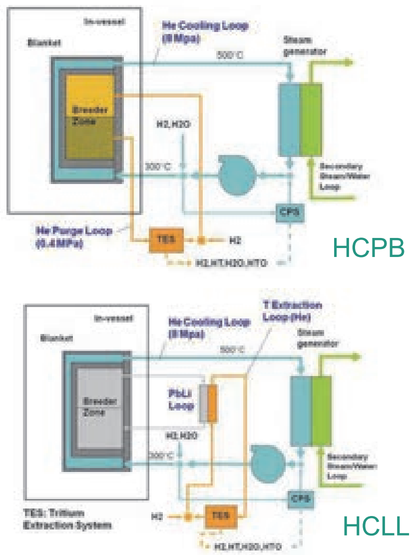

- The coolant primary circuit exchanges heat through a helium-water steam generator to a Rankine circuit at ~500°C max temperature.
- According to a study for DEMONET configuration, the primary coolant can be subdivided in several loops (each line with a own blower and steam generator handling about 180 MW of the reactor thermal power).
- The main difference is the mechanism of T extraction:
  - in the HCPB a low pressure He purge flow extracts T from the ceramic pebble beds;
  - In the HCLL the PbLi re-circulates slowly (~10 PbLi inventaries pro day) for a T extraction outside the VV (He stripping or permeator).

EU Test Blanket Modules

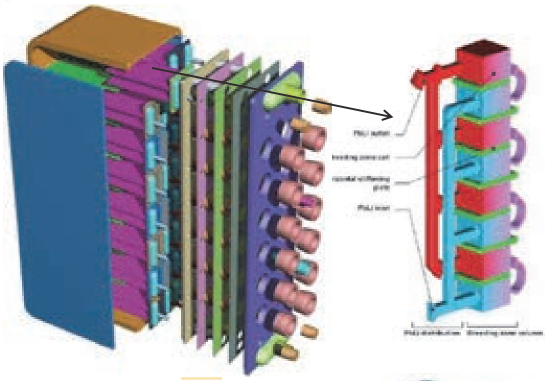

HCLL TBM

L.V. Boccaccini, A. Aiello, O. Bede, F. Cismondi, L. Kosek, T. Ilkei, J.-F. Salavy, P. Sardain, L. Sedano, Present status of the conceptual design of the EU test blanket systems, Fusion Engineering and Design 86 (2011) 478-483.

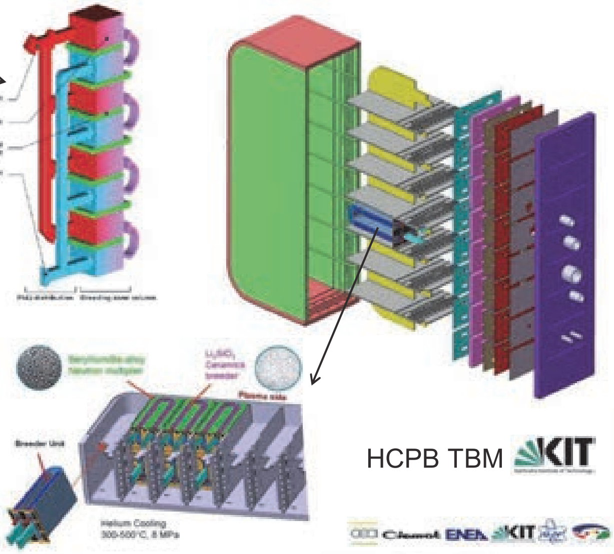

HCPB TBM

6 L.V. Boccaccini

The WCLL Design: DEMONET configuration

- This concept has been proposed by CEA in the 90-ties. It use water as coolant at PWR conditions (285-325°C at 15.5 Mpa) and PbLi in quasi stagnant condition as breeder.
- **Advantages:**
  - Water is an **exceptional coolant**, largely **available** and the **PWR cooling technology** is well proved (Balance of Plant).
  - Contribute to neutron shielding in the manifold region.
- **Issues:**
  - **Eurofer embrittlement:** because the entrance temperature of the coolant is low (285°C), the effect of embrittlement could be a stringent constraint for the concept
  - **Water / PbLi reaction:** concerns for a possible large peak of pressure during in-box LOCA.
  - **Tritium permeation and extraction:** possible T contamination of the primary coolant with T permeating from the PbLi; issue in the purification of large amount of tritiated water.

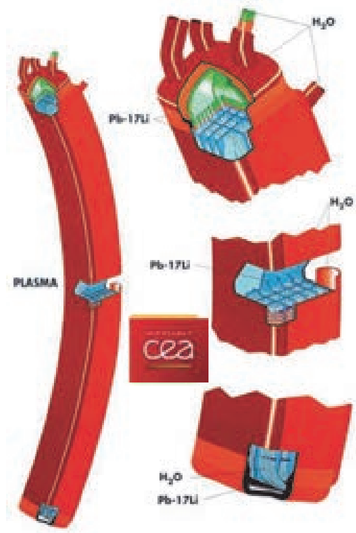

7 L.V. Boccaccini

The WCLL Design: PPP&T DEMO configuration

Design of the blanket module

- Vertical stiffening plates to reinforce the box against EM loads and pressurisation
- Waved FW to reduce steel thickness (TBR) and max temp

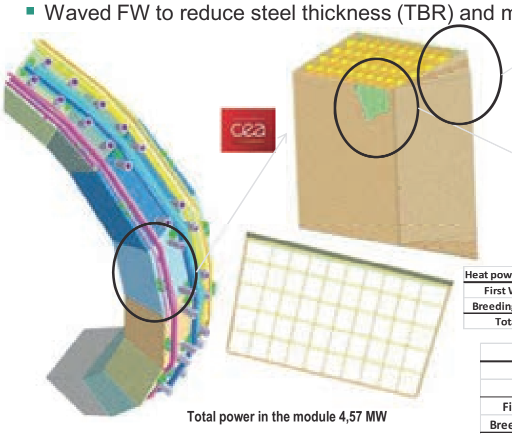

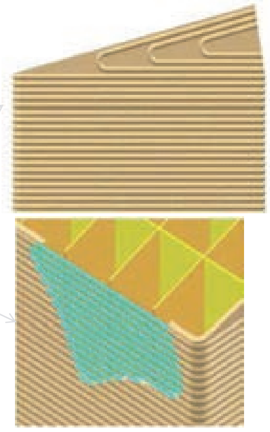

Heat power density - Ph (MW)	
First Wall	1,09
Breeding Zone	0,00
Total	1,09

Neutron power density - Pn (MW)				
	Materials			Total
	Eurofer	H2O	Pb-17Li	
First Wall	0,32	0,03	0,00	0,35
Breeding Zone	0,13	0,12	2,89	3,14
Total	0,45	0,15	2,89	3,49

The Dual Coolant Blanket

- This concept has been proposed by Malang [Malang, 1994] at KIT and developed in the US ARIES-ST studies [Tillack, 1997 and 2003].
- Reference Blanket in the EU PPCS for Mod-C plant configuration.
- The main idea is to have a PbLi cooling (at least partially) still adopting steel as structural material. This is possible if the PbLi flow insulated (electrical and thermal insulation) from conductive walls by means of flow channel insert (FCI).
- Allumina sandwich was the first choice for the FCI in [Malang, 1994]. Selection of SiC_f/SiC-FCI in the present reference designs.
- The insulating channels allow to reaching (the only one of the proposed concepts using a RAFM of first generation) outlet temperatures up to 700°C.
- For an application on an early DEMO a version at only ~500°C could be taken into account.

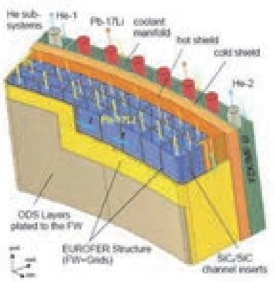

Main features:

- helium-cooled RAFM steel structures (EUROFER)
- ODS plated FW to use the high-temperature strength of ODS
- self-cooled breeding zone with Pb17Li as breeder and coolant
- SiC/SiC flow channel inserts as electrical (MHD) and thermal insulators leading to high exit temperature and high thermal efficiency

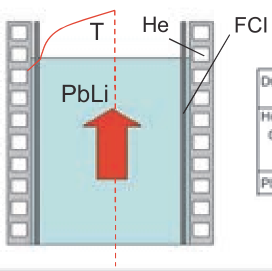

Dual Coolants	T_{Inlet} (°C)	T_{Outlet} (°C)	ΔT (K)
Helium (8 MPa)			
Overall blanket	300	480	180
FW	300	450	150
Grids	450	480	30
Pb-17Li	480	700	220

DEMO Configuration and the HCPB Segmentation

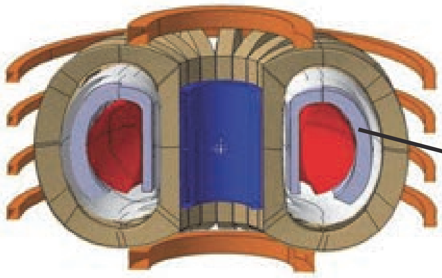

16 TF -> 16 Blanket Sectors

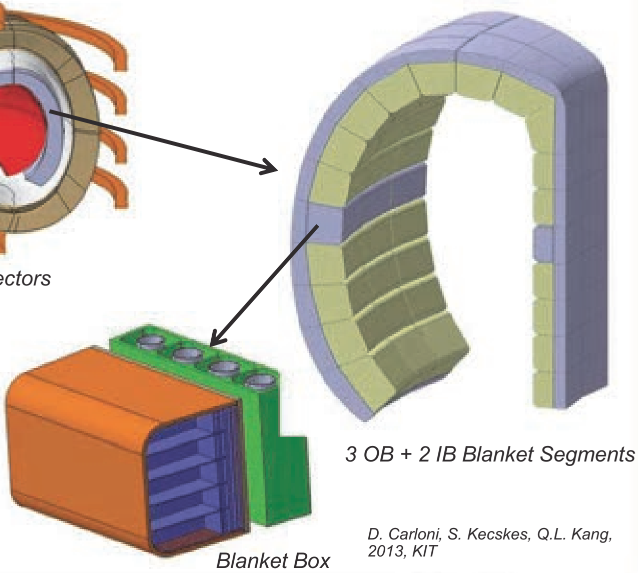

3 OB + 2 IB Blanket Segments

Blanket Box

- Maintenance concept based on the Vertical Replacement Concept
- Design of the blanket segment based on the Multi Module Design

D. Carloni, S. Kecskes, Q.L. Kang, 2013, KIT

HCPB Blanket for PPP&T DEMO

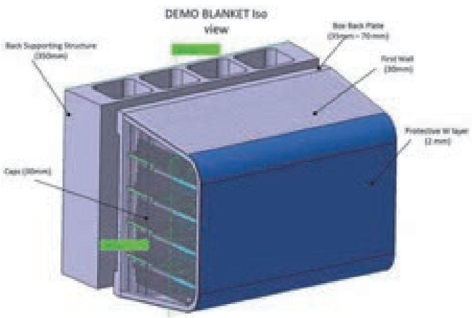

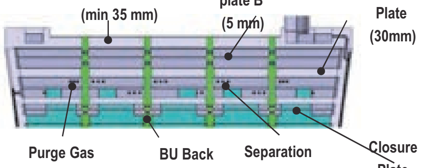

- **Loading:** Thermal load conditions based on a steady state plasma (or pulses >2-8h) with a max surface heating of 0.5 MW/m^2 and a max neutron wall load (at the OB equatorial blanket) of 1.5 MW/m2.
- **Blanket in form** of large modules (up to 1 m x 2 m). This modules are arranged for vertical maintenance in a removable segment.
- **The box** containing the breeders is designed for low operational pressure (about 0.2 MPa) and accidental pressure of 8 MPa to cope with a possible over-pressurisation caused by an in-box LOCA. The grid provide this feature.
- **The Helium** in the different structures (FW, CAP, Grid and Breeder Units) is supply by manifold located in the rear part of the box. The manifold structure is enclosed between two thick closure plates that are connected by stiffening grids.

Breeder Units Design

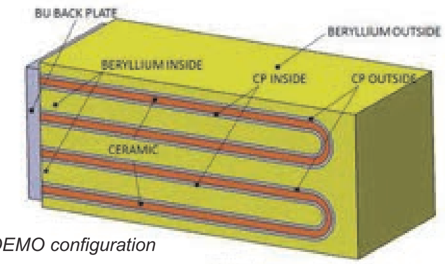

DEMO configuration

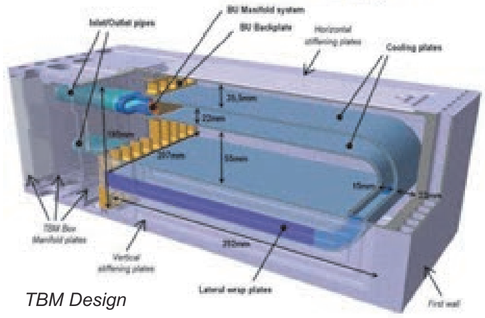

TBM Design

- **Breeder Units:** Located into the cells formed by the grid. U-shaped Cooling Plate design. The ceramic fills the gap between the 2 Cooling Plates, whilst Be fills the remaining space of the cell.
- **Ceramic Breeder (CB):** Li_4SiO_4 in form of pebble bed of 0.2-0.6 mm at ~63% packing factor. Li_2TiO_3 is an alternative candidate (1mm pebble).
- **Beryllium:** Be or Be12-Ti pebbles. In a ratio of 4:1 respect to the CB. Reference 1mm pebbles.
- **Purge flow:** a low pressure He flow purges the Be and CB pebble beds extracting T. The recovery of T from He is done outside the VV.

Purge schema in the HCPB Breeder Units

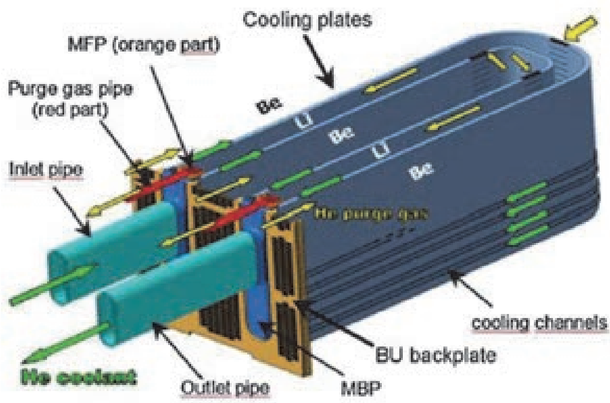

- In TBM the scheme foreseen the injection of purge in Be beds and then in the front part in the Ceramic breeder.
- The He loop at low pressure (few bars) has H addition at 0.1%.

F. Hernández, F. Cismondi, B. Kiss, Thermo-mechanical analyses and assessment with respect to the design codes and standards of the HCPB-TBM Breeder Unit, Fusion Eng. 87 (2012) 1111– 1117

The Coolant and the Tritium Extraction Systems

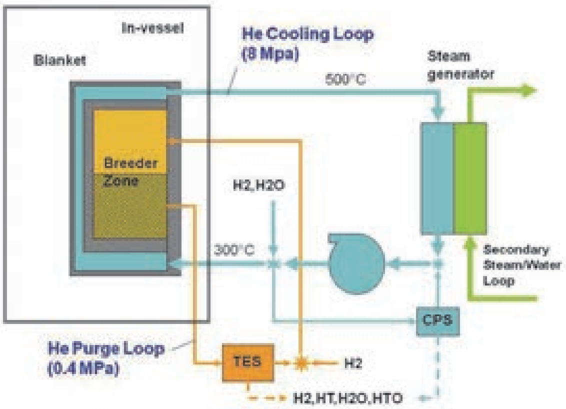

- **Helium Coolant System:** helium temperature between 300 to 500°C at 8 MPa. The blanket system is feeded by four independent loops (2 IB, 2 OB with redundant cooling).
- **Tritium Extraction System (TES):** to extract T from the pebble beds and remove it from the He carrier. Low pressure loop.
- **Coolant Purification System (CPS):** to remove T (and others impurities) from the high pressure Helium Coolant. Only a small fraction of helium is treated (<1%).

14 L.V. Boccaccini

Tritium Extraction System (DEMONET 1995)

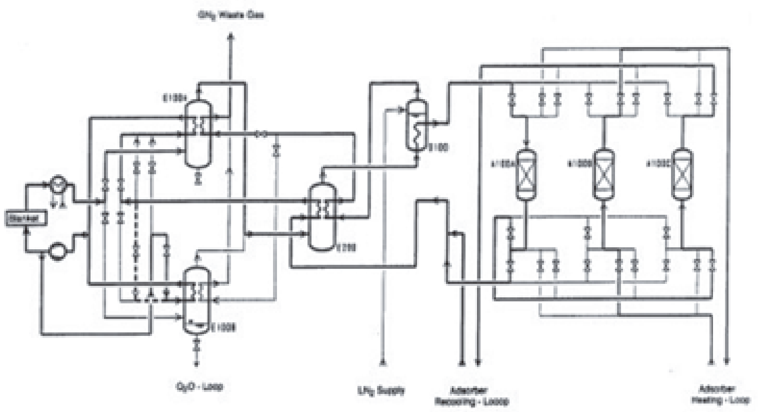

- The process was proposed by KIT in collaboration with LINDE. It is based on the use of cold traps (at 173K) and cryogenic 5A molecular sieves (at ~77 K).

M. Dalle Donne, H. Albrecht, L.V. Boccaccini, U. Fischer, S. Gordeev, E. Hutter, K. Kleefeldt, P. Norajitra, G. Reimann, P. Ruatto, K. Schleisiek and H. Schnauder, European Helium Cooled Pebble Bed blanket design of blanket test module to be tested in ITER, Fusion Engineering and Design 39-40 (1998) 825-833

15 L.V. Boccaccini

Tritium permeation control in HCPB blanket

- The definition of the mitigation techniques has been performed identifying all the values of Permeation Reduction Factors (PRF_{BB} for blanket cooling structure, PRF_{SG} for SG tubes) and the recirculation rate into CPS (α_{CPS}) allowing the tritium releases to be lower than 20 Ci/d.
- The results showed that it is possible to mitigate tritium migration in in He-cooled blankets without excessively stressing the purification system and without too demanding permeation barriers.
- High uncertainties affecting the performances attainable from the permeation barriers.

F. Franza, L.V. Boccaccini, A. Ciampichetti, D. Demange, M. Zucchetti, Tritium Permeation Issues for Helium-Cooled Breeding Blankets, presented to SOFE-25.

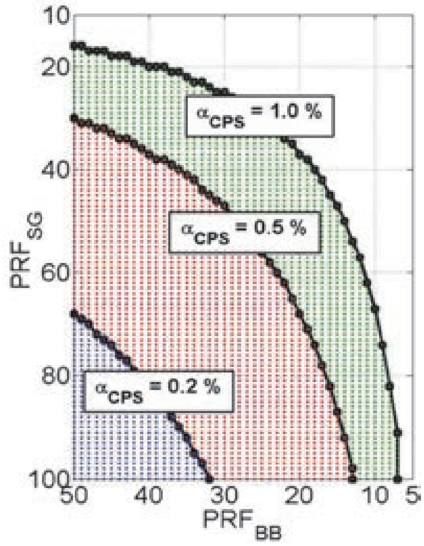

16 L.V. Boccaccini

Conclusions

- The EU breeder blanket programme is entering in a new phase facing the opportunities and the challenges of the Roadmap 2013 that leads to the definition of a DEMO with start construction in 2030. The selection of blanket concepts, materials and technologies for the new machine will be one of the main task in the next years as well as the choice of the right development strategy in view of a commercial FPP .
- EU has a portfolio of blanket concepts developed in the last 20 years that covers a large spectrum of possibilities in term of coolants and breeder materials.
- The helium cooled blankets (HCPB and HCLL) remain the first choice also for the Early DEMO; the R&D programme is in an advanced stage and they will be tested in ITER. They present very favourable characteristics of safety in term of compatibility with all the reactor materials and T processes. In addition He open future development for reactor systems with high thermal efficiency. Issues are high pumping power, balance of plant maturity and he availability as natural resource.
- Water cooled concepts will be assessed as back-up solution, in particular the WCLL. R&D will be re-open to clarify the issues in term of material compatibility, safety and T coolant purification
- The DCLL is also under assessment as possible transition to more advanced self-cooled blanket concepts. However, in an Early DEMO only a low performance version could be developed in time.
- New design work have been performed to adapt and further develop the HCPB concept for the new DEMO conditions.

17 L.V. Boccaccini

TOPICAL DISCUSSION: LIFE LIMITING FACTORS AND ACHIEVABLE PEAK POWER DENSITY FOR SOLID BREEDER BLANKETS (summarized by A. Ying)

Under this topic, we discussed the following questions (each question is followed by the discussions that took placed):

(1) How much is the current solid breeder blanket design condition with regard to neutron wall load (NWL)? How was it decided?

The EU considered an average and maximum neutron wall loads of 2.1 and 2.5 MW/m^2, respectively for the solid breeder blanket designs in FPP (fusion power plant) study. The JA has considered a solid breeder blanket design for a neutron wall load of 5 MW/m^2 with a corresponding width of the ceramic breeder pebble bed region of 7 mm in her past DEMO/power plant design studies. In recent design studies, the neutron wall load has come down to 3.5 MW/m^2. China has considered a neutron wall load of 1.5 MW/m^2 primarily for CFETR.

(2) What is the life limiting factor for solid breeder caused by neutron irradiation and NWL? (such as lithium burnup, breeder breakage/sintering, nuclear heating and temperature control, irradiation damage, etc.)

The life limiting factors for solid breeders can be due to Li burn-up, TBR degradation, loss of temperature control of the ceramic breeders due to pebble breakage and mechanical property degradation under irradiation, excess mass transfer due to the existence of moisture/vapor, and compatibility problems. JA has considered 20 to 35% Li burn-up as a life limiting factor. However, there is not enough knowledge to make any definite conclusions. The PIE of the HICU data may help to answer this question to some extent, which is still yet to be performed. The goal is to ensure that the life limiting factor for a solid breeder blanket is on the structural material irradiation lifetime and is not caused by the material and operational degradations of the ceramic breeder materials.

(3) What is the critical characteristic of the breeder material? What is the current performance of blanket? (such as the maximum allowable temperature and temperature windows for different breeders, as a function of fluence)

The solid breeder material has a low thermal conductivity and a relatively narrow operational temperature window. The minimum operational temperature of a solid breeder material is determined by its tritium release characteristics, which sits at about 350 to 400^oC. This temperature range is consistent with the coolant operational temperature, whereas the maximum operational temperature of a solid breeder can be limited in a first approximation by the sintering temperature (80 % of melting temperature), or at the temperature where decomposition or evaporation occurs. The maximum temperature for the Li_4SiO_4 is currently set at 930^oC. The maximum for the Li_2TiO_3 is set at 900 but with 1000^oC as the limit. A question was asked why it is still not converged with respect to the maximum operational temperature for solid breeder material.

In conclusion: There appear no definite answers to those critical questions. Irradiation experiments tend to take a much longer time than one would expect, during which the irradiated materials might be no longer relevant or the budget situation changed and no funding for PIE, etc. Hopefully, with China, Korea and India’s interests on the solid breeder blanket concepts these questions can be addressed in more systematic and efficient ways.

ISBN 978-3-7315-0101-5

ISSN 1869-9669
ISBN 978-3-7315-0101-5